UNSW SYDNEY

Characterisation and production of pancreatic islet extracellular matrix for sustaining islet function after isolation

Author:
Cheng, Jennifer Yun-Ching

Publication Date:
2012

DOI:
https://doi.org/10.26190/unsworks/16117

License:
https://creativecommons.org/licenses/by-nc-nd/3.0/au/
Link to license to see what you are allowed to do with this resource.

Downloaded from http://hdl.handle.net/1959.4/52611 in https://unsworks.unsw.edu.au on 2024-05-01

Characterisation and production of pancreatic islet extracellular matrix for sustaining islet function after isolation

by

Jennifer Yun-Ching Cheng

A Thesis submitted for the Degree of Doctor of Philosophy

Graduate School of Biomedical Engineering

University of New South Wales

August 2012

Originality Statement

I hereby declare that this submission is my own work and to the best of my knowledge it contains no materials previously published or written by another person, or substantial proportions of material which have been accepted for the award of any other degree or diploma at UNSW or any other educational institution, except where due acknowledgement is made in the thesis. Any contribution made to the research by others, with whom I have worked at UNSW or elsewhere, is explicitly acknowledged in the thesis. I also declare that the intellectual content of this thesis is the product of my own work, except to the extent that assistance from others in the project's design and conception or in style, presentation and linguistic expression is acknowledged.

Signed: …….....

Date:…….....

Copyright Statement

‘I hereby grant the University of New South Wales or its agents the right to archive and to make available my thesis or dissertation in whole or part in the University libraries in all forms of media, now or here after known, subject to the provisions of the Copyright Act 1968. I retain all proprietary rights, such as patent rights. I also retain the right to use in future works (such as articles or books) all or part of this thesis or dissertation.

I also authorise University Microfilms to use the 350 word abstract of my thesis in Dissertation Abstract International (this is applicable to doctoral theses only). I have either used no substantial portions of copyright material in my thesis or I have obtained permission to use copyright material; where permission has not been granted I have applied/will apply for a partial restriction of the digital copy of my thesis or dissertation.'

Signed …….....

Date …….....

Authenticity Statement

‘I certify that the Library deposit digital copy is a direct equivalent of the final officially approved version of my thesis. No emendation of content has occurred and if there are any minor variations in formatting, they are the result of the conversion to digital format.’

Signed …….....

Date …….....

Abstract

Loss of extracellular matrix (ECM) is known to result in low pancreatic islet survival rates post-isolation and result in poor transplantation outcomes in the treatment of diabetes. Several approaches to ECM supplementation have been used to help improve islet longevity, however, long-term culture of isolated islets is currently unachievable and rates of clinical insulin independence from islet transplantation is still less than 50%. The causes of this are multi-faceted, however, the kind of ECM components that constitutes a healthy islet is still not known. Healthy, adult rodent ECM was characterized by immunohistochemistry and immunoblotting. The basement membrane was distributed throughout the islet in a pattern that was tightly associated with the interweaving endothelium. In contrast, heparan sulfate (HS) was the predominant glycosaminoglycan found in the islet and was mainly on or in the beta-cells. The novel localization of the HS proteoglycan, syndecan-4, showed a similar distribution pattern to the HS within the rodent islet, thus suggesting that the islet HS is attached to syndecan-4. Human umbilical cord vein endothelial cells (HUVECs) were found to be capable of producing ECM components that included collagen IV, fibronectin, laminin, perlecan and HS. Macromolecular crowding enhanced the deposition of ECM components by 2-6 fold. These results showed that HUVECs could produce ECM similar in composition to those observed in healthy, adult islets and macromolecular crowding could increase the quantity of these deposited components.

The crowded and decellularized HUVEC ECM facilitated the maintenance of glucose stimulated insulin secretion and did not increase the occurrence of apoptosis and necrosis in the MIN6 beta-cell line more than that of tissue culture plastic. The

crowded HUVEC ECM extended the life of primary islets by maintaining hormone expression and genetic expression of important -cell-specific markers. In addition to this, primary islets cultured on the crowded HUVEC ECM tended to maintain their spherical morphology. This work demonstrated that in vitro endothelial cells can simulate ECM produced by islet vasculature. Furthermore, enhancing ECM by macromolecular crowding can produce better quality and quantity of ECM to support and maintain islet function and structure in extended culture. These methods can be used to increase longevity of islets in culture and better prepare isolated islets for transplantation.

Acknowledgements

It has been a rollercoaster ride of joy and despair, but I have come out on top and do not regret a moment of this journey. This thesis is dedicated to all those that made this journey worthwhile.

I owe the utmost thanks and gratitude to Laura Poole-Warren for being nothing but supportive and encouraging, especially during moments when I could not see the light at the end of the tunnel. To my co-supervisors John Whitelock and Penny Martens, thank you for being there when Laura could not. To Michael Raghunath and the Tissue Modulation Lab at the National University of Singapore, thank you for welcoming me into Singapore and teaching me so much. To Jenny Gunton and the Gunton Lab (especially Rebecca Stokes, Kim Cheng, Kuan Minn Cha and Christian Girgis) at the Garvan Institute, there is just not enough gratitude to send your way - I thank my lucky stars everyday to have been able to collaborate with you, as I would not have survived without all your help. I also have to thank Jennifer Gamble at the Centenary Institute for generously providing me with an unlimited supply of HUVECs.

Then there are the friends that became my family along the way. Khoon and Yogi, I am truly sorry to leave you both behind. The "Teletubbies" can still hold our "international conferences" in the future by Skype! Eman and Cara, it has been a privilege to be working on the "Pancreas Project" with you both. To the ex-Hydrogel members, Naat and Helene, I am missing our conversations and gatherings at your house, everyday. Bill, Johnson and MJ - you guys were the best office buddies ever! Thanks to my "sister", Wendy, for introducing me to Garvan and going on so many adventures with me. I wish I could give special thanks to each and every wonderful friend I have made at GSBME, BABS and Garvan, but that list would be never ending. Then there is the UNSW Outdoors Club and all of its crazy members for running such amazing trips that kept me sane in between experiments.

Finally, I must give thanks to my pillars of support - Steve, mum, dad and sister. I am the luckiest girl to have you all as family and truly appreciate how much you believe in me.

This work would not have been possible without the ARC Discovery Grant DP0986447 and the animals that sacrificed their lives for this cause.

May all beings be happy and free,
and may the thoughts, words and actions of my life contribute
in some way to that happiness and to that freedom for all

List of Publications

Journal Publications

1. Cheng JYC, Whitelock J, Poole-Warren LA. (2012) Syndecan-4 is associated with beta-cells in the pancreas and the MIN6 beta-cell line. *Journal of Histochemistry and Cell Biology*. DOI: 10.1007/s00418-012-1004-6 (in press)

2. Cheng JYC, Raghunath M, Whitelock J, Poole-Warren LA. (2011) Matrix components and scaffolds for sustained islet function. *Tissue Engineering Part B: Reviews*. 17(4): 235-47

Conference Presentations

1. Cheng JYC, Chuang C, Whitelock J, Poole-Warren LA. "Characterisation of pancreatic islet extracellular matrix and its role in beta-cell function". International Conference on Proteoglycans and Matrix Biology, 2011, Manly, Australia (poster presentation)

2. Cheng JYC, Raghunath M, Poole-Warren LA. "Enhanced *in vitro* production of endothelial cell matrix by macromolecular crowding". TERMIS-EU, 2011, Granada, Spain (oral presentation)

3. Cheng JYC, Chuang C, Whitelock J, Poole-Warren LA. "Characterisation of islet extracellular matrix". TERMIS-AP, 2010, Sydney, Australia (oral presentation)

4. Martens P, Cheng JYC, Young CJ, Nafea E, Poole-Warren LA. “Encapsulation of Pancreatic Cells for Tissue Engineering”. International Nanomedicine Conference, 2012, Sydney, Australia (oral presentation)

5. Martens P, Cheng JYC, Young CJ, Poole-Warren LA. “Improving Islet Cell Survival in a Biosynthetic Hydrogel Microencapsulation System”. TERMIS, 2012 (oral presentation)

6. Young CJ, Cheng JYC, Whitelock J, Martens P, Poole-Warren LA. “Islet Matrix Identification for use in Biosynthetic Microencapsulation”. European Society of Biomaterials Conference, 2011, Dublin, Ireland (oral presentation)

7. Martens P, Young C, Nafea E, Cheng JYC, Poole-Warren LA. “Characterisation of a Poly (Vinyl Alcohol) Hydrogel Cell Encapsulation System”. Australian Polymer Symposium, 2011, Coffs Harbour, Australia (oral presentation)

Table of Contents

List of Figures

List of Tables

Chapter 1

1 Introduction

The World Health Organization states that diabetes affects 346 million people worldwide and will become the seventh leading cause of death in the world, by the year 2030 (WHO, 2011). Figure 1.1 shows the current treatments available for diabetes. The first line of treatment include insulin injections (for type 1) and the intake of blood-glucose-lowering agents (for type 2) (Devendra et al., 2004; Nathan et al., 2009). Whole organ transplants are largely only applied to type 1 diabetics requiring simultaneous kidney transplants and are having secondary complications to the disease (Sutherland et al., 2001). Although whole pancreatic grafts facilitate greater than 1 year of insulin independence in more than 80% of recipients (Sutherland et al., 2001), the approach is plagued with organ shortages and retains the risks involved with major surgical procedures as well as long-term immunosuppression (Ricordi and Strom, 2004). Islet transplantation, on the other hand, does not require significant surgery and opens up the potential for xenotransplantation as well as a reduction in immunosuppressive drug therapy, if coupled with the technology of immunoisolation. Islet allografts have already had some success, whereby insulin independence was achieved in 100% of type 1 diabetic people (n=7) treated by islet transplantation in conjunction with a glucocorticoid-free immunosuppression regimen (Shapiro et al., 2000).

Since then, it has been reported that 80% of patients treated with islet transplantation could achieve insulin independence within the first year of the transplant (Shapiro et al., 2003).

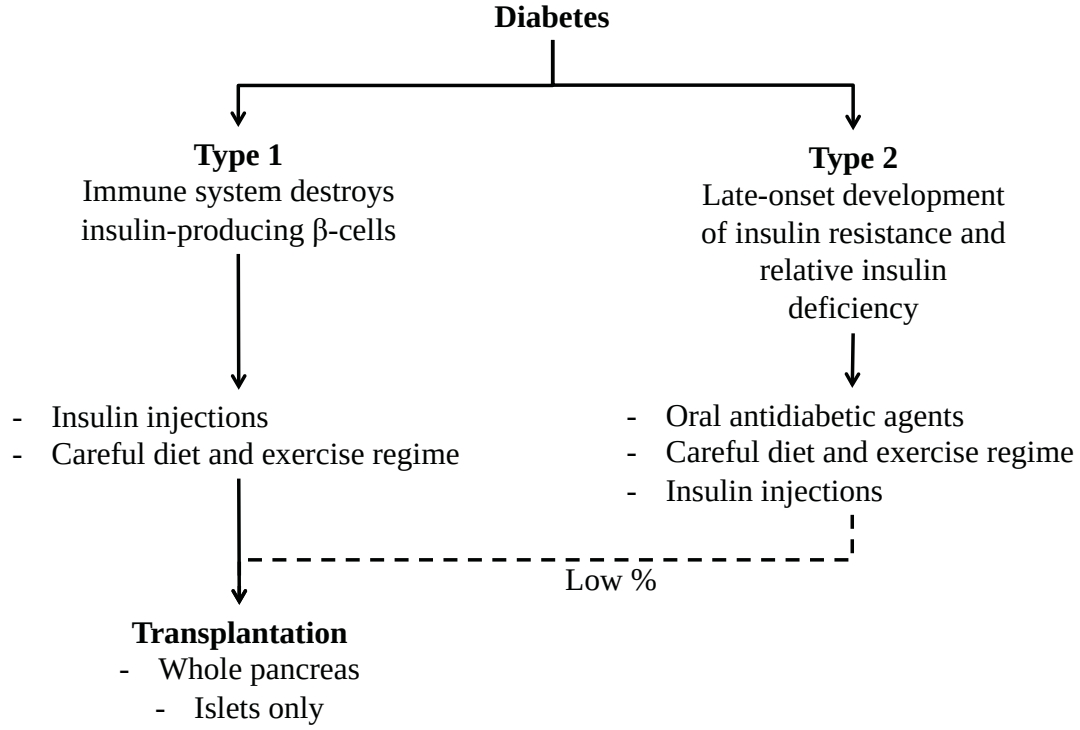

Figure 1.1 Flow diagram of the different types of diabetes and treatments that are currently available

Nevertheless, a current problem facing this therapy is that isolated islets have limited lifespan with recipient insulin independence lasting from 22 days to 48 months (Robertson, 2004b). As few as 14% of patients given islet transplants remain insulin independent by the fifth year (Ryan et al., 2005). The overall process of islet transplantation is a lengthy and stressful process that only provides good yields and quality islets if performed rigorously. The pancreata are digested with collagenase, which disintegrates the intercellular matrix of collagen and release the islets from the rest of the organ (Szot et al., 2007). The islets are subsequently filtered and purified

by a density gradient centrifugation created by Ficoll (which is itself, islet-toxic), then cultured before being transplanted into the recipient. It is therefore unsurprising that islet isolation may result in low survival rates. There are various factors that affect the clinical outcome of the islet transplant and these include limited islet viability during and after isolation, failure to revascularize and immune attack from the inflammatory response (Deters et al., 2011; Narang and Mahato, 2006).

The pancreas contains exocrine, endocrine and ductal cells. There are at least four types of endocrine cells within the pancreatic islets themselves - α, β, δ and PP cells – each of which secrete specific hormones that modulate the metabolism of carbohydrates, lipids and proteins (Islam, 2010). In addition to these cell types, the islet vasculature is important for maintaining glucose homeostasis because it is necessary for the time-critical responses to changes in the balance of blood glucose concentrations and islet hormone release in the body. It is also imperative for supplying the high oxygen demand of pancreatic β-cells. Islet capillaries are five-times more dense and ten-fold more fenestrated than the exocrine capillaries and the β-cells are generally bordered by at least one capillary (Ballian and Brunicardi, 2007; Henderson and Moss, 1985). During islet isolation, the islets are dissociated from the surrounding exocrine tissue and blood vessels by enzymatic digestion and mechanical agitation. The enzyme digest disrupts the cell-to-cell and cell-to-matrix associations between islets and the exocrine tissue, and to some extent, also between cells within the islet (van Deijnen et al., 1992b; Wolters et al., 1992).

The isolation process also causes significant β-cell death, by both necrosis and apoptosis (Islam, 2010). Islets placed in culture have an apoptosis rate of between 2-

20%, which is markedly higher than rates observed *in vivo* (Dror et al., 2007; Thomas et al., 1999). Furthermore, up to 70% of transplanted β-cell mass may be destroyed during the early engraftment period (Biarnes et al., 2002; Davalli et al., 1995; Ryan et al., 2005). Apoptosis begins during the isolation process, peaks at 2-3 days post-transplantation as they are exposed to proinflammatory cytokines, hypoxia and nutrient deprivation, and continues for a further 2 weeks until what remains of the graft stabilizes and revascularizes (Biarnes et al., 2002; Carlsson et al., 2002; Davalli et al., 1995; Davalli et al., 1996; Giuliani et al., 2005; Paraskevas et al., 2000; Stokes et al., 2012). In addition to apoptosis, the β-cell phenotype is fragile and easily lost once islets are removed from their native environment (Russ et al., 2009; Weinberg et al., 2007). Gene expression of a number of important β-cell-specific transcription factors has been shown to decline after isolation (Negi et al., 2012). Therefore, the maintenance of functional and viable β-cell mass after the isolation process is a critical step for successful and efficient islet transplantation.

Interestingly, when islets are maintained in their original 3D cluster conformation, improved islet viability and function was observed when compared to monolayer cultures of islets (Lucas-clerc et al., 1993). Furthermore, the use of partially isolated islets in conjunction with the addition extracellular matrix (ECM) components such as collagen and fibronectin has demonstrated even more promise in enhancing islet function and viability (Daoud et al., 2009; Nagata et al., 2001). Various combinations of ECM components have also been tried and have shown improved islet survival and transplant outcomes (Cheng et al., 2011). However, despite these developments, long-term culture of isolated islets as well as long-term clinical

insulin independence from islet transplantation is still currently unachievable. The causes to this dilemma is multi-faceted and yet even just one facet – that is, what kind of ECM components constitutes a healthy islet - is still not known.

1.1 Aims of Thesis

It is hypothesised that endothelial cells from islet vasculature produce ECM that can support islet function and that enhancing ECM deposition through macromolecular crowding would produce better quality and quantity of endothelial ECM for promoting islet health. This thesis describes the characterisation of pancreatic islet ECM and the use of *in vitro* cells to produce ECM of a similar composition for extending the longevity of isolated islets. The overall objectives of this thesis were to:

1) Identify and study the distribution of ECM proteins, proteoglycans and glycosaminoglycans within healthy, adult pancreatic islets
2) Use *in vitro* cultured endothelial cells and macromolecular crowding techniques to enhance production of ECM of a similar constitution to ECM components identified
3) Study the function, viability and differentiation of β-cells cultured on normal and enhanced endothelial ECM

Chapter 2

2 Literature Review

This literature review was in part published in Tissue Engineering Part B: Reviews and permission was granted by the publishers for use in this thesis. The concepts and writing of this paper was largely under the control of Cheng JYC (90% input). The other authors contributed to the analysis and interpretation of the literature and assisted in the development of the arguments.

Paper citation:

Cheng JYC, Raghunath M, Whitelock J, Poole-Warren LA. (2011) Matrix components and scaffolds for sustained islet function. *Tissue Engineering Part B: Reviews*. 17(4): 235-47

2.1 Introduction

The extracellular matrix (ECM) makes up a substantial part of any given tissue. The ECM is a scaffold of proteins and polysaccharides by which cells are supported and anchored. Most importantly, it is involved in providing molecular cues that regulate cell behaviour. The intricate relationship between the cellular and acellular components of a tissue drives its healthy development, homeostasis and recovery from stress or injury (Bowers et al.; Lelièvre et al., 1996; Parnaud et al., 2006; Rozario and DeSimone). It is thus in the cell matrix that lies the key to determining essential design principles for engineering long-lasting and functional tissues.

The ECM is secreted locally by resident cells and forms an organised meshwork closely associated with cell surfaces. Depending on the functional requirements of the tissue, cells adapt and vary the amount and types of matrix molecules they secrete. This dynamic process makes natural matrix highly variable in its composition and mechanical properties. Examples of this include the calcified matrix produced to form hard structures found in teeth and bones, the rope-like fibres assembled to give tendons tensile strength, and the transparent gel-matrices with glass-like refractive properties found in the cornea. The matrix can also form thin sheets of fibres surrounding the surfaces of cells and organs known as the basement membrane. This membrane matrix is critical for facilitating cell-to-cell signalling, proliferation, development, migration and function. Understanding the nature of the matrix and how it interacts with resident cells is the next step to the recreation of biochemical cues for directing cell function in an artificial organ.

The major components of extracellular macromolecules are polypeptide chains of collagen, laminin, fibronectin and elastin interlaced with polysaccharide chains called glycosaminoglycans that are covalently linked to protein cores of proteoglycans via serine residues. Together, these natural polymers provide structure as well as contribute to the microenvironment of the tissue through signalling moieties and their ability to bind growth factors, cytokines, enzymes and other effector molecules. However, detailed knowledge of the matrix molecular composition and how it guides cell function still remains incomplete. This holds especially true for the islets of Langerhans of the pancreas. Islets isolated from the pancreas for transplantation tend to suffer from anoikis, or "homelessness", as the commonly used Edmonton protocol for islet isolation requires collagenase to dislodge the islets from their native environment (Linetsky et al., 1997). The sudden loss of the pancreatic environment and subsequent interruption of cell-matrix interactions leads to cell apoptosis (Frisch and Screaton, 2001). Thus transplanted islets are often associated with significantly lower engraftment efficiencies than whole pancreas transplants. The survival rate after pancreas transplant surgery is approximately 86%, whereas islet graft success remains at only 10% or less (Ryan et al., 2001). Although other factors such as poor transplant site and hypoxia may also contribute to low graft success, by understanding the crucial role ECM plays in maintaining and driving endocrine function, the optimal bioartificial scaffold for supporting islet function may be designed to improve glucose responsiveness, islet survival and maintenance of differentiation. This review summarizes current knowledge of the ECM in pancreatic islets and the *in vitro* attempts that have been made to simulate this microenvironment to improve islet survival and function.

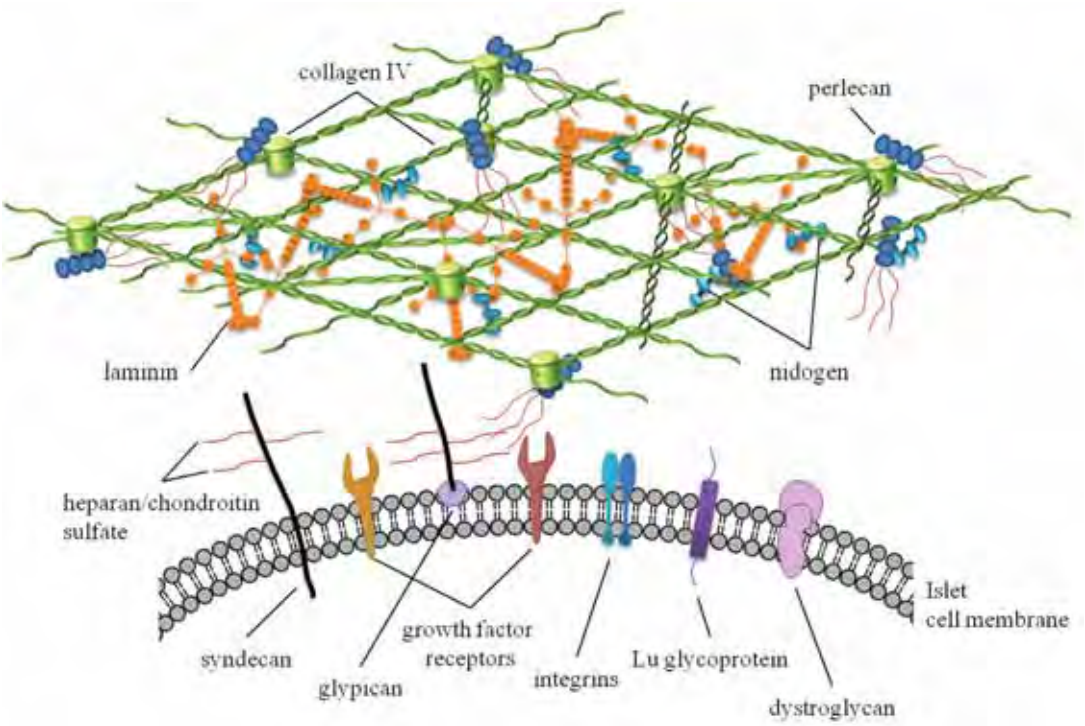

Figure 2.1 Islet matrix components and their potential receptors. The schematic shows the major components of islet extracellular matrix (ECM) and the cell surface receptors that are known for these components. The ECM consists of collagen IV, fibronectin, laminin, perlecan, and other components that are yet to be discovered. Potential receptors such as syndecan and glypican may aid in growth factor signaling, and together with other receptors, such as integrins, dystroglycan, and Lu glycoprotein, interact with the surrounding ECM network to maintain endocrine viability and functionality.

2.2 In vivo function of matrix in the islets of Langerhans

The cell matrix is made up of a complex mixture of carbohydrates and proteins that dictate the structure, mechanical forces and functional signals surrounding a cell community. The basement membrane is in closest proximity to cells and is an assembly of matrix molecules that can have the significant tensile strength of collagen, can act as molecular sieves with the help of proteoglycans and also facilitate the attachment of cells via laminin (Iozzo, 2000). Matrix interactions with surface receptors, such as those illustrated in the schematic in Figure 1.2, mediate cell adhesion and potentiate downstream biochemical pathways that influence cell proliferation, migration, differentiation and homeostasis. Each matrix component may have more than one receptor. Identifying these cell surface receptors, their downstream signalling pathways and understanding their interactions with matrix components can help to provide insight into the functional role of islet ECM. Table 1.1 summarises the major integrin receptors known. It should be noted that the integrin receptor composition of islets remains controversial, with various differences observed across species (Wang et al., 1999). For a detailed overview of integrin expression in human islets, see Stendahl et al, 2009 (Stendahl et al., 2009).

Table 2.1 Known integrin receptors to different ECM components

ECM component	**Integrin**	**Reference**
Collagen	α1β1, α2β1, α10β1, α11β1	(Tumova et al., 2000)
Laminin	α1β1, α2β1, α3β1, α6β1, α7β1, α9β1, αvβ3, αvβ5, αvβ8, α6β4	(Colognato et al., 1997; Kühn and Eble, 1994; Mercurio, 1995; Mizushima et al., 1997; Nomizu et al., 1997)
Fibronectin	α3β1, α4β1, α5β1, α4β7, α8β1, αvβ1, αvβ3, αvβ5, αvβ6, αIIbβ3	(Johansson et al., 1997)
Nidogen/entactin	α3β1 and αvβ3	(Dedhar et al., 1992; Yuan et al., 2008)
Vitronectin	αvβ1, αvβ3, αvβ5, αIIbβ3	(Felding-Habermann and Cheresh, 1993)
Perlecan	α2β1	(Bix et al., 2004)

2.2.1 Basement membrane proteins

2.2.1.1 Collagen

Collagen fibres have great tensile strength that not only provide structural support for cells internally and externally, they are also required for cell growth adhesion and migration, differentiation, morphogenesis and injury repair (McCall-Culbreath and Zutter, 2008). Collagen I, II, III, IV, V, VI, have all been reported in the peripheral ECM of mature human islets (Deijnen et al., 1994; Meyer et al., 1998a; Meyer et al., 1998b; van Deijnen et al., 1992a; Wang and Rosenberg, 1999). However, their role in endocrine function is not clear. Though collagen IV has been shown to promote the survival of intact islets when compared to collagen I (Pinkse et al., 2006), another study has shown it to decrease insulin production and secretion in purified β-cells (Kaido et al., 2006).

Integrins are important for cellular signal transduction and the role of collagen-integrin binding is important for a variety of functions that range from osteoblast differentiation (Jikko et al., 1999) and dermal fibroblast cell proliferation (Pozzi et al., 1998) to the regulation of myofibrillar patterning (Ross and Borg, 2001). Four integrins, namely α1β1, α2β1, α10β1, and α11β1, have been shown to mediate cellular interactions with the GFOGER sequence in domain I of the α subunit of collagen (McCall-Culbreath and Zutter, 2008). Though the β1-integrin chain has been previously reported to be expressed by islet cells (Cirulli et al., 2000; Kaido et al., 2004a; Kaido et al., 2004b; Ris et al., 2002; Virtanen et al., 2008; Wang et al., 1999), only the α1-chain has also been found in islets, and this finding remains controversial (Kaido et al., 2004b; Wang et al., 1999). Kaido and colleagues

observed that the α1β1 integrin enabled human fetal β-cell attach, migrate and secrete insulin when exposed to collagen IV (Kaido et al., 2004b), whereas Wang and colleagues did not observe the α1 integrin chain in islets isolated from the hamster, canine, porcine, and human pancreas (Wang et al., 1999). Thus despite the abundance of collagen IV in the islet matrix, there is no clear evidence for a collagen and integrin binding pathway. This suggests that non-integrin interactions with collagen may play a more significant functional role in the pancreatic endocrine system. Discoidin domain receptors are non-integrin receptors for collagen I-V, and play an important role in regulating cell adhesion, migration, differentiation, proliferation and ECM production (Chin et al., 2001). Discoidin domain receptor-1 expression has been found in the islet cells but not in the surrounding exocrine tissue (Alves et al., 1995).

2.2.1.2 Laminin

In addition to collagen IV, laminins are a major structural component of basement membranes. Collagen IV and laminin both form stabilized polymer networks bound together by nidogen and the glycosaminoglycan chains of perlecan (Antonio et al., 1993; Mayer et al., 1997). Laminin's cross-shaped trimeric proteins have three short arms that bind other laminin molecules to form sheets and one long arm able to bind cell membranes (Tunggal et al., 2000). Laminin is prevalent in the islet ECM (Meyer et al., 1998a; Meyer et al., 1998b; Parnaud et al., 2006; van Deijnen et al., 1992a; Virtanen et al., 2008; Wang and Rosenberg, 1999) and studies in mouse islets have indicated that pancreatic endocrine cells interact with laminin associated with the pervading microvasculature, specifically laminin-2/-211, laminin-8/-411 and

laminin-10/-511 (Jiang et al., 2002; Kaido et al., 2004b; Nikolova et al., 2006; van Deijnen et al., 1992a; Virtanen et al., 2008). It is still unclear which cell type contributes which laminin to the islet microenvironment. Immunolocalisation for laminin-5/-332 in rat and human islets demonstrated heterogeneous intracellular staining according to islet cell type, with stronger labeling on non-β-cells than β-cells, and negative labeling on the endothelial cells or their associated basement membranes (Armanet et al., 2009; Parnaud et al., 2006). Interestingly, the Armanet study was only able to detect extracellular laminin-5/-332 by immunoblotting the islet conditioned medium(Armanet et al., 2009).

Laminin interacts with cells via integrin and non-integrin mediators. The integrin receptors include six members of the β1 subfamily (α1β1, α2β1, α3β1, α6β1, α7β1 and α9β1), three of the αv subfamily (αvβ3, αvβ5, αvβ8) and the α6β4 integrin (Colognato et al., 1997; Kühn and Eble, 1994; Mercurio, 1995; Mizushima et al., 1997; Nomizu et al., 1997). Non-integrin receptors of laminin include the dystroglycan protein complex, the Lutheran blood group glycoprotein (Lu) and laminin receptor-1 (Hinek, 1996; Kikkawa and Miner, 2005; Miner and Yurchenco, 2004; Simoneau et al., 2003).

Some laminin receptors have been identified on the cells of the islets of Langerhans. The α3 and β1 integrins and dystroglycan were found to be distributed on the endocrine cells throughout the islet with no apparent polarisation towards the microvascular basement membranes (Kantengwa et al., 1997; Virtanen et al., 2008), while the α6 integrin has been co-localised with laminin in the developing pancreas (Wang et al., 2005b). Dystroglycan has been implicated to play a role in laminin-1-

induced β-cell differentiation and survival in fetal mouse pancreas (Jiang et al., 2001). The Lu glycoprotein was prominently immunolocalised to the surface of adult human islet cells facing the basement membranes and the invading microvasculature (Virtanen et al., 2008), which is consistent with previous findings that indicate its specific affinity for the laminin α5 chain (Kikkawa and Miner, 2005; Kikkawa et al., 2002; Vainionpää et al., 2006). However, expression of Lu varies between species as it is found on human β-cells but is absent from rodent β-cells, suggesting that ECM functions may differ between species (Otonkoski et al., 2008; Virtanen et al., 2008). Laminin receptor-1 may also play a role in the regulation of gene expression as it is essential for the 20S rRNA-precursor to mature 18S rRNA in the late step of 40S ribosomal subunit maturation (Jackers et al., 1996). Interestingly, laminin receptor-1 is also able to bind independent of species, elastin and collagen IV, if they form similar secondary conformations to laminin (Hinek, 1996; Mecham and Heuser, 1991).

2.2.1.3 Fibronectin

Fibronectin is a dimeric glycoprotein that exists in soluble and fibrillar forms, with the latter being a common extracellular matrix component of a variety of cells. Fibronectin has several domains that create non-covalent adhesion of various other ECM components within the tissue. Its interacting partners include collagen, heparin and chondroitin sulfate proteoglycans, specific receptors such as integrin on the surface of various cell types as well as fibronectin itself (Alberts et al., 2007). Multiple splicing variants of fibronectin exists and their expression is influenced by the types of growth factors present and the age of the producing cell (Magnuson et

al., 1991). Cells adhere to fibronectin via its distinct Arg-Gly-Asp (RGD) loop (de Pereda et al., 1999). This RGD sequence is recognised by a range of integrins including α3β1, α4β1, α5β1, α4β7, α8β1, αvβ1, αvβ3, αvβ5, αvβ6 and αIIbβ3 (Johansson et al., 1997). In addition, non-integrin receptors of fibronectin include dystroglycan (Belkin and Smalheiser, 1996; Hall et al., 2003) and syndecan (Bernfield and Sanderson, 1990; Woods et al., 2000a).

Fibronectin has been immunolocalised in the adult islet periphery, islet ductal pole and perivascular areas, and is often associated with collagens I, III, IV and laminin (Geutskens et al., 2004; Meyer et al., 1998a; Meyer et al., 1998b; Parnaud et al., 2006). Integrin subunits α3 and α5 have been co-localised with fibronectin in developing pancreatic tissue and is thus speculated to be responsible for endocrine cell interactions with fibronectin during morphogenesis (Wang et al., 2005b; Wang and Rosenberg, 1999). In addition to this, the α5β1 integrin has been implicated to signal cell survival through the transcriptional upregulation of the anti-apoptotic protein, Bcl-2 (Lee et al., 2005), thus suggesting that fibronectin may play a role in controlling anoikis via this integrin pathway.

2.2.1.4 Nidogen/entactin

Nidogen, also known as entactin, is a globular glycoprotein found in basement membranes that links together perlecan, collagen IV, fibulin and laminin (Iozzo, 2000). The globular domains of nidogen can bind to the protein core of perlecan, collagen IV and the short arm of the laminin trimer (Mann et al., 1988). Cell adherence to nidogen is facilitated by an RGD sequence found in its central domain (Chakravarti et al., 1990), as well as the integrins α3β1 and αvβ3 (Dedhar et al.,

1992; Yi et al., 1998) The two isoforms of nidogen, nidogen-1 and nidogen-2, have both been immunolocalised to the peri-islet and sub-endothelial basement membranes (Irving-Rodgers et al., 2008), however, their role in β-cell function remains unknown.

2.2.1.5 Vitronectin

Vitronectin is a glycoprotein that occurs in plasma as well as the ECM and has previously been co-localised with fibronectin within the collagenous bundles of retinal matrix (Marano and Vilaró, 1994). It consists of three domains, one of which regulates proteolysis by binding and stabilizing plasminogen activator inhibitor-1 (Blasi, 1997), another contains an RGD sequence that recognises integrin receptors (αvβ1, αvβ3, αvβ5 and αIIbβ3) (Felding-Habermann and Cheresh, 1993) and a third that binds heparin following its activation by the thrombin-antithrombin III complex (Høgåsen et al., 1992). The signalling pathway through the αvβ5 integrin can direct cell migration (Smith and Cheresh, 1990), and studies have shown that both αvβ3 and αvβ5 are involved in angiogenic pathways (Friedlander et al., 1995).

Vitronectin is only found in human fetal islet tissue, emerging from pancreatic ducts in early precursor tissue (Cirulli et al., 2000). The importance of vitronectin in early islet development was also suggested when an upregulation of the vitronectin receptor, αvβ1, in fetal compared to that of mature β-cells was observed (Kaido et al., 2004b). In addition to this, the integrin αvβ1 was found to be essential for the spread and migration of fetal β-cells grown on vitronectin, while αvβ5 supported the adhesion of both mature and immature beta-cell populations. This suggests that

vitronectin may play an important role in the motile processes required during the early stages of islet morphogenesis.

2.2.2 Proteoglycans

Proteoglycans are heavily glycosylated glycoproteins found in the ECM. They have a core protein decorated with long carbohydrate side chains, namely glycosaminoglycans (GAGs), that are post-translationally attached and negatively charged under physiological conditions (Iozzo, 2000). This negative charge provides the ECM with sieving properties and allows it to bind and sequester growth factors and cytokines, where they function as a reserve to be released when required (Griffith and Swartz, 2006). Currently, little is known about the presence and role of proteoglycans within the islet ECM. Early studies of toadfish islets showed their synthesis of heparan sulfate predominantly, as well as chondroitin 4- and 6-sulfates and dermatan sulfate (Watkins et al., 1968). However, there have been no studies to date, on islets and dermatan sulfate, thus this review will focus on the more extensively studied heparan sulfate and chondroitin sulfate proteoglycans and explore their functions in the pancreatic islet.

2.2.2.1 Heparan sulfate proteoglycans

Heparan sulfate proteoglycans (HSPG) are decorated with long, linear polymer chains of alternating N-acetylglucosamine and glucuronic acid, and have multiple binding domains for various other ECM components and cell surface receptors (Iozzo, 2000). The branched and negatively charged sugar residues bind to growth factors such as fibroblast growth factors, vascular endothelial growth factors and

hepatocyte growth factors (Lin, 2004), and influences their distribution and diffusion throughout the ECM (Strigini, 2005).

2.2.2.1.1 Perlecan

Perlecan demonstrates a wide range of regulatory control, binding properties and interactions as it is found in all basement membranes, cartilage and several mesenchymal tissues during development (Costell et al., 2002; Iozzo, 1984). Mammalian perlecan is comprised of five domains, four of which share some homology with other proteoglycans present in the basement membrane such as agrin and collagen XVIII (Iozzo, 2000).

Perlecan is functionally diverse as it has a plethora of partners that interact either directly with its protein core, with its GAG chains or with growth factors bound to these GAG chains. Perlecan may also be decorated with other GAGs like chondroitin sulfate (CS) and keratin sulfate (KS), however, the nomenclature has remained "HSPG" as it was first identified with heparan sulfate (HS) decoration (Chuang et al., 2010; Knox et al., 2005). Aided by HS chains, perlecan can bind to growth factors (Aviezer et al., 1994; Mongiat et al., 2001; Mongiat et al., 2000), growth-promoting ECM components (Bengtsson et al., 2002; González-Iriarte et al., 2003; Mongiat et al., 2003; Vischer et al., 1997), α2β1 integrin (Bix et al., 2004) and ECM proteins including laminin-1, collagens and fibronectin (Ettner et al., 1998; Heremans et al., 1990; Villar et al., 1999; Whitelock et al., 1999). As a result of this, perlecan helps to stabilise the overall ECM network. Furthermore, the binding of growth factors, chemokines and signalling molecules to perlecan protects them from proteolytic degradation and misfolding (Knox et al., 2002; Whitelock et al., 1996).

Perlecan's HS chains also allow for better cellular control of local effector molecule gradients, which can be stored and proteolytically released as needed. It has thus been proposed that perlecan modulates angiogenesis via the interaction of growth factors with its protein core and HS chains (Bix and Iozzo, 2008; Whitelock et al., 1996). In addition to this, HSPGs including perlecan were observed to physically obstruct the migration/invasion of cells, preventing monocytes from binding to the subendothelial matrix as well as provide adhesion ligands for transmigrating leukocytes during inflammation (Parish, 2006; Parish et al., 2001; Pillarisetti, 2000).

Despite the extensive knowledge of perlecan in other systems, the function of perlecan in islets is poorly understood. Perlecan has been immunolocalised to the capillaries within the islet and basement membranes surrounding the exocrine acini of a healthy adult mouse pancreas (Irving-Rodgers et al., 2008). Interestingly, a strong staining of perlecan was observed around the islet in prediabetic mice pancreas, but was absent in the diabetic murine pancreas (Irving-Rodgers et al., 2008). This suggests that the absence of perlecan and/or its GAG chains may play a role in the loss of function of the islet cells in diabetes. It is further speculated that perlecan may act as a protective barrier for the islets in the inflamed pancreas, as there is usually an accumulation of insulitis mononuclear cells around the boundary of the islets during the non-destructive phase of type II diabetes in the NOD mouse model (Irving-Rodgers et al., 2008; Wang et al., 2005a).

2.2.2.1.2 Syndecan

Syndecan is a cell surface, transmembrane HSPG that usually carries HS chains and sometimes additional CS chains (Bernfield et al., 1999). There are 4 mammalian

syndecans known to date and they modulate the interaction of cell surface receptors with ligands such as growth factors and other ECM components (Bernfield and Sanderson, 1990). Syndecan's HS chains have varied interactions with different types of collagen and exhibits the highest affinity to collagen V, while collagens I, III, IV and VI all interacted with intermediate affinities (Antonio et al., 1994). Similarly, syndecans can bind to fibronectin's heparin-binding domain and localise into focal adhesion contacts to participate in downstream intracellular signaling (Lee et al., 1998; Tumova et al., 2000).

Syndecans are able to promote the recruitment of leukocytes by creating a chemokine gradient at the endothelium surface through HS interactions with growth factors and chemokines (Salek-Ardakani et al., 2000). This chemokine gradient has the ability to regulate the activation of the cell surface integrins (Hoogewerf et al., 1997) and the permeabilisation of the vascular endothelium in preparation for leukocyte extravasation (Miller et al., 1998; Wrenshall et al., 1999). In addition to this, syndecan's HS and CS chains can also inhibit leukocyte binding to endothelial cells by binding to E-selectins and collagen I (Gotte, 2003; Luo and Shoichet, 2004). The binding of heparin-binding proteins to syndecan further helps to protect endothelial cells from apoptosis (Olofsson et al., 1999). Furthermore, syndecan has the abilty to modulate the inflammation pathway, as well as promote wound healing via the degradation of HS that consequently enhances the bioavailability of FGF-2, a growth factor critical for tissue repair (Kato et al., 1998).

The function of syndecan on the islet cell surface is not clear. Syndecan has been co-localised with thrombospondin which has been shown to stain strongly in developing

murine pancreatic islets (Corless et al., 1992). The mRNA of syndecan-2, -3 and -4 has previously been detected in isolated murine islets (Takahashi et al., 2009). Studies have shown that the binding of syndecan-1 to laminin-322 (a highly controversial finding that is yet to be confirmed, the only ECM protein recently found to be "produced" by endocrine cells (Armanet et al., 2009)) regulates cell adhesion and migration by suppressing signalling via the β4 integrin in immortalised and tumorigenic human cell lines (Ogawa et al., 2007). Similarly, it was found that syndecan-1 supports α2β1 integrin adhesion to collagen in chinese hamster ovary cells and enhances the downstream transcription pathway of metalloproteinase-1 (Vuoriluoto et al., 2008). Interestingly, collagens I, IV, V and particularly VI are major components of the islet-exocrine and the intra-islet microvascular interface (Hughes et al., 2006). Therefore, considering the ECM-binding properties of syndecans in inhibiting leukocyte extravasation and in CHO cell adhesion, it is speculated that cell surface syndecan may function to help islet cells bind to collagen and laminin.

2.2.2.1.3 Glypican

Glypicans are cell surface HSPGs that are attached to the cell membrane via a glycosyl phosphatidyl inositol anchor in the outer leaflet of the lipid bilayer (Fransson et al., 2004). Glypican has the ability to bind to the heparin-binding domain of fibronectin via its HS chains (Tumova et al., 2000). There are six isoforms of mammalian glypican known and they are expressed predominantly during development. Glypican plays a potential role in the regulation of growth factors during morphogenesis as its expression fluctuates in a development stage- and

tissue-specific manner (Filmus, 2001). Specifically, glypican-3 may be a negative regulator of cell proliferation as its mutation results in an overgrowth and dysmorphic syndrome (Chiao et al., 2002). Furthermore, glypican-3 has been shown to induce apoptosis in a cell-specific manner (Gonzalez et al., 1998). It is therefore not surprising that the abnormal expression of glypican-1 and glypican-3 have both been associated with the development of cancer. Different types of cancers influence the expression of glypican differently. Glypican-1 is essential for mitogenic signaling of growth factors in pancreatic cancer cells, where normal adult pancreas exhibit low levels of glypican-1 and pancreatic carcinoma cells demonstrate a significant upregulation (Kleeff et al., 1998; Whipple et al., 2008). However, in ovarian cancer, glypican-3 is downregulated (Buchanan et al., 2010), and in hepatocellular carcinomas and colorectal tumours, it is upregulated (Wang et al., 2010; Yuan et al., 2008).

The mRNA of glypican-1 and -4 have both been detected in isolated murine islet cells (Takahashi et al., 2009). In another islet genetic study, the expression of glypican-1, -2, -3 and -5 appeared to be downregulated after pancreatic differentiation (Zertal-Zidani et al., 2007). This suggests that glypican may also play a role in directing the morphogenesis of islets during pancreatic development.

2.2.2.1.4 Betaglycan

Betaglycan is a transmembrane HS and CS proteoglycan that functions as a co-receptor for the growth factor TGF-β (López-Casillas et al., 1991). This HSPG is unique in that it binds TGF-β via its protein core and not its HS and CS chains (Andres et al., 1991). It attenuates the affinity of TGF-β for two high-affinity kinase

receptors, thus upregulating the TGF-β signalling pathway (Eickelberg et al., 2002). Betaglycan also exists in a soluble form in serum and the ECM, which can act as an antagonist for TGF-β and provide a negative feedback loop for ECM and TGF-β expression (Juárez et al., 2007; Velasco-Loyden et al., 2004). In addition to its role in TGF-β signalling, betaglycan can function to re-organise the cytoskeleton and inhibit cell migration (Mythreye and Blobe, 2009).

Betaglycans have not been studied in islets. However, a loss of betaglycan expression has been observed in pancreatic cancer (Mythreye and Blobe, 2009; Venkatasubbarao et al., 2000). Interestingly, TGF-β is essential for islet morphogenesis and endocrine cell development, particularly the insulin-containing β-cells (Miralles et al., 1999; Sanvito et al., 1994), while overexpression of TGF-β in the mouse also demonstrated a protective effect against the onset of insulin dependent diabetes mellitus (Grewal et al., 2002).

Betaglycans are co-receptors of several growth factors and can act as anatagonists to other growth factor signalling. One such example is its ability to bind inhibin and facilitate the antagonism of activin, thus potentially contributing to the regulation of islet development and functional maturation (Lewis et al., 2000; Yamaoka et al., 1998). In a similar manner, betaglycan is able to block BMP signalling through inhibin blockade. In light of the fact that BMP and Activin play major roles in promoting the differentiation of *Pdx1*$^{+}$ cells from human embryonic stem cells (Xu et al., 2011), betaglycan may be an important co-receptor for facilitating this signalling pathway in the developing pancreas.

2.2.2.1.5 Agrin

Even though agrin contains both CS and HS chains, it is part of the heparan sulfate proteoglycan family and is crucial for post-synaptic differentiation at the neuromuscular junction (Bezakova and Ruegg, 2003). In agrin knockout mice, the embryos develop normally but with severe malformations of the synapse and die *in utero* or are stillborn (Kröger and Schröder, 2002). Very little is known about agrin in the context of the pancreas. Nevertheless, agrin mRNA has been detected in murine islets (Takahashi et al., 2009).

2.2.2.2 Chondroitin sulfate proteoglycans

Chondroitin sulfate proteoglycans (CSPGs) consist of a protein core glycosylated with chains of alternating sugars, N-acetylgalactosamine and glucuronic acid (Iozzo, 2000). CSPGs are major components of cartilage and are known to regulate neuronal differentiation and development in the central nervous system (Gu et al., 2009). Immunostaining for general basement membrane CSPGs in the rat pancreas showed localisation to the basement membrane surrounding the islet as well as the blood vessels within the islet, but not the islet itself (McCarthy and Couchman, 1990). However, the exact role of CSPGs on islet function is not clear and very few have been studied in the pancreas.

2.2.2.2.1 Versican

Versican is a CSPG with four isoforms, (Naso et al., 1994) and consists of three domains that can interact with hyaluronan, selectins, CD44, integrins and chemokines (Wu et al., 2005b). Even though the versican protein core does not contain any RGD sequences, it is able to bind integrin β1 and increase focal

adhesion and reduce oxidative stress-induced apoptosis (Wu et al., 2002; Wu et al., 2005a). Versican can also bind to ECM proteins fibulins, fibrillin, and collagen I (Wu et al., 2005b), and is able to reduce cell-binding to fibronectin by sequestering fibronectin's RGD domains (Sakko et al., 2003).

In the adult human pancreas, versican was immunolocalized to the connective tissues surrounding the exocrine acini, ducts and blood vessels (Bode-Lesniewska et al., 1996). However, no labeling was observed within the islets (Bode-Lesniewska et al., 1996). Interestingly, versican is upregulated in pancreatic carcinoma (Skandalis et al., 2006) and are released by pancreatic cancer cells *in vitro* (Mauri et al., 2005).

2.3 In vitro simulations of matrix components and effects on β-cells

Pancreatic β-cells have very stringent requirements of their surrounding matrix for the maintenance of function and differentiation (Green et al., 2010b; Thivolet et al., 1985). The matrix presented to these cells must therefore provide the correct structural and soluble cues to elicit a functional cellular response and may be mediated by the incorporation of biomolecular recognition components into the scaffold similar to that of native cell matrix. It is therefore of great interest to render scaffolds biomimetic by specific surface modifications rather than non-specific adsorption of matrix components. The biomimetic material must have an informational function that potentially mimics the many roles native matrix components play in tissues and organs. In this way, hormonal expression may be directed by interactions with the scaffold that can also be manipulated by altering

certain design parameters. The matricellular components found in native matrix are good candidates for these informational parameters. Though some matrix constituents may perform more than one function, matricellular components are those that do not contribute directly to the structural aspects of the matrix, but serve to modulate cell-matrix interactions as well as cell function (Bornstein and Sage, 2002). The chemical processes required to incorporate has the potential to reduce the biological activity of these matricellular components. Nevertheless, preservation of bioactivity in biomimetic scaffolds can and has been achieved (Green et al., 2010a; Nilasaroya et al., 2008). There are several approaches for rendering a scaffold biomimetic, and in doing so, maintaining and directing β-cell function. These include the use of extracted biological matrix, whole chains of matrix proteins, short bioactive peptide fragments, glycoasaminoglycans and cell-modulating factors to simulate the natural environment of β-cells.

2.3.1 Use of extracted extracellular matrix

The importance of matrix on pancreatic islet cell differentiation, attachment and proliferation was first realised in the early 80's (Montesano et al., 1983; Thivolet et al., 1985). Since then, there have been many attempts to present isolated islets with biological matrix in order to prolong their functional viability pre- and post-transplantation.

Initial studies on enhancing growth of pancreatic islet cells in culture began with the use of extracellular matrices derived from endothelial cell cultures. Bovine corneal and human umbilical cord vein endothelial cells were previously used to produce a layer of matrix onto which islet cells were seeded (Hayek et al., 1989; Hulinsky et

al., 1995b; Kaiser et al., 1988; Thivolet et al., 1985). The endothelial-derived matrix was able to enhance islet cell attachment, proliferation, DNA synthesis and increase mitotic index (Hayek et al., 1989; Thivolet et al., 1985). A more appropriate insulin response to glucose starvation and stimulation was also observed when compared to suspended islets (Hulinsky et al., 1995b). In one study, the islet cell responsiveness to glucose, glucagon and somatostatin was retained for 2-4 weeks in culture (Kaiser et al., 1988). However, the majority of these studies were not performed for more than nine days, with the one exception, and all studies observed the islets to form monolayers when exposed to the *in vitro* endothelial-derived matrix.

The use of ECM has also demonstrated promise in the protection of β-cells from apoptosis. ECM produced by the rat bladder carcinoma cell line 804G was shown to reduce serum deprivation-induced and IL-1β-induced apoptosis in isolated β-cells when compared to poly-L-lysine (Hammar et al., 2004). The 804G ECM was able to facilitate adhesion and spreading of isolated rat β-cells in a glucose-dependent manner via the α6β1 integrin (Bosco et al., 2000).

Currently, Matrigel® is the most widely used matrix for the culturing of isolated islets, pre-transplantation (Nolan, 2009). It is extracted from the Englebreth-Holm-Swarm (EHS) carcinoma that has been propagated in mice for over thirty years (Swarm, 1963) and is a crude source of laminin, collagen IV, perlecan, entactin as well as a plethora of growth factors (Hughes et al., 2010; Vukicevic et al., 1992). Primary cultures of rat and porcine islets on Matrigel® all demonstrated a trophic effect on maintaining normal β-cell function (Nagata et al., 2001; Oberg-Welsh, 2001; Perfetti et al., 1996) as well as islet cluster-like morphology (Hayek et al.,

1989). The longest study to date demonstrated the ability of Matrigel® to maintain β-cell differentiation and insulin-secretion for up to six weeks (Perfetti et al., 1996). Matrigel® have also been shown to promote the differentiation and formation of islet-like clusters from adult ductal epithelial cells (Bonner-Weir et al., 2000; Gao et al., 2003), fetal porcine islet-like cells (Oberg-Welsh, 2001) and adult human pancreatic progenitor cells (Lechner et al., 2005). However, due to the fact that Matrigel® is a crude extract with the presence of growth factors, the role of specific ECM components on β-cell function remains undefined. Interestingly, a comparison of collagens and Matrigel® demonstrated collagen to be sufficient for maintaining glucose-responsiveness but was not as effective as Matrigel® in maintaining cellular viability (Nagata et al., 2001).

2.3.2 Use of basement membrane proteins

One of the major difficulties with the engineering of tissue scaffolds is its ability to provide sites for cell adhesion. Cell attachment to a scaffold is the initial step required to facilitate cell growth, differentiation, viability and spreading. Biomaterial surface modification with biomolecular recognition components initially involved the use of whole matrix proteins such as collagen, fibrin and laminin to increase their cell adhesiveness and general bioactivity. Some studies using collagen gels or biomaterials coated with similar proteins have shown promise in promoting endocrine function.

Early work on matrix proteins demonstrated that collagen I gels were able to reorganise neonatal rat islet cell monolayers into islet-like clusters (Montesano et al., 1983). Subsequently, it was discovered that gels composed of collagen I and/or IV

were also able to maintain glucose responsiveness of isolated islets *in vitro* (Nagata et al., 2001). This has proved to be promising as mice transplanted with islets seeded onto scaffolds containing non-specifically adsorbed collagen IV achieved euglycemia fastest and had a glucose challenge response most similar to non-diabetic mice even 10 months post-transplantation. In comparison, mice that had received scaffolds that had been coated with fibronectin, laminin and serum proteins did not show a similar outcome (Salvay et al., 2008). Similarly, Pinkse and colleagues found that collagen IV and laminin were the most potent in promoting rat islet survival in a 24 hour study (Pinkse et al., 2006). Furthermore, in a study of human islets embedded in collagen gels, cell viability was maintained for up to 8 weeks and glucose-responsive insulin secretion for 17 days (Lucas-clerc et al., 1993).

Fibronectin has been associated with strong cell adhesion and spreading but its influence on insulin production varies between species and commercial preparations are made from plasma fibronectin. Porcine islet insulin production was not improved by fibronectin whereas human islet structural integrity and insulin content distribution were maintained (Daoud et al., 2009). Conversely, the addition of soluble fibronectin to isolated islets has been shown to preserve their integrin expression and the maintenance of β-cell mass and function (Wang and Rosenberg, 1999).

Fibrin gels have also been used to maintain the 3D configuration of human islets and enhance the effects of added growth factors hepatocyte growth factor, fibroblast growth factor and nicotinamide (Beattie et al., 2002). In a 6-day study, insulin

content of the islets was increased and proliferation was observed only in the presence of both fibrin and growth factors.

It is therefore evident that use of singular matrix proteins indeed enhances islet viability and function, but not for a long enough timeframe to make islet transplantation a long-term solution. The use of matrix proteins is also limited by their potential for eliciting an immunological response as they are isolated from different xenogenic sources and also may potentiate cross-source infection (Kumar, 2006). In addition, the exposure of human cells to non-human ECM may cause undesired effects. It was recently found that human embryonic stem cells exposed to animal-derived products expressed Neu5Gc, an immunogenic non-human sialic acid, thus rendering them unsuitable for clinical transplantation into humans (Martin et al., 2005).

Another serious limitation is that the bioactivity of extracted matrix proteins is often compromised, as the extraction processes used can strip major ECM molecules of crucial ligands, or denature molecules. Adsorption of extracted ECM proteins to synthetic surfaces may also change their orientation and conformation (Kumar, 2006). These long protein chains tend to fold randomly upon adsorption such that their bioactivity becomes greatly reduced or sterically unavailable. In addition to this, the low stability of matrix proteins and their susceptibility to proteolytic degradation can also reduce the lifetime of the scaffold (Kumar, 2006). Furthermore, the mechanical properties of matrix gels have also been problematic and thus more recent interest has been focused on combining natural ECM with synthetic scaffold materials.

Synthetic scaffolds blended or functionalised with basement membrane proteins have recently demonstrated potential in the enhancement of β-cell function. Insulinoma cells encapsulated with polyethylene glycol functionalised with collagen IV and laminin induced a two-fold and four-fold increase in insulin secretion, respectively (Weber and Anseth, 2008). In addition, a combination of collagen IV and laminin resulted in higher β-cell insulin secretion than when the ECM proteins were used individually (Weber et al., 2008).

2.3.3 Immobilisation of oligopeptides

Since the discovery that matrix protein-derived peptide sequence motifs also had the potential to modulate cellular behaviour and are easier to incorporate into biomaterials than full matrix protein sequences, interest in these short signalling domains have increased significantly. In 1984, Pierschbacher and Ruoslahti identified the RGD tripeptide motif as the minimal peptide sequence required for cell adhesion in fibronectin (Pierschbacher and Rouslahti, 1984). Since then, RGD sites have been identified in many other matrix components including vitronectin, fibrinogen, collagen, laminin and tenascin (Horton, 1999). Approximately half of the 24 known integrins are able to bind matrix components in an RGD-dependent manner. Additionally, other cell-adhesive motifs such as YIGSR (laminin B1-derived), REDV (fibronectin-derived) and IKVAV (laminin-derived) have also been

identified (Shin et al., 2003). As these sequence motifs are conserved in multiple matrix proteins, a broad range of cell types can respond to the same sequence.

RGD peptides have been used to not only enhance islet cell adhesion, but also prolong cell survival. Pinkse and colleagues demonstrated that the RGD peptide on its own had the ability to mimic matrix ligation to rat islets and in doing so, prevent anoikis of the cells (Pinkse et al., 2006). Similarly, Weber and colleagues showed the influence of various short oligopeptides over β-cell survival and insulin release (Weber et al., 2007). A 10-day study demonstrated laminin-derived sequences IKLLI and IKVAV to promote insulinoma viability and insulin secretion. The importance of synergy between various matrix components was observed when viability and insulin secretion were enhanced only in the presence of both oligopeptides PDSGR and YIGSR.

2.3.4 Immobilisation of proteoglycans and glycosaminoglycans

GAGs and proteoglycans are important regulators of the cellular response and cell phenotype. Consequently, there is a growing interest in the immobilisation of GAGs into biomimetic scaffolds. GAGs are often incorporated into scaffolds to bind, store and control release of signalling molecules such as growth factors. It is also used to provide local concentration gradients within the scaffold and influence the diffusion of these molecules to their receptors. GAGs may be a better scaffold component than whole proteins as they are intrinsically more stable and have lower immunogenicity compared to ECM proteins (Uygun et al., 2009). The bioactivity of GAGs has been used in a number of tissue engineering applications that involve angiogenesis (Sakiyama-Elbert and Hubbell, 2000; Taylor et al., 2004), blood compatibility

(Murugesan et al., 2008), sustained release of growth factors (Ferdous and Grande-Allen, 2007; Steffens et al., 2004) and hematopoietic and mesenchymal stem cell differentiation (Buruzula et al., 2004; Cho et al., 2008; Javazon et al., 2001; Madihally et al., 1999; Uygun et al., 2009).

Despite the functional diversity of proteoglycans and GAGs, there are very few studies available that have used the immobilization of GAGs in a scaffold to enhance islet endocrine function. Nevertheless, GAGs such as heparin have been incorporated into synthetic scaffolds to improve their growth factor-binding ability. Heparin-binding peptide amphiphile nanofibres in fibrous poly(L-lactic acid) matrices significantly increased the blood vessel density with the presence of vascular endothelial growth factor (VEGF) and basic fibroblast growth factor (FGF-2) (Stendahl et al., 2008). Similarly, in an islet re-vascularisation study, Cabric and colleagues anchored VEGF to surface heparinized islets in order to promote the attachment and proliferation of human dermal microvascular endothelial cells on the islet's outer surfaces (Cabric et al., 2010). The coated heparin improved the adhesion of the endothelial cells onto the islet surfaces, though insulin release remained unaffected.

Hyaluronate is another GAG that has been used to enhance islet viability and function. Velten and colleagues impregnated cuprophane hollow fibres with alginate or hyaluronate and observed higher insulin secretion and cell viability in the presence of hyaluronate when compared to alginate (Velten et al., 1999).

2.3.5 Immobilisation of growth factors and other small molecules

The native ECM acts as a reservoir that protects cytokines, chemokines and growth factors from degradation and allows them to be presented to cell receptors more efficiently. Thus studies of biomimetic scaffolds also aim to recapitulate growth factor presentation and their controlled release to promote a functional cellular response. The covalent immobilisation of cytokines and growth factors to surfaces has been shown to increase their stability as well as bioactivity. This was demonstrated in a study where glucagon-like peptide 1 (GLP-1) grafted onto poly(N-vinyl-2-pyrroridone-co-acrylic acid) appeared to improve the insulinotropic activity of encapsulated islets when compared to GLP-1-zinc crystal co-encapsulated and control islets (Kim et al., 2005). More recently, the immobilisation of glucagon-like peptide-1 (GLP-1) within poly(ethylene glycol) for the encapsulation of isolated islets maintained cell viability and insulin secretion one week after isolation (Lin and Anseth, 2009).

Inadequate vascularisation of tissue scaffolds seeded with cells is a constant problem in tissue engineering as it leads to apoptotic death due to hypoxia and lack of nutrients. Thus the incorporation of growth factors has also been a strategy used to induce vascularisation and re-establish capillary networks (Linn et al., 2003). The co-encapsulation of islets within a collagen matrix immobilised with VEGF resulted in an increase in vasculature to the transplant site, which consequently improved insulin secretion and glycemic control in the diabetic mice (Sigrist et al., 2003). In addition to this, the Stendahl study previously mentioned, not only demonstrated increased vascularisation when VEGF and FGF-2 were incorporated into a poly(L-lactic acid) hydrogel, but also showed that normoglycemia was achieved at a higher rate than those without growth factors or with growth factors separately (Stendahl et

al., 2008). Similarly, rat islets encapsulated in chitosan and PLGA scaffolds impregnated with VEGF presented with higher insulin content compared to scaffolds without VEGF, two weeks post-transplantation (Linn et al., 2003).

2.4 Enhancing matrix deposition by macromolecular crowding

The importance of ECM, particularly those produced by the adjacent endothelial cells, in the maintenance and function of pancreatic islets is evident. If endothelial cells can be harnessed to produce ECM containing the essential components required for facilitating β-cell health and function, then the endothelial cell ECM can be incorporated into bioscaffolds to improve the success rates of islet transplantations. However, the majority of ECM components produced under normal *in vitro* culture conditions are secreted into the culture medium and removed with each media change before it can be deposited. This was particularly evident in fibroblasts, where biochemical analyses revealed that most of the collagen present in the culture was in the form of unprocessed procollagen (Lareu et al., 2007a). Unlike collagen, procollagen is soluble and was mostly found in the culture medium only. The reason for this occurrence was hypothesised to be due to the lack of a crowded environment in an *in vitro* cell culture system (Phillips et al., 2008). The animal serum proteins normally used to supplement cell culture media typically comprises only 1-10 g/L, which is considerably lower than that of interstitial fluids (30-70 g/L), blood plasma (80 g/L) and the cell interior (200-350 g/L) (Aukland et al., 1984; Bates et al., 1993; Ellis, 2001; Wadsworth and Oliveiro, 1953).

The concept of macromolecular crowding describes the ability of macromolecules to induce entropic segregation of other molecules via the excluded volume effect (Madden and Herzfeld, 1993). It has been shown that even as little as 1 volume percent of macromolecules added to the *in vitro* environment can sufficiently crowd the functional proteins of interest to enhance biochemical reactions such as enzymatic, binding and folding kinetics to that of *in vivo* levels (Drenckhahn and Pollard, 1986; Minton, 1997).

Neutral (670 kD) and negatively (500, 10 kD) charged dextran sulfate, dextran T-40, Ficoll 400 kD and 70 kD, polyethylene glycol (PEG) polysodium-4-styrene sulfonate (PSS) and polyvinyl pyrrolidone (PVP) have all been used to crowd *in vitro* culture conditions in order to enhance ECM deposition (Bateman et al., 1986; Chen et al., 2009; Lareu et al., 2007a; Lareu et al., 2007b; Lareu et al., 2007c; Zeiger et al., 2012). Cell types investigated under macromolecular crowding have thus far included human embryonic lung and adult hypertrophic scar fibroblasts and human bone marrow-derived mesenchymal stem cells (Chen et al., 2009; Lareu et al., 2007a; Zeiger et al., 2012). Negatively charged dextran sulfate and a cocktail of Ficoll 70 and 400 were both found to enhance procollagen conversion to insoluble collagen by procollagen-C-proteinase and its enhancer, PCOLCE1 (Chen et al., 2009; Hojima et al., 1994; Lareu et al., 2007a; Lareu et al., 2007b; Lareu et al., 2007c). Consequently, the deposition of collagen can be enhanced by >6-fold compared to normal uncrowded culture conditions (Lareu et al., 2007a). The use of macromolecular crowders also influences the spatial orientation and pattern of the ECM deposited. Collagen I and fibronectin matrices produced under Ficoll crowding by fibroblasts appeared reticular, whereas dextran sulfate produced a course granular

pattern (Lareu et al., 2007c). Similarly, Ficoll crowded mesenchymal stem cells produced ECM fibers (fibronectin and collagen IV) that were more aligned than uncrowded cells and in doing so, increased the actin cytoskeleton alignment of the mesenchymal stem cells seeded onto this ECM (Zeiger et al., 2012).

2.5 Conclusion

There is currently a significant lack of knowledge about the role of the ECM in the functioning of the pancreatic endocrine system. Without an understanding of the natural matrix environment of the endocrine cells, a sustainable bioartifical pancreas will be difficult to develop. Furthermore, understanding of islet matrix components may also provide insight into the development of pancreatic diseases. Once this knowledge is provided and the optimal islet ECM can be produced in clinically relevant quantities, synthetic scaffold systems can be combined with the appropriate biological matrix components to improve islet viability and enhance endocrine function post-transplantation. Current scaffold systems do not provide islet longevity and it is through the synergistic workings of biological signals with the desirable and tailorable mechanical properties of synthetic matrices that long-term health and differentiation may be achieved. This will be followed by the potential for differentiating stem cells into islet cell types by the incorporation of growth factors and effector molecules into these biomimetic systems to promote appropriate angiogenesis and bioartificial tissue development.

The following chapters describe an in-depth characterisation of healthy adult rodent islet ECM, which was then used as a basis for comparison with the *in vitro*-produced endothelial ECM. The technique of macromolecular crowding was then applied to

enhance ECM production and deposition by the cell lines and the composition of the ECM produced was then studied. Finally, the suitability of the *in vitro*-produced ECM for supporting and extending islet health and function was then investigated.

Chapter 3

3 Characterisation of extracellular matrix in the pancreatic islet

This chapter was in part published in the Journal of Histochemistry and Cell Biology and permission was granted by the publishers for use in this thesis. The concepts and writing of this paper was largely under the control of Cheng JYC (90% input). The other authors contributed to the analysis and interpretation of the literature and assisted in the development of the arguments.

Paper citation:

Cheng JYC, Whitelock J, Poole-Warren LA. (2012) Syndecan-4 is associated with beta-cells in the pancreas and the MIN6 beta-cell line. *Journal of Histochemistry and Cell Biology*. DOI: 10.1007/s00418-012-1004-6 (in press)

3.1 Introduction

The current focus of tissue engineering for pancreatic islet transplantation has been to provide biological or biosynthetic scaffolds to mimic the extracellular matrix (ECM) of islets in order to prolong their survival and function after isolation. There is indeed considerable evidence supporting the significant influence of cell-ECM interactions on islet survival and function (Stendahl et al., 2009). However, much of the research to date has focussed on BM proteins in the islet, while proteoglycans and glycosaminoglycans have been largely unexplored.

Studies of islet BMs have generated some confusion due to reports of species differences in islet ECM composition and morphology. van Deijnen et al reported a collagen IV and laminin-containing peri-islet capsule that was continuous in canine islets, fragmentary in porcine islets and discontinuous in the rat and human islets (Deijnen et al., 1994; van Deijnen et al., 1992a). Conversely, another study reported that peri-islet BM was absent in porcine islets, while human, canine and hamster islets have a continuous BM that forms a barrier between the exocrine and endocrine cells (Otonkoski et al., 2008; Wang et al., 1999). Furthermore, major differences of BM structure between rodent and human islets have also been observed. Human islets were found to possess a double-layered BM organisation with each layer containing different laminin types, whereas only one endothelial BM was localised in the murine islet (Otonkoski et al., 2008; Virtanen et al., 2008). Therefore, unlike the mouse, human β-cells may not be in direct contact with the endothelial BM.

Added to this divergence of findings is the uncertainty as to which cell types, endocrine, exocrine or the intra- and peri-islet endothelial cells, in the islet produce the BM. There have been several reports of a peri- and intra-islet BM containing various types of collagens, laminins, fibronectin, vitronectin, nidogen and perlecan (Geutskens et al., 2004; Irving-Rodgers et al., 2008; Meyer et al., 1998a; Meyer et al., 1998b; Parnaud et al., 2006). These studies have all suggested that the main depositors of ECM in the pancreatic islets to be from the intra-islet endothelium. Furthermore, laminin chains α4, α5 and collagen IV have been co-localised with the endothelial cell marker, PECAM1, and through the comparison of laminin (α4, α5) and collagen IV (α1, α2) gene expression in islet endothelial and β-cells, it was even proposed that β-cells are unable to form BMs (Nikolova et al., 2006). Controversially, one study to date, demonstrated the co-localisation of intracellular laminin-332 with insulin- and glucagon-positive cells in human islets, though extracellular laminin-332 could only be detected by immunoblotting the islet conditioned medium (Armanet et al., 2009).

Recently, immunohistochemical and chemical staining have shown an abundant presence of heparan sulfate (HS) within the whole islet region of the murine pancreas (Takahashi et al., 2009; Ziolkowski et al., 2012) and a role in the survival, differentiation and function of islets has been suggested (Noguchi et al., 2007; Takahashi et al., 2009; Ueda et al., 2008). The HS eptitopes that have thus far been identified within the islet include the 3G10 (heparitinase-digested stub) and HepSS-1 (*O*-sulfated *N*-acetylated domains) epitopes (Kure and Yoshie, 1986; Takahashi et al., 2009; Ziolkowski et al., 2012). In the Ziolkowski study, it was demonstrated that β-cells tended to lose 50% of their HS content after isolation, which led to a 2-fold

increase in β-cell death (Ziolkowski et al., 2012). Interestingly, this research also suggested that most of the HS present in the islet resided intracellularly within the insulin-positive cells and that inhibition of HS degradation prevented destructive autoimmunity and the progression of type 1 diabetes. It was therefore hypothesised that loss of HS and perhaps degradation of its associated proteoglycan is the key to the decline of islet function post-isolation.

Despite the importance of HS in islet homeostasis, their associated proteoglycans are yet to be confirmed. Perlecan has been immunolocalised in the BMs of islets (Irving-Rodgers et al., 2008) and has been suggested to play a role in obstructing mononuclear cell migration during destructive insulitis (Parish, 2006). However, the staining pattern of perlecan is vastly different to that of HS and the proteoglycans to which this extraordinary amount of HS is attached remain uncharacterised (Irving-Rodgers et al., 2008; Takahashi et al., 2009; Ziolkowski et al., 2012). Nevertheless, gene expression of the HS-associated proteoglycans syndecan, glypican and type XVIII collagen, have previously been detected in murine islets (Takahashi et al., 2009; Zertal-Zidani et al., 2007). Cell surface HS proteoglycans include syndecans (4 isoforms), glypicans (6 isoforms) and betaglycan, with a repertoire of roles depending on the ligands to which they bind. In many cell types, syndecans can promote the recruitment of leukocytes, mediate wound healing and also have roles in cell-ECM interactions and ECM assembly (Xian et al., 2010). The mRNA of syndecan-2, -3, -4 and glypican-1 and -4 was detected in healthy adult mouse islets (Takahashi et al., 2009). While in another study, semi-quantitated expression of glypican-1, -2, -3 and -5 appeared to be downregulated after pancreatic differentiation, and syndecan-1 to -4 expression remained constant during

development (Zertal-Zidani et al., 2007). However, protein expression of these proteoglycans has not yet been confirmed.

The major objective of this research was to identify and study the distribution of BM proteins and proteoglycans within the pancreatic islet. Specifically, the aims were to evaluate inter-species differences in ECM morphology, distribution and composition by examining mouse, rat and rabbit pancreata and to compare ECM associated with the MIN6 insulinoma cell line in order to assess its suitability as a model for future studies in β-cell-matrix responses.

3.2 Materials and Methods

3.2.1 Equipment and reagents for immunohistochemistry

Primary antibodies were either commercially purchased or generously donated from collaborating laboratories. Refer to Table 3.1 for the sources and dilutions of primary and secondary antibodies. Fluorescently labelled secondaries were heavy and light chain-recognising AlexaFluor IgG from Molecular Probes through Invitrogen. The NovaRed® chromogen substrate, haemotoxylin and Imm-Edge® wax pen were from Vector Laboratories, Inc. UK. The antigen retrieval buffer sodium citrate was from Sigma Aldrich USA, while the decloaking chamber (DC-2002) and the TissueTek trays were from Applied Medical.

3.2.2 Cell culture

The MIN6 mouse insulinoma cell line was a kind gift from Dr Jenny Gunton (The Garvan Institute, Sydney) and permission granted for its use was given by Dr Junichi Miyazaki (Kumamoto University Medical School, Japan). MIN6 cells were cultured in high glucose DMEM (Gibco) containing 10% heat inactivated foetal bovine serum, 20mM HEPES, 20 mM L-glut, β-mercaptoethanol and 3.7g/L sodium bicarbonate and pH adjusted to 7.4 (Miyazaki et al., 1990).

3.2.3 Pancreas samples

Adult Wister rat pancreata were donated by Professor Lynne Bilston from the Prince of Wales Medical Research Institute, harvested under ACEC approval 07/136B. Adult New Zealand White rabbit pancreata were donated by Dr Socrates Dokos and

Professor Nigel Lovell from the Graduate School of Biomedical Engineering, University of New South Wales, sacrificed under ACEC approval 08/03B. Adult C57BL/6 mouse pancreata were donated by Dr Jenny Gunton from the Garvan Research Institute under AEC 08.12 and 09.13.

3.2.4 Pancreas processing

Rabbit, rat and mouse pancreata were fixed for 24 to 48 hrs at room temperature in 10% neutral buffered formalin (Confix "Clear" pH 7.0). Formalin-fixed specimens were dehydrated (2× 1h 70% ethanol, 2× 1h 80% ethanol, 2× 1h 95% ethanol, 3× 1h 100% ethanol, 3× 1h xylene) embedded in paraffin wax (2× 1.5h at 58°C), embedded into paraffin blocks then sectioned (5-10 µm) and mounted on positively-charged silane slides.

Snap-frozen pancreata were embedded in OCT compound (Thermo Scientific), sectioned (5-10 µm) and mounted on Knittel-Glaser Starfrost adhesive glass slides (Surgipath Medical).

3.2.5 Haematoxylin and eosin staining

Sections were stained in Harris haematoxylin (Surgipath Medical) for 4 minutes, washed in water, differentiated in 1% acid alcohol for 2 seconds and washed again in water. Sections were then placed in Scott's Blueing solution (Fronine) for 20 seconds, washed and then counterstained in Eosin (Surgipath Medical) for 3 minutes and dehydrated, cleared and mounted with Ultramount (Fronine).

3.2.6 Masson's trichrome staining

Formalin-fixed sections were deparaffinized (2× xylene for 5 min) and rehydrated through a graded series of alcohols (2× 100% ethanol for 3 min, 1× 95% ethanol for 3 min, 1× 70% ethanol for 3 min) then incubated in Bouins Solution for 1 h at 57ºC. Sections were placed in Celestine Blue for 5 min, rinsed with tap water, stained with Harris Haematoxylin for 4 min and rinsed again with tap water. Sections were then dipped in Scott's Blue six times, rinsed with tap water, dipped in acid alcohol, rinsed with tap water, dipped in Scott's Bluing solution six times and rinsed with tap water. Slides were then stained with Briebrich Scarlet-Acid Fuchsin for 2 min, rinsed with distilled water, differentiated in 1% phosphomolybdic acid, rinsed with distilled water, placed in Aniline Blue solution, then 1% acetic acid for 1 min, dehydrated, cleared and mounted with Ultramount (Fronine).

3.2.7 Grocott-Gomori methenamine silver staining

Formalin-fixed sections were deparaffinized (2× xylene for 5 min) and rehydrated through a graded series of alcohols (2× 100% ethanol for 3 min, 1× 95% ethanol for 3 min, 1× 70% ethanol for 3 min). Sections were oxidised by 5% (w/v) chromic acid for 1 h then washed under running tap water, rinsed for 1 min with 1% sodium bisulphate, washed for 5 min under running tap water and then washed three times with distilled water. Slides were stained with methenamine-silver for 30 min-2 h at 58ºC, washed six times with distilled water, incubated with 0.1% gold chloride for 30-60 s, rinsed with distilled water, incubated with 2% (w/v) sodium thiosulphate for 2-5 min then washed thoroughly with tap water. Sections were stained with Light

Green SF Green (C.I. 34043) for 30 s, rinsed quickly with absolute alcohol twice, dehydrated and mounted with Ultramount (Fronine).

3.2.8 Immunohistochemical staining

Slides were placed in a 60ºC oven for 3 min and then deparaffinised twice in xylene for 5 min. Slides were then immersed in a series of 3 min ethanol washes (2x in 100% (v/v), 1x in 95% (v/v) and 1x in 70% (v/v) ethanol) followed by a 2 min rinsing in water to re-hydrate the tissue sections. A circle was drawn around the tissue section on each slide with a wax pen to allow different treatments on multiple tissues on the same slide. Antigen epitope retrieval was performed via a decloaking chamber. A tray of slides in either 0.01 M sodium citrate at pH 6 or Tris-EDTA buffer (10 mM Tris, 1 mM EDTA, 0.05% (w/v) Tween 20, pH 9.0) was placed in the decloaking chamber and processed at 121ºC for 3 min. The slides were rinsed in deionized water for a few minutes and blocked with 3% H_2O_2 (v/v) in water for 5 min followed by another water rinse. Some slides were treated with 0.01 U/mL of heparitinase in DPBS at pH 7.2 for 3 h at 37ºC.

Slides were washed three times with TBST (0.05 M Tris, 0.15 M NaCl and 0.05% (w/v) Tween-20 at pH 7.6) for 5 min each. Tissue sections were blocked with 3% (w/v) BSA/TBST for 1 h at room temperature. Primary antibodies (Table 3.1) were diluted in blocking buffer and incubated overnight at 4ºC. Control sections were incubated with isotype control Ig. The slides were left at room temperature for 30 min and washed twice with TBST for 5 min. Slides were incubated with biotinylated secondary antibody (1:500) diluted with blocking buffer for 1 h at room temperature and then washed twice with TBST, followed by a 30 min incubation with

streptavidin-HRP (1:250). The slides were then washed four times with TBST before developing with NovaRED® (Vector) stain and counterstained with haemotoxylin for 30 s-2 min and rinsed with deionized water. Sections were dehydrated with the same ethanol series in reverse order and finally with xylene. Sections were mounted with UltraMount Plus (Thermo Scientific) and covered with glass coverslips.

3.2.9 Immunfluorescence and immunocytochemical staining

Frozen sections were fixed with ice-cold methanol for 10 min and allowed to air dry. Tissue sections were blocked with 3% (w/v) BSA/TBST for 30 min-1 h at room temperature. Primary antibodies (Table 3.1) were diluted in Dulbecco's Phosphate Buffered Saline (DPBS, Sigma) and incubated for 1.5 h at room temperature or overnight at 4ºC. Control sections were incubated with isotype control Ig. Slides were washed three times by immersing in DPBS for 10 min. Sections were incubated with AlexaFluor-conjugated secondaries (Molecular Probes/Invitrogen), diluted 1:400 with DPBS, in the dark at room temperature for 30 min. Slides were washed three times by immersing in DPBS for 10 min. Sections were incubated with 4',6-diamidino-2-phenylindole, dilactate (DAPI, Molecular Probes/Invitrogen), diluted 1:1000 with DPBS, in the dark at room temperature for 10 min. Slides were washed three times by immersing in DPBS for 10 min, mounted with Fluorescence Mounting Medium (DAKO), and then covered with glass coverslips.

Tissue sections and cells were viewed at 20× and 40× magnification with the epifluorescence microscope, Leica DMIL, and/or confocal microscope, Olympus FV1000. Voltage and gain were maintained across samples and controls for each experiment.

Table 3.1 Primary antibodies and fixative/s used for immunohistochemistry

Antigen (clone)	**Host species**	**Code**	**Source**	**Dilution**	**Fixative**
Agrin	Mouse	MAB5204	Millipore	1:50-200	Methanol
Chondroitin sulfate (CS-56)	Mouse	ab11570	Abcam	1:50-200	Formalin
Collagen IV	Rabbit	ab6586	Abcam	1:100	Methanol
Collagen XVIII	Rabbit	ab85661	Abcam	1:50-100	Methanol/Formalin
Fibronectin	Rabbit	A0245	DAKO	1:100	Methanol
Glucagon	Rabbit	ab18461	Abcam	1:50	Formalin
Glypican-1	Rabbit	ab73979	Abcam	1:50-100	Methanol/Formalin
Glypican-1 (4D1)	Mouse	MAB2600	Millipore	1:20-50	Methanol/Formalin
Heparan sulfate (10E4)	Mouse	F58-10E4	Seikagaku	1:100	Formalin
Heparan sulfate (3G10)	Mouse	F69-3G10	Seikagaku	1:200	Formalin
Insulin	Guinea Pig	ab7842	Abcam	1:100	Formalin
Laminin EHS/Laminin-121	Rabbit	ab11575	Abcam	1:100	Methanol
Perlecan (A7L6)	Rat	ab2501	Abcam	1:100	Methanol
Syndecan-1 (B-A38)	Mouse	ab82200	Abcam	1:20-50	Methanol/Formalin
Syndecan-4	Rabbit	ab24511	Abcam	1:30	Methanol/Formalin
von Willebrand Factor	Rabbit	A0082	DAKO	1:100	Methanol

3.2.10 Mouse islet isolation

Pancreatic islets were isolated using the collagenase method from male C57BL/6 mice aged 10–12 weeks, as previously described by Kulkarni et al (Kulkarni et al., 1999).

3.2.11 SDS-PAGE and mass spectrometry

After isolation, islets from 3 mice were pooled and either directly trypsinised for mass spectrometry or the proteins were extracted overnight at 4°C by 5M guanidine-HCl and ethanol precipitated overnight at -20℃. Samples were spun down at 4°C, supernatant discarded, washed with 90% ethanol, spun down, supernatant discarded then allowed to air dry. Protein extracts were resuspended in 1x NuPAGE loading buffer (Sigma), boiled at 95℃ for 10 min and loaded onto on 3-8% NuPAGE Tris-Acetate Pre-Cast gels (Sigma) for 1 h at 160V then stained with Simply Safe Coomassie G250 dye for 30 min. Gels were destained in water for 30 min- 1 h and bands were excised with a scalpel. Excised gel bands of ~1x1 mm were washed with 50 mM NH_4HCO_3 for 20 min, vortexed briefly, spun down and liquid discarded. Gel pieces were then washed in a wash solution of 50% v/v acetonitrile/25 mM NH_4HCO_3 until completely destained of Coomassie. After discarding the wash solution, 100% acetonitrile was added and incubated at room temperature for 5-10 min, spun down and all liquid discarded. Gels were then incubated in 25 mM iodoacetamide at room temperature and in the dark for 20 min. The iodoacetamide solution was discarded, gels washed in 50 mM NH_4HCO_3 for 15 min, spun down and liquid discarded. Gel pieces were shrunk with 100%

acetonitrile, spun down, liquid discarded and placed in a 50°C oven for 20 min. Gels were trypsinised (0.02 μg/mL in 50 mM NH4HCO3, sequencing grade modified trypsin, Promega) overnight at 37℃ then sonicated for 10-15 min. Gel pieces were spun down and supernatant kept at 4℃ for mass spectrometry.

Peptides were separated by the Ultimate 3000 HPLC and autosampler system (Dionex, Amsterdam, the Netherlands) and analysed by LTQ Velos Orbitrap mass spectrometer (Thermo Electron, Bremen, Germany). The database search program Mascot (Version 2.2, Matrix Science) was used for peptide sequence identification. Search parameters included precursor tolerance of 4 p.p.m., product ion tolerances were ±0.4 Da; Met(O) were specified as a variable modification, enzyme specificity was trypsin, one missed cleavage was possible and the NCBI database was used.

3.2.12 Semi-purification of total proteoglycan

After lifting MIN6 cells with 0.02% (w/v) EDTA or islet isolation, cell pellets were lysed with buffer containing 1% Triton X-100, 10 mM Tris (pH 7.6), 150 mM NaCl, 1 mM EDTA and 1x protease inhibitor cocktail (Roche) in DPBS. Cell lysates were shaken for 1h at 4℃ and stored at -80℃ until use.

Cell lysates were diluted by 10x with DPBS and DEAE-Sepharose anion beads (Sigma) at 1/20th of the lysate volume were added and shaken for 1h at 4℃. After quick centrifugation, supernatant was removed and beads were washed twice with DPBS. To elute,1M NaCl pH 7.5 was added and shaken for 1h at 4℃. After quick centrifugation, supernatant was removed and stored at -80℃ for Western blotting.

3.2.13 Western blot analysis

For the immunoblotting of proteoglycans, semi-purified total proteolgycan from MIN6 and mouse islets were thawed on ice and resuspended with1x NuPAGE loading buffer (Sigma). For the immunoblotting of ECM proteins, isolated islets were lysed with 1x NuPAGE loading buffer directly. Samples were boiled at 95℃ for 10 min and loaded onto 4-12% NuPAGE Bis-Tris Pre-Cast Gels (Sigma). Precision Plus Protein All Blue Standards (Bio-Rad) was used as protein ladder. Gels were run in MES buffer (50 mM MES, 50 mM Tris base, 0.1% SDS, 1 mM EDTA, pH 7.3) at 200V for 30 min and transferred onto 0.45 μm PVDF membranes (Millipore) for 1h at 20V, using the Novex Semi-Dry Blotter (Invitrogen) in 2x NuPAGE transfer buffer, containing methanol at 1/10th the final volume.

Membranes were blocked for 1h at room temperature with 5% (w/v) BSA/TBST then incubated with primary antibodies overnight at 4℃. Membranes were washed 3x 10 min with TBST, briefly rinsed with TBS and then incubated with HRP-conjugated secondary antibodies for 1h at room temperature. The membranes were then washed 4x 10 min with TBST, rinsed 2x with TBS, incubated with SuperSignal West Femto Maximum Sensitivity Substrate (Thermo Scientific) and developed on x-ray films in the dark.

3.3 Results

3.3.1 Chemical characterization of pancreatic islet ECM

Chemical stains, Masson's trichrome and methenamine silver, were used to compare the presence and distribution of ECM components in the islet of Langerhans of mouse, rat and rabbit pancreas. Masson's trichrome stained collagen around the acinar cells, in the pancreatic duct and blood vessel walls, but did not show staining within the islet region in all three species (Figure 3.1). Methenamine silver, on the other hand, showed the presence of basement membranes (BM) in pancreatic sections of all three species. The BM capsules surrounding the acinus and the blood vessels were stained black and were observed in the connective tissue associated with the capillaries within and surrounding the islet (Figure 3.2).

In the mouse pancreas, larger islets tended to be completely enclosed by BM, whereas small islets (< 200 μm) tended to have a discontinuous enclosure (Figure 3.2 a-b). In contrast, islets in the rabbit and rat pancreas did not have a BM "capsule" surrounding the entire islet, but had a staining pattern that appeared to follow the course of the interweaving microvasculature (Figure 3.2 c-f).

3.3.2 Immunohistochemical characterisation of pancreatic islet ECM

Immunohistochemical localisation identified the BM components of the mouse islet to contain collagen IV (Figure 3.3A), at least one of the laminin chains of mouse Engelbreth-Holm-Swarm (EHS) tumour (α1, β2, γ1) (Figure 3.3B), fibronectin

(Figure 3.3C) and perlecan (Figure 3.3D). The staining pattern of these components showed a similar organisation to that of the invading microvasculature observed with the methenamine silver staining (Figure 3.2). Furthermore, multiple staining of these four components directly overlapped with that of the endothelial cell marker, von Willebrand Factor (Figure 3.3).

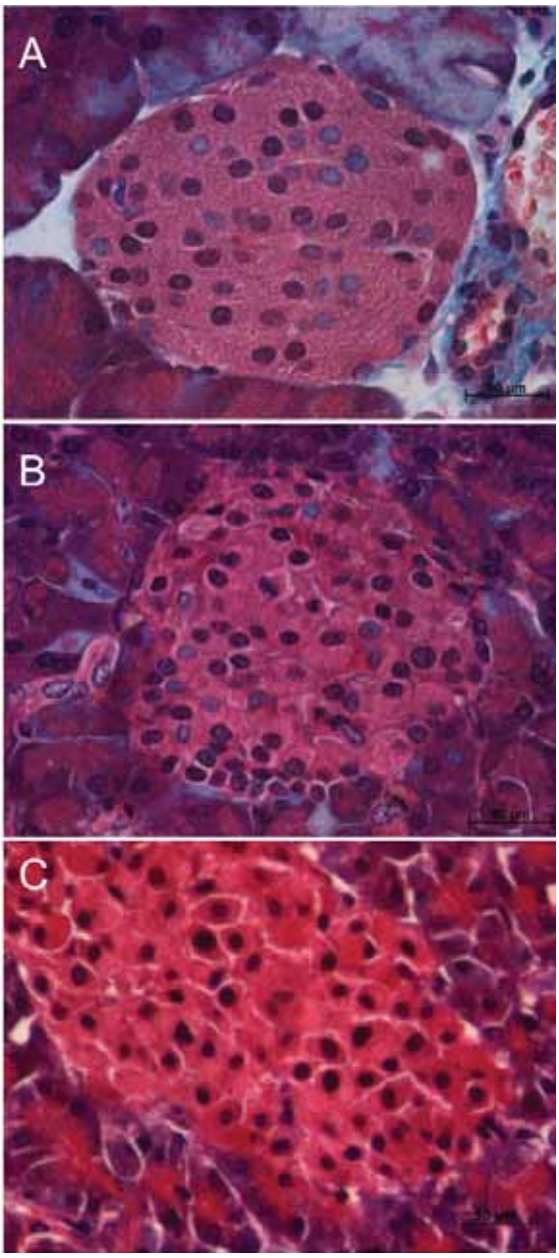

Figure 3.1 Masson's trichrome stain for collagen in murine (a), rat (b) and rabbit (c) pancreatic sections. Collagen should be stained blue, however, no collagen was detected using this method in either of the species. Scale bar: 50 μm

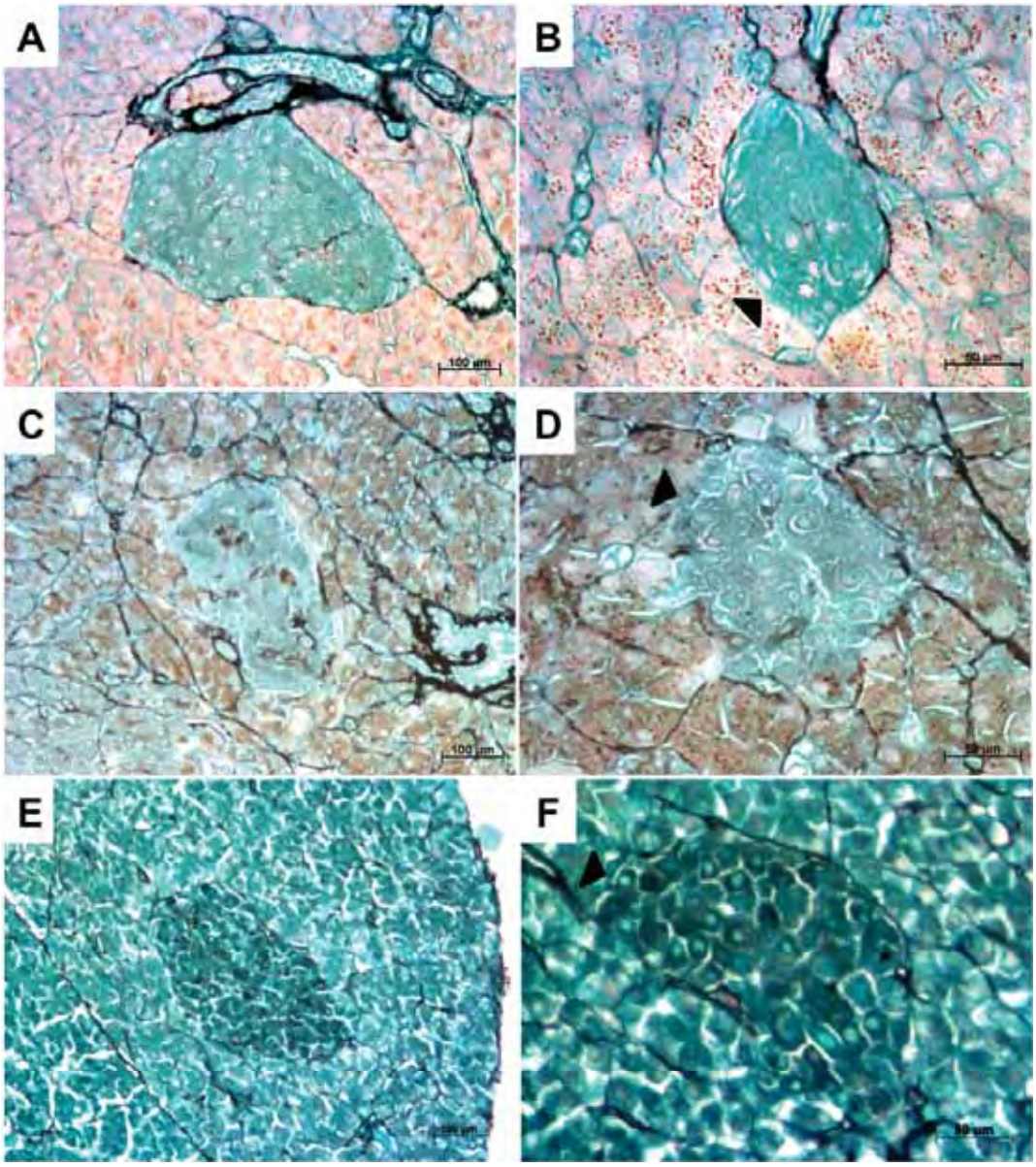

Figure 3.2 Methenamine silver stained mouse (A, B), rat (C, D) and rabbit (E, F) pancreatic sections. Basement membranes appear black and species-specific differences in morphology can be observed. ► indicates areas of discontinuous basement membrane enclosure. Scale bar on left panel: 100 μm; right panel: 50 μm

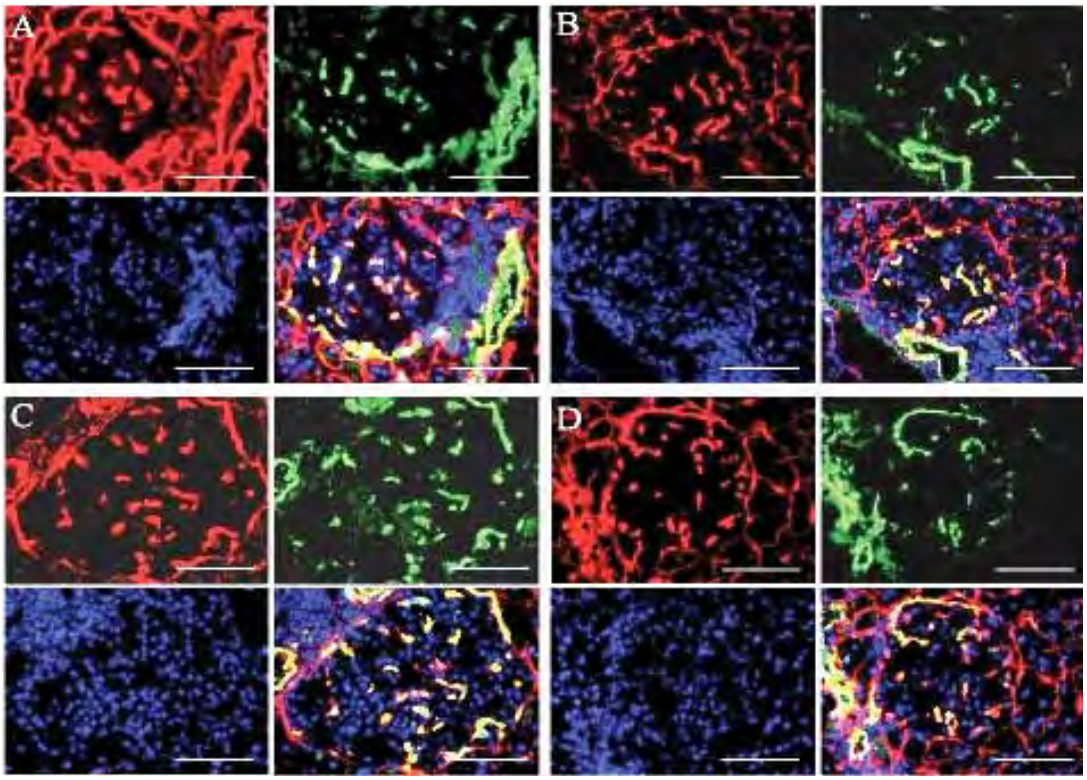

Figure 3.3 Mouse islets labeled with von Willibrand factor in green, cell nuclei in blue, collagen IV (A), laminin-121 (B), fibronectin (C) and perlecan (D) in red, demonstrates co-localisation of basement membranes with endothelial cells. Scale bar: 100 μm

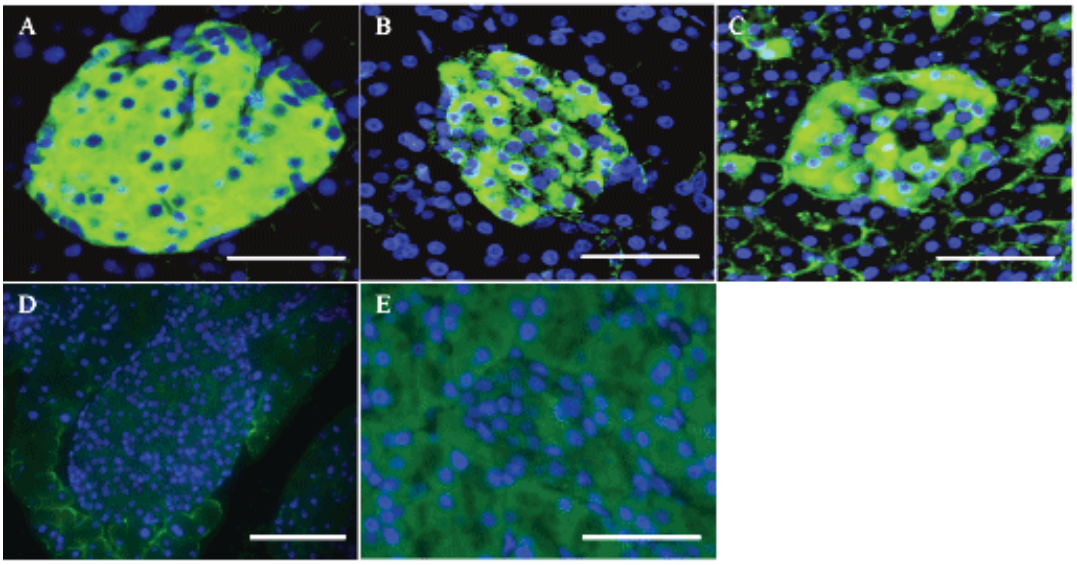

Figure 3.4 HS 3G10 stub (A, B, C) and HS 10E4 (D, E) staining of mouse (A, D), rat (B, E) and rabbit (C) islets in green. The 3G10 epitope can be seen dispersed throughout cells of the islet, while the 10E4 epitope is absent. Cell nuclei were stained blue. Scale bar: 50 μm

In contrast, immunolocalisation for the 3G10 stub epitope of heparan sulfate (HS) that emerges after heparitinase digestion stained the majority of cells within the islet in the mouse, rat and rabbit pancreas (Figure 3.4). The HS stub localisation was very different to the perlecan staining morphology and appeared to be distributed throughout the islet either on the cell surfaces or intracellularly. The rabbit HS immunostaining was inconsistent within repeats and thus further characterisation was not pursued. Interestingly, the 10E4 antibody for the *N*-sulfated and *N*-acetylated form of HS (David et al., 1992; van den Born et al., 2005) (Figure 3.4) and the CS-56 antibody for chondroitin sulfate (data not shown) did not positively stain the islet region in any of the species. Overlaying of insulin or glucagon (red) with the HS stub (green) demonstrated that the eptitope was mainly present on the insulin-positive cells and not the glucagon-positive cells within the mouse and rat islets (Figure 3.5). As a confirmation of antibody specificity, HS stub antibody did not bind prior to heparitinase digestion, though antigen retrieval was at times enough to expose some of the stub epitope without heparitinase digestion (data not shown).

For the characterisation of HS-associated proteoglycans, the syndecan-1, glypican-1, betaglycan and type XVIII collagen antibodies used in this study were unsuccessful in detecting these proteoglycans in the pancreas of both the mouse and rat. Staining for syndecan-4, however, revealed the significant presence of the transmembrane HS proteoglycan in both mouse and rat islets (Figure 3.6). The stain was distributed throughout the islet in a similar manner to that of the HS stub, and appeared to be either on the cell surfaces and/or within the cells. Interestingly, the syndecan-4 epitope was better immunodetected after the HS was digested from the tissue section with heparitinase.

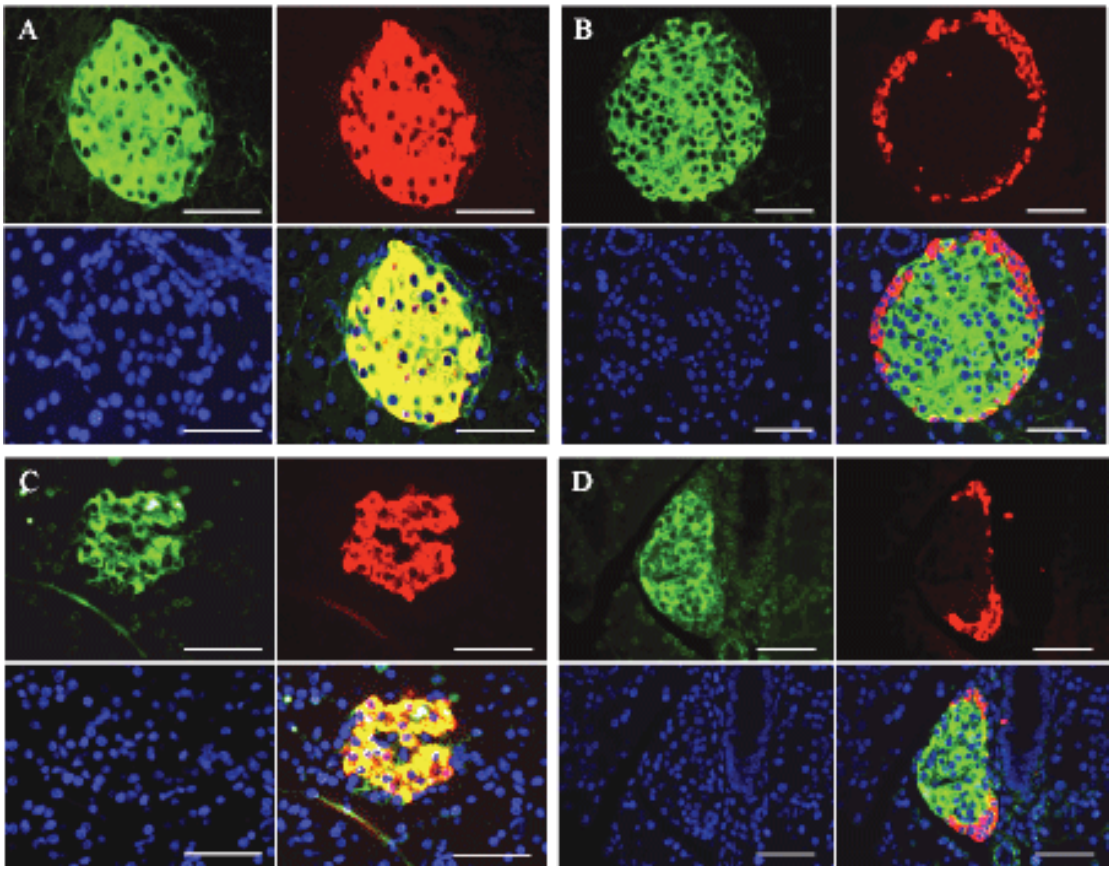

Figure 3.5 Multiple staining of HS stub in green with insulin (A, C) and glucagon (B, D) in red. Panels A and B are of mouse islets and panels C and D are of rat islets. Cell nuclei were stained blue. Scale bar: 50 μm

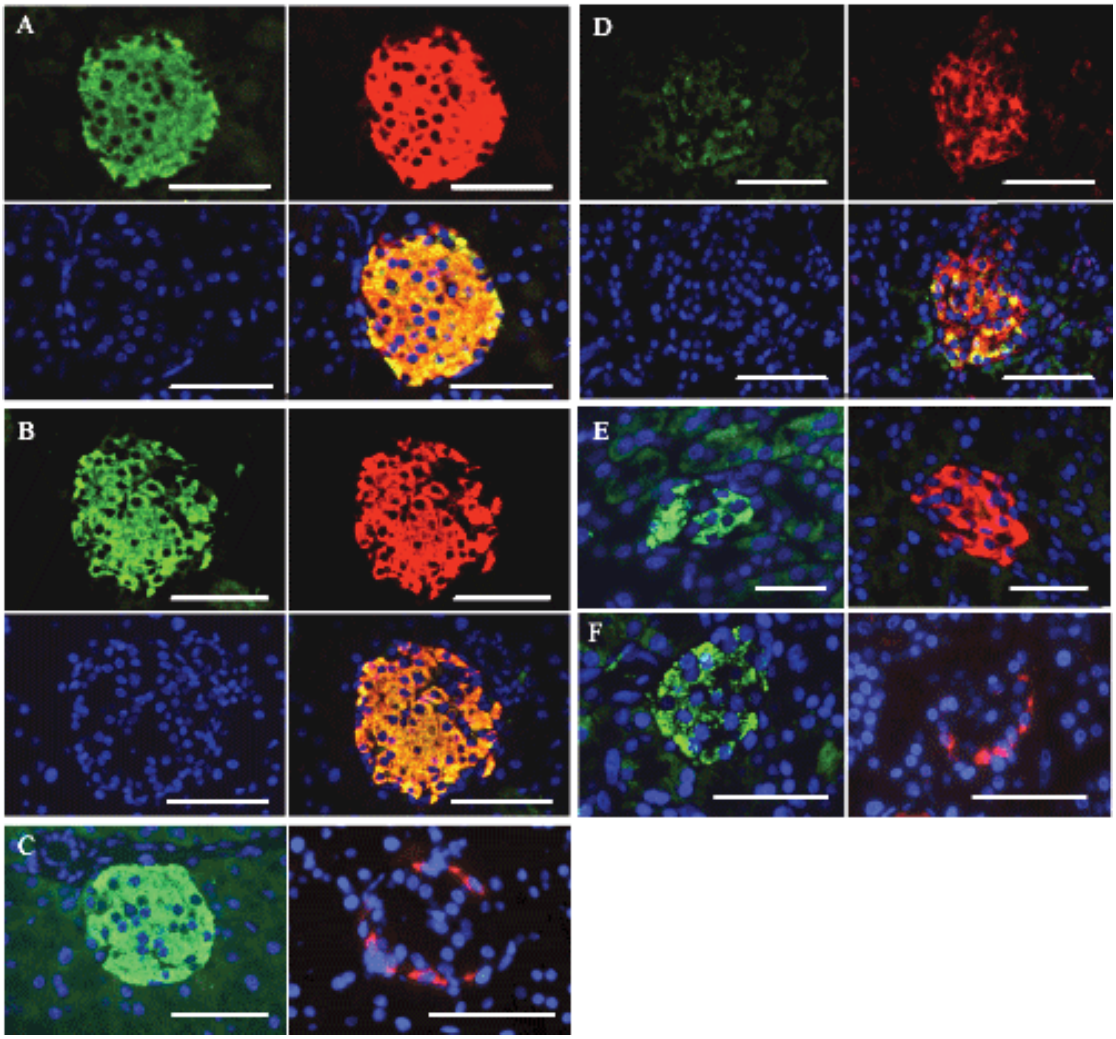

Figure 3.6 Immunohistochemical staining of syndecan-4 in mouse (A, B, C) and rat (D, E, F) islets in green overlayed with HS stub (A, D) and insulin (B). C, E and F shows separate sections individually stained with sydnecan-4 in green, insulin (E) and glucagon (C, F) in red. Cell nuclei were stained blue. Scale bar: 50 μm

Multiple staining of syndecan-4 with HS stub showed a direct overlap of the two antigens (Figure 3.6A). Furthermore, syndecan-4 also overlapped directly with the insulin staining in the mouse islet (Figure 3.6B). In contrast, multiple localisation of syndecan-4 with the HS stub and insulin in the rat was unsuccessful, but the staining patterns were very similar in morphology (Figure 3.6E). Nevertheless, a comparison of the individual staining patterns of syndecan-4 and glucagon showed syndecan-4 (green) to be mainly in the inner region of the islet, similar to that of the insulin (red) stain (3.6B and E), while glucagon (red) remained only in the periphery (Figure 3.6C and F) in both the mouse and rat islets.

3.3.3 Determination of intracellular or extracellular HS and syndecan-4 localization by confocal microscopy

In order to determine the intracellular or extracellular localization of HS within the mouse islet, confocal microscopy was used to construct 3D overlayed images of fluorescently labeled HS stub and insulin. Although the HS stub appeared to be localized to the β-cell surface in single-plane images, 3D z-stack images were not definitively extracellular. Figure 3.7 shows a single-plane image of HS stub staining following the curvature of some β-cell surfaces that did not overlap with the intracellular insulin stain (arrowheads), however, green fluorescence can be seen in the image cross section scattered across the distance of the 10 μm section, adjacent to the nuclei. Similarly, the cellular proximity of syndecan-4 was not definitively extracellular from single-plane and 3D z-stack images as well (Figure 3.8). This was perhaps compounded by the fact that the syndecan-4 antibody used binds the cytoplasmic domain of the core protein.

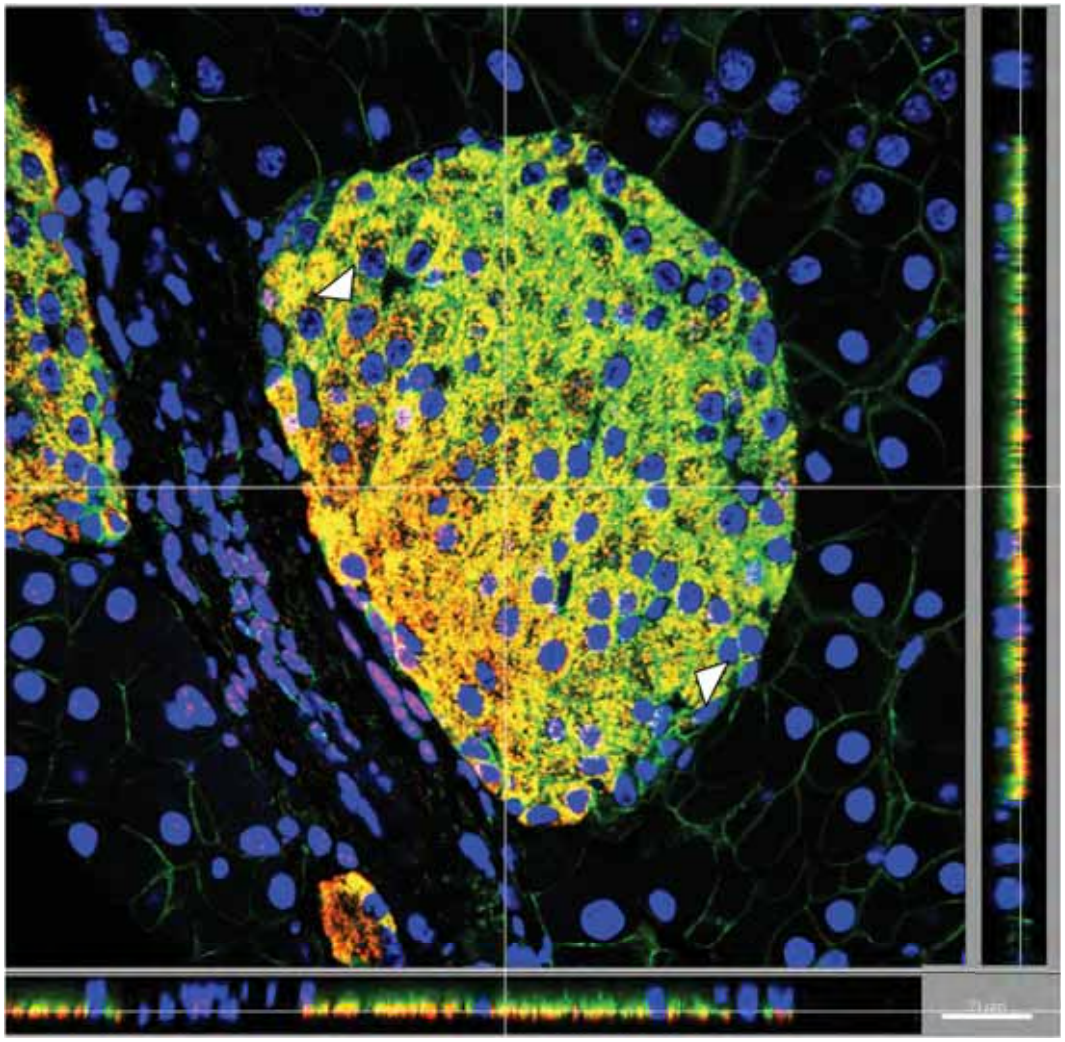

Figure 3.7 Confocal single-plane image of a 10 μm mouse islet section. Image is an overlay of HS 3G10 stub labelled in green, insulin in red and cell nuclei in blue. Arrowheads show HS stub staining following the curvature of some β-cell surfaces. Scale bar: 20 μm

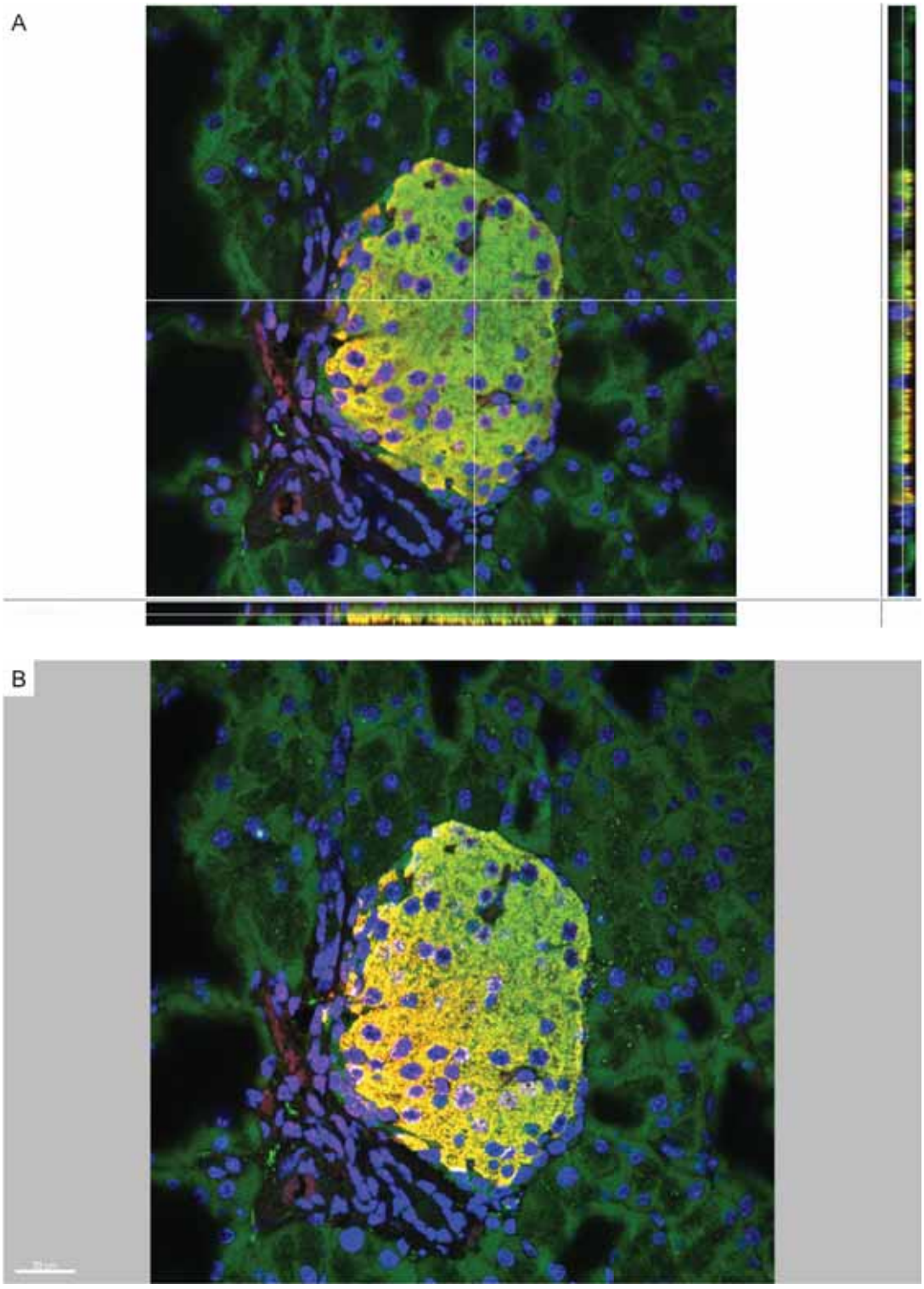

Figure 3.8 Confocal single-plane (A) and z-stack (B) images of a 10 μm mouse islet section. Images are overlays of syndecan-4 labeled in green, insulin in red and cell nuclei in blue. Cross-sections of the 10μm slice on the side panel provides an indication for the location of the labeled antigen in relation to the cell nuclei. Scale bar: 20 μm

3.3.4 Identification of islet ECM by SDS-PAGE and mass spectrometry

Identification of ECM proteins and/or proteoglycans was attempted by mass spectrometry (MS) as an alternative method to immunohistochemistry. Direct tryptic digestion of protein extracts resulted in identification of intracellular proteins only (Appendix A). In order to reduce the amount of proteins per sample for a potentially more stringent identification, protein extracts were separated by SDS-PAGE and an in-gel tryptic digest was performed prior to HPLC separation and MS. Distinct protein bands in the SDS-PAGE demonstrated the presence of intact islet proteins (Figure 3.9). Nevertheless, despite the additional protein separation step, no ECM protein or proteoglycan was identified in the Mascot peptide search (Appendix A). Further experiments using this methodology were therefore not conducted.

3.3.5 Immunohistochemical characterisation of MIN6 cell line

Comparable to the pancreatic tissue staining, strong immunoreactions with the HS stub antibody was observed on the cell surfaces of MIN6, while HS 10E4 (*N*-sulfated and *N*-acetylated) was weak in staining and could only be seen on some cells in the MIN6 cell layer (Figure 3.10). The MIN6 cells also stained strongly for syndecan-4 and pre-treatment with heparitinase was not required for immunoreactivity to occur. The syndecan-4 staining appeared to be intracellular due to the fact that the antibody used recognises the cytoplasmic domain of the core protein.

3.3.6 Western blot analysis of syndecan-4 in islets and MIN6 cell line

Western blotting for syndecan-4 was not as effective without pre-deglycosylation of the total proteoglycan fraction in both islets and MIN6. Overnight treatment with heparitinase increased the presence of non-specific bands and a sharp, distinct 75 kD band appeared in both digested and undigested MIN6 fraction (Figure 3.11). While in the islet fraction, an 80 kD band appeared after the heparitinase digest. Interestingly, a 35kD band appeared in both MIN6 and islet lysate only after digestion. As syndecan-4 has often been shown to produce a smear of high molecular weight multimers in Western blots unless deglycosylated by heparitinase and chondroitinases (Drzeniek et al., 1999; Hamon et al., 2004; Schofield et al., 1999), the 80 kD band in the islet fraction may thus be a syndecan-4 dimer, while the bands above 50 kD in the MIN6 lysates were most likely due to non-specific binding of the syndecan-4 antibody.

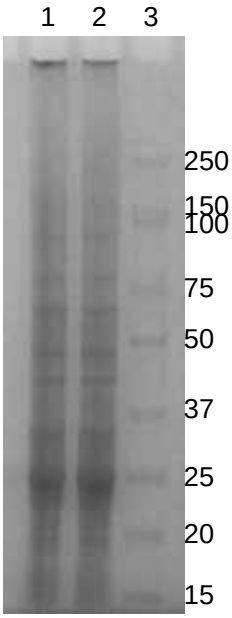

Figure 3.9 SDS-PAGE of guanidine-HCl-extracted mouse islet proteins. Lane 1 & 2: islet proteins; lane 3: ladder. Ladder sizes in kD

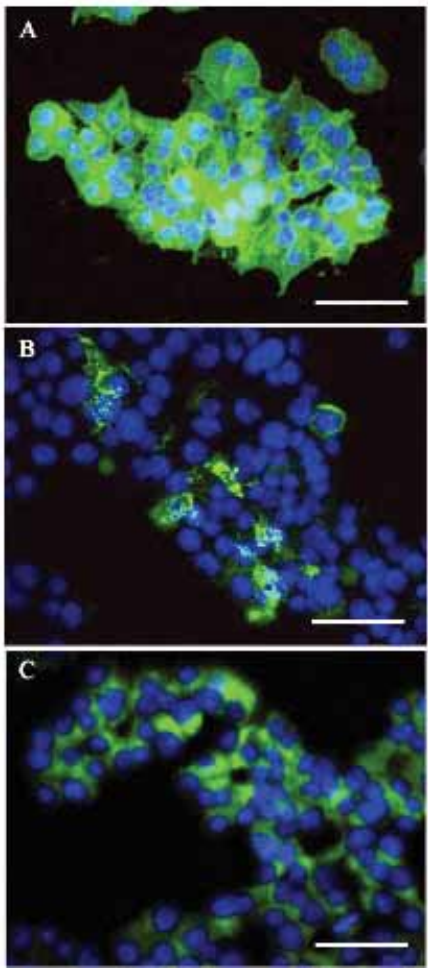

Figure 3.10 Immunohistochemical staining of the MIN6 cell line. HS 3G10 stub (A), HS 10E4 (B) and syndecan-4 (C) were stained in green and cell nuclei in blue. Scale bar: 50 μm

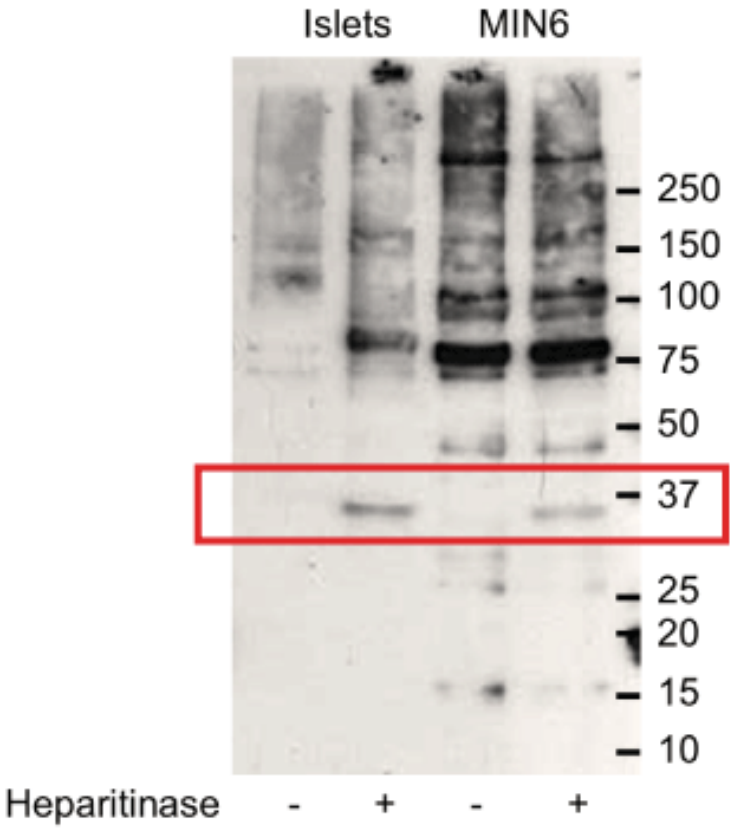

Figure 3.11 Western blot of syndecan-4 in semi-purified proteoglycan fraction from MIN6 cells and mouse islets, with and without heparitinase digest. Deglycosylated syndecan-4 core protein is boxed in red. Ladder sizes in kD

3.4 Discussion

The presence of a BM in the pancreatic islets of the mouse, rat and rabbit was confirmed in this study. In contrast to previous studies (Irving-Rodgers et al., 2008; Nikolova et al., 2006), this BM did not always form a peri-islet capsule around the entire islet in the mouse species (Figure 3.2). Nevertheless, the BM tightly followed the interweaving blood vessels in all three species. This BM morphology was similar to those previously observed by Hughes et al, Irving-Rodgers et al and Ontokoski et al in the mouse species (Hughes et al., 2006; Irving-Rodgers et al., 2008; Otonkoski et al., 2008). The rat and rabbit species were found to be extremely difficult to immunostain due to the high levels of non-specific binding and inconsistencies within staining repeats. Consequently, this chapter primarily focused on the mouse species and found that the endothelial cell marker, von Willebrand factor, overlapped directly with the BM components collagen IV, fibronectin, laminin-121 and perlecan (Figures 3.3), thus confirming a tight association of these components with the underlying endothelium. Previous studies have only shown the association of laminin-α1 and collagen IV with the endothelium (Nikolova et al., 2006), therefore this is the first study to also demonstrate the endothelial localisation of fibronectin and perlecan. HS on the other hand, was distributed throughout the islet, particularly in the mouse species (Figure 3.4). Furthermore, only the 3G10 stub epitope was observed, but not the 10E4 N-sulfated and N-acetylated form of HS. The HS stub distribution was similar to those observed by Takahashi et al and Ziolkowski et al (Takahashi et al., 2009; Ziolkowski et al., 2012).

The sulfation pattern of heparan sulfate is important for its interactions with growth factor ligands and receptors (Turnbull et al., 1992). During murine lens development, N-sulfation is essential for binding to FGF2 (Pan et al., 2006). Differential activation of FGF-1 and FGF-2 may also be mediated by both oligosaccharide length and sulfation pattern, with different O-sulfation positioning being implicated for promoting binding to different FGFs (Pye et al., 2000). In addition, structural differences in heparan sulfate chains also determine whether a cell undergoes differentiation in human colon carcinoma cells (Salmivirta et al., 1998). It is therefore interesting to observe a lack of 10E4 HS epitopes in the islet region, despite the abundance of HS 3G10 stubs. The recent identification of HepSS-1 epitopes (Ziolkowski et al., 2012) perhaps indicates the importance of O-sulfated and N-acetylated HS domains in the function of islets.

However, HS does not exist in the extracellular space on its own (Iozzo, 2001), and thus presence of an associated proteoglycan must exist in the islet. Perlecan is currently the only HS-associated proteoglycan shown to be present in the extracellular matrix of the pancreatic islet by various methods. Gene expression by isolated islets (Takahashi et al., 2009) and immunohistochemical detection (Irving-Rodgers et al., 2008) have both confirmed its presence in the islet and is expressed mainly in the intra-islet vascular BMs. However, perlecan is unlikely to be the proteoglycan on which the islet HS are attached as the HS staining occurred profusely dispersed throughout the mouse and rat islet in a pattern not only different to that of perlecan, but also the intra-islet endothelium. The immunoreaction appeared to be specifically associated with the β-cells (Figure 3.5) but not the

glucagon-positive α-cells. This indicated that there must exist other HS proteolgycan/s in the islet to which the abundant levels of HS are attached.

Due to the fact that protein identification by antibody requires a trial and error approach for determining whether a certain protein is present in a tissue, mass spectrometry was an alternative method used to overcome this issue. Nevertheless, attempts to identify all the possible ECM components present in a healthy murine pancreatic islet by mass spectrometry were unsuccessful. Peptide matches that resulted from each attempt were always outnumbered with intracellular proteins, even after crude separation of the proteins and total proteoglycan by SDS-PAGE and anion bead chromatography, respectively. In 2009, Waanders et al endeavored a similar study and identified collagen I, IV, VI, XIV, laminin and fibronectin in their mass spectrometry analyses of isolated murine islets (Waanders et al., 2009). However, the only proteoglycans found were fibrillin-2, chondroitin sulfate proteoglycan-4, syndecan-4 and agrin, all of which were near the limit of detection. This suggests that ECM components, especially proteoglycans, are perhaps at a very low concentration compared to cellular proteins within the islet, and thus mass spectrometry may not be the best method used for detecting their presence.

Other known HS-associated proteoglycans include syndecans, glypicans, betaglycans and type XIII collagen (Iozzo, 2001). Membrane associated HS proteoglycans include syndecan-1-4, glypican-1-6 and betaglycan and genetic expression of syndecans, glypicans by isolated islets have previously been reported (Takahashi et al., 2009; Zertal-Zidani et al., 2007). The mRNA of the pericellular HS proteoglycan, type XIII collagen, was also detected by Takahashi et al (Takahashi et

al., 2009). Nevertheless, attempts to detect syndecan-1, glypican-1, betaglycan and type VIII collagen in this study by immunohistochemistry have thus far been unsuccessful. This however, does not suggest the absence of these proteoglycans and may merely be a function of the antibodies and technique used.

Syndecan-4 on the other hand showed strong immunolabeling that was distributed throughout the mouse and rat islets, similar to that of the HS (Figure 3.6). Merging of the two stains showed a direct overlap, thus suggesting the two antigens to be associated with each other within the islet. Interestingly, there was such an abundance of HS that heparitinase digestion was required in order for the syndecan-4 antibody to react with the core protein. Furthermore, double labelling of syndecan-4 with insulin or glucagon revealed that, like HS, syndecan-4 was present on the insulin-positive and not the glucagon-positive cells (Figure 3.6). Together, this strongly indicates that there is an abundance of HS on the β-cells, not α-cells, and large portion of the HS found in the islet may originate from the membrane-associated syndecan-4 proteoglycan.

Previous studies have shown that cell surface HS plays an important role in the regulation of islet differentiation, maturation and is also required to maintain normal glucose-stimulated insulin secretion (Noguchi et al., 2007; Takahashi et al., 2009; Ueda et al., 2008; Zertal-Zidani et al., 2007). The function of syndecan-4 in β-cells on the other hand remains unknown.

The predicted molecular weight of a syndecan-4 monomer is 22 kD, with an observed band size of 24 kD due to its glycosylation. Syndecans have also been shown to form multimers that are SDS- and reduction-resistant (Oh et al., 1997).

Western blot analysis of MIN6 and islet semi-purified lysate both showed the appearance of a ~37 kD band after heparitinase digestion (Figure 3.11). Though protein bands of other sizes were detected, it is believed that they were of a non-specific nature as syndecan-4 is known to have a core polypeptide molecular weight of ~35 kD after heparitinase digestion (Bao et al.; Drzeniek et al., 1999; Echtermeyer et al., 1999). In the islet total proteoglycan, however, there was an appearance of a ~37 kD and ~85 kD band post-heparitinase digestion. It is believed that the ~85 kD represents the oligomeric form of syndecan-4 core protein, which is consistent with previous findings that show syndecan to form SDS- and reduction-resistant oligomers (Asundi and Carey, 1995; Kojima et al., 1992; Yung et al., 2001).

Although syndecan-4 was the only syndecan identified thus far by this study, it is postulated that other syndecans may be present. Previous work on syndecan-4 knockout mice did not specifically study the pancreas/islets and thus impact on pancreatic function was not described. However, the knockout mice displayed delayed wound-healing of the skin possibly due to slower cell migration, impaired blood vessel formation in the placenta and defective cell adhesion (Simons and Horowitz, 2001). There is also a potential for isoform redundancy to exist between the syndecans, whereby certain isoforms are upregulated in order to compensate for the knocked out isoform thus making a phenotype difficult to observe.

It was recently discovered that the abundance of HS present in the islet actually resides within the β-cells themselves and not in the peri- or extracellular space (Ziolkowski et al., 2012). The study found that there was a decrease in intracellular HS and an increase in cell surface HS after two days in culture that correlated with

an increase in β-cell apoptosis and death. Furthermore, supplementation of intracellular HS with highly sulfated heparin protected the β-cells from apoptosis. However, the function of the intracellular HS and whether it exists as free polysaccharide chains or is attached to a proteoglycan still remains to be confirmed. Confocal microscopy of HS with an antibody that recognizes a neo-epitope generated after heparitinase digestion did not conclusively show whether it was intracellularly or membrane localized in mouse islets (Figure 3.7). In fact, the HS stub appeared to be present both inside and on the cell surface. Use of a syndecan-4 antibody specific to the cytoplasmic region of the core protein also did not definitively demonstrate its cellular localization (Figure 3.8).

When comparing the tissue ECM results with isolated β-cells, HS stub appeared distinctly on the cell surfaces of the MIN6 murine insulinoma cell line, whereas *N*-sulfated and *N*-acetylated HS (via the 10E4 antibody) was only present in/around a few cells and was not definitively intracellular (Figure 3.10 a-b). Syndecan-4, on the other hand, appeared to be intracellular (Figure 3.10 c), but this may be due to the nature of the antibody being specific for the cytoplasmic region of the proteoglycan. Interestingly, similar to the immunohistochemical findings for the islet tissue sections, collagen IV, laminin-121, fibronectin and perlecan were not detected in the MIN6 cell layer by immunocytochemistry (data not shown). This somewhat confirms the speculation by Nikolova et al that β-cells cannot form BMs (Nikolova et al., 2006). Though these components have been identified in isolated islets (Irving-Rodgers et al., 2008; Waanders et al., 2009), it must be remembered that islets comprise of a number of different cell types, including the endothelial cells.

Therefore, gene expression of these ECM components detected from islets may have been from transcripts expressed by the intra-islet endothelial cells or other cell types present within the islet.

Syndecan-4 has been demonstrated to be involved in FGF-2 signaling by facilitating FGF-2 internalization via an endocytic pathway in endothelial cells (Tkachenko et al., 2004). Clustering of syndecan-4 lead to the internalization of both itself and FGF-2 and the majority of FGF-2 internalized by rat fat pad endothelial cells was facilitated via the syndecan-4 pathway. A more recent study has shown that co-delivery of FGF-2 with syndecan-4 increased FGF-2 cellular signaling, uptake and nuclear localization in endothelial cells when compared with FGF-2 alone (Jang et al.). Furthermore, mutations of the cytoplasmc tail of syndecan-4 disrupted signal transduction by FGF-2 (Horowitz et al., 2002; Murakami et al., 2002). FGF-2 is also an important growth factor for pancreatic cell proliferation and differentiation during the early stages of development (Hardikar et al., 2003; Ogneva and Martinova, 2002). Further to this, FGF-10 is also an important player in the development of islets. FGF-10 was shown to positively influence β-cell mass by increasing early precursor proliferation and extending the expression of the endocrine precursor marker, *Ngn3* (Duvillie et al., 2007). Therefore, syndecan-4 and its associated HS may potentially play an important role in signal transduction in pancreatic β-cells through the FGF signalling pathway.

Although current studies of syndecan-4 in islets have predominantly been in the rodent model, microarray data from healthy and Type 2 diabetic human islets is available on the website of the Diabetes Genome Anatomy Project (Gunton et al.,

2005; Kahn, 2005). Analysis of syndecan-4 mRNA expression from this data showed a 2-fold down-regulation of syndecan-4 in diabetic islets. However, due to the fact that the sample size was so small (7 normal glucose tolerance, 5 type 2 diabetic), this result was not statistically significant (*P-value = 0.065*) (See Appendix A). Nevertheless, these results provide some insight into the importance of syndecan-4 in the function of human pancreatic islets.

3.5 Conclusion

In summary, the islet contains a basement membrane that may or may not completely enclose the individual islet, depending on the islet size and species (Figure 3.2), and is distributed throughout the islet in a pattern that appears to follow the interweaving endothelium. In the mouse species, the basement membrane contains collagen IV, laminin-121, fibronectin and perlecan that are tightly associated with the intra- and peri-islet endothelial cells (Figure 3.3), and are therefore potentially produced by the endothelial cells rather than the endocrine cells themselves. This was further suggested by the absence of positive immunostaining of these ECM components in the MIN6 insulinoma cell layer.

Isolated islets contained a higher proportion of cellular proteins than ECM components and proteoglycans. As a result, these components were virtually undetectable by mass spectrometry. Nevertheless, immunohistochemial localisation demonstrated that HS comprises a major portion of the islet ECM and was found on the cell surface of the β-cells but not the α-cells. Whether the HS is within the β-cells attached to proteoglycans, such as syndecan-4, or occurs as free polysaccharide chains remains to be confirmed.

Syndecan-4 was found to be mainly expressed primarily by the β-cells and not the α-cells in the murine and rat islets. This suggests that the HS found in the islets are mostly attached to the syndecan-4 core protein found in the β-cells. Whether syndecan-4 is strictly on the cell surfaces, or whether it is endocytosed into the β-cells with the HS, requires further study and is outside the scope of this thesis. Immunohistochemistry and confocal microscopy in this instance did not definitively

demonstrate the cellular localization of both syndecan-4 and the HS stub in the β-cells.

Although the function of syndecan-4 in β-cells requires further investigation, its co-localization with HS (Figure 3.6) suggests that together they may play a synergistic role in maintaining the health of islets. Syndecan-4 was shown in endothelial cells to be crucial for FGF-2 signaling (Tkachenko et al., 2004) and potentially, the HS proteoglycan may play a similar role in pancreatic β-cells. Syndecan-4 core protein extracted from MIN6 β-cells and islets were approximately 37 kD in size (Figure 3.11) and is a similar core protein size to the syndecan-4 produced by endothelial cells (Bao et al.; Olofsson et al., 1999).

Though syndecan-4 was the only transmembrane HS proteoglycan detected in this study, this does not suggest the absence of other forms of syndecans in the islet. Studies of syndecan-4 knockout mice did not report of any pancreatic dysfunction, thus implicating the presence of other isoforms (Simons and Horowitz, 2001; Takahashi et al., 2009).

The MIN6 insulinoma cell line expressed both syndecan-4 and HS, with the HS stub existing mainly on the cell surfaces. Extracted syndecan-4 from both islets and MIN6's had core proteins of an identical size. Furthermore, similar to in vivo β-cells, MIN6 did not immunostain positive for collagen IV, laminin, fibronectin and perlecan. In this way, the MIN6 cell line showed very similar ECM characteristics to those of in vivo β-cells and thus may be a good model for the study of β-cell interactions with various ECM components.

These results indicate that although the basement membrane components such as collagens, fibronectin and laminin may be important for providing molecular cues to pancreatic endocrine cells, it is the more abundant HS and proteoglycans, such as syndecan-4, that may be crucial to supporting β-cell-specific function, viability and differentiation in the rodent model. Due to the fact that species differences exist between the rodent and human species, these results will need to be verified in the human species in order for it to be clinically relevant. However, the human species is outside the scope of this thesis and thus will not be explored.

Further to the immunohistochemical findings in this chapter, the basement membrane-associated endothelial cells are a potential cell type that may be ideal for the production of islet-compatible ECM containing all the required components in the appropriate concentrations. Therefore, the next chapter will characterize the ECM proteins, proteoglycans and glycosaminoglycans (in particular syndecans and HS) produced and deposited by endothelial cells.

Chapter 4

4 Enhanced production of endothelial cell extracellular matrix

4.1 Introduction

Endothelial cells (EC) have previously been shown to produce a wide variety of ECM components (Davis and Senger, 2005). As demonstrated in Chapter 3, ECM found in the islet is tightly associated with the intra-islet ECs and thus there is potential for *in vitro* endothelial cells to be used as a "factory" for producing the ideal β-cell sustaining ECM. Early studies of endothelial-produced ECM for the support of islets have proven to be promising (Hayek et al., 1989; Hulinsky et al., 1995b; Kaiser et al., 1988; Thivolet et al., 1985). However, common protocols for EC culture require a pre-coating of ECM, such as gelatin or fibronectin, on the tissue culture plastic (TCP) in order for the ECs to adhere and propagate. Furthermore, previous studies have shown that much of the matrix produced in culture is released into the supernatant and discarded with each media-change instead of being deposited onto the culture plate (Lareu et al., 2007a; Lareu et al., 2007b; Lareu et al., 2007c). Therefore, the aim of this study was to investigate the use of macromolecular crowding conditions for the enhancement of endothelial ECM deposition.

The adult pancreatic islet is one of the most vascularised organs in the body. Blood vessels form dense networks of fenestrated capillaries within the islet that are five times higher in density than those found in the neighbouring exocrine tissue (Kuroda et al., 1995; Lammert et al., 2003). Each endocrine cell is in one-to-one proximity to an endothelial cell, with β-cell apices oriented towards the capillaries, thus facilitating rapid exchange of signals between the two cell-types (Zanone et al., 2008). Studies of the murine pancreas, have suggested that β-cells do not form their own basement membranes (BM), but produce vascular endothelial growth factor A (VEGF-A) that recruit endothelial cells to form capillaries with vascular BM next to the β-cells (Jiang et al., 2002; Nikolova et al., 2006). Deletion of VEGF-A under the *Pdx-1* promoter resulted in a loss of intra-islet endothelial cells and the basement membranes laminin and collagen IV. In turn, these vascular BM components were able to regulate the expression of insulin and β-cell proliferation (Nikolova et al., 2006). Furthermore, treatment of islets with endothelial-conditioned media resulted in an increased glucose-stimulated insulin secretion and islet insulin content (Johansson et al., 2009). Many other studies have observed isolated ECM components found within the intra-islet endothelial basement membrane, such as collagen IV, laminin and fibronectin, to enhance isolated islet function. For an in-depth review, refer to Cheng et al, 2011 (Cheng et al., 2011).

Currently, Matrigel® is the most widely used matrix for the preservation of isolated islets, prior to transplantation (Nolan, 2009). It is a crude source of ECM components extracted from the mouse Engelbreth-Holm-Swarm carcinoma and contains a plethora of growth factors. Since Matrigel® currently functions either as a

short term carrier of β-cells after isolation or transplanted with the islets to improve vascularization, the long term effects of Matrigel® on maintaining β-cell differentiation is largely unknown. One study showed that without the addition of activating factors, Matrigel® alone could not induce the differentiation of acinar-derived cells, which express both exocrine and neuroendocrine properties, into insulin-positive cells (Hamamoto et al., 2011). Another study observed that the addition of Matrigel® did not offer a more suitable environment to further improve the islet engraftment (Caiazzo et al., 2007). The longest study of mature islets on Matrigel® to date demonstrated its ability to maintain rat islet function for up to 6 weeks (Perfetti et al., 1996). It is therefore evident that ECM components and their ability to present the right kind of growth factors to the β-cells is important, however, perhaps endothelial cells may be better geared to producing ECM of the optimal composition for the long term maintenance of β-cells.

Bovine corneal and human umbilical cord vein endothelial cells have previously been used to produce a layer of matrix on which islet cells were seeded (Hayek et al., 1989; Hulinsky et al., 1995b; Kaiser et al., 1988; Thivolet et al., 1985). The endothelial-derived matrix was able to enhance islet attachment and proliferation (Hayek et al., 1989; Thivolet et al., 1985). A more appropriate insulin response to glucose starvation was observed when compared to suspended islets, though insulin secretion itself was not enhanced (Hulinsky et al., 1995b). In one study, the islets' responsiveness to glucose, glucagon and somatostatin was retained for 2-4 weeks in culture (Kaiser et al., 1988). Despite these promising results, all studies observed the

islets to form monolayers when seeded onto the endothelial matrix and the majority of these studies were not performed for longer than 9 days.

It is generally known that there is difficulty in producing significant amounts of ECM under normal 2D *in vitro* culture conditions. One reason for this may be the absence in a tissue culture flask of the crowded environment, normally found around the exterior of cells within multicellular organisms (Phillips et al., 2008). Normal crowding elements include proteins, carbohydrates and lipids that form supramolecular assemblies such as cellular organelles and membranes that occupy volume. The volume of cytoplasm that is usually occupied by macromolecules is estimated to be at least 20-30% (Kim and Yethiraj, 2009). Extracellular fluid containing interstitial fluid and blood plasma also contains proteinaceous macromolecules that occupy between 7-8% of total fluid volume that translates to a protein concentration of approximately 20.6 g/L (Foghandersen et al., 1995; Ross and Pawlina, 2006). On the other hand, cell culture conditions are typically supplemented with 5-10% fetal bovine serum that results in a protein concentration of 4-16 g/L. The vast differences in crowdedness between cell culture conditions and those normally found in a living organism thus leads to inefficiencies in ECM deposition.

Macromolecular crowders, such as dextran sulfate and Ficoll, have previously been used to simulate an *in vivo* crowded environment in *in vitro* cell cultures (Chen et al., 2011). Collagen I deposition was enhanced when dextran sulfate crowders were supplemented in fibroblast culture medium (Lareu et al., 2007c). Under normal tissue culture conditions, collagen is secreted as pro-collagen into the culture media

until it is cleaved by procollagen-C-proteinase (PCP) and deposited as insoluble collagen on the tissue culture plastic. Under non-crowded conditions, PCP activity is low and most of the water-soluble collagen is lost during media-changes, thus only small amounts of insoluble collagen are deposited. Dextran sulfate in the culture media enhances enzyme-protein interactions, thus leading to more procollagen being cleaved into its insoluble counterpart.

Macromolecular crowders also have the added benefit of enhancing ECM stabilization by enzymatic and non-enzymatic crosslinking that protects it from proteolytic attack (Chen et al., 2011). Fibroblasts grown under crowded conditions produced collagen matrices with a higher ratio of β-chains to α-chains, thus suggesting an increase in lysyl oxidase-mediated crosslinking of the deposited collagen (Chen et al., 2009; Lareu et al., 2007c).

It would therefore be useful to enhance endothelial cell deposition of ECM by macromolecular crowding for the production of a better β-cell function-supporting substrate. The effects of crowding on ECM deposition have previously been studied in human fibroblasts, human embryonic and mesenchymal stem cells (Chen et al., 2011; Lareu et al., 2007c), but have not yet been explored in endothelial cells. The specific aims of this research were to quantify the amount and to characterise the ECM components, in particular syndecans and HS, deposited by endothelial cells under normal and crowded conditions. In addition, the study aimed to evaluate whether there was matrix production by MIN6 cells and if expression of syndecan-4 and HS could be enhanced under the two conditions. Finally, two different

detergents, Nonidet P-40 and sodium deoxycholate, were compared for efficiency in removal of cellular material and maintenance of ECM integrity.

4.2 Materials and Methods

4.2.1 Endothelial cell culture

In order to enhance endothelial cell ECM production, two types of endothelial cells were cultured under normal and crowded conditions. Normal primary human umbilical cord vein endothelial cells (HUVEC) and transformed human microvascular endothelial cells (HMEC-1) were compared for ECM deposition. Cell layers from Simian virus 40 (SV-40) transformed human dermal microvascular endothelial cells (HMEC-1) and primary human umbilical cord vein endothelial cells (HUVECs) were screened for various ECM components by immunocytochemistry cultured under normal and crowded conditions.

The HUVECs were a kind donation from Professor Jennifer Gamble of the Centenary Insitute, Sydney. The HUVECs were cultured at low passage (3-5) and seeded on 6-well plates at $5x10^4$ cells/well in EGM-2 BulletKit (Lonza), 5% CO_2 at 37℃. Normal conditions required continued culture in unsupplemented media.

Ficoll was chosen as the crowding agent due to its hydrodynamic charge and relatively small hydrodynamic radius. Ficoll has a neutral net charge and hydrodynamic radii of 4 and 8 nm for the 70 kD and 400 kD molecular weights, respectively (Zeiger et al., 2012). For crowded conditions, EGM-2 media was removed after 4 h, and replaced with fresh EGM-2 or EGM-2 containing a mixture of 37.5 mg/mL Ficoll 70 kD and 25 mg/mL Ficoll 400 kD (GE Healthcare) and 100 μm L-ascorbic acid 2-phosphate (WAKO) (Chen et al., 2009). EGM-2-MV BulletKit (Lonza) was used in the same culturing method for HMEC-1. Cells were

cultured for 5 days under both normal and crowded conditions without media change. On day 6 of culture, the media was removed and cell layers were washed twice with DPBS. Cell layers were either fixed with ice-cold methanol or 4% formaldehyde for immunocytochemical staining or decellularised for ECM harvesting.

4.2.2 ECM harvesting

The *in situ* HUVEC cell layer was decellularised by detergent-based lysis washing. Cells were initially detached with 0.2% (w/v) ethylenediaminetetraacetic acid (EDTA) for ~5 min at 37℃. Remaining cells were lysed on a rocker at 4℃ with either 0.5% (w/v) sodium deoxycholate (DOC, Sigma) or 1% (v/v) Nonidet P-40 solution containing 0.5x protease inhibitor cocktail (Roche) for 10 min. The lysis was repeated a total of five to eight times, with a final lysis step replacing the DOC solution with 0.5% (w/v) DOC/DPBS. The ECM was then washed three times with DPBS and stored at 4℃ until use. Fluorescence staining for F-actin (phalloidin), nuclear material (DAPI) and/or protein disulfide isomerase were used to gauge the efficiency of cell material removal. ECM integrity was characterised by immunfluorescence staining for various ECM components (see Section 4.2.3).

4.2.3 MIN6 β-cell culture

The MIN6 insulinoma cell line was cultured as previously described in Chapter 3. Briefly, cells were cultured in high glucose DMEM (Gibco) with or without the addition of the macromolecular cocktail, 37.5 mg/mL Ficoll 70 kD and 25 mg/mL Ficoll 400 kD (GE Healthcare) (Chen et al., 2009). Cells were cultured for 5 days

with one media change on the third day. Cells were then washed three times with DPBS and fixed with methanol for immunocytochemical staining.

4.2.4 Immunocytochemistry

Primary antibodies were either commercially purchased or generously donated from collaborating laboratories. Refer to Table 3.1 for the sources and dilutions of primary and fluorescent secondary antibodies. Fluorescently labelled secondary antibodies were heavy and light chain-recognising AlexaFluor IgG from Molecular Probes through Invitrogen.

In situ HUVEC cell layers or decellularised ECM were fixed with ice-cold methanol for 10 min and allowed to air-dry. Samples were blocked with 3% (w/v) bovine serum albumin in Dulbecco's phosphate-buffered saline (BSA/DPBS, Sigma) for 30 min-1 h at room temperature. Primary antibodies (Table 3.1) were diluted in 3% (w/v) BSA/DPBS and incubated for 1.5 h at room temperature or overnight at 4ºC. Conjugate controls were incubated with 3% (w/v) BSA/DPBS only. Isotype controls were normal IgG of the same species and at the same concentration as the primary antibody. Samples were washed for 10 min with DPBS for three times. Samples were incubated with AlexaFluor-conjugated secondaries (Molecular Probes/Invitrogen), diluted 1:400 with 3% BSA/DPBS, in the dark at room temperature for 30 min. Samples were washed three times with DPBS for 10 min. Samples were incubated with 4',6-diamidino-2-phenylindole, dilactate (DAPI, Molecular Probes/Invitrogen), diluted 1:1000 with DPBS, in the dark at room temperature for 10 min. Slides were washed three times with DPBS for 10 min and

stored in DPBS at 4℃. Three images per well were taken at either 20x or 40x magnification with a Leica DMIL microscope.

4.2.5 Semi-quantitative analysis of ECM

4.2.5.1 Bicinchoninic acid (BCA) assay

The bicinchoninic acid (BCA) assay (BCA kit for protein determination, Pierce) was used to quantify the amount of ECM proteins that were present in the HUVEC ECM. After DOC decellularisation, the BCA reagents were added directly to the HUVEC ECM, and then measured for absorbance at 562 nm. Varying concentrations of BSA was used to create a standard curve and the proteins present in the HUVEC ECM were then extrapolated.

4.2.5.2 Dimethylmethylene blue binding (DMMB) Assay

To quantify the amount of glycosaminoglycans that were present in the HUVEC ECM, the 1,9-dimethylmethylene blue (DMMB) assay was used. After DOC decellularisation of the HUVEC ECM, DMMB was added directly onto the ECM and incubated for 30 min. Heparin was used to create a concentration standard curve and the heparan sulfate concentrations in the crowded and uncrowded HUVEC ECM was thus extrapolated.

4.2.5.3 Quantitative pixel analysis

Immunofluorescent pixels of three images of three trials and taken under the same magnification were quantified by ImageJ software and normalised to the number of DAPI-stained nuclei observed in the same image. Cell-normalised pixels from three

images per batch of staining were averaged and three batches of crowded and non-crowded HUVEC cell layers were compared.

4.2.6 Morphology of β-cells and HUVEC ECM after 2 days of culture

The MIN6 insulinoma cell line was seeded onto HUVEC ECM (made with and without crowders), tissue culture plastic or Matrigel® (BD Biosciences) and cultured in high glucose DMEM (Gibco) for 2–5 days. Cells were washed with DPBS and fixed with either 4% formaldehyde or ice-cold methanol. Collagen IV, fibronectin, laminin, perlecan, syndecan-4 and heparan sulfate were stained using the immunocytochemical staining methodology described in Section 4.2.3.

4.2.7 Statistical analysis

Statistical analyses were performed using the Minitab software. The General Linear Model of ANOVA was used to compare significance of difference between ECM components deposited under crowded and uncrowded conditions.

4.3 Results

4.3.1 Cell line vs. primary endothelial cells

Low amounts of matrix were produced by HMEC-1 cell line in comparison with primary HUVECs, which produced significant amounts of ECM. In both cell types, crowded conditions enhanced matrix production. As seen in Figure 4.1, the majority of collagen IV, fibronectin and laminin detected in HMEC-1 matrix was intracellular and there appeared to be more staining of each component in cells grown under crowded conditions (b, d, f) compared to the normal control (a, c, e). After decellularisation with 0.5% DOC, almost no ECM remained from the normal HMEC-1s, and very little ECM was observed on the tissue culture plastic of the crowded HMEC-1s (Figure 4.2).

In contrast, primary HUVECs appeared to deposit a significant amount of various ECM components into the extracellular space under both normal and crowded conditions. Collagen IV, VI and XVIII, fibronectin, laminin, perlecan, nidogen, von Willebrand factor, syndecan-1 and -4, glypican-1, heparan sulfate and chondroitin sulfate were all detected in the cell layer (Figures 4.3-4.6). HUVECs grown in the presence of crowders appeared to have more ECM deposited into the extracellular space, whereas uncrowded HUVECs tended to retain their ECM intracellularly or within close proximity to the cell surface. During methanol fixation, crowded cells also remained adherent on the tissue culture plastic (TCP) more readily than those grown without crowders. Therefore, the observed increase in presence of ECM in crowded HUVECs may have been a result of better adherence as opposed to

increased production and/or deposition of ECM. However, better adherence may also have resulted from increased ECM deposition and stabilization as a function of the crowders. In addition, uncrowded cells appeared to either adhere to each other rather than the TCP, or the ECM they deposited tended to delaminate off the TCP quite easily during methanol fixation. It was therefore crucial to quantitate the relative amounts of ECM produced on a per cell basis under both conditions to verify whether ECM deposition was enhanced.

4.3.2 Quantitation of ECM deposition in the HUVEC cell layer

Cell number-normalised pixel quantitation of collagen IV, laminin, fibronectin, perlecan and heparan sulfate all showed a statistically significant 2-6 fold increase in deposition under crowded conditions (Table 4.1, Figures 4.7-4.8). Deposition of perlecan and heparan sulfate into the cell layer showed the highest difference between crowded and uncrowded HUVECs.

Table 4.1 Comparison of quantitated fluorescent pixel counts of ECM components in the HUVEC cell layer, deposited under crowded and uncrowded conditions.

ECM component	-MMC (pixels)	+MMC (pixels)	Fold change	P-value
Collagen IV	1363 ± 294	2805 ± 909	2.1	0.012
Laminin	1255 ± 344	5086 ± 778	4.1	0.013
Fibronectin	1242 ± 55	4217 ± 264	3.4	0.004
Perlecan	643 ± 60	3959 ± 927	6.2	0.037
Heparan sulfate (10E4)	678 ± 51	3551 ± 303	5.2	0.001

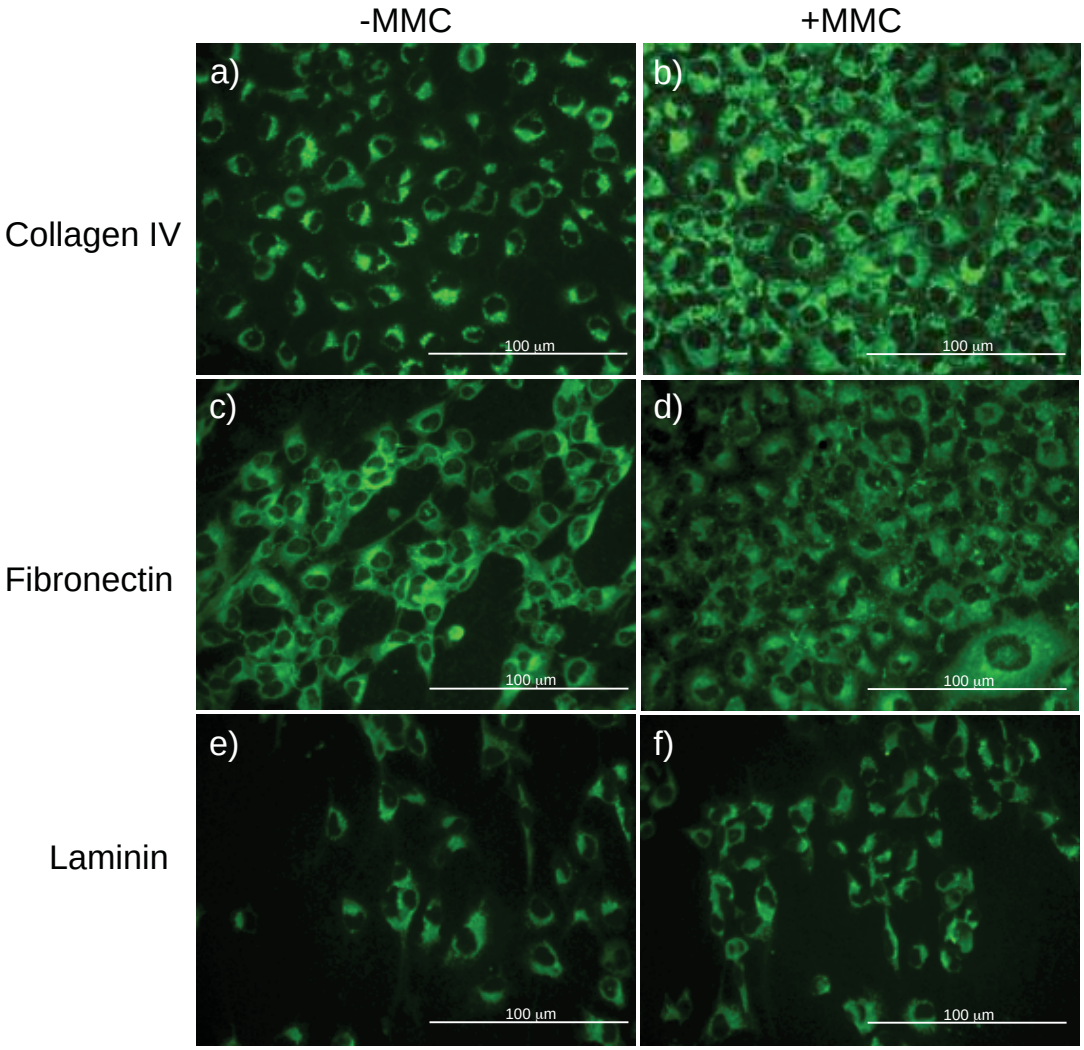

Figure 4.1 Immunocytochemical staining of collagen IV (a, b), fibronectin (c, d) and laminin (e, f) in human microvascular endothelial cell layer under normal (-MMC) or crowded (+MMC) conditions. Scale bar: 100 μm

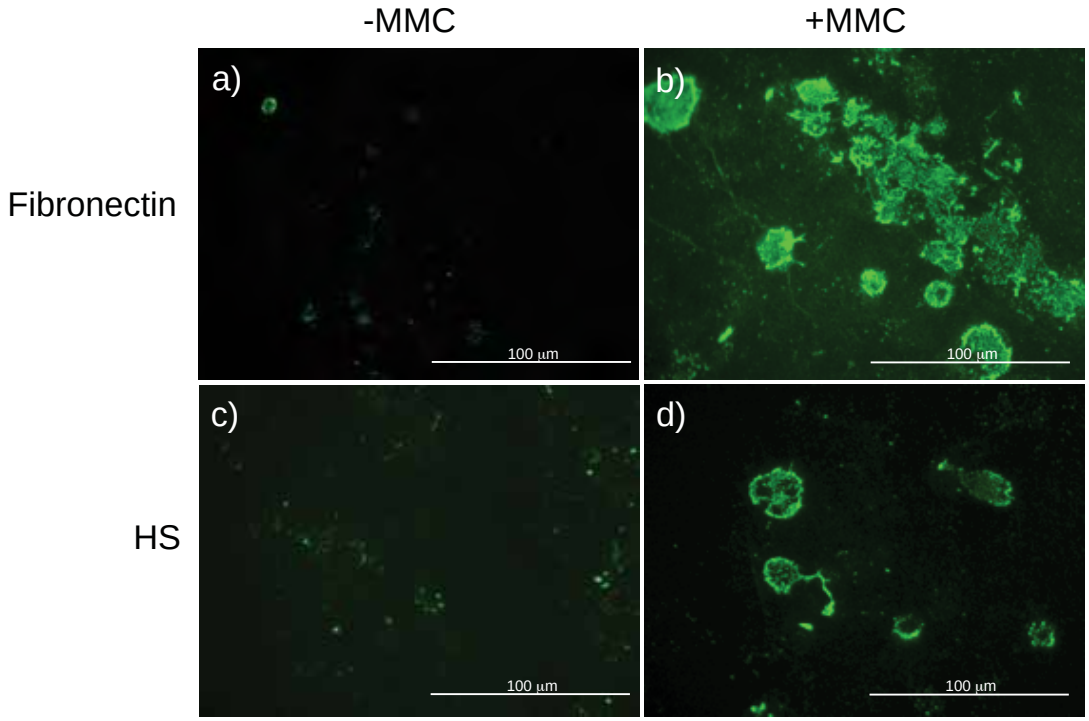

Figure 4.2 Immunocytochemical staining of fibronectin (a, b) and HS 10E4 (c, d) in human microvascular endothelial ECM deposited under normal (-MMC) or crowded (+MMC) conditions.

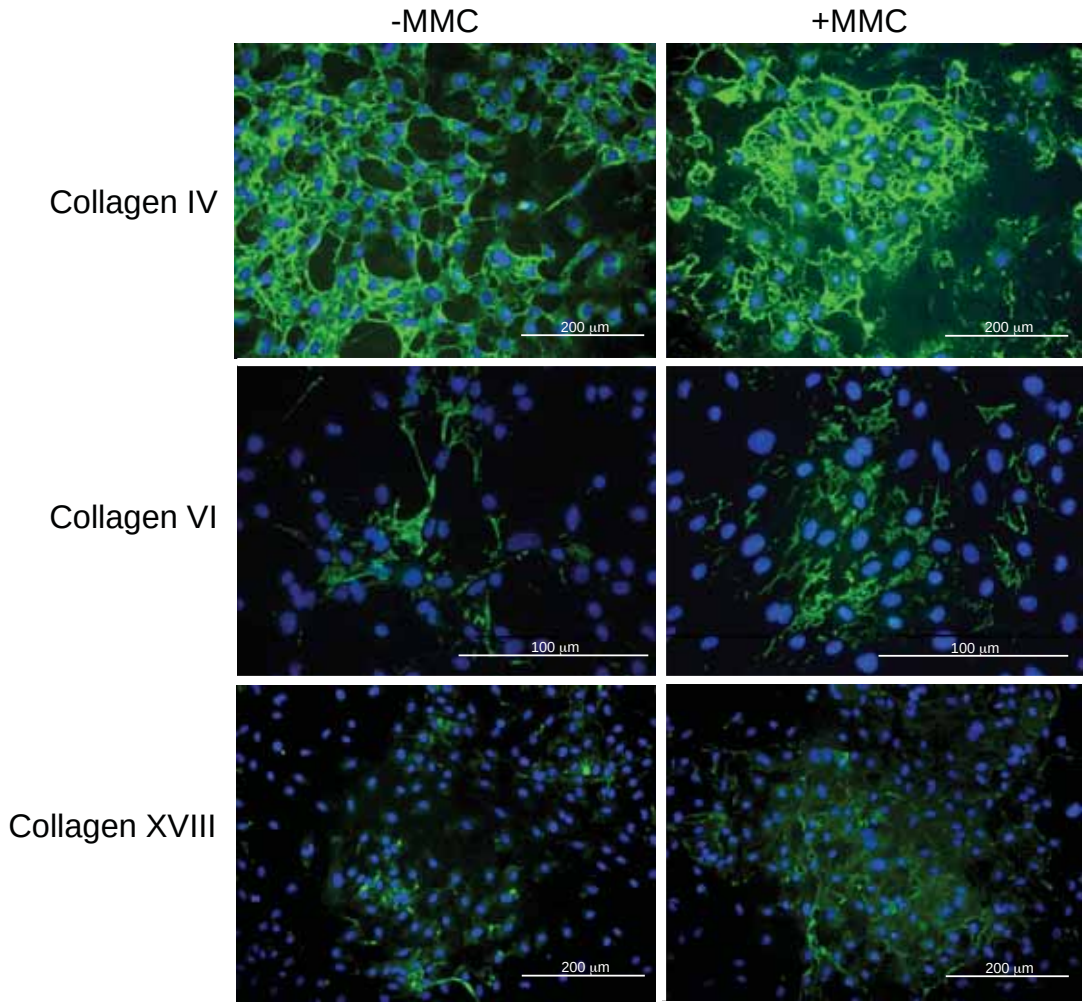

Figure 4.3 Immunocytochemical staining of collagen IV, VI and XVIII in human umbilical cord vein endothelial cells (HUVECs) under normal (-MMC) or crowded (+MMC) conditions.

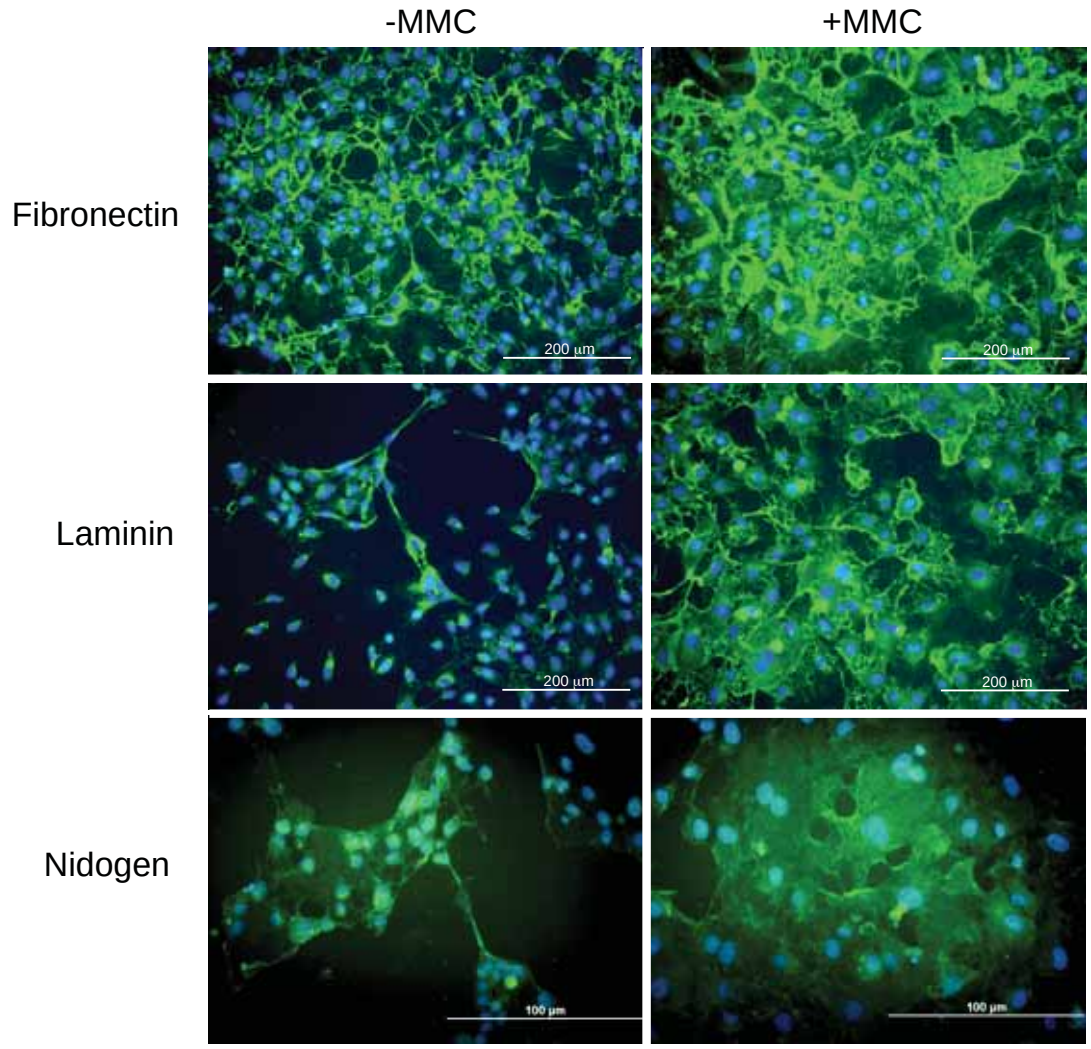

Figure 4.4 Immunocytochemical staining of fibronectin, laminin and nidogen in human umbilical cord vein endothelial cells (HUVECs) under normal (-MMC) or crowded (+MMC) conditions.

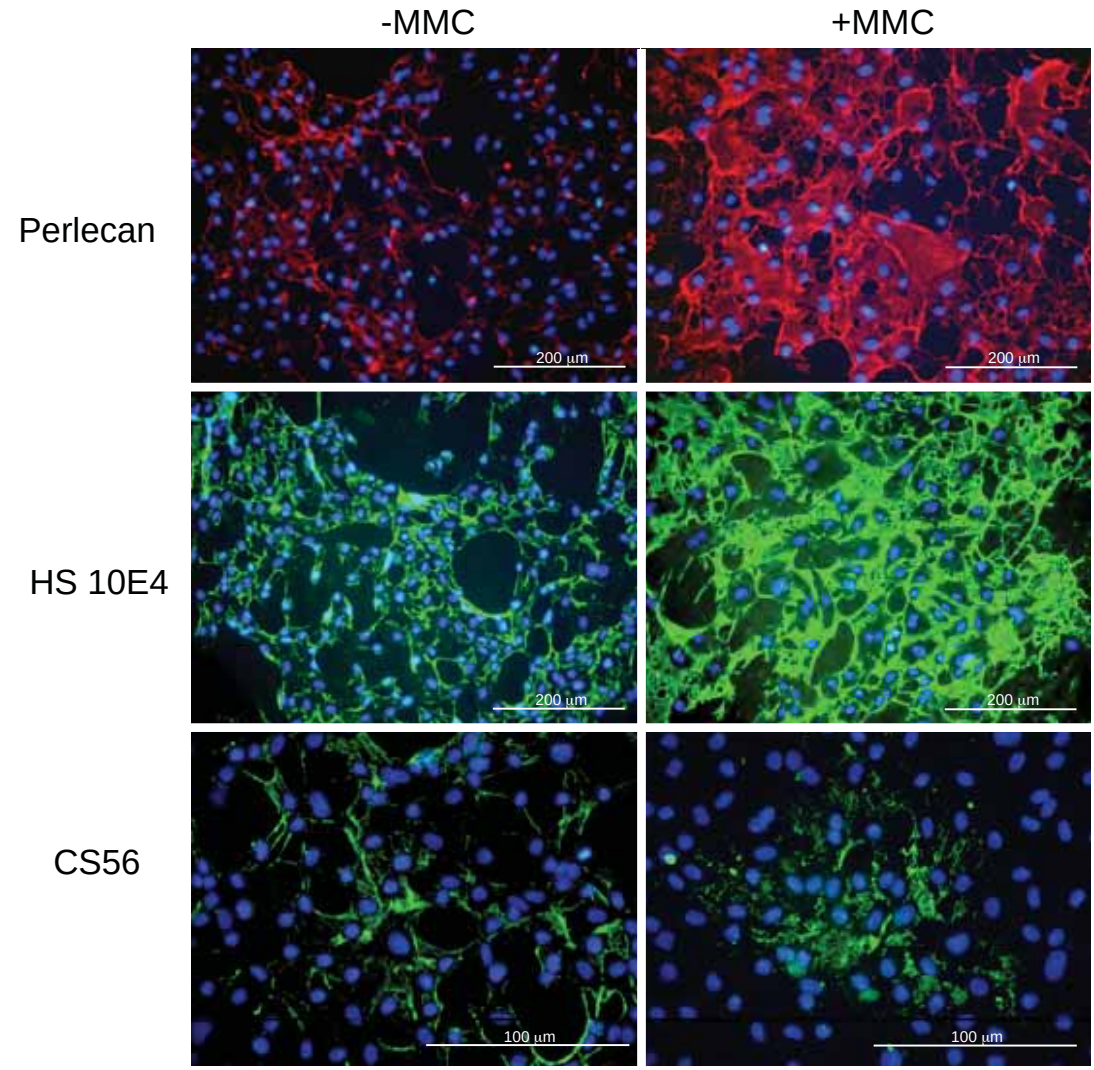

Figure 4.5 Immunocytochemical staining of perlecan, heparan sulfate (HS 10E4) and chondroitin sulfate (CS56) in human umbilical cord vein endothelial cells (HUVECs) under normal (-MMC) or crowded (+MMC) conditions.

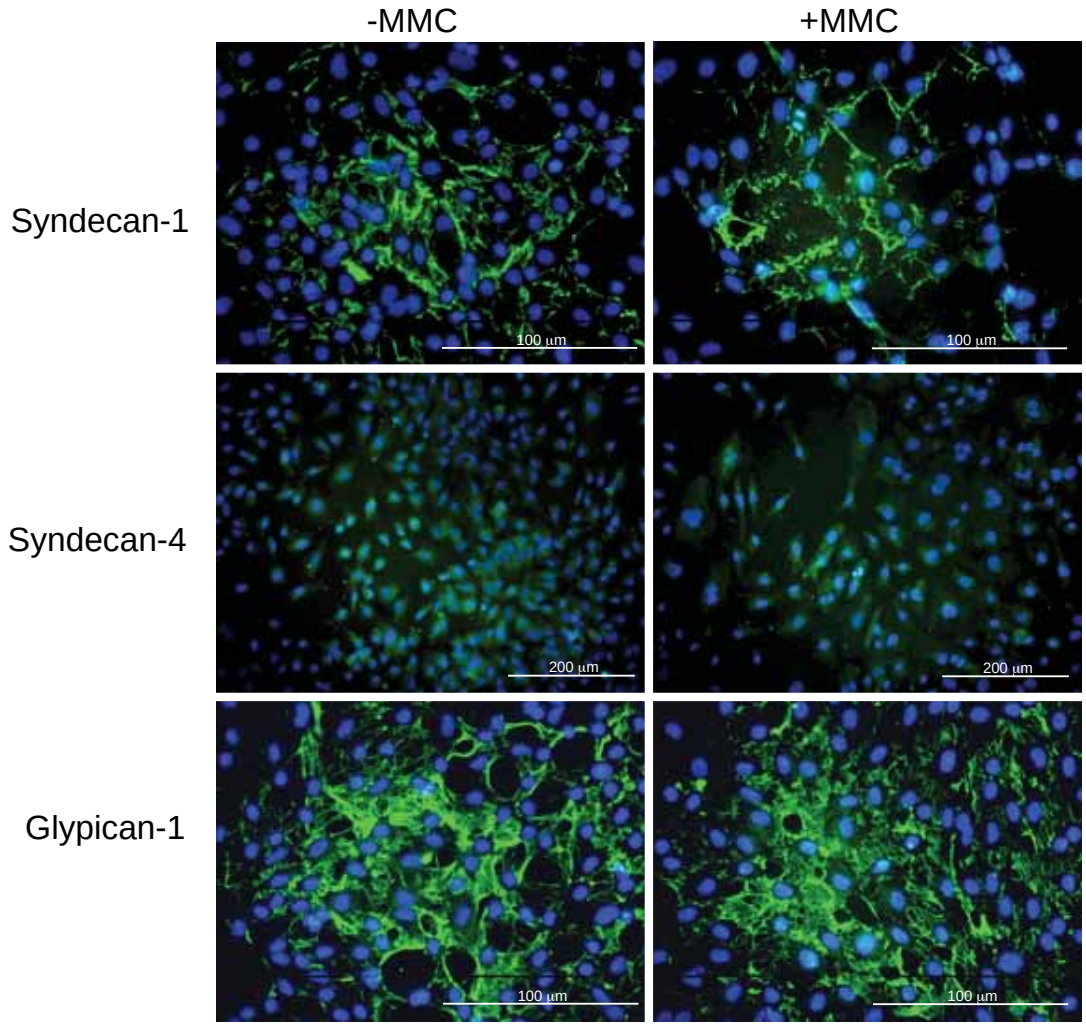

Figure 4.6 Immunocytochemical staining of syndecan-1, syndecan-4 and glypican-1 in human umbilical cord vein endothelial cells (HUVECs) under normal (-MMC) or crowded (+MMC) conditions.

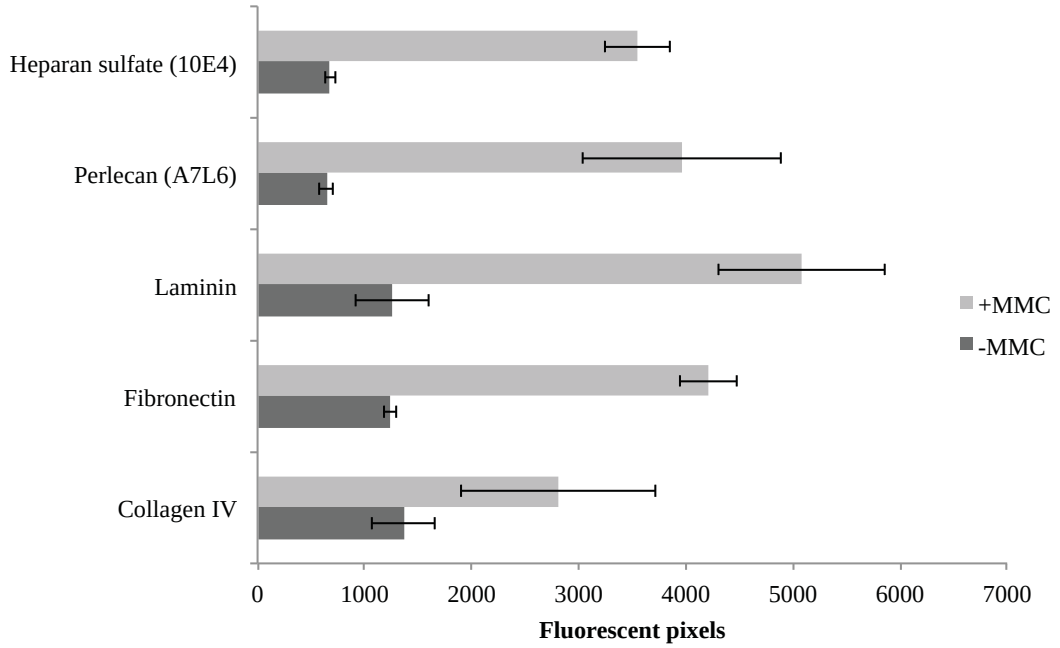

Figure 4.7 Comparison of quantitated fluorescently stained components deposited under normal (-MMC) or crowded (+MMC) conditions.

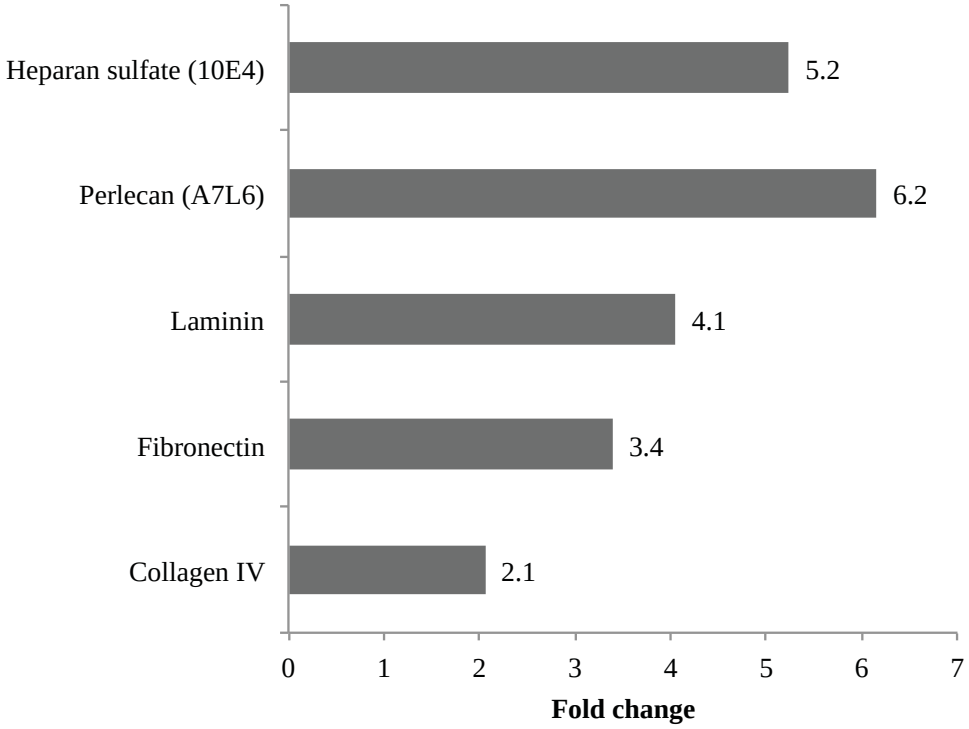

Figure 4.8 Fold change of quantitated fluorescently stained components deposited under crowded conditions normalised to normal conditions.

4.3.3 Endothelial cell ECM harvesting

Comparison of Nonidet P-40 (NP-40) and sodium deoxycholate (DOC) for effectiveness in removing cellular material from the HUVEC layer without causing damage to or loss of the various ECM components showed that DOC was more effective. NP-40 was found to be ineffective in the complete removal of cell material. In Figure 4.9, remaining presence of cell nuclei (DAPI) and F-actin (phalloidin) could be observed in both crowded and uncrowded cell layers. DOC on the other hand, was generally successful in removing most of the cell material from the TCP (Figure 4.10). However, crowded HUVECs required several more rounds of DOC and DPBS washes, as cell debris and remnant nuclei would remain in the cell layers when three rounds of DOC washing were implemented. In contrast, three rounds of DOC washing were sufficient in removing most of the cellular material from the TCP in the uncrowded HUVECs.

After DOC lysis, ECM components were detected by immunocytochemistry. Collagen IV, fibronectin, laminin, perlecan and heparan sulfate all remained intact in the ECM that was made with crowders (Figures 4.11-12), and remnants of collagen VI and XVIII, syndecan-1, glypican-1 and CS were also detectable. In contrast, a substantial amount of these components were washed away from the TCP in the ECM that were made without crowders (Figures 4.13-14). Interestingly, despite the presence of syndecan-4 detected in the HUVEC cell layer, this HS-proteoglycan was not detected in the HUVEC ECM after DOC decellularisation (Figure 4.12c and 4.14c), whereas syndecan-1 and glypican-1 were detected even after DOC.

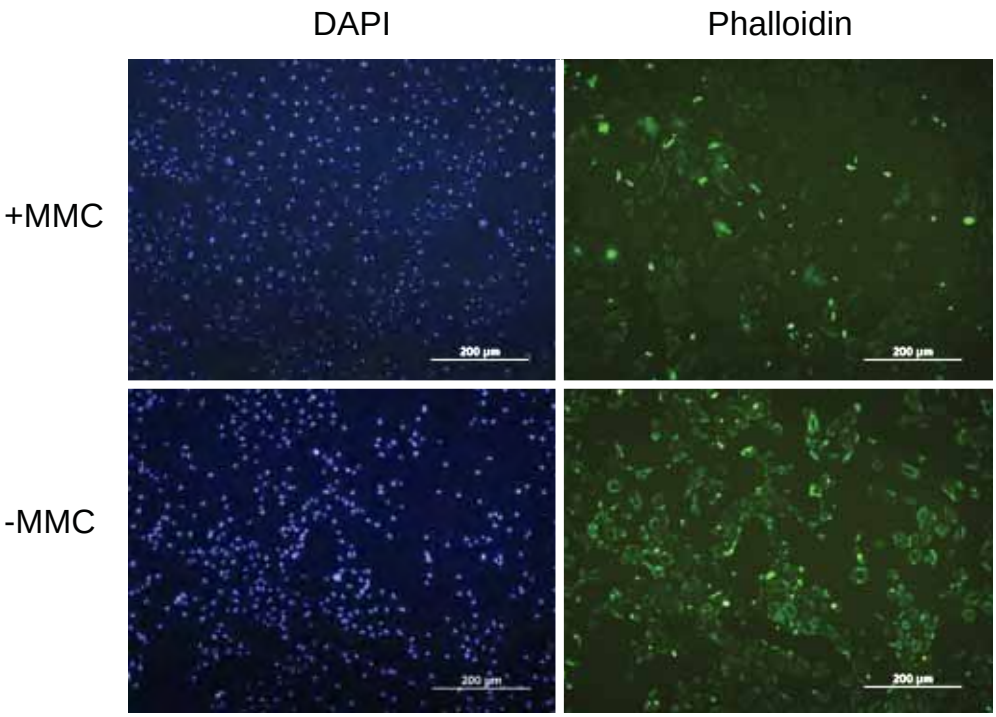

Figure 4.9 Fluorescently labeled nuclear material (DAPI, blue) and F-actin (Phalloidin, green) in HUVEC ECM after NP-40 decellularisation.

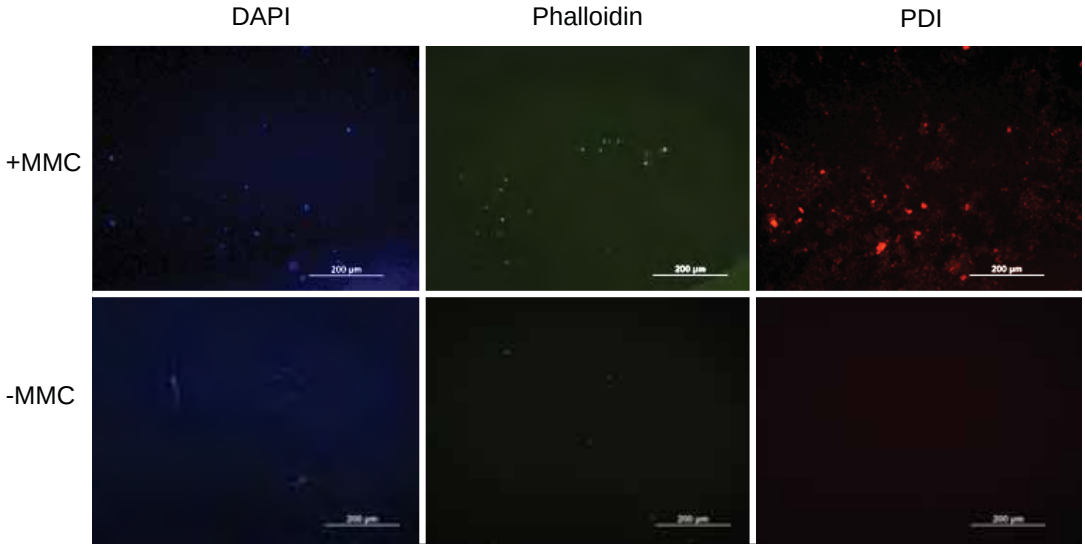

Figure 4.10 Fluorescently labeled nuclear material (DAPI, blue), F-actin (Phalloidin, green) and protein disulfide isomerase (PDI, red) in HUVEC ECM after sodium deoxycholate decellularisation.

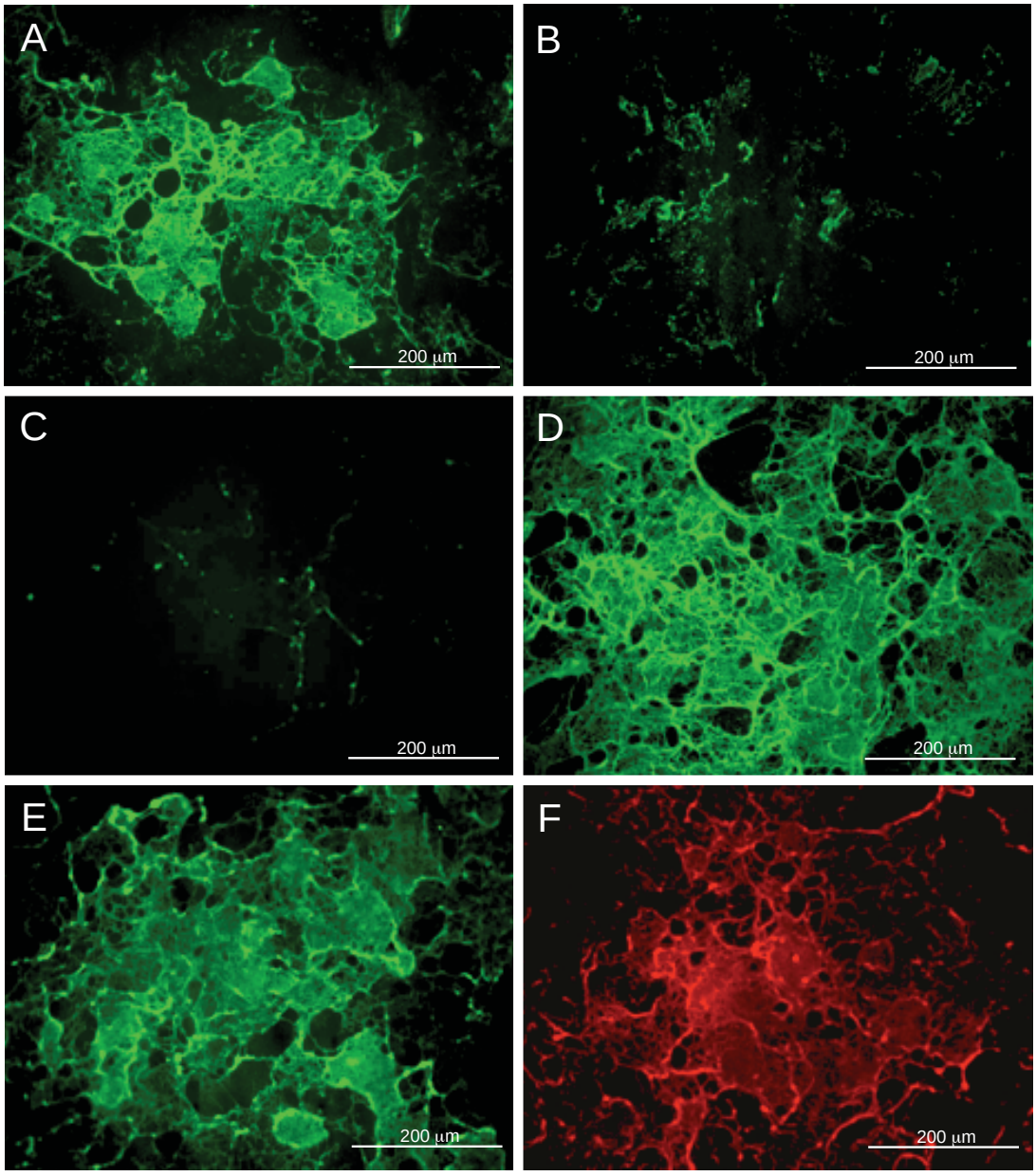

Figure 4.11 Immunocytochemical staining of collagen IV (A), VI (B) and XVIII (C), fibronectin (D), laminin (E) and perlecan (F) in HUVEC ECM deposited under crowded conditions.

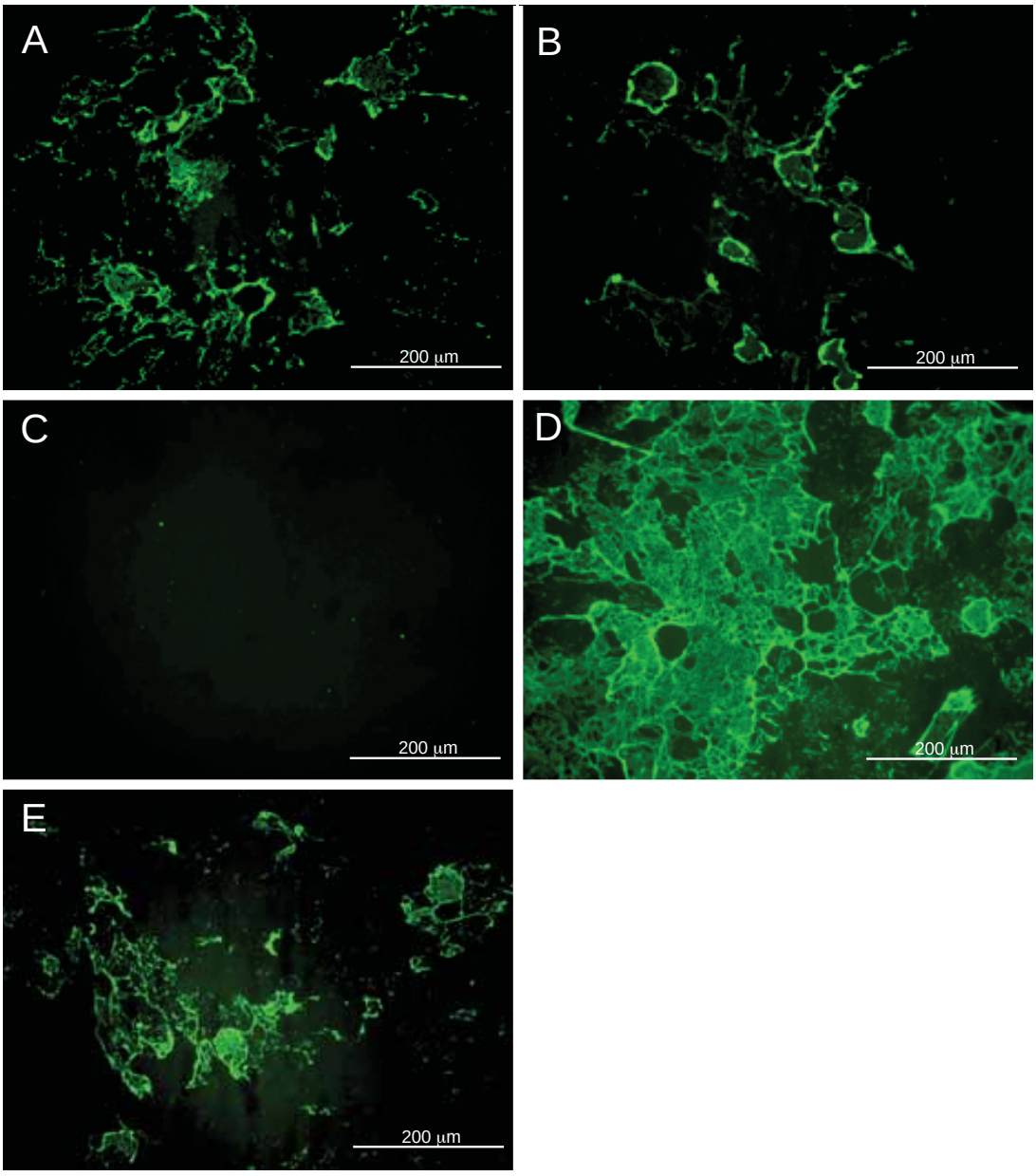

Figure 4.12 Immunocytochemical staining of syndecan-1 (A), glypican-1 (B) syndecan-4 (C), HS 10E4 (D) and CS56 (E) in HUVEC ECM deposited under crowded conditions.

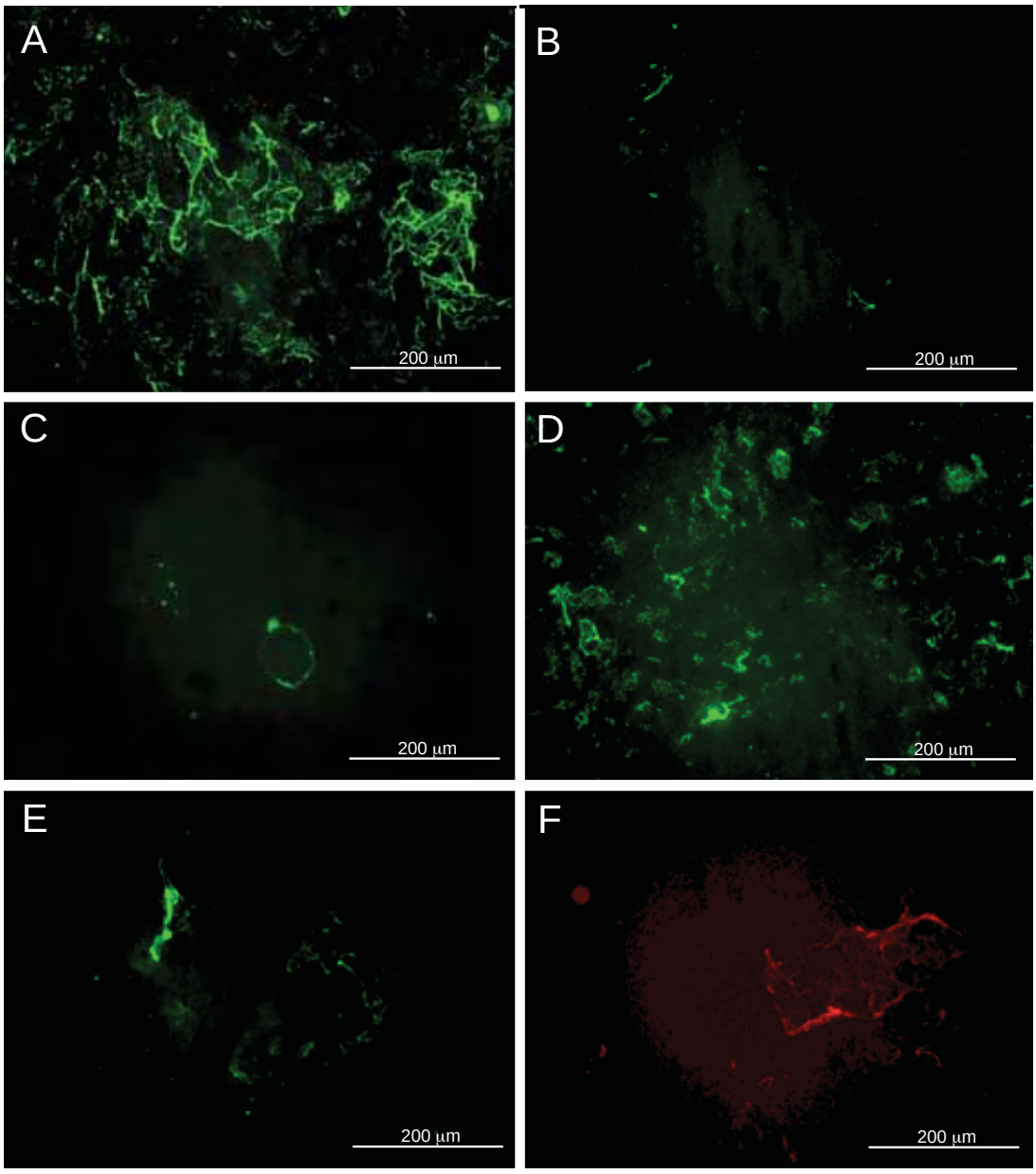

Figure 4.13 Immunocytochemical staining of collagen IV (A), VI (B) and XVIII (C), fibronectin (D), laminin (E) and perlecan (F) in HUVEC ECM deposited under normal conditions.

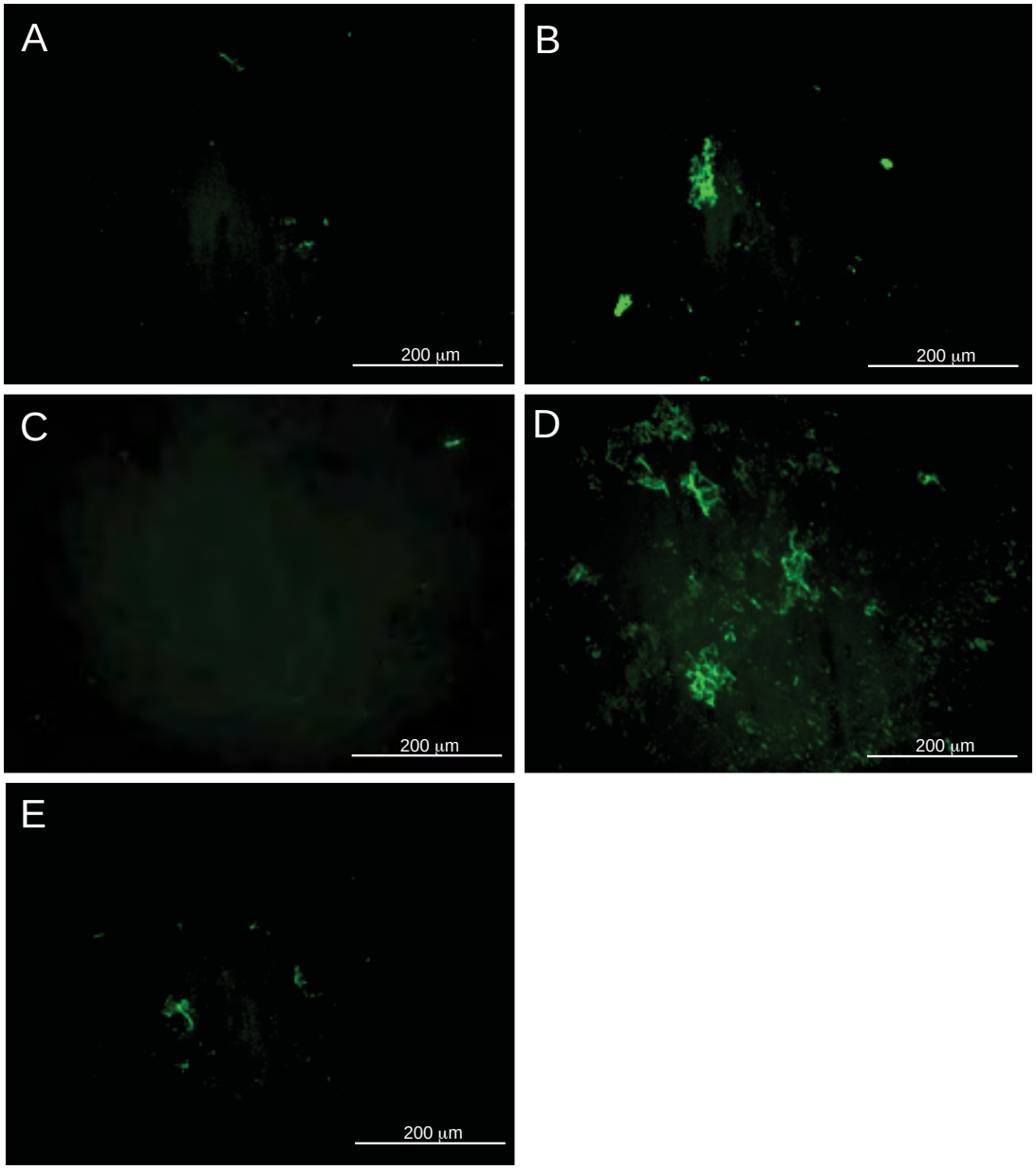

Figure 4.14 Immunocytochemical staining of syndecan-1 (A), glypican-1 (B) syndecan-4 (C), HS 10E4 (D) and CS (E) in HUVEC ECM deposited under normal conditions.

4.3.4 Quantitation of ECM content after decellularisation

Fluorescent images of immunostained ECM components obtained after decellularisation were not normalised as all cellular material were removed. Quantitated pixels of laminin, fibronectin, perlecan and heparan sulfate all showed a statistically significant 7.8-47.1-fold increase in remaining ECM under crowded conditions (Table 4.2, Figures 4.15-16). Though collagen IV also showed a 2.4-fold increase, this was not significant. The components laminin and fibronectin showed the highest fold difference between crowded and uncrowded decellularised HUVEC ECM.

Table 4.2 Comparison of quantitated pixel counts of ECM components deposited under crowded and uncrowded conditions, after decellularisation

ECM component	-MMC (pixels)	+MMC (pixels)	Fold change	P-value
Collagen IV	98437 ± 32711	237113 ± 98125	2.4	0.162
Laminin	10878 ± 4078	512095 ± 46459	47.1	0.001
Fibronectin	34384 ± 757	742031 ± 90779	21.6	0.002
Perlecan	14265 ± 9738	270856 ± 36953	19.0	0.003
Heparan sulfate (10E4)	50937 ± 11290	397120 ± 85104	7.8	0.006

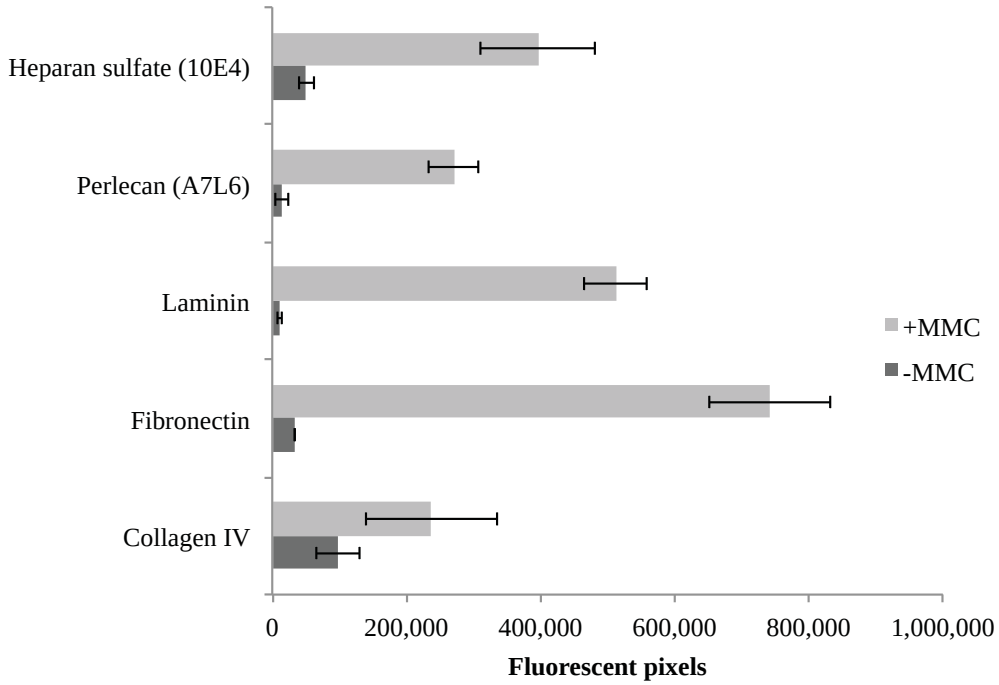

Figure 4.15 Comparison of quantitated, DOC decellularized, fluorescently stained components that were deposited under normal (-MMC) or crowded (+MMC) conditions.

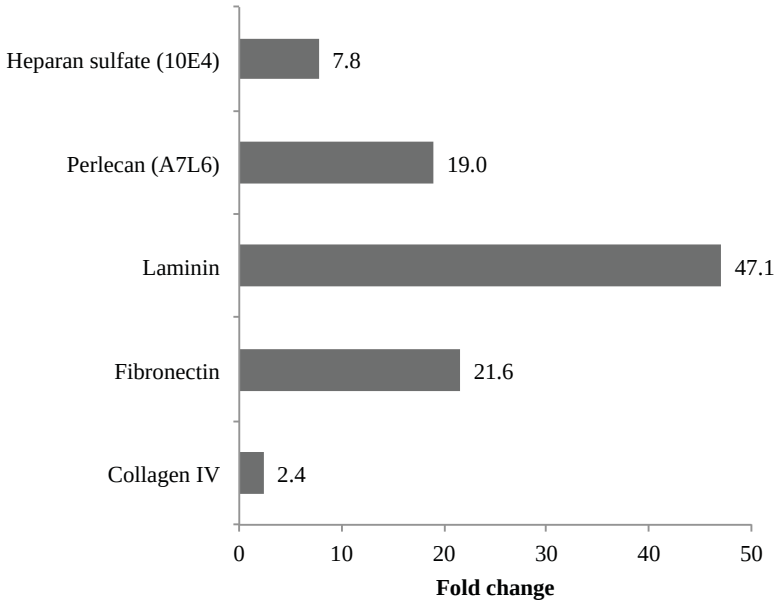

Figure 4.16 Fold change of quantitated, DOC decellularized, fluorescently stained components that were deposited under crowded conditions normalised to normal conditions.

Protein and glycosaminoglycan (GAG) content in the sodium deoxycholate-decellularised ECM were also quantified by BCA and DMMB assay (Table 4.3). The BCA assay showed a statistically significant 1.1-fold increase in protein content, while the DMMB assay only showed a 1.2-fold change in GAG content. It should be noted that BSA and heparin were used as standards in the BCA and DMMB assays, respectively, which may have lead to an underestimation of the results.

Table 4.3 Protein and glycosaminoglycan (GAG) concentrations in normal (-MMC) and (+MMC) crowded HUVEC ECM after decellularisation, as quantitated by BCA and DMMB assays. BSA and heparin were used as standards in the BCA and DMMB assays, respectively.

		Concentration (μg/mL)			
Assay	**Component measured**	**-MMC**	**+MMC**	**Fold change**	**P-value**
BCA	Protein	26.91 ± 1.63	29.52 ± 1.68	1.1	0.004
DMMB	GAG	15.20 ± 0.91	17.58 ± 1.19	1.2	0.003

4.3.5 Enhancing MIN6 ECM production by macromolecular crowding

The antibodies for collagen IV and XVIII, fibronectin, EHS laminin and perlecan used in this study did not react with any of these ECM components in the MIN6 cell layer under normal and crowded conditions (data not shown). Furthermore, crowding did not increase or decrease staining for syndecan-4 and the heparan sulfate stub (Figure 4.17).

4.3.6 MIN6 morphology when in contact with HUVEC ECM

Matrigel® was initially used as a positive control but was not used in subsequent experiments as the MIN6s did not respond well to it. The MIN6s became irregularly clustered at day 2 and formed abnormal tubular-like patterns by day 5 of culture (Figure 4.18b). In contrast, the morphology of the MIN6s at 2 and 5 days after seeding onto the decellularised HUVEC ECM did not appear to be markedly different to those cultured on tissue culture plastic (TCP). Continued proliferation of the MIN6s was observed at both time points. Furthermore, the method of DOC decellularisation did not have an adverse effect on the MIN6s. After 2 days of culture, collagen IV, fibronectin, laminin and HS 10E4 were all still visible at the bottom of each well (Figure 4.19). However, similar to previous findings, less of these ECM components were detected in HUVEC ECM that were made without crowders (Figure 4.20). Syndecan-4 expression on the MIN6 cell surfaces was not affected by any of the cell supports (TCP, HUVEC ECM made with and without crowders) (Figure 4.21).

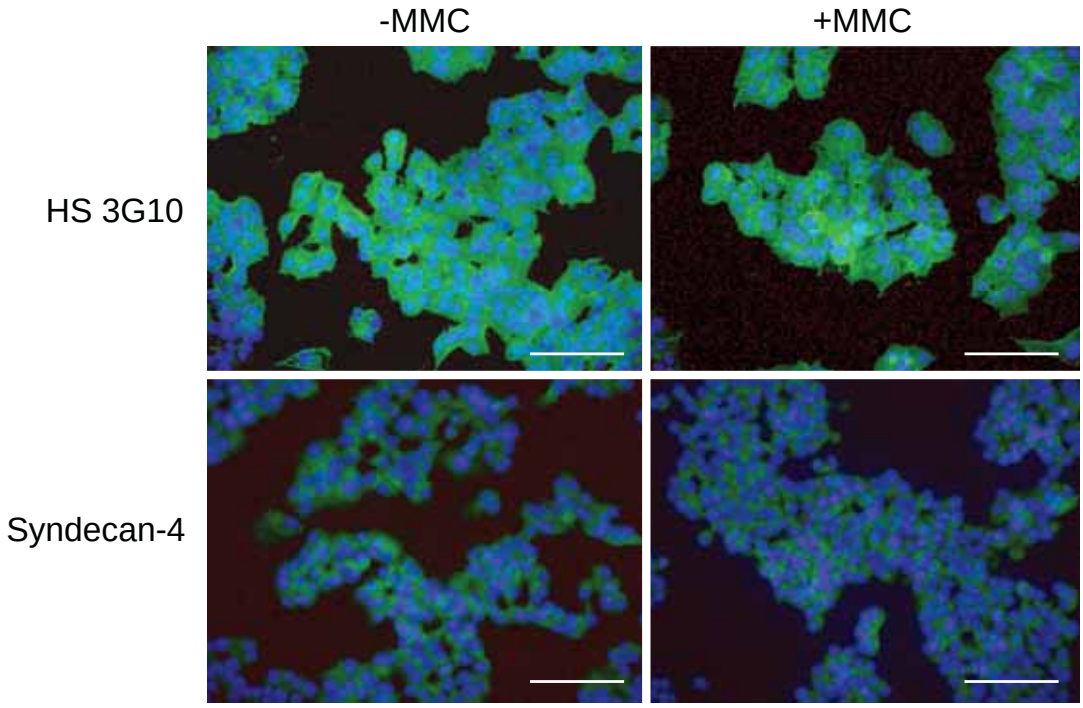

Figure 4.17 Immunostaining for heparan sulfate stub (HS 3G10) and syndecan-4 in the MIN6 cell layer cultured under normal (-MMC) and crowded (+MMC) conditions. Scale bar: 50 μm

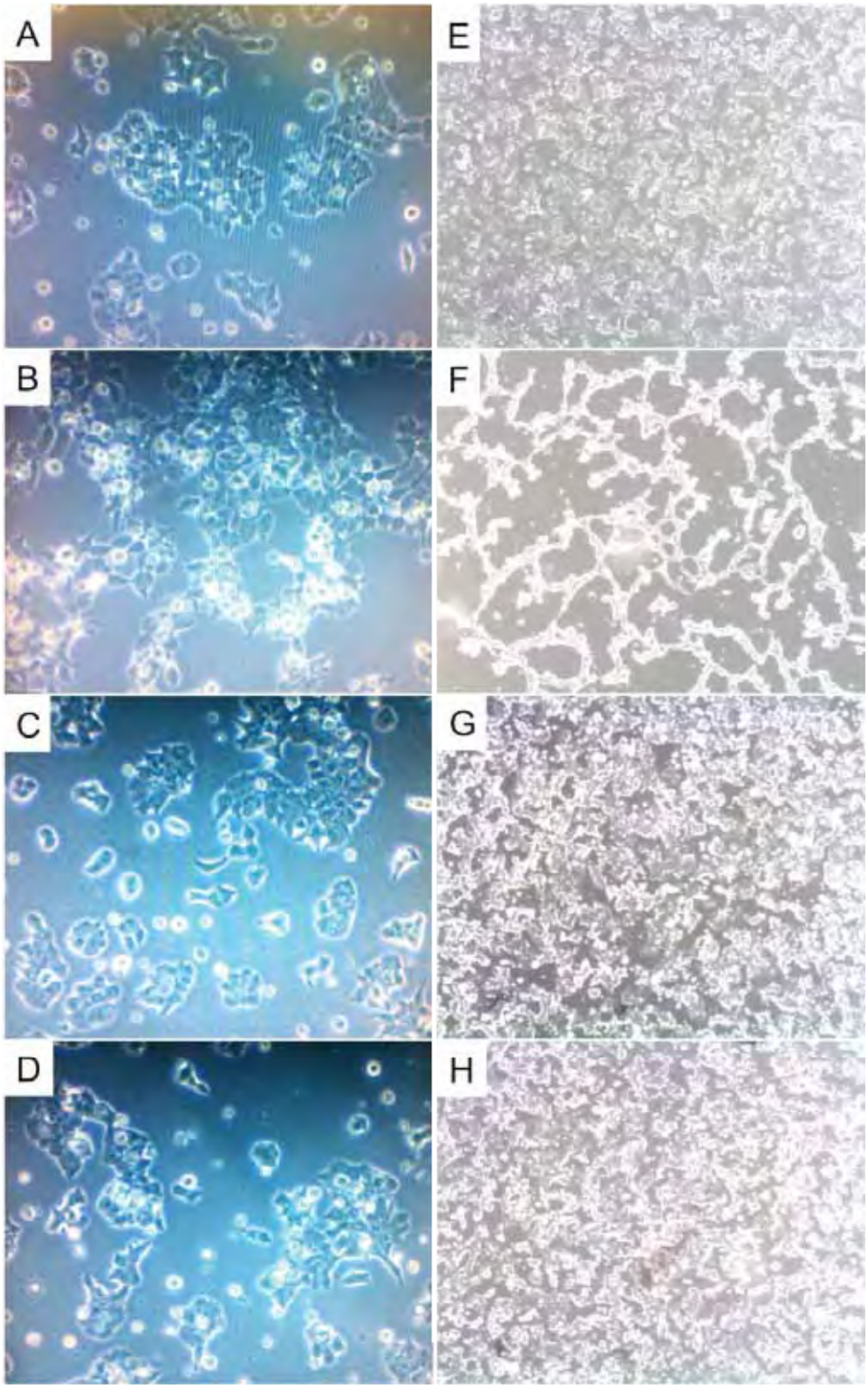

Figure 4.18 Morphology of MIN6 cells after 2 (left panel) and 5 days (right panel) of culture on (A, E) TCP, (B, F) Matrigel®, HUVEC ECM made (C, G) without and (E, H) with crowders.

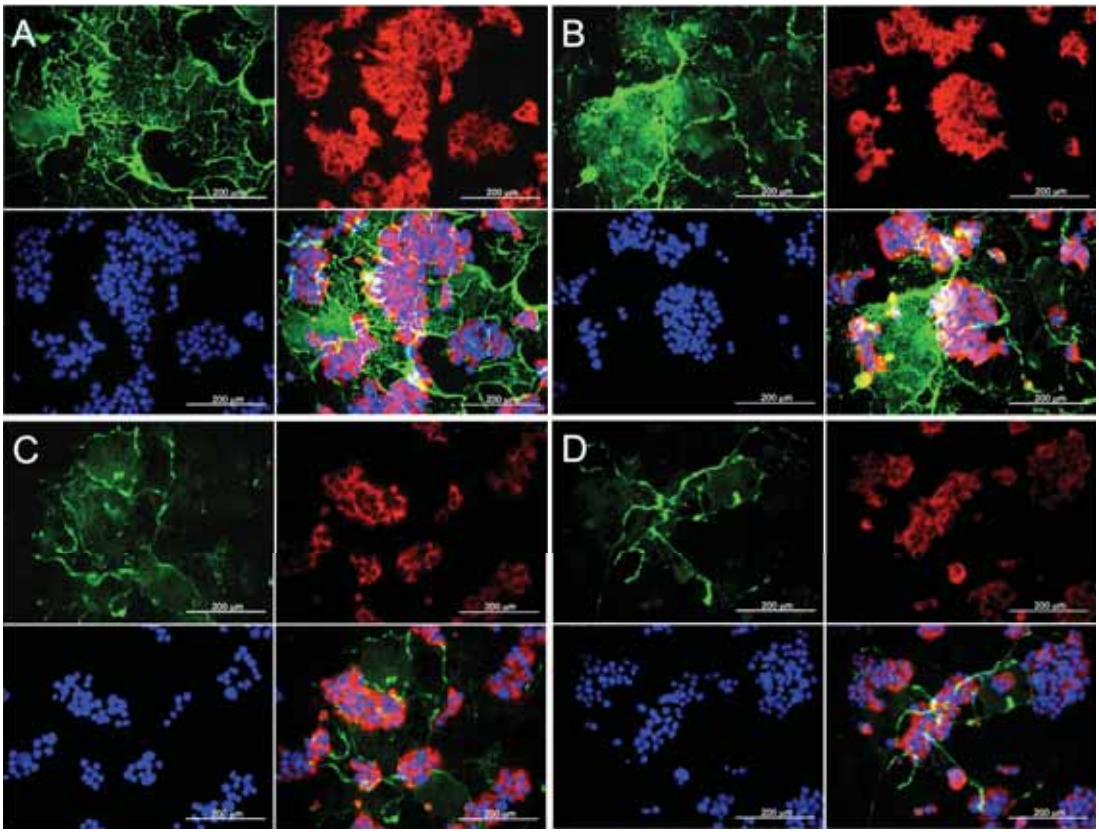

Figure 4.19 Immunolabelling of (a) collagen IV, (b) fibronectin, (c) laminin and (d) HS 10E4 (made with crowders) in green after 2 days of MIN6 seeding. Insulin is labelled in red and cell nuclei in blue. Scale bar: 200 μm

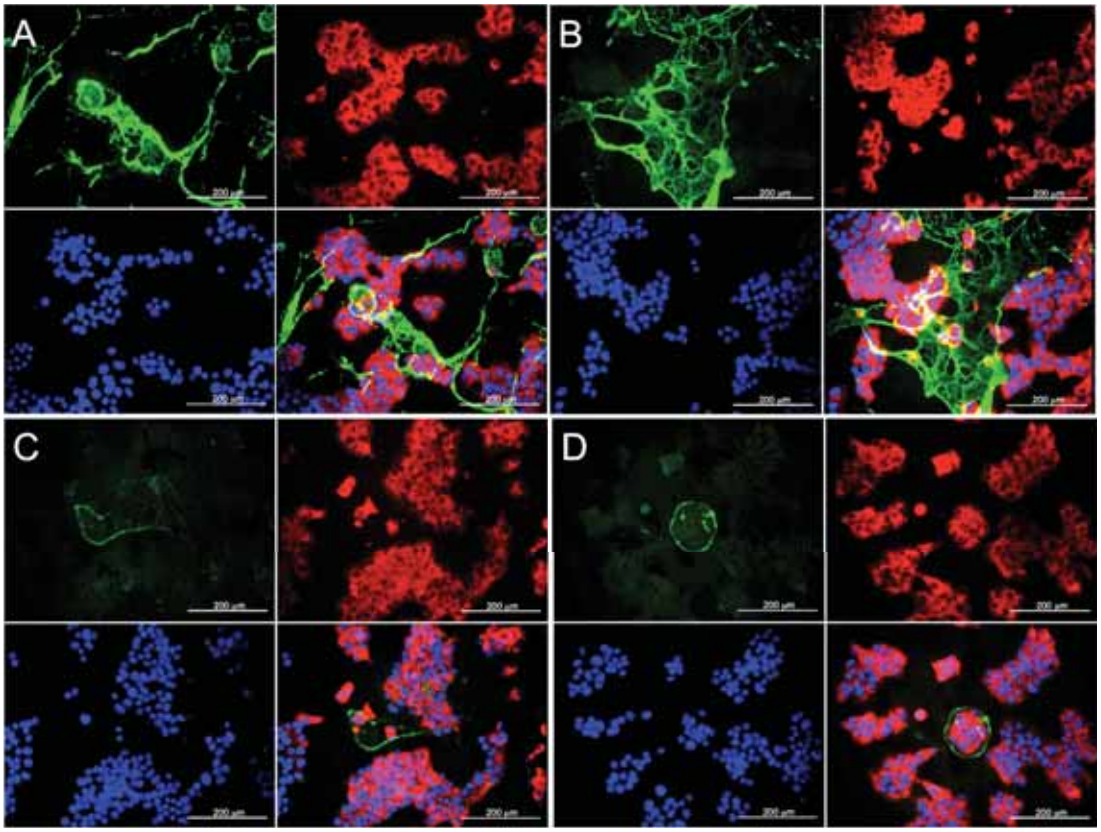

Figure 4.20 Immunolabelling of (a) collagen IV, (b) fibronectin, (c) laminin and (d) HS 10E4 (made without crowders) in green after 2 days of MIN6 seeding. Insulin is labelled in red and cell nuclei in blue. Scale bar: 200 μm

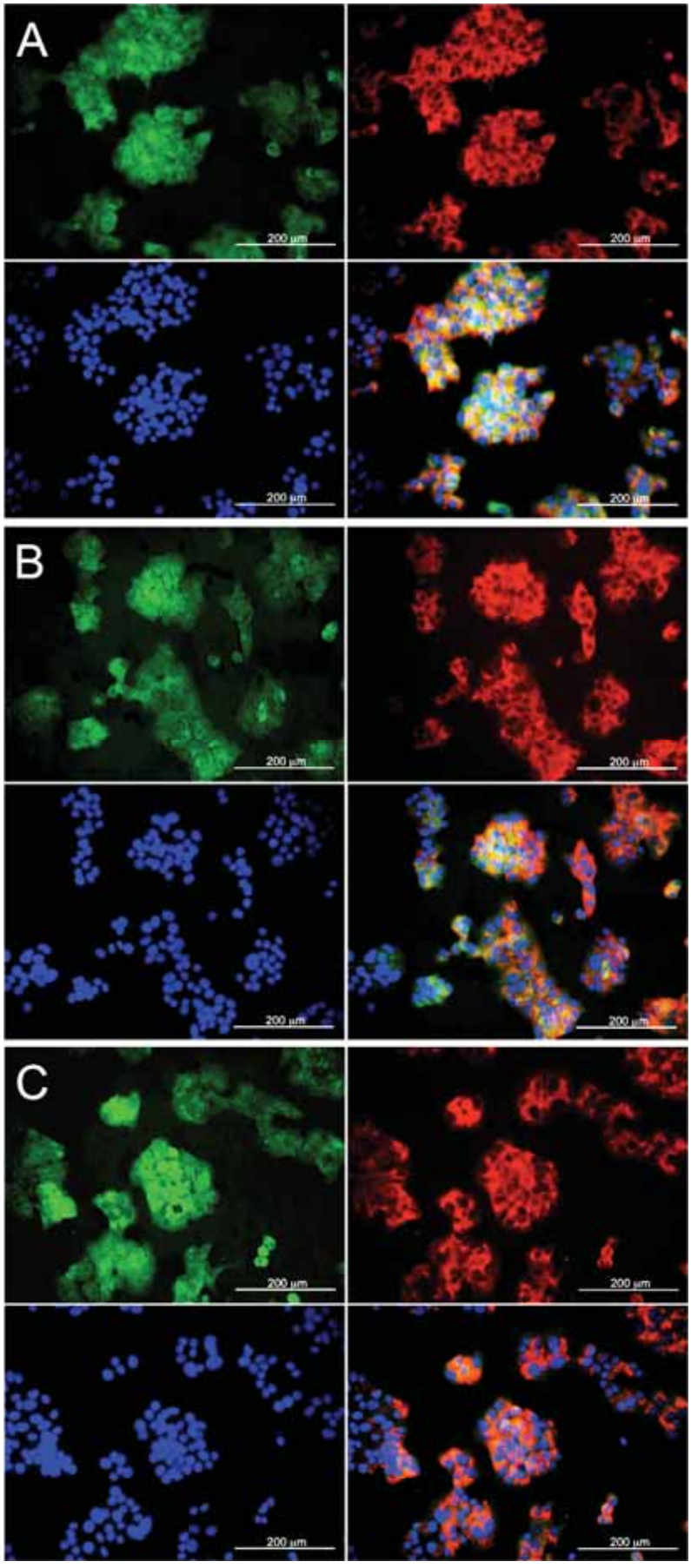

Figure 4.21
Immunolabelling for syndecan-4 on MIN6 cells cultured on (a) crowded, (b) uncrowded ECM and (c) TCP for 2 days. Insulin is labelled in red and cell nuclei in blue. Scale bar: 200 µm

4.4 Discussion

Extracellular crowding was increased by the non-interacting, neutral polymers Ficoll 70 and 400. This copolymer of sucrose and epichlorhydrine exhibits a mean hydrodynamic radius of ~4 nm (Fc70) or ~8 nm (Fc400) (Chen et al., 2011), is non-cytotoxic and does not significantly impact the viscosity of solutions at relevant concentrations (Folkow et al., 1971). Lareu et al. previously demonstrated that the addition of these macromolecules to the culture media of fibroblasts accelerated the enzymatic conversion of pro-collagen to collagen (Lareu et al., 2007a; Lareu et al., 2007b; Lareu et al., 2007c), which is a crucial prerequisite for the formation of insoluble collagen matrix. However, whether this could be achieved with endothelial cells and the effect of the enhanced ECM on the function of other cell types (eg. β-cells) have not yet been explored. This chapter studied the ECM produced by HMEC-1 and HUVECs under Ficoll crowding and whether the endothelial ECM had adverse effects on MIN6 β-cells. The concentration of macromolecule used represented the same order of magnitude as the total protein concentration found in blood plasma (80 mg/mL) (Chebotareva et al., 2004).

HMEC-1 produced low amounts of ECM and macromolecular crowding with Ficoll 70/400 could only slightly enhance the deposition (Figure 4.1-2). Nevertheless, collagen IV, laminin and fibronectin were detected in the cell layer and appeared to be mostly intracellular. The lack of ECM expression in HMEC-1 may be due to the fact the cells are a transformed cell line and there have been previous studies that show transformed cells to produce less ECM (Woods et al., 1984).

In contrast, HUVECs produced significantly more ECM and when cultured under crowded conditions, did not require an initial coating of ECM (such as gelatin or fibronectin) normally required for cell adherence to occur (Baudin et al., 2007; Cheung, 2007). The crowded HUVECs were also more resistant to de-lamination and deposited 2-6 times more ECM than cells that were cultured without crowders (Figure 4.7-8). Immunocytochemical staining of the HUVECs identified collagen IV, VI and XVIII, fibronectin, laminin, perlecan, nidogen, syndecan-1, glypican-1, heparan sulfate and chondroitin sulfate within the *in situ* cell layer (Figures 4.3-6). NP-40 was insufficient in removing cellular and nuclear material from the HUVEC ECM (Figure 4.9), while DOC was able to remove most of the cell debris and allowed ECM components including collagen IV, fibronectin, laminin, perlecan and HS to remain intact (Figures 4.11-14). ECM that were made with crowders were also more resistant to sodium deoxycholate (Figure 4.10) and 2-47 times more ECM remained on the well-plate after decellularisation compared to ECM that were made without crowders (Figures 4.15-16). The DOC-decellularised ECM did not have an adverse effect on the MIN6 β-cell line, while a Matrigel® control led to the formation of unusual "tubular" structures by day 5 of culture (Figure 4.18). Expression of insulin and syndecan-4 were still observed at 2 (Figure 4.21) and 5 days (data not shown) of culture on the HUVEC ECM. HUVEC ECM made with or without crowders could still be observed in the well plate after 2 days of MIN6 culture (Figures 4.19-20). By day 5, some ECM that were made with crowders could still be observed, while the majority of ECM made without crowders had either been metabolised or degraded (data not shown). ECM components such as collagen IV, fibronectin, laminin and perlecan were not detected in the MIN6 cell layer, even

under crowded conditions (data not shown). This somewhat confirms previous conjecture that β-cells do not produce these ECM components (Nikolova et al., 2006). Furthermore, presence of crowders did not enhance expression of syndecan-4 or HS by the MIN6 cells (Figure 4.17).

The ECM components produced by the primary HUVECs in this study matched those found in the murine pancreatic islet basement membranes studied in Chapter 3. The morphology of deposited ECM was markedly different between crowded and uncrowded ECs. Similar to results observed by Lareu et al with adult hypertrophic scar fibroblasts (Lareu et al., 2007a), the ECs that were cultured with crowders tended to deposit more stabilised ECM into the extracellular space, whereas ECs without crowders produced ECM that lifted off the TCP easily, demonstrated by the "holes" observed in uncrowded HUVEC cell layers, and remained mostly associated with or inside the ECs. Quantitation of fluorescently stained ECM showed a marked increase in the presence of ECM under crowded conditions, with fold differences ranging from 2-6, across various ECM components in the cell layer (Figure 4.8).

Similar enhancement of ECM deposition have been observed in murine transformed astrocytes, WI-38 fibroblasts and bone marrow-derived mesenchymal stem cells, whereby the supramolecular assembly of ECM components and their ligands were accelerated by macromolecular crowding (Chen et al., 2011). The crowders were shown to accelerate the assembly of collagen triple helices into collagen fibres by the enhancement of enzymatic and non-enzymatic crosslinking. It is therefore speculated that a similar process of accelerated ECM assembly was occurring in the HUVECs cultured with crowders.

To optimise ECM harvesting for the support of β-cells, sodium deoxycholate (DOC) and Nonidet P-40 (NP-40) were compared for effectiveness in the removal of cell debris and nucleic material while maintaining the integrity of the remaining ECM. DOC was found to be more successful at removing cellular debris from the HUVEC ECM than NP-40. NP-40 is a non-ionic, non-denaturing detergent often used for lysing cells and cytoplasmic protein isolation (Borun et al., 1967). However, NP-40 was not strong enough to lyse the nuclear membrane, and was also unable to clear the HUVEC ECM of most of the cellular material (Figure 4.9).

In contrast, DOC is a water-soluble, bile-acid, ionic detergent that is effective in disrupting and dissociating various protein interactions. DOC is much stronger than Nonidet P-40 as a cell-lysing agent and thus was much more effective in the removal of cell debris from the ECM. Nonetheless, an interesting difference in the ability for DOC to remove debris from crowded and uncrowded ECM was observed. Crowded ECs were much more difficult to remove and the number of washes normally sufficient for removing cells from uncrowded ECM had to be increased in order for complete removal to occur (Figure 4.10). Macromolecular crowders have been shown to stabilise protein-protein and protein-DNA interactions (Harve et al., 2010; Jarvis et al., 1990; Lareu et al., 2007b). Furthermore, the presence of more ECM may have all lead to an increased retention of ECs in the crowded ECM.

Immunocytochemistry of the HUVEC ECM after DOC lysis demonstrated that the ECM components, such as collagen IV, fibronectin, laminin, perlecan and heparan sulfate, were all better adhered to the TCP when made under crowded conditions

(Figures 4.11-12). This correlated well with previous observations of cell layers lifting during methanol fixation in HUVECs that were not cultured with crowders.

Fluorescently stained pixel quantitation of decellularised ECM demonstrated a 2.4-47.1-fold difference between crowded and uncrowded ECM (Figure 4.16). While the BCA and DMMB assays, used as alternative methods for the relative quantitation of ECM protein and glycosaminoglycan (GAG) content, respectively, showed a statistically significant 1.1-fold increase in protein content and a 1.2-fold change in GAG content in the crowded ECM (Figures 4.17-18). The discrepancies between these two methods and the pixel quantitation method may have been a result of the standards used in both assays. Bovine serum albumin (BSA) was used as the protein concentration standard in the BCA assay and heparin was used as the GAG standard in the DMMB assay. From the immuncytochemical staining, it was shown that the HUVEC ECM contains a plethora of ECM proteins and at least heparan sulfate and chondroitin sulfate. Thus, quantitation via a BSA and heparin standard may have caused an underestimation and a better representative of these components may have been needed as standards in order for a more accurate quantitation of protein and GAG content. Nevertheless, all three methods showed significantly higher amounts of residual ECM left by the crowded HUVECs compared to the uncrowded HUVECs.

In order to investigate whether the HUVEC ECM and DOC decellularisation method had any adverse effects on β-cells, the MIN6 insulinoma cell line was directly cultured on the HUVEC ECM. Interestingly, Matrigel® appeared to adversely affect the MIN6 morphology, as the cells began to form abnormal tubular-like structures on

the thin coating after 5 days of culture (Figure 4.18). This phenomenon has not yet been reported in the literature perhaps due to the fact that most studies use thick coatings of Matrigel® for β-cell culture (Kidszun et al., 2006; Knight et al., 2006b; Laschke et al., 2008; Nagata et al., 2001; Oberg-Welsh, 2001). In contrast, the decellularised HUVEC ECM did not adversely affect the general viability and morphology of the MIN6 β-cells when compared to a tissue culture plastic control. Furthermore, proliferation was unhindered, as confluence was similar across all the cell supports (TCP, crowded ECM and uncrowded ECM) at 2 and 5 days after seeding. The presence of ECM components after 2 days of MIN6 culture demonstrated that the integrity of some ECM components were still intact, with more being available in the crowded ECM (Figure 4.19) compared to the uncrowded ECM (Figure 4.20). In addition, expression of insulin and syndecan-4 by the β-cells were also unaffected by the HUVEC ECM (Figure 4.21).

4.5 Conclusion

This chapter has demonstrated that the neutral macromolecular crowder cocktail of Ficoll 70 and 400 indeed enhances *in vitro* ECM deposition by endothelial cell lines. Even in a cell type that did not produce very much ECM such as the transformed HMEC-1s, more ECM was observed in cells cultured under crowded conditions. Furthermore, the primary HUVEC line produced more ECM than the HMEC-1s, and deposition of various ECM components was enhanced 2 to 6-fold by macromolecular crowders.

The *in vitro*-produced HUVEC ECM was cleared of cellular material by DOC lysis but not NP-40 and the increased stability of deposited ECM under crowded conditions was made even more obvious after decellularisation. There was 2 to 47-fold more ECM components remaining on the TCP after DOC lysis in ECM that were made with crowders compared to ECM that were made in the absence of crowders. Syndecan-1, -4 and glypican-1 were found on HUVEC cell surfaces, but only syndecan-1 and glypican-1 remained in the ECM after decelluarization. Furthermore, HS was found to be abundantly expressed by the HUVECs and remained on the culture plate after DOC lysis. Other major ECM components present after decellularisation included collagen IV, fibronectin, laminin and perlecan. The identified HUVEC ECM components matches quite well with those identified within the murine pancreatic islet in Chapter 3 and thus may potentially be suitable for supporting islet health and function.

Preliminary investigations of β-cell response to the HUVEC ECM showed that the ECM and decellularisation method used were not toxic to the MIN6 insulinoma cell line and did not hinder proliferation or insulin expression. However, the effect of the ECM on other functional aspects such as insulin secretion, apoptosis and differentiation are still unknown and will be evaluated in Chapter 5. Due to the finding that some ECM components were still present after 2 days of MIN6 culture, this will be the time point used to assess β-cell function on HUVEC ECM.

Chapter 5

5 Characterisation of β-cell response to endothelial matrix

5.1 Introduction

In the preceding chapter, it was shown that HUVEC ECM made under normal or crowded conditions were not deleterious to β-cell proliferation, expression of insulin and cell surface markers syndecan-4 and HS. However, the impact of the ECM mixture on β-cell health and survival is still unknown. Therefore, the characterisation of the β-cell response will form the main focus of this chapter.

The extracellular matrix (ECM) has previously been shown to function as a survival factor for cells and its destruction during the islet isolation process heavily contributes to the demise of pancreatic islets (Cheng et al., 2011; Pinkse et al., 2006; Wang and Rosenberg, 1999; Ziolkowski et al., 2012). In contrast to motile cells, cells of the islet require signals from the ECM to survive and maintain their characteristic topographical arrangement for their secretory function to remain in tact (Lucas-clerc et al., 1993). When islets are detached from their microenvironment in the isolation process, communication between cell surface receptors and ECM components are disrupted and apoptosis induced. However, when islet are incompletely separated from their ECM, a reduction in anoikis is observed and the islets tend to remain viable for longer periods of time (Thomas et al., 1999).

In addition to anoikis, once isolated islets are placed in *in vitro* culture, they tend to lose their differentiation within a period of days (Negi et al., 2012; Weinberg et al., 2007). This is due to the fact that islets in conventional *in vitro* culture on hydrophilic plastic tend to adhere and lose their 3-dimensional structure (Lucas-clerc et al., 1993). However, when islets are cultured as 3D clusters with some ECM in tact on non-adherent, hydrophobic plastic, they tend to retain their differentiated phenotype for extended periods (weeks) compared to dissociated islet cells (days) (Weinberg et al., 2007). It was in this same study, that the islet vasculature and its associated ECM was speculated to contribute not only to insulin expression, but also the entire β-cell programming and maintenance of differentiation.

Further to the disruption of the islet microenvironment, the isolation process is one that triggers a cascade of stressful events that include the activation of apoptosis and production of pro-inflammatory molecules (Cowley et al., 2012; Negi et al., 2012; Paraskevas et al., 2000). Although the events involved that causes β-cell dysfunction and death are not well characterised, research on rodents and humans have indicated that oxidative stress may play a major role in the induction of apoptosis (Blinman et al., 2000; Bottino et al., 2002; Pileggi et al., 2001; Robertson, 2004a; Robertson et al., 2004). The link between glucose sensing/stimuli and insulin secretion is highly dependent on the mitochondrial glucose metabolism (Maechler et al., 1999; Malaisse, 1997; Meglasson and Matschinsky, 1986). Oxidative stress is particularly damaging to the mitochondria and consequently reduces insulin gene expression and secretion and increases apoptosis of β-cells (Maechler et al., 1999). Furthermore, β-cells are highly susceptible to oxidative stress due to their reduced levels of

endogenous antioxidants (Azevedo-Martins et al., 2003; Evans et al., 2003; Kajikawa et al., 2002). Thus stress induced during isolation, cold storage and transplantation contributes to lowering the survival rates of transplanted islets.

In order to prolong islet function after isolation, previous studies using bovine corneal endothelial cells (BCEC) and human umbilical cord vein endothelial cells (HUVEC) to produce a layer of matrix on which primary islets were seeded and cultured have shown some positive impact (Hayek et al., 1989; Hulinsky et al., 1995b; Kaiser et al., 1988; Thivolet et al., 1985). The BCEC ECM was able to enhance islet attachment and DNA synthesis was increased when media was supplemented with glucose and insulin (Hayek et al., 1989; Thivolet et al., 1985), but limited cell viability with a decrease in insulin output after nine days in culture was also reported. Furthermore, a better stimulation index was observed in islets cultured on HUVEC ECM when compared to free-floating islets, though the spontaneous and basal insulin release was not enhanced and low DNA synthesis was observed (Hulinsky et al., 1995b). In another study with BCEC ECM, the rat islets' responsiveness to glucose, glucagon and somatostatin was retained for 2-4 weeks in culture and secondary cultures were successfully obtained with functional insulin secretion for up to 9 weeks (Kaiser et al., 1988). Similarly, Schuppin et al observed continued insulin secretion in the islet monolayers for up to 7 days and demonstrated proliferative activity in these insulin-positive, islet-derived cells (Schuppin et al., 1993).

Nevertheless, most of these studies characterised islet morphology, DNA synthesis and insulin profiling, but did not examine other functional aspects of β-cells such as

recovery from stress, differentiation and apoptosis when cultured on the endothelial ECM. Moreover, despite these promising results, all studies involving the culture of islets on endothelial matrix resulted in the formation of islet "monolayers" that are normally described of islets undergoing de-differentiation in long-term culture (Gershengorn et al., 2004; Hanley et al., 2008; Weinberg et al., 2007). It is thus interesting for continued glucose-responsive insulin secretion to be observed in both the Schuppin and Kaiser studies (Kaiser et al., 1988; Schuppin et al., 1993).

The overall objective of this thesis was to study the function, ability to recover from stress, viability and differentiation of β-cells cultured on normal and enhanced endothelial ECM. Specifically these studies aimed to:

(a) understand the effect of crowded ECM on glucose stimulated insulin secretion from MIN6 insulinoma cell lines before and after exposure to oxidative stress conditions;

(b) study apoptosis in MIN6 cells under stressed and unstressed conditions and understand the effect of crowded ECM on rescuing stressed cells; and

(c) understand the impact of crowded ECM on primary islet morphology and de-differentation

5.2 Materials and Methods

The MIN6 insulinoma cell line was used as a model for islet β-cells. As a simulation of islets undergoing oxidative stress, MIN6s were exposed to hydrogen peroxide then cultured on tissue culture plastic (TCP), sodium deoxycholate-decellularised HUVEC ECM (Chapter 4, Section 4.2.2) that were made with crowders (+MMC ECM) and without crowders (-MMC ECM). Normal and H_2O_2-stressed MIN6s were then tested for function (glucose-stimulated insulin secretion) and apoptosis gene expression.

Primary mouse islets were used to test for morphological responses (shape, structure, and spread as well as insulin and glucagon expression) and differentiation marker expression after culture on TCP, +MMC ECM and -MMC ECM.

5.2.1 MIN6 cell culture

The MIN6 insulinoma cell line was cultured as previously described in Chapter 3. Normal cells were seeded onto TCP, +MMC ECM and -MMC ECM at 1×10^6 cells/well in 6-well plates and cultured without media change for 48 h.

5.2.2 H_2O_2 stress induction

MIN6 exposure to hydrogen peroxide was used as a model for β-cells undergoing oxidative stress. Prior to seeding MIN6 cells onto each cell support, the cells were exposed to 150 μM H_2O_2 for 30 min then trypsinized and seeded onto TCP, +MMC ECM and –MMC ECM at 1×10^6 cells/well in 6-well plates and cultured with one media change for 48 h.

5.2.3 MIN6 glucose-stimulated insulin secretion (GSIS) assay

Phase 1 (15 min after glucose challenge from stored insulin) and Phase 2 (1 h after glucose challenge from newly expressed) insulin secretion were compared across the three cell supports. Serum-free DMEM (Gibco) containing 20 mM L-glut and 1M HEPES was used throughout the GSIS assay. MIN6 cells were washed three times with DPBS (Gibco) and incubated with serum-free DMEM containing 1 mM glucose (Sigma) for 2 h at 37℃. Cells were then washed once with 1 mM glucose DMEM and incubated with 1 mL of fresh 1 mM glucose DMEM at 37℃. Samples of 10 μL was taken from the media supernatant at 15 min (phase 1 insulin secretion) and 1 h (phase 2 insulin secretion) and diluted with 490 μL of 1% (w/v) BSA/DPBS. The 1 mM glucose DMEM media supernatant was removed and replaced with 1 mL of 25 mM glucose DMEM and incubated at 37℃. Samples of 10 μL was taken from the media supernatant at 15 min (phase 1) and 1 h (phase 2) and diluted with 490 μL of 1% (w/v) BSA/DPBS. Diluted samples were vortexed and stored at -20℃ until required for ELISA.

The rest of the 25 mM glucose DMEM media supernatant was removed and cells were stored overnight at -80℃. Cells were then thawed to room temperature and collected with a cell scraper in 1 mL of 1× cell-lysis buffer (CyQUANT Cell Proliferation Assay Kit) for total DNA quanititation. Total insulin was extracted by diluting 50 μL of MIN6 lysate in 450 μL of acidic-ethanol (70% ethanol, 10 mM HCl) and stored at -20℃ until required for ELISA.

5.2.4 Total DNA quantitation

MIN6 lysates were diluted 1:20 and total DNA content was measured using the CyQUANT Cell Proliferation Assay Kit (Invitrogen/Molecular Probes). Briefly, a DNA standard curve was obtained using known concentrations of λDNA. CyQUANT GR fluorescence dye was added (1:400) to the MIN6 DNA samples and the standard. Fluorescence was measured at excitation maximum of 480 nm and emission maximum of 520 nm.

5.2.5 Insulin ELISA

Samples were diluted by 1:1000 and total insulin samples were diluted by 1:5000 in 1% BSA/DPBS. Insulin concentrations from all samples were determined by ELISA via the Chrystal Chem Rat Insulin ELISA kit. The amount of insulin secreted in response to the low and high glucose challenges were normalised to total insulin and total DNA content. The stimulation index (SI) reflects the insulin releasing ability of the β-cells and was calculated by dividing the insulin value obtained after a high glucose challenge by insulin value obtained after a low glucose challenge. The SI is relatively independent of cell number and was used to statistically compare the difference between the 3 cell supports as well as the 3 trials.

5.2.6 Flow cytometry

Proportions of MIN6 cell populations that were apoptotic or necrotic on each cell support were measured by reactivity with Annexin V-FITC and propidium idodide. After 48 h of culture on the 3 cell supports, cells were washed twice with DPBS then trypsinised. The tryptic digest was neutralised with DMEM and cells were spun

down at 800 rpm for 5 min. Supernatant was discarded and 50 µL of 1:50 dilution of FITC-conjugated Annexin-V was added and incubated in the dark for 30 min at room temperature. Another 150 µL of 1:50 dilution of propidium idodide was added onto the cells. The cells were then passed through a 70 µm cell strainer and put through the BDFACSCanto flow cytometer immediately. Unstained and single-stained controls were used for compensation.

5.2.7 Primary mouse islet culture

Primary pancreatic islets were subsequently used to assess islet de-differentiation in culture on the 3 different cell supports. As test samples required adherence of islets onto a 2D surface of ECM, non-adherent 3D suspension culture of islets was deemed inappropriate as an additional control. Islets were isolated using the collagenase method from male C57BL/6 mice aged 10–12 weeks, as previously described (Kulkarni et al., 1999). Islets were handpicked under the dissecting microscope (Leica M60) to further remove acinar contaminants. Islets from 3 mice were pooled and plated onto TCP, +MMC ECM and -MMC ECM at ~50-80 islets/well in 6-well plates and cultured in RPMI (Gibco) containing 10% heat inactivated foetal bovine serum, 1M HEPES and 20 mM L-glut for 5-7days. Half of the media was changed on a daily basis. Islet morphology was monitored with a Zeiss ICM 405 light microscope. Islets were counted into groups that were rated on the basis of their morphology as “normal”, “fibroblastic” and “de-differentiated” on day 5 and 7 (Figure 5.10).

5.2.8 RNA extraction and cDNA synthesis

The ability for the HUVEC ECM to modulate gene expression of apoptosis markers was studied in the MIN6 cells, while differentiation markers were studied in primary islets.

MIN6 cells were washed twice with DPBS and lysed with RLT lysis buffer. A cell scraper was used to scrape cells off the well plate. In the case of islets, media supernatant and DPBS used to wash the wells were spun down and removed and cell pellets were lysed with RLT buffer and combined with islets lysed and scraped from the well plate. MIN6 and islet lysates were subsequently homogenised with a QIAshredder (QIAGEN) and RNA was extracted with the QIAGEN RNeasy Mini Kit. RNA concentrations were measured by a NanoDrop ND1000 Spectrophotometer. RNA samples were resuspended in RNase-free water and stored at -80°C. First-Strand cDNA was synthesised using the Invitrogen SuperScript III First-Strand Synthesis SuperMix. All samples were amplified using random hexamers by a BIO-RAD DNAEngine Peltier Thermal Cycler with 1 µg of RNA per sample. cDNA samples were resuspended in DNase-free water and stored at -20°C.

5.2.9 Quantitative real-time PCR

Table 5.1 Primers and primer sequences used in this study

Target gene	**Function**	**Forward sequence (5'-3')**	**Reverse Sequence (5'-3')**
A20	Anti-apoptotic	TGCCCTTGGGTACTGGATAG	GGCTCGACCCCAGATGTCAG
Bax	Pro-apoptotic	TGCAGAGGATGATTGCTGAC	GATCAGCTCGGGCACTTTAG
Bcl-2	Anti-apoptotic	TCTGAAGGATTGATGGCAGA	TCTGAAGGATTGATGGCAGA
Bcl-XL	Anti-apoptotic	CCATTGCTACCAGGAGAACC	AGGAGCTGGTTTAGGGGAAA
Glut-1	Glucose transporter	ACCTATGGCCAAGGACACAC	CTGGTCTCAGGCAAGGAAAG
Glut-2	Glucose transporter (β-cell specific)	CATGCTGAGCTCTGCTGAAG	ACAGTCCAACGGATCCACTC
Pdx-1	Transcription factor	GAAATCCACCAAAGCTCACG	TTCAACATCACTGCCAGCTC
NeuroD1	Transcription factor	GGAGGAGGAGGAAGATGAGG	TGGGTCTTGGAGTAGCAAGG
HNF-1α	Transcription factor	ACTTGCAGCAGCACAACATC	GAATTGCTGAGCCACCTCTC
ID1	DNA-binding protein inhibitor	CGTCAACGACTTCGACCTGATG	GCAGGTCCCTGATGTAGTCGATTAC
MafA	Transcription factor	CGTCAACGACTTCGACCTGATG	CGTCAACGACTTCGACCTGATG
Proinsulin	Immature form of insulin	TTTGTCAAGCAGCACCTTTG	TCTACAATGCCACGCTTCTG
18S	Housekeeping gene	GGTGCATGGCCGTTCTTA	TGCCAGAGTCTCGTTCGTTA
Cyclophilin	Housekeeping gene	TGGACCAAACACAAACGGTTCC	ACATTGCGAGCAGATGGGGTAG
TBP	Housekeeping gene	TATCACTCCTGCCACACCAG	ATGATGACTGCAGCAAATCG

Real-time PCR was performed as previously described in Cheng et al 2010 (Cheng et al., 2010).

5.2.10 Statistical Analysis

All experiments were done with 3 samples per condition and entire experiments were repeated 3 times. Values are reported as mean ± standard deviation. One-way ANOVA was used to determine significance for stimulation indexes, total insulin and fold-change of gene expression data using Minitab 15 statistical analysis software. The one-way ANOVA was also used to determine significance of changes in Annexin V- positive and propidium iodide-positive MIN6 populations. The Chi-square (Fisher's exact) test and the Bonferroni's multiple comparison method were used to determine the significance of de-differentiated islet proportions using the GraphPad Prism5 software.

5.3 Results

5.3.1 Glucose-stimulated insulin secretion (GSIS) of normal and stressed MIN6 after culture on ECM

5.3.1.1 Comparison of stimulation indexes on each cell support

Insulin secretion from normal MIN6s cultured on TCP, -MMC ECM and +MMC ECM did not show significant differences in stimulation indexes (SI) across the three supports in three separate experiments (Figure 5.1). SI remained consistent at Phase 1 and 2 and indexes ranged from 2-3 in all of the experiments.

In contrast, stressed MIN6s showed a decrease in SI on all cell supports at Phase 2 insulin secretion compared to Phase 1 (Figure 5.2). Stressed cells at Phase 1 had SI of 1.5-2, which subsequently dropped down to 1-1.5 at Phase 2. Nevertheless, a comparison of indexes across the three cell supports did not demonstrate any significant differences between ECM and TCP.

5.3.1.2 Normalisation to total insulin content

Normalisation of raw secreted insulin values at low and high glucose challenges to total insulin resulted in a general trend of lower insulin secretion in normal MIN6s cultured on both –MMC ECM and +MMC ECM compared to that of TCP (Figures 5.3) in both phases of insulin secretion. This was due to the fact that normal MIN6s cultured on ECM tended to possess higher levels of intracellular insulin content. This trend was observed in both phase 1 and phase 2 insulin secretions of normal MIN6 but not stressed MIN6 cells (Figure 5.5).

In contrast, a difference in response to glucose was observed in MIN6s that had been pre-exposed to oxidative stress. Statistically significant response to glucose was observed only on +MMC ECM and TCP but not –MMC ECM in the first phase of insulin secretion. In the second phase of insulin secretion, significant responses to glucose was only observed on +MMC ECM.

5.3.1.3 Normalisation to total DNA content

Total DNA content across all samples tended to be consistent in value in both normal and stressed MIN6s. Normalisation of insulin concentrations to DNA demonstrated no significant difference of insulin secretion in β-cells on all three cell supports in normal MIN6s (Figure 5.4). This lack of effect was again seen in both phase 1 and 2 insulin secretions. Further to this, the ratio of total intracellular insulin to total DNA content confirmed that MIN6s cultured on ECM indeed had higher total insulin than cells cultured on TCP (Figure 5.7). In particular, cells cultured on non-crowded HUVEC ECM were significantly 1.7-1.9-fold ($P<0.05$) higher in total insulin content.

Interestingly, statistically significant glucose responsiveness was only observed in stressed MIN6s cultured on +MMC ECM at the first phase of insulin secretion when the insulin concentrations were normalized to total DNA. Cells were no longer responsive to glucose at Phase 2 insulin secretion on all three cell supports.

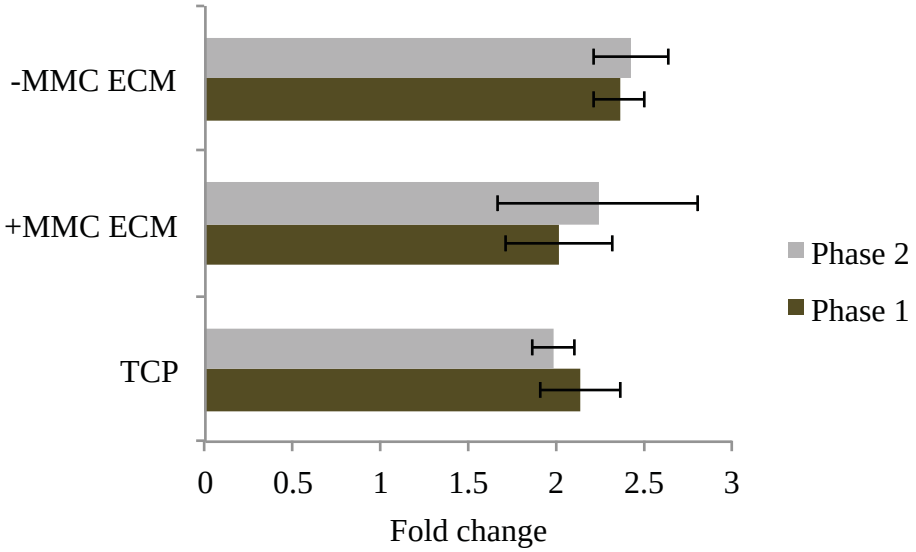

Figure 5.1 Phase 1 and Phase 2 stimulation indexes of MIN6 cultured on tissue culture plastic (TCP), matrix made with crowders (+MMC ECM) and matrix made without crowders (-MMC ECM).

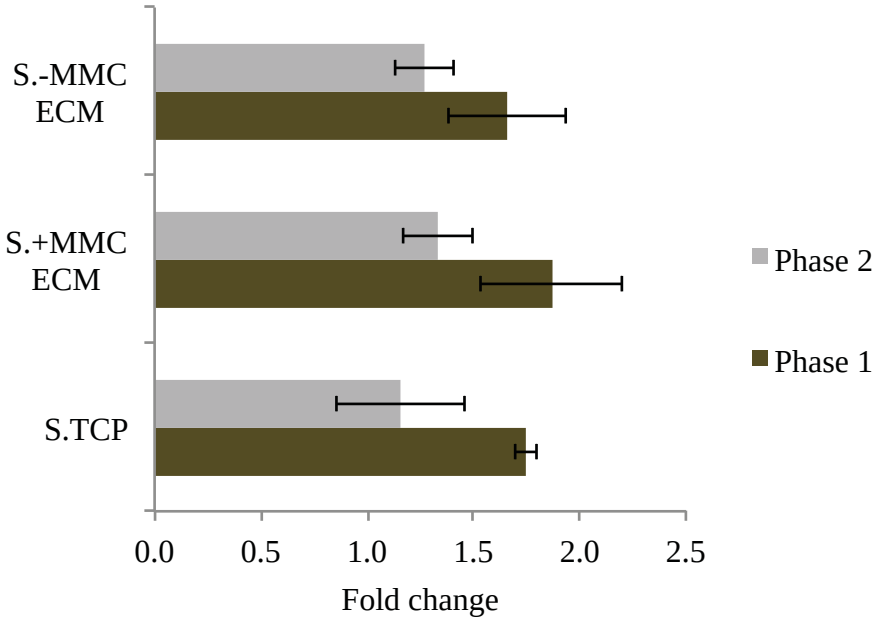

Figure 5.2 Phase 1 and Phase 2 stimulation indexes of H_2O_2-stressed MIN6 cultured on tissue culture plastic (S.TCP), matrix made with crowders (S.+MMC ECM) and matrix made without crowders (S.-MMC ECM). Normal MIN6 on TCP (NS.TCP) was used as a GSIS assay control.

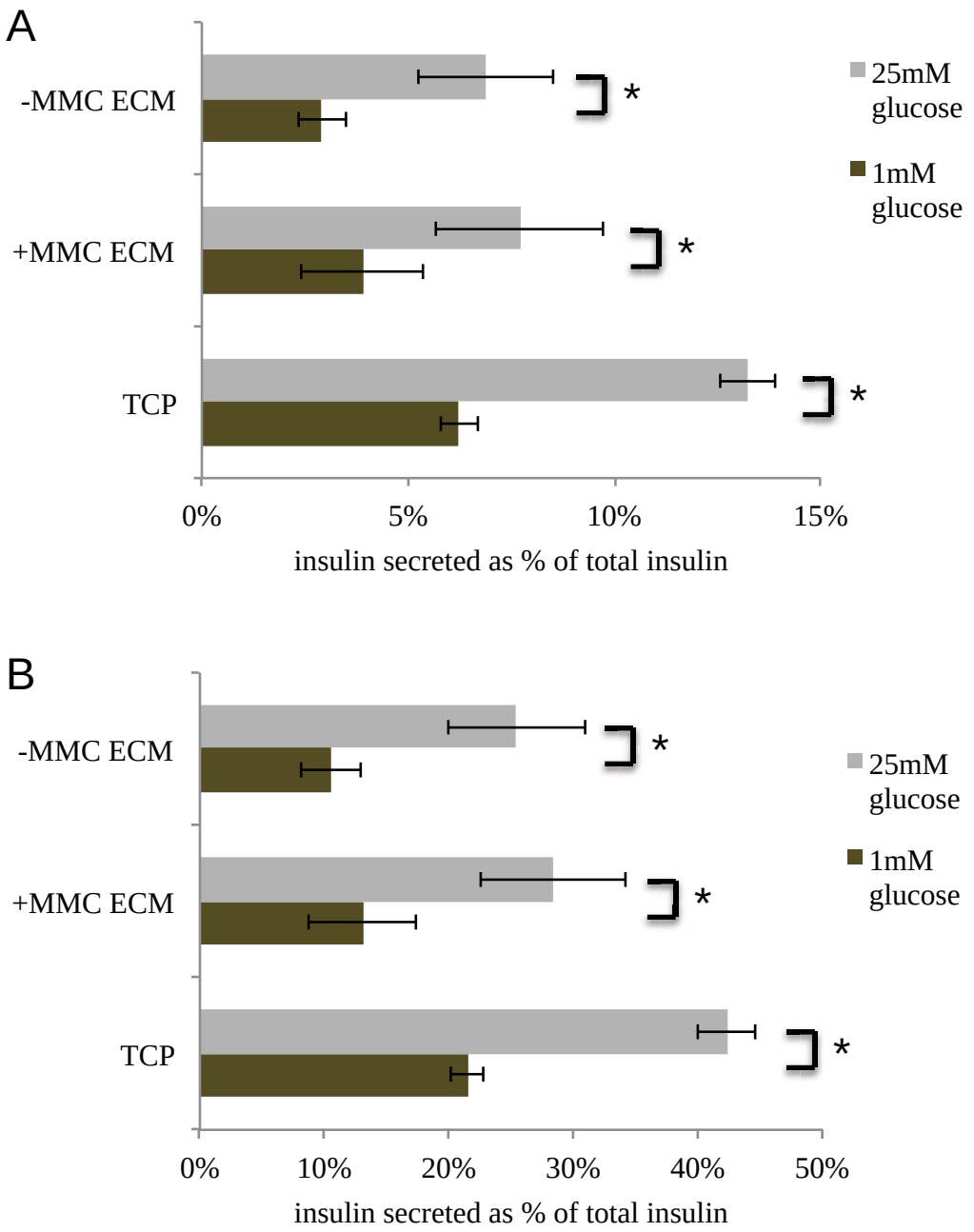

Figure 5.3 Raw phase 1 (A) and phase 2 (B) insulin concentrations normalised to total insulin content of normal MIN6 after 2 days of culture on tissue culture plastic (TCP), matrix made with crowders (+MMC ECM) and matrix made without crowders (-MMC ECM). * represents significance in relation to the basal insulin secretion level (1 mM Glucose) as calculated by the one-way ANOVA test ($n = 3$; $P < 0.05$).

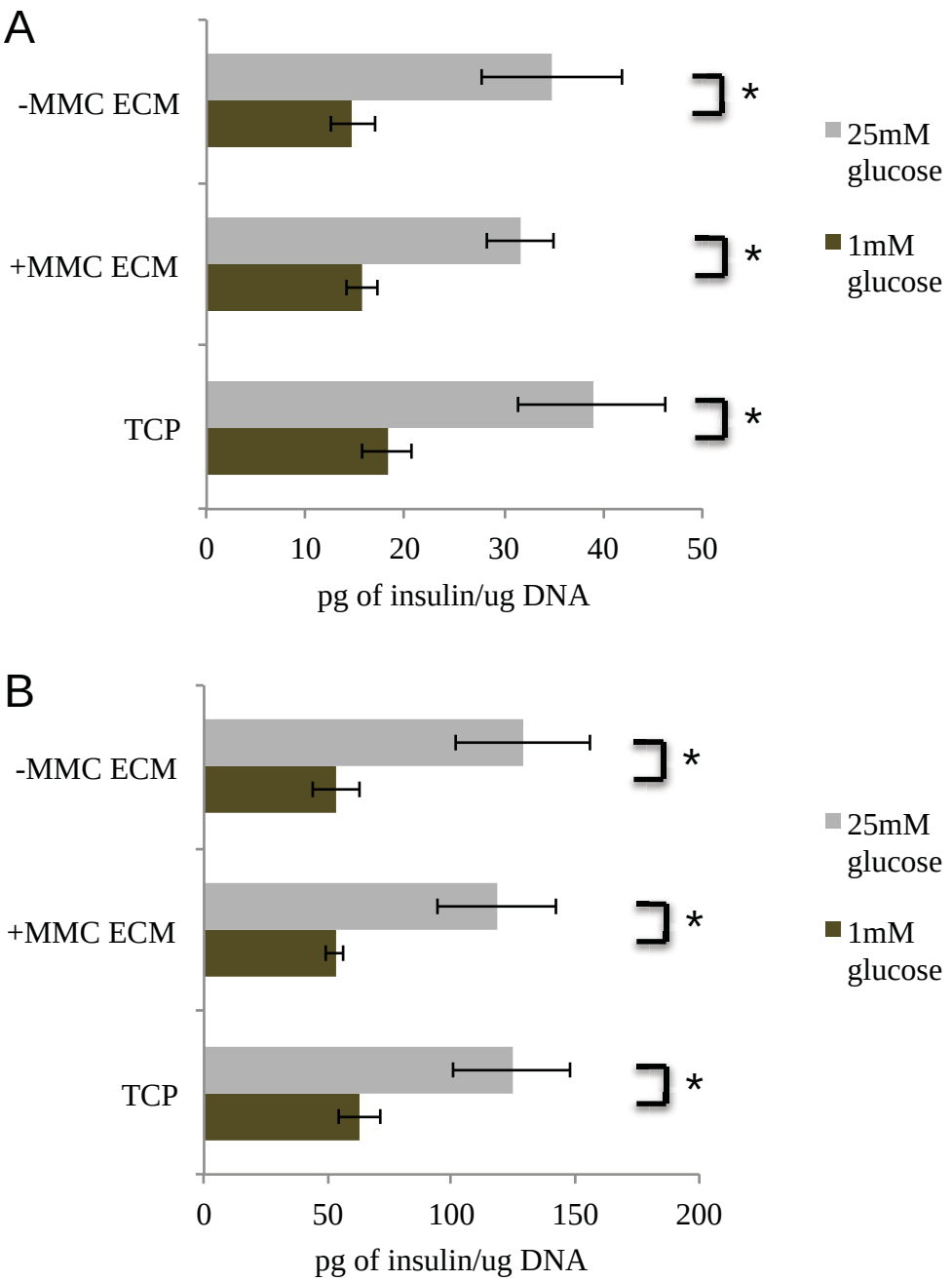

Figure 5.4 Raw phase 1 (A) and 2 (B) insulin concentrations normalised to total DNA content of normal MIN6 after 2 days of culture on tissue culture plastic (TCP), matrix made with crowders (+MMC ECM) and matrix made without crowders (-MMC ECM). * represents significance in relation to the basal insulin secretion level (1 mM Glucose) as calculated by the one-way ANOVA test ($n = 3$; $P < 0.05$).

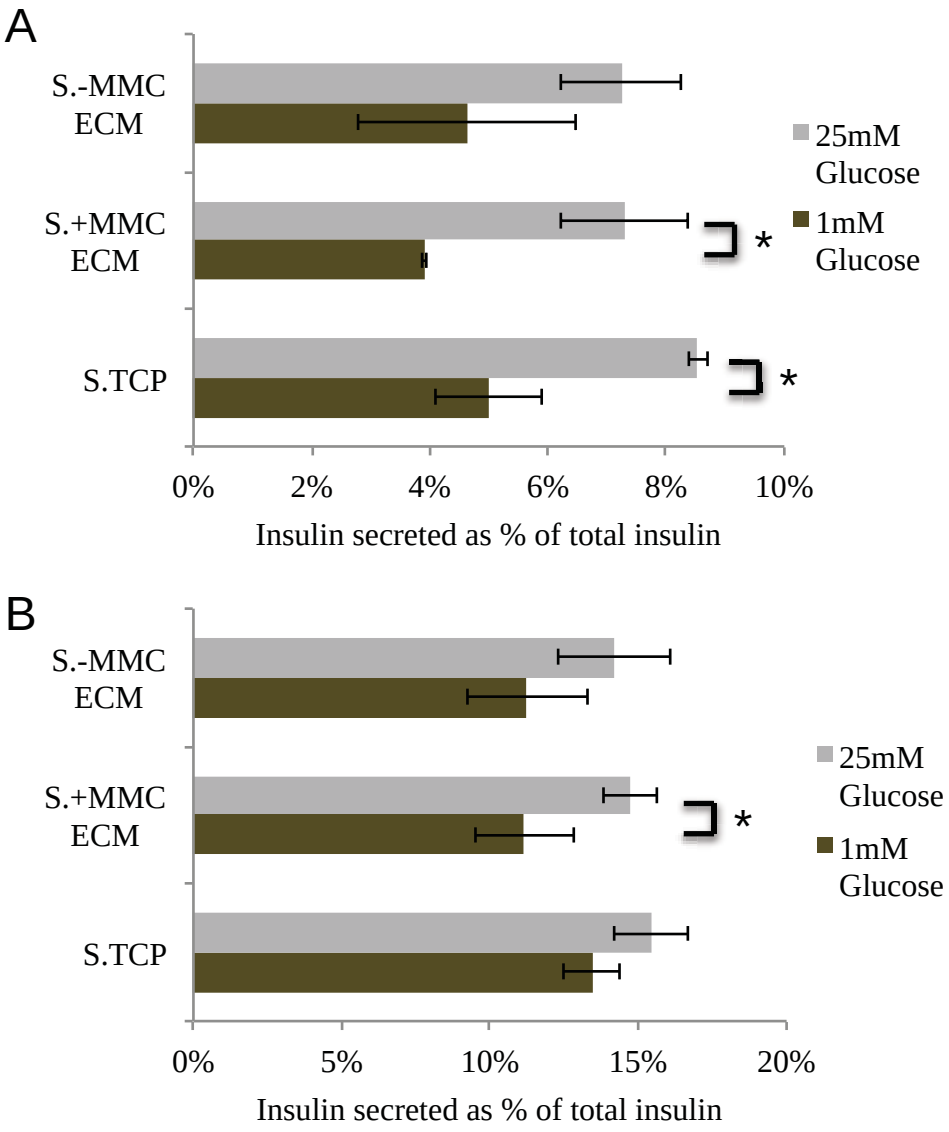

Figure 5.5 Raw phase 1 (A) and 2 (B) insulin concentrations normalised to total insulin content of H_2O_2-stressed MIN6 after 2 days culture on tissue culture plastic (S.TCP), matrix made with crowders (S.+MMC ECM) and matrix made without crowders (S.-MMC ECM). * represents significance in relation to the basal insulin secretion level (1 mM Glucose) as calculated by the one-way ANOVA test ($n = 3$; $P < 0.05$).

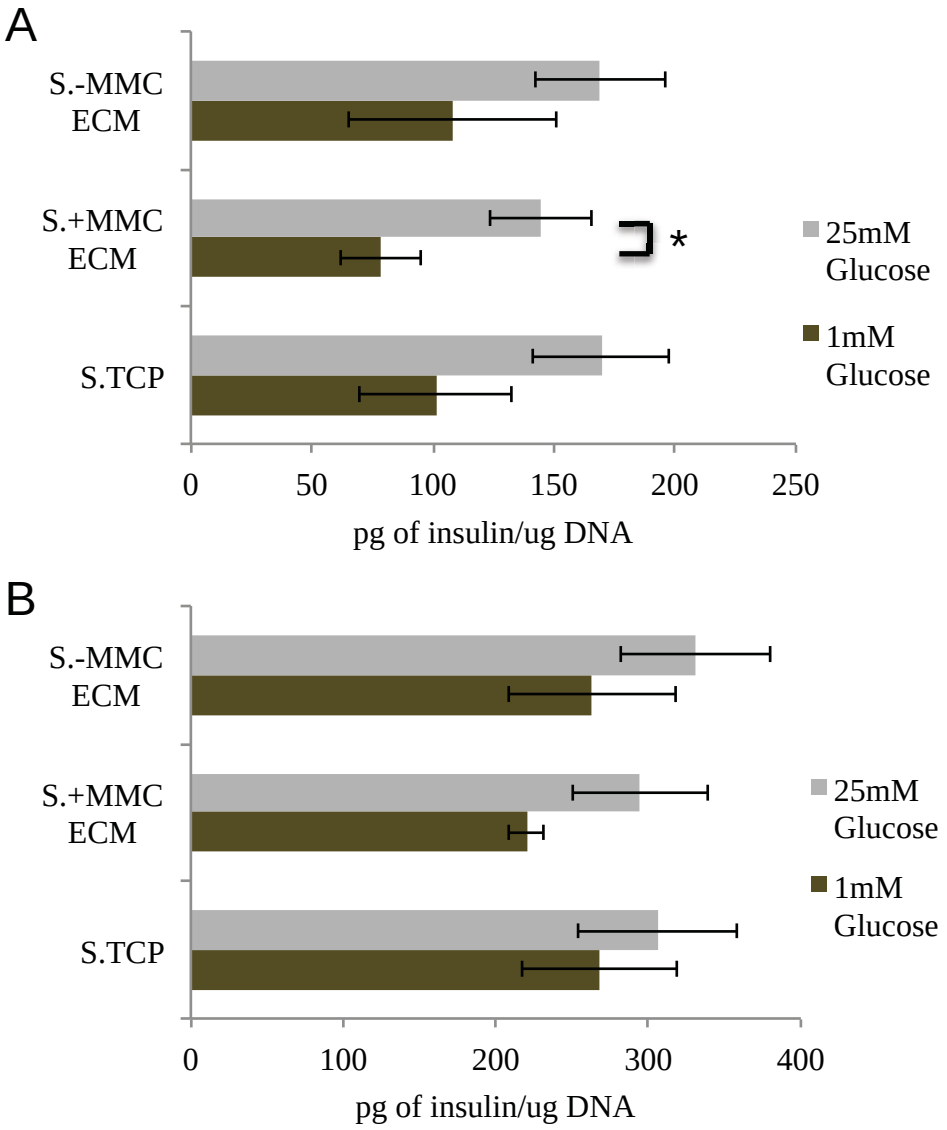

Figure 5.6 Raw phase 1 (A) and 2 (B) insulin concentrations normalised to total DNA content of H_2O_2-stressed MIN6 after 2 days culture on tissue culture plastic (S.TCP), matrix made with crowders (S.+MMC ECM) and matrix made without crowders (S.-MMC ECM). Normal MIN6 on TCP (NS.TCP) was used as a GSIS assay control. * represents significance in relation to the basal insulin secretion level (1 mM Glucose) as calculated by the one-way ANOVA test ($n = 3$; $P < 0.05$).

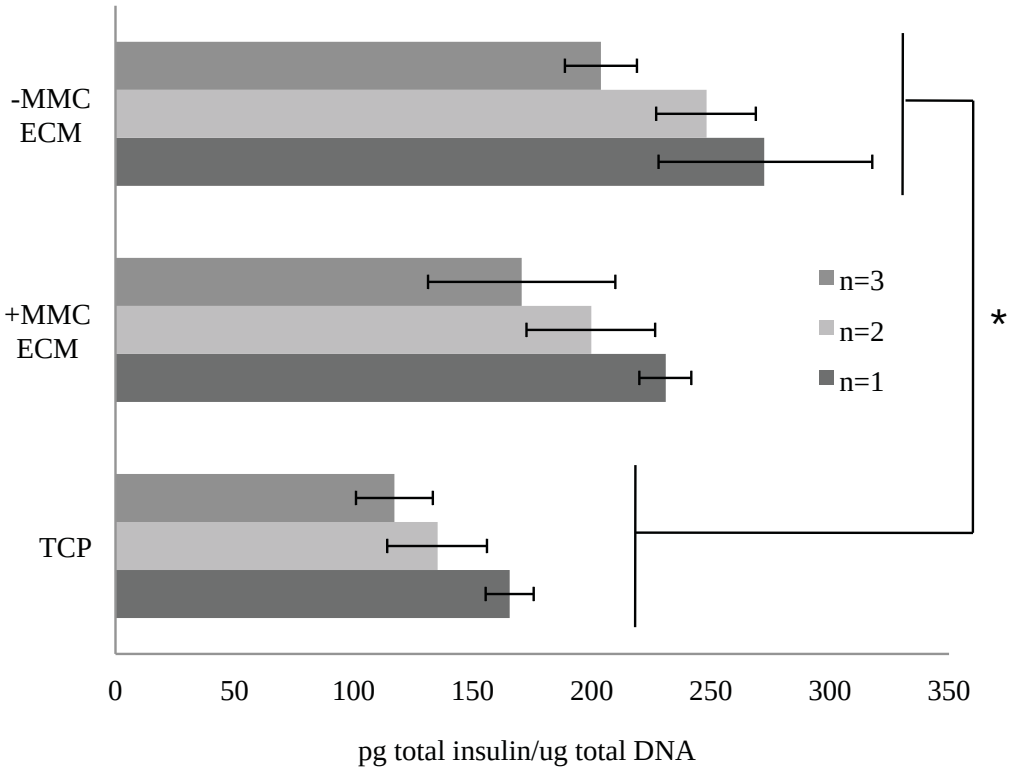

Figure 5.7 Total insulin content normalised to total DNA content from MIN6 cultured on tissue culture plastic (TCP), matrix made with crowders (+MMC ECM) and matrix made without crowders (-MMC ECM). * represents significance ($P<0.05$) in relation to the TCP control as calculated by the one-way ANOVA test.

5.3.2 Expression of apoptotic markers in normal and stressed MIN6

The housekeeping gene, *18S*, was chosen for normalization in MIN6 cells as it was found to be the most consistent in expression across all three cell supports (Appendix B). In normal MIN6 cells, significant upregulation of anti-apoptotic genes *A20* (1.5-1.9 fold) and (1.5-1.6 fold) *Bcl-XL* were observed in cell cultured on +MMC ECM (Figure 5.8). A similar trend was observed in the H_2O_2 stressed MIN6 cells, where *A20* was upregulated by 1.2-1.3 fold and *Bcl-XL* by 1.1-1.4 fold, though the upregulation was not as pronounced as that of the normal cells (Figure 5.9). The anti-apoptotic gene *Bcl-2*, however, did not vary across the 3 cell supports in both normal and stressed cells. Interestingly, there was a slight down regulation of the pro-apoptotic marker, *Bax*, in both normal and stressed MIN6 cultured on -MMC ECM, while a significant upregulation of *Bax* (1.2-1.3 fold) was observed in the stressed MIN6 cultured on +MMC ECM. Together, these results indicate that β-cells respond differently to HUVEC ECM that were made with or without crowders.

5.3.3 Apoptosis analysis by flow cytometry in normal and stressed MIN6

Despite the upregulation of anti-apoptotic genes in normal and stressed MIN6 cells cultured on crowded ECM, no significant difference in Annexin V-positive (apoptotic) and propidium iodide-positive (necrotic) populations were observed across the 3 cell supports in normal (Figure 5.10) and stressed (Figure 5.11) MIN6 cells.

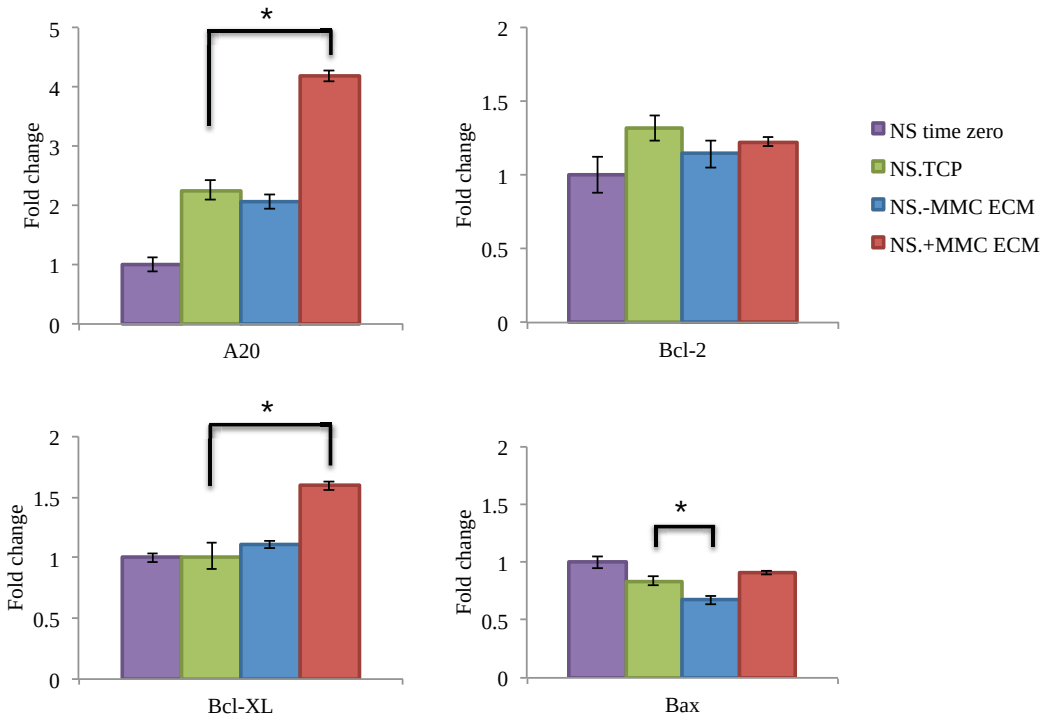

Figure 5.8 Expression levels of apoptosis markers in normal MIN6 cells directly after trypsinization (NS time zero) and at 2 days after culture on TCP (NS TCP), uncrowded matrix (NS –MMC ECM) and crowded matrix (NS +MMC ECM). * represents significance in relation to the TCP control as calculated by the one-way ANOVA test ($n = 3$; $P < 0.05$).

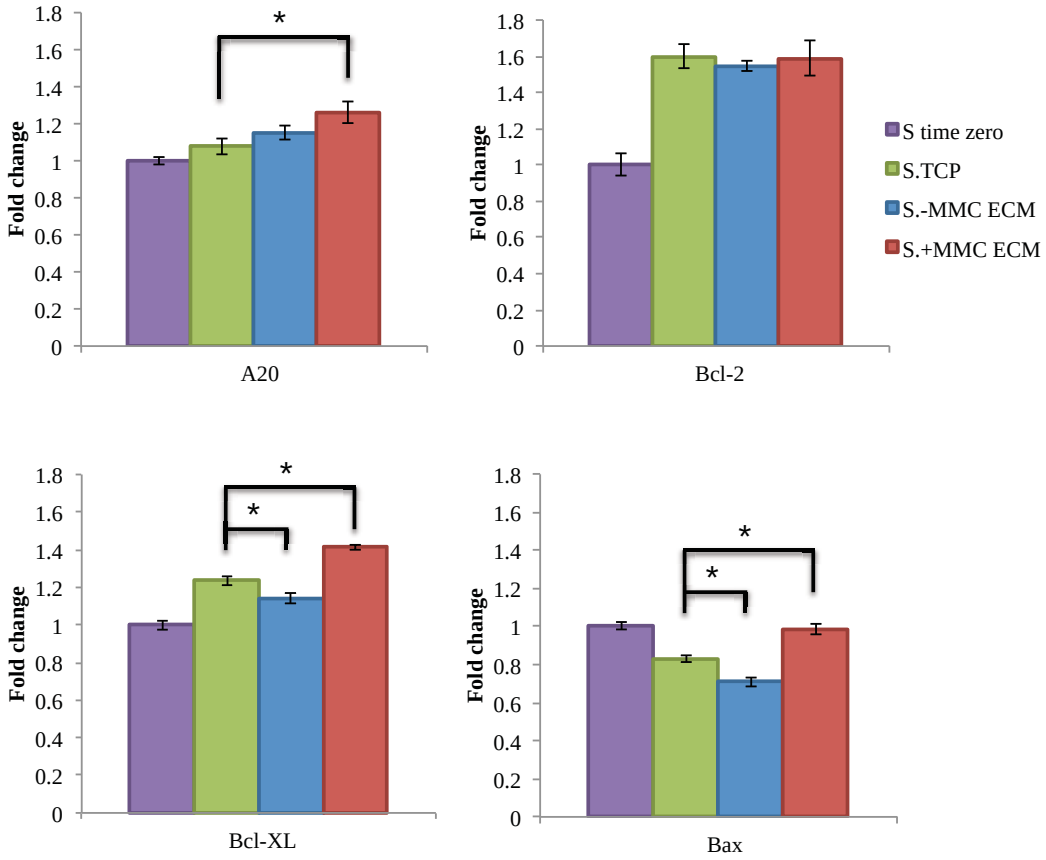

Figure 5.9 Expression levels of apoptosis markers in H_2O_2-stressed MIN6 cells directly after trypsinization (S time zero) and at 2 days after culture on TCP (S TCP), uncrowded matrix (S –MMC ECM) and crowded matrix (S +MMC ECM). * represents significance in relation to the TCP control as calculated by the one-way ANOVA test ($n = 3$; $P < 0.05$).

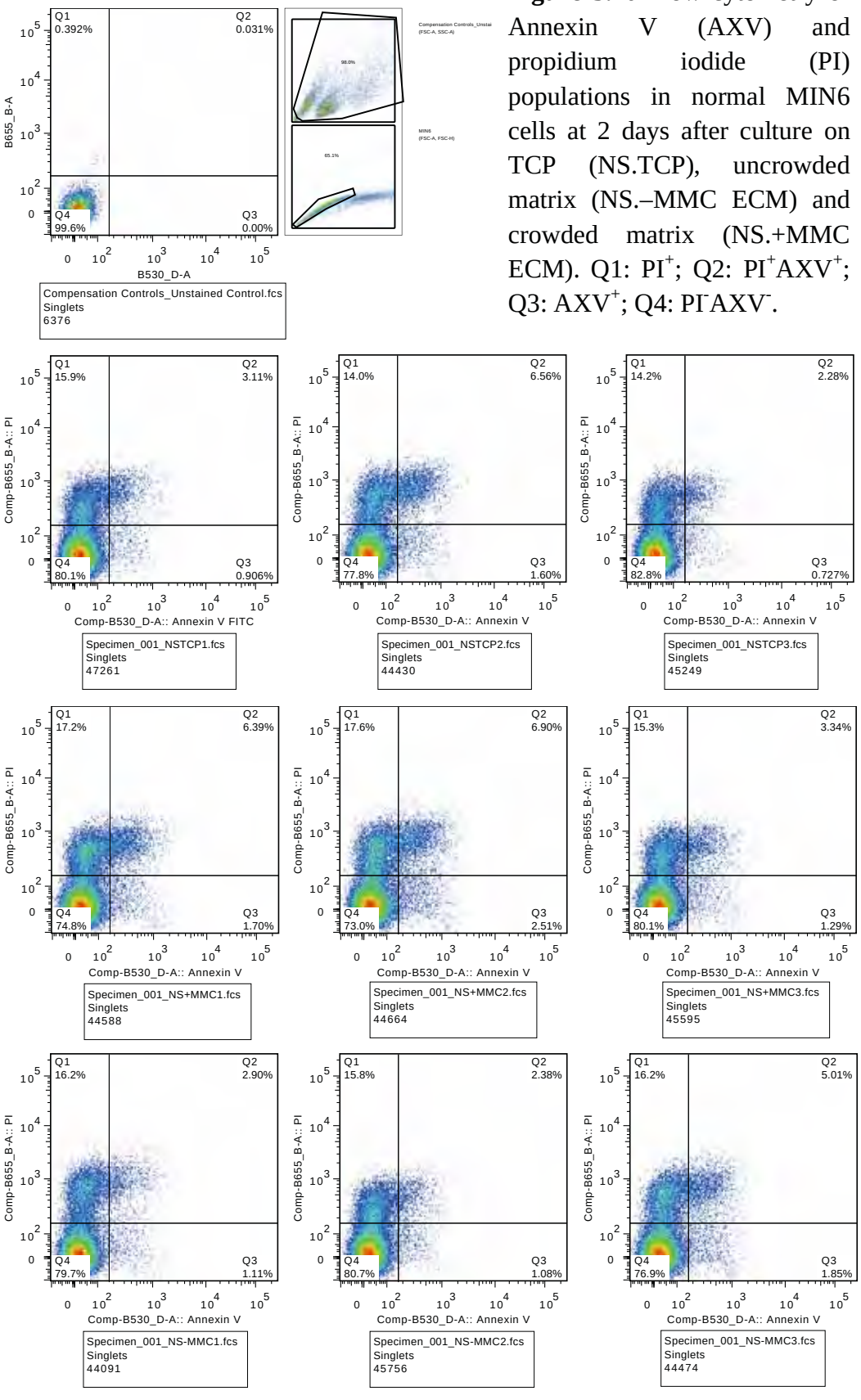

Figure 5.10 Flow cytometry of Annexin V (AXV) and propidium iodide (PI) populations in normal MIN6 cells at 2 days after culture on TCP (NS.TCP), uncrowded matrix (NS.–MMC ECM) and crowded matrix (NS.+MMC ECM). Q1: PI^+; Q2: PI^+AXV^+; Q3: AXV^+; Q4: PI^-AXV^-.

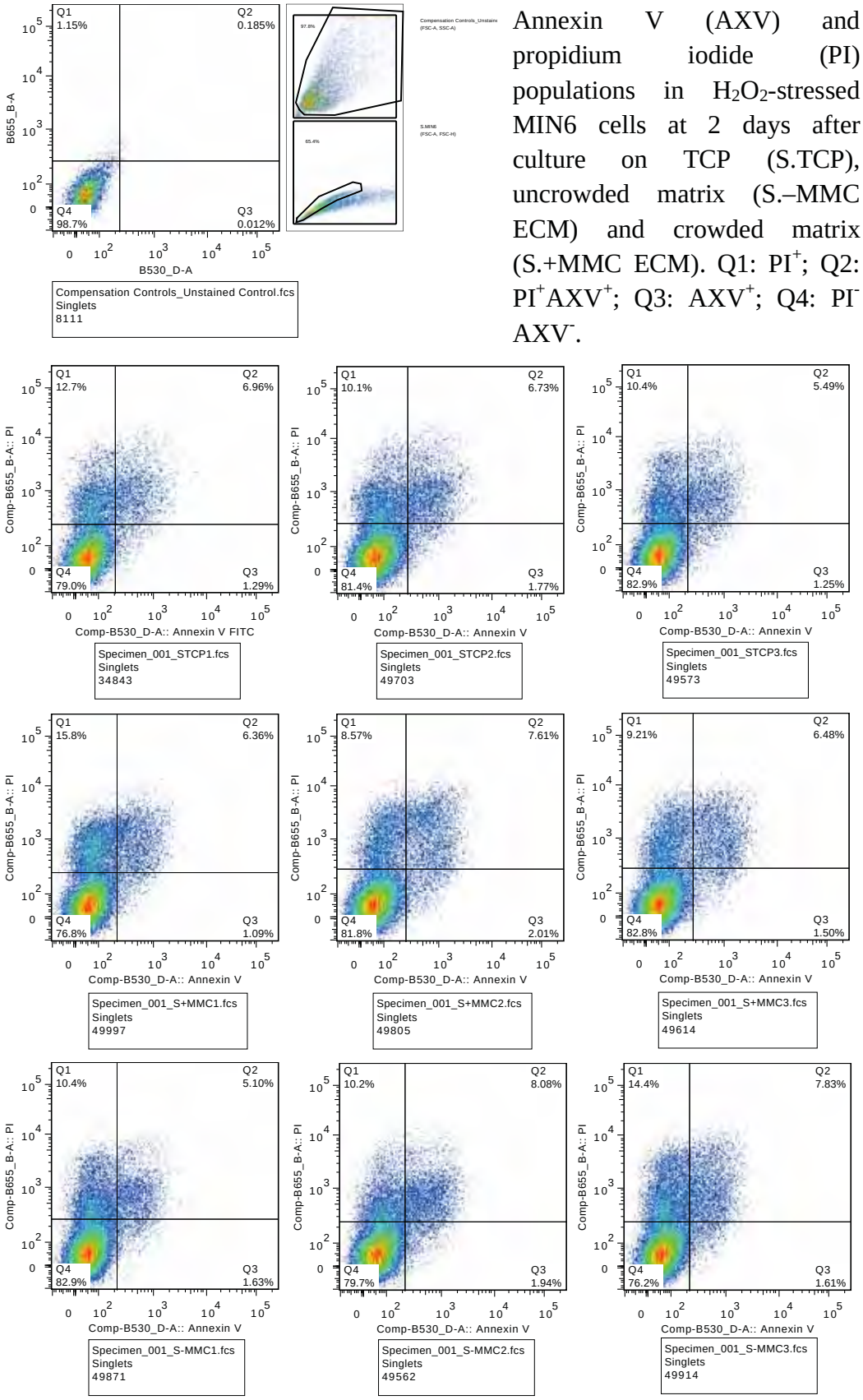

Figure 5.11 Flow cytometry of Annexin V (AXV) and propidium iodide (PI) populations in H_2O_2-stressed MIN6 cells at 2 days after culture on TCP (S.TCP), uncrowded matrix (S.–MMC ECM) and crowded matrix (S.+MMC ECM). Q1: PI^+; Q2: PI^+AXV^+; Q3: AXV^+; Q4: PI^-AXV^-.

5.3.4 Primary islet morphology on ECM

Islets categorized as "normal" were fully rounded in morphology, especially around the periphery of the islet cluster (Figure 5.12). "Fibroblastic" islets were fully rounded whilst being surrounded by fibroblastic growth on the culture plate. Islets beginning to form or had formed monolayers were categorized as "forming monolayers". These islets were spread around the edges of the normally rounded cluster, with outgrowths of cells directly from the islet cluster onto the culture plate.

A higher proportion of islets cultured on TCP and –MMC ECM tended to form monolayers within 3 days of seeding on the cell support, than when cultured on +MMC ECM. This observation was statistically significant, compared to the TCP control, 7 days after seeding (Table 5.2). Interestingly, there appeared to be more "fibroblastic" islets when cultured on ECM, however this observation was not significant. Nevertheless, even when the categories "fibroblastic" and "forming monolayers" were combined, there were significantly lower proportions of islets in the combined category when cultured on +MMC ECM compared to the TCP control at day 7 (data not shown).

5.3.5 Immunohistochemical staining of primary islets on ECM

Immunostaining for insulin and glucagon revealed that even though islets were forming monolayers in culture (up to ~11% on TCP and –MMC ECM), the clusters continued to express insulin and glucagon, even 7 days after culture on all 3 cell supports (Figure 5.13). Interestingly, some β-cells from islets that were forming monolayers were able to retain insulin expression despite having migrated from the

main islet cluster on TCP and –MMC ECM. In contrast, islets on +MMC ECM tended to stay in spherical clusters of insulin and glucagon-expressing cells, with only ~4% of islets forming monolayers that were generally smaller, only spread around the edge of the cluster and rarely ever completely flat, even at 7 days of culture.

5.3.6 Expression of differentiation markers in primary islets

The housekeeping gene, *18S*, was chosen for normalization in islets as it was found to be the most consistent in expression across all three cell supports (Appendix B). Consistent with a de-differentiated islet gene expression profile, transcription factor *ID1* was upregulated by 1.2-1.3-fold and the glucose transporter gene, *glut1*, was upregulated by 1.6-1.8-fold, while the transcription factor, *mafA*, was downregulated (0.6-0.7-fold change) in islets cultured on –MMC ECM compared to the TCP control (Figure 5.14).

Nevertheless, genes specific to β-cell differentiation, *NeuroD1* transcription factor (1.2-fold), *proinsulin* (1.1-fold) and glucose transporter gene, *glut2* (1.6 and 1.8-fold), were all significantly upregulated in islets cultured on both +MMC ECM and –MMC ECM, respectively, compared to the TCP control. Interestingly, the β-cell-specific transcription factor, *pdx1*, was downregulated (0.9-fold change) in islets on +MMC ECM.

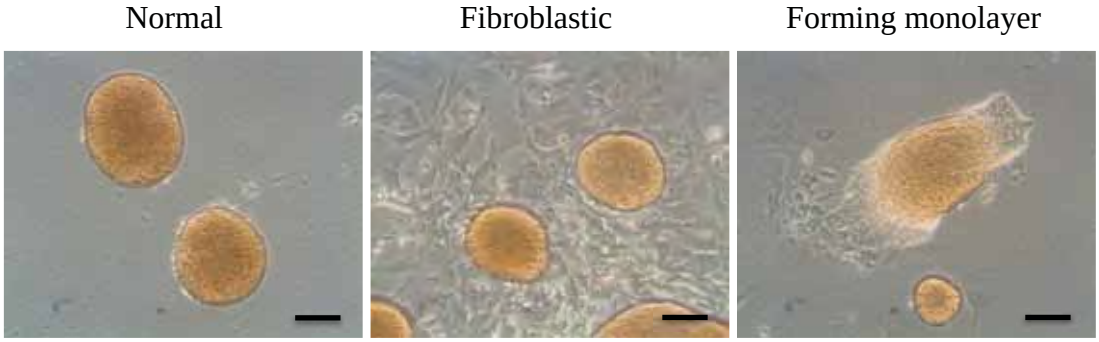

Figure 5.12 Primary mouse islets were cultured on TCP, -MMC ECM and +MMC ECM for 7 days and categorised as either "normal", "fibroblastic" and "forming monolayer" based on these morphological features. Scale bar: 100 μm.

Table 5.2 Proportions of islet populations becoming fibroblastic or forming monolayers 3 and 7 days after culture on tissue culture plastic (TCP), -MMC ECM (uncrowded matrix) and +MMC ECM (crowded matrix). *represents significance (*P<0.0083*) compared to the TCP control as calculated by Chi square (Fisher's exact) test with the Bonferroni correction for multiple comparisons.

Day	Support	Normal (%)	Fibroblastic (%)	Forming monolayer (%)
3	TCP	92 ± 2.25	1 ± 1.41	6 ± 0.83
	-MMC ECM	93 ± 0.31	1 ± 0.45	7 ± 0.53
	+MMC ECM	95 ± 1.28	0 ± 0.56	5 ± 0.72
7	TCP	87 ± 2.50	2 ± 0.97	11 ± 2.64
	-MMC ECM	86 ± 1.04	5 ± 0.91	10 ± 1.56
	+MMC ECM	92 ± 2.65	3 ± 1.22	4 ± 1.37*

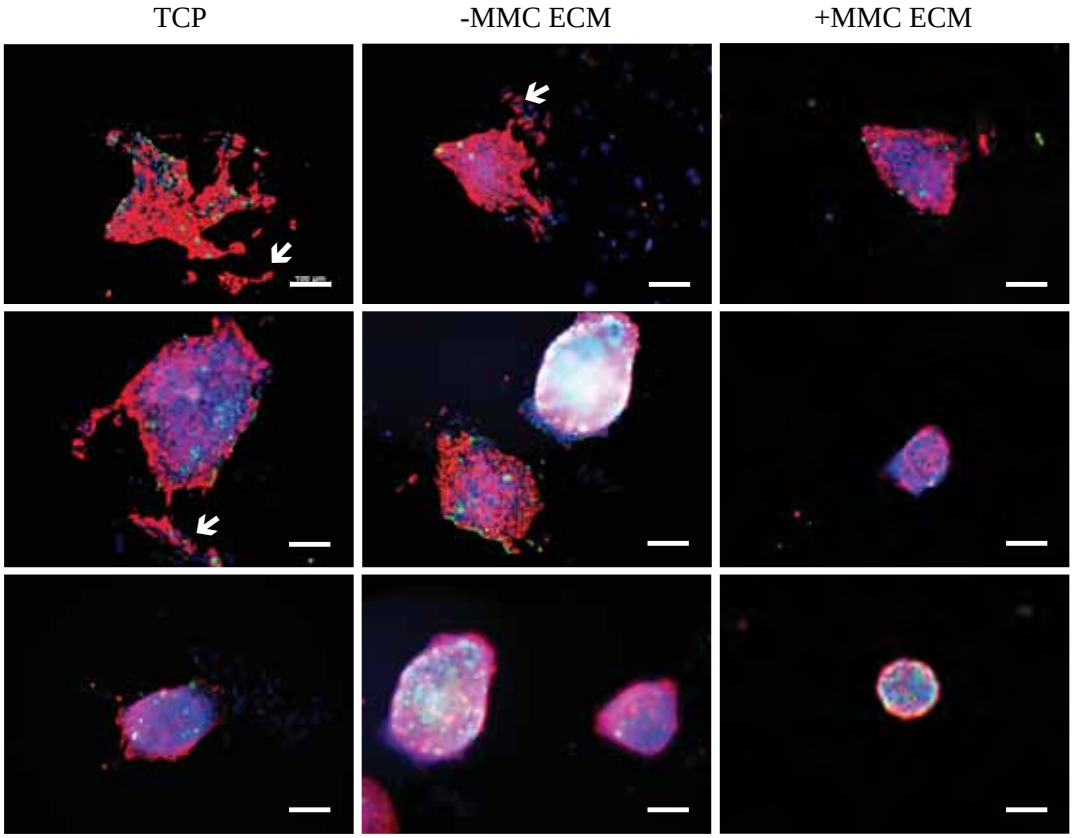

Figure 5.13 Morphological differences observed in primary mouse islets cultured on TCP, -MMC ECM and +MMC ECM for 7 days and stained for insulin (red), glucagon (green) and nuclei (blue). Scale bar: 100 μm. Arrows show β-cells that have migrated away from the main islet cluster.

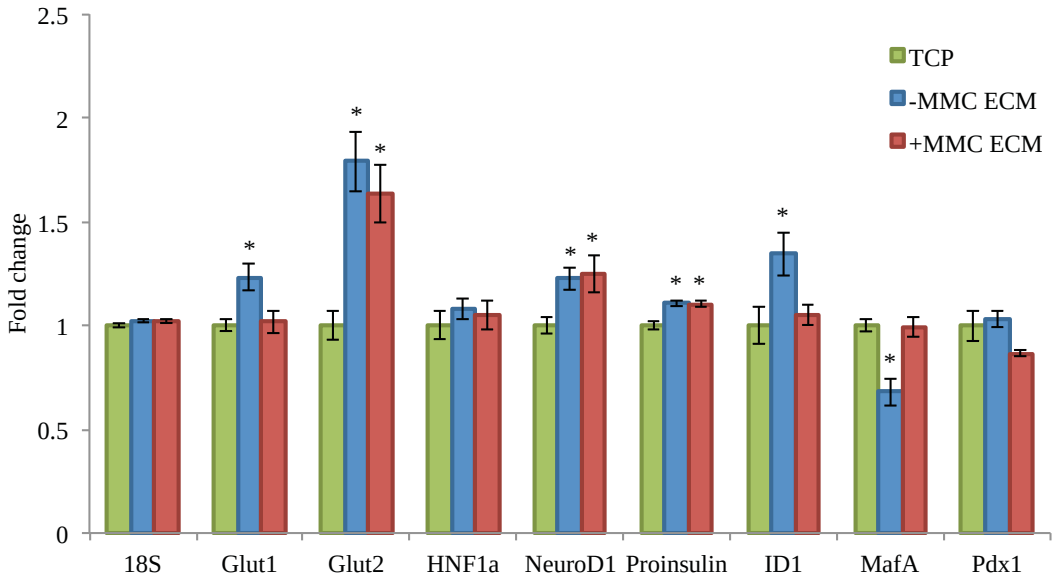

Figure 5.14 Relative expression levels of β-cell markers and transcription factors in islets cultured for 7 days on TCP, +MMC ECM and –MMC ECM. Each transcript is normalised to expression levels on TCP. * represents significance in relation to the TCP control as calculated by the one-way ANOVA test ($n = 3$; $P < 0.05$).

5.4 Discussion

Sodium deoxycholate-decellularized HUVEC ECM that was made with or without crowders was not deleterious to the insulin secretory function of MIN6 β-cell line. Glucose stimulated insulin secretion (GSIS) was maintained in both normal and H_2O_2-stressed MIN6 cells when cultured on both –MMC ECM and +MMC ECM. In normal MIN6, the SI were similar in Phase 1 and 2 insulin secretion (ranging between 2-2.5) and was not markedly different to that of the TCP control at 2 days of culture (Figure 5.1). Although SI did not differ between the cell supports in the H_2O_2-stressed MIN6 cells, a reduction of the index was observed at Phase 2 insulin secretion (Figure 5.2). This was perhaps due to the fact that the cells were still in a highly stressed state, at 2 days after the H_2O_2 exposure. These results indicate that the HUVEC ECM was not able to enhance the insulin secretory function of MIN6 cells before and after oxidative stress more than that of TCP.

Furthermore, DNA synthesis was not different across the cell supports, as total DNA content remained consistent after 2 days of culture in both normal and stressed cells. Nevertheless, normal MIN6s cultured on both ECMs had up to two-fold higher total intracellular insulin content than the TCP control, with particularly higher total insulin content in cells cultured on –MMC ECM, despite having unchanged stimulation indexes across the 3 cell supports (Figure 5.7). This would suggest that the ECM is somehow inducing the cells to express and store more insulin hormone. This phenomenon was only observed in the normal but not the H_2O_2-stressed MIN6 cells. Previous studies involving ECM such as fibrin gels with added growth factors have demonstrated increase in total insulin content by three-fold but did not change

the stimulation indexes in human adult islets (Beattie et al., 2002; Otonkoski et al., 1994). Perhaps residual growth factors produced by HUVECs present in the ECM after decellularisation were influencing the behavior of the MIN6 cells in a similar manner to that of the human islets.

These observations were also somewhat similar to those observed of rat islets cultured on normal HUVEC ECM, where DNA synthesis and spontaneous insulin release were not enhanced, compared to free-floating islets, though a better stimulation index was observed (Hulinsky et al., 1995b). Rat islets cultured on normal BCEC ECM showed enhanced DNA synthesis only when media was supplemented with glucose and insulin (Hayek et al., 1989; Thivolet et al., 1985). In the Thivolet study, the effect of ECM on insulin was only observed on day 9 of culture on BCEC ECM, where insulin secretion was 2.6-fold higher in cells on ECM compared to TCP. Interestingly, in the same study, the RINm5F insulinoma cell line did not show different insulin secretion levels on BCEC ECM compared to TCP at day 3, 4 and 5 of culture. Similarly, insulin secretion at 5 days of culture of normal MIN6 cells on TCP, -MMC ECM and +MMC ECM again, did not show significant differences in SI between the cell supports (data not shown). It should be noted that insulinoma cell lines are selected to be able to maintain function and viability on TCP, and thus may not be the ideal model for demonstrating differences in insulin secretion levels when comparing ECM to TCP in MIN6 (this study) and RINm5F (Thivolet et al., 1985) cell lines.

It was therefore interesting to observe a difference in the MIN6 response to the three cell supports after exposure to oxidative stress. When insulin levels were normalized

to total intracellular insulin content, a significant glucose response throughout the first and second phases of insulin secretion was only observed in pre-stressed MIN6s cultured on crowded matrix. Similarly, when the insulin levels were normalized to total DNA content, a significant response to the glucose challenge was only observed in the first phase of insulin secretion in stressed cells cultured on crowded matrix. Perhaps due to their highly stressed states, none of the three supports were able to sustain the GSIS function of the MIN6 cells by the second phase of insulin secretion. Previous studies with transient oxidative stressing of β-cells demonstrated loss of GSIS function at 3 days after exposure due to damages to the mitochondrial machinery (Li et al., 2009). In the same study, revival of the secretory responses was only observed three weeks after the hydrogen peroxide exposure. In this study however, it only took two days, post-exposure, for the crowded matrix to facilitate a partial recovery of the GSIS function. This suggests that the crowded matrix, but not the uncrowded matrix and TCP, enabled the MIN6 cells to regain their mitochondrial health and thus their ability to respond to glucose in a short period of time.

In addition to maintaining GSIS, the HUVEC ECM did not increase or decrease the overall apoptotic and necrotic populations in the MIN6 β-cell line compared to the TCP control in both the normal and H_2O_2-stressed cells (Figure 5.10 and 5.11). Nevertheless, at the genetic level, +MMC ECM induced increased expression of anti-apoptotic genes *A20* and *Bcl-XL* as well as the pro-apoptotic gene *Bax* in both normal and H_2O_2-stressed MIN6, while –MMC ECM reduced *Bax* expression in both normal and stressed cells and reduced *Bcl-XL* expression in stressed cells (Figure 5.9-5.10). A20 is a zinc-ring finger protein that prevents the activation of

NF- κB by the inflammatory response and in doing so, prevents the upregulation of pro-inflammatory genes (Heyninck and Beyaert, 2005; Ho and Bray, 1999). A20 overexpression has been associated with improved islet survival *in vivo*, where 75% of recipients were reversed of diabetes compared to 20% of the control islet recipients (Grey et al., 2003). However, it was shown in the same study that there was still evidence of caspase-3 in islet grafts of both cohorts, thus indicating that A20 is not able to inhibit all pathways of apoptosis. Bcl-XL is another anti-apoptotic protein that prevents the formation of pores in the mitochondrial membrane by pro-apoptotic proteins such as Bax triggered by intrinsic cues such as DNA damage, hypoxia and reactive oxygen species (Chan and Yu, 2004). Apoptosis only occurs when concentrations of pro-apoptotic proteins exceeds that of the anti-apoptotic proteins at the mitochondrial membrane (Chan and Yu, 2004). Overexpression of Bcl-XL in islets has previously been shown to prevent ROS-induced apoptosis *in vitro* (Zhou et al., 2000). An upregulation of both *Bcl-XL* and *Bax* in both normal and stressed MIN6s cultured on +MMC ECM may have neutralized the effect of both, while a lack of inflammatory factors such as cytokines in normal culture media may have rendered the anti-apoptotic effects of upregulated A20 to go unnoticed. The same reasoning could be used to explain the lack of change in apoptotic populations in stressed MIN6s cultured on –MMC ECM, whereby downregulation of both *Bcl-XL* and *Bax* may have negated the effect of both.

Nevertheless, morphological responses and genetic markers for β-cell differentiation were investigated in mouse primary islets cultured on HUVEC ECM. It was previously documented that ECM enhances islet adhesion, monolayer formation and

DNA synthesis (Hulinsky et al., 1995a; Hulinsky et al., 1995b; Kaiser et al., 1988; Schuppin et al., 1993; Thivolet et al., 1985). In contrast to these studies, primary mouse islets did attach more readily to HUVEC ECM than TCP, but did not form monolayers as readily on +MMC ECM. Less than 6% (at a maximum) of islets cultured on ECM formed monolayers within 7 days of culture on +MMC ECM (Table 5.2), which was vastly different to the 62% observed by Hayek et al on BCEC ECM at 5 days of culture (Hayek et al., 1989). Even on –MMC ECM, only up to 11% of islets were forming monolayers at 7 days of culture. The most surprising contrast was that up to 14% of islets were forming monolayers on TCP at 7 days of culture, whereas none were observed in the Hayek study.

The number of fibroblastic islets was not different across the three cell supports, and by day 7 of culture only made up to 6% of the islet populations. Interestingly, migration of β-cells away from monolayer-forming clusters were observed on TCP and –MMC ECM but was not as prevalent on +MMC ECM (Figure 5.13). A similar phenomenon was observed on BCEC ECM in the Schuppin and Thivolet studies (Schuppin et al., 1993; Thivolet et al., 1985). In contrast, islets cultured on +MMC ECM tended to remain in spherical clusters, did not form completely flat monolayers and were less spread compared to TCP and –MMC ECM. Though the formation of islet monolayers may have potential to be maintained in *in vitro* cultures, as previously demonstrated by Kaiser et al (Kaiser et al., 1988), the ability for +MMC ECM to maintain the spherical architecture and function of islets will mean easier harvesting from *in vitro* culture to *in vivo* transplantation.

β-cells within islets undergo dedifferentiation once isolated and placed in *in vitro* cultures. By 7-15 days after initiation of islet cultures, loss of important β-cell markers such as pdx1, insulin and glut2 can be observed (Weinberg et al., 2007). In the Weinberg study, 27% of β-cells were insulin-negative by day 8 and as high as 74% by day 21 in culture. The gene expression profile and phenotype of dedifferentiating islets is summarized in Table 5.3.

Table 5.3 Genetic markers and corresponding phenotypes for β-cells undergoing dedifferentiation.

Gene	**Expression level during dedifferentiation**	**Phenotype**	**Reference**
Glut1	Upregulation	Impaired GSIS	(Hughes et al., 1993)
Glut2	Downregulation	Impaired GSIS, loss of insulin expression control	(Guillam et al., 1997)
HNF1a	Downregulation	Reduction in glucose-stimulated insulin release	(Pontoglio et al., 1998)
NeuroD1	Downregulation	Development of diabetes and reduction in the number of endocrine cells	(Chao et al., 2007)
Proinsulin	Downregulation	Depletion of islet insulin content	(Leibowitz et al., 2002)
ID1	Upregulation	Inhibits differentiated β-cell function	(Akerfeldt and Laybutt, 2011; Billestrup, 2011)
MafA	Downregulation	Glucose intolerance, impaired GSIS	(Zhang et al., 2005)
Pdx1	Downregulation	Pancreas agenesis and impaired glucose tolerance	(Gauthier et al., 2004)

The downregulation of transcription factor mafA is associated with glucose intolerance and impaired GSIS (Zhang et al., 2005) and an upregulation of the transcriptional regulator ID1 inhibits differentiated β-cell function and is prevalent in type 2 diabetes (Akerfeldt and Laybutt, 2011; Billestrup, 2011). This phenotype was observed in islets cultured on –MMC ECM (Figure 5.16). Further confirmation of dedifferentiation is the upregulation of the glucose transporter, *glut1*, in islets on –MMC ECM, as rodent β-cells predominantly express *glut2* (De Vos et al., 1995). Nevertheless, islets on –MMC ECM also showed increases in β-cell-promoting markers such as *glut2*, *neuroD1* and *proinsulin*. Islets cultured on +MMC ECM, on the other hand, showed increased levels of *glut2*, *neuroD1* and *proinsulin* with unchanged expression levels of *glut1*, *ID1* and *mafA* compared to the TCP control. These results indicate that major differences in either structure, quantity of ECM components (verified in Chapter 4) and perhaps growth factors exist between –MMC and +MMC ECM. These differences have major influences on the β-cell/islet response in extended *in vitro* culture. The upregulation of both dedifferentiation and differentiation markers in islets on –MMC ECM may have been the result of only some islets being in contact with the correct amount of ECM components. Previous staining of ECM components in –MMC ECM (Chapter 4, Figure 4.14) demonstrated uneven residual ECM on the well plate after decellularisation. Whereas the more uniform and abundant presence of ECM components in +MMC ECM (Chapter 4, Figure 4.12-13) may have facilitated a more even exposure of the islets to these components and thus been more beneficial at maintaining β-cell-specific markers.

The primary islet gene expression and morphology studies provide a glimpse into the beneficial affect endothelial ECM has on isolated islets. Nevertheless, the differences in cell spreading and de-differentiation between the cell supports could potentially be further augmented by the use of dissociated islets in order to increase cell stress via the disruption of cell-to-cell contact.

5.5 Conclusion

These studies have demonstrated that enhancing HUVEC ECM deposition by macromolecular crowding extended the *in vitro* life of primary islets by maintaining insulin and glucagon hormone expression as well as genetic expression of important β-cell-specific markers that promote β-cell function. Furthermore, the method developed in Chapter 4 for the production and decellularisation of HUVEC ECM was not deleterious to primary mouse islets and the MIN6 β-cell line. This method allowed for the easy production of a β-cell-promoting mixture of ECM components that facilitated the maintenance of glucose stimulated insulin secretion and did not increase the occurrence of apoptosis and necrosis in the MIN6 β-cell line more than that of the TCP control.

This study also demonstrated better recovery of glucose responsiveness after oxidative stress by means of the crowded HUVEC ECM. Furthermore, the HUVEC ECM may have potential for protecting β-cells from the inflammatory response by increasing the expression of the anti-apoptotic/inflammatory gene, *A20*. An added advantage of the crowded ECM was its ability to preserve the spherical structure of islets in culture. Up to 95% of islets cultured on the crowded ECM maintained their 3D clustered structure at 7 days of culture, which would allow for easier downstream harvesting of the islets for *in vivo* transplantation.

These results show potential for crowded HUVEC ECM to maintain function, viability and differentiation of isolated islets in culture. The crowded HUVEC ECM provides a good basis for increasing the longevity of isolated islets by providing a "2.5D" scaffold on which islets may be supported and has the potential to be

harnessed into a microencapsulation system if the crowding technique can be applied into a 3D hydrogel system.

Chapter 6

6 Conclusions and Future Recommendations

Maintaining viable and functional β-cells after islet isolation is a critical step for successful and efficient islet transplantation. Although a variety of approaches have been developed to prolong islet longevity, current procedures still result in moderate islet recovery that is even further reduced following any period of *in vitro* culture. Many factors contribute to the demise of islets. These include enzymatic and mechanical stresses during isolation as well as exposure to proinflammatory cytokines, hypoxia and nutrient deprivation during the first stages of transplantation. Furthermore, islets are disrupted from their native environment, which contains important cell-to-cell and cell-to-matrix associations, and are expected to survive transplantation in their already compromised state. It would therefore be beneficial to develop an environment in which islets can recover from isolation and better gear them to survive the engraftment process.

This thesis aimed to understand the islet environment by characterizing the constitution of healthy adult pancreatic islet ECM and to produce ECM of a similar composition using *in vitro*-cultured cells. Macromolecular crowding was used to enhance *in vitro* deposition of ECM and it was hypothesized that endothelial cells under crowded conditions would produce ECM of a better quality and quantity for supporting islet function. The major objective was then to examine whether the crowded matrix was able to extend or enhance the function, viability and differentiation of β-cells in culture.

6.1 Conclusions

In Chapter 3, it was shown that basement membranes in the rodent islet are tightly associated with the endothelium and are thus possibly produced by the endothelium to facilitate communication between the different cell types within the islet. How the islets receive these molecular cues are through cell surface receptors previously to be identified as integrins (Cheng et al., 2011; Virtanen et al., 2008; Wang et al., 2005b; Wang et al., 1999; Wang and Rosenberg, 1999). However, this thesis has shown the presence of other cell surface molecules, HS and syndecan-4, which may also play a crucial role in the endocrine signalling pathway as they were mostly found on/in the β-cells. Consequently, it is hypothesised that these cell surface proteoglycans and their associated HS play a major role in the function and health of β-cells, perhaps by binding to important factors. However, the exact role of these components is still unknown. It would therefore be interesting to investigate whether β-cells lose syndecan-4 expression in long-term culture and thus lose their differentiation or are directed down the apoptosis pathway. In addition to this, the fate of syndecan-4 expression after transplantation would also be intriguing to determine.

In Chapter 4, it was identified that HUVECs were an abundant source of ECM components. Interestingly, the primary endothelial cells produced ECM components similar to those identified in the *in vivo* rodent islets in Chapter 3. This further supports the hypothesis that the endothelium supplies the majority of the basement membrane components within the islet of Langerhans. Considering syndecan-4 and HS may play a crucial role in β-cells, it was then ideal for HUVECs to also produce these components in order to supplement isolated islets with these components.

However, even though syndecan-4 was expressed by the HUVECs, the proteoglycan was destroyed or washed away in the decellularisation process. Nevertheless, other HS proteoglycans such as syndecan-1, glypican-1 and HS itself were all expressed by the HUVECs and remained in the ECM after decellularisation.

For *in vitro*-produced ECM to be clinically viable, production and deposition of ECM needs to be enhanced. Macromolecular crowding of the HUVEC culture media with a Ficoll cocktail was able to enhance ECM yield by up to 47-fold after decellularisation. Furthermore, the crowded matrix was also more uniformly spread and layered across the well plate. This was perhaps the reason for which differences in β-cell responses were observed in Chapter 5. Compared to TCP and normal HUVEC ECM, the crowded matrix was better at restoring glucose-responsiveness in the oxidative-stressed MIN6 cell line. In addition to this, the crowded matrix also better retained the spherical structure of isolated primary islets and maintained the expression of β-cell-specific differentiation markers in extended culture. It was, however, interesting to observe that islets cultured on normal HUVEC ECM showed more dedifferentiation gene expression than TCP. Not only were the islets forming monolayers at approximately the same rate as islets cultured on TCP, islets on normal HUVEC ECM showed expression profiles that demonstrated both dedifferentiation and differentiation genetic markers. The uneven distribution of uncrowded ECM components, as shown in Chapter 4, may have contributed to these unusual observations.

These results indicate that perhaps HUVEC ECM components need to be at a specific concentration, structure or orientation in order for the ECM to positively

influence isolated islets. Moreover, these specific ECM criteria may have been better achieved under macromolecular crowding conditions. It would therefore be crucial to study quantitative and qualitative differences between crowded and uncrowded matrix in order to determine the essential components that allowed crowded matrix to positively influence islet differentiation and structure.

Even though this thesis has shown interesting findings related to islets in the rodent species, inter-species differences discussed in Chapter 3 should not be forgotten. Further to this, though these results may provide some insight into the human species, verification of these studies need to be confirmed with human islets in order for this thesis to be clinically relevant.

In conclusion, the major findings from this work are summarised below:

- Islet basement membrane components are mostly associated with islet endothelium
- HS and syndecan-4 are more cell-associated, and localised to the β-cells but not the α-cells
- HUVECs produce many of the ECM components found in islet ECM, including HS and syndecans
- Macromolecular crowders enhances deposition of ECM and also facilitates more uniform layering of ECM on the well plate
- Normal and ECM that is enhanced by crowders are not deleterious to viability, GSIS function and proliferation of β-cells
- Crowder-enhanced ECM restores glucose-responsiveness in stressed β-cells

- Crowder-enhanced ECM extends β-cell differentiation and maintains the islet spherical topography better than normal HUVEC ECM and tissue culture plastic

6.2 Future Recommendations

The ECM is the key to determining the essential design principles for engineering long-lasting and functional tissues. This is because the ECM provides the correct molecular cues required by the cells to facilitate blood vessel formation, which then provides sufficient oxygen and nutrient/growth factor transfer that are essential for cell survival. Further investigations into the ratio in which the various ECM components exists in the islet ECM and how sydnecans interact with these components, will provide important insights into the exact composition by which a bioartificial pancreatic scaffold should be designed. As islets do not naturally produce very much ECM and loses the little ECM it has during isolation and transplantation, it therefore may be crucial to overcompensate the levels of ECM in the bioartifical scaffold.

Macromolecular crowding is a means by which ECM production can be enhanced. Therefore, the incorporation of crowders into a 3D system may potentially be a way in which the essential molecular cues may be provided in abundance to islets at the initial stages of seeding in the bioscaffold. The following sections describe the steps that will need to be taken in order to determine the parameters for designing a bioartificial pancreas.

6.2.1 Further characterisation of syndecans in islets

Further investigation into the functions of syndecans in β-cells may help to elucidate the reasons why islets cannot survive for extended periods once isolated. Even though syndecan-4 was the only cell surface HS proteoglycan detected in this thesis,

other isoforms of syndecan are likely to be present due to the lack of pancreatic dysfunction reported in syndecan-4 knockout mice (Simons and Horowitz, 2001). In addition, gene expression of syndecan-2, -3 and -4 has previously been detected in pancreatic islets (Takahashi et al., 2009). The syndecan-4 knockout mice is currently the most well-characterized out of the four isoforms, however, the phenotypes of defective wound healing and decreased angiogenesis have dominated reports without any mention of islet function (Alexopoulou et al., 2007).

There are several ways in which syndecans and islet function may be studied. Islets from syndecan knockout mice as well as mice with knockouts of each isoform may be isolated and compared. Considering islet capillaries are five-times (Larrain et al., 1997) more dense and ten-fold more fenestrated than the exocrine capillaries and the β-cells are generally bordered by at least one capillary (Ballian and Brunicardi, 2007; Henderson and Moss, 1985), it would be interesting to study the vascularization and basement membranes of islets from these knockout mice. Another approach would be to knockdown syndecans in the MIN6 insulinoma cell line using siRNA technology. Subsequent studies of the syndecan knockout islets or knocked down MIN6s could include cell proliferation (Su et al., 2007), cell adhesion to various ECM components (Utani et al., 2001; Woods et al., 2000b), glucose-stimulated insulin secretion, apoptosis and necrosis (Modrowski et al., 2005), differentiation (Dhodapkar et al., 1998; Larrain et al., 1997) and cell interaction with growth factors such as FGF (Carey, 1997; Tkachenko et al., 2004). Together, these experiments could help explain the mechanisms by which syndecans help β-cells function and potentially survive *in vitro* culture and ultimately, transplantation.

6.2.2 Further assessment of HUVEC ECM and macromolecular crowding

Chapter 4 showed differences in quantity of ECM components between HUVEC ECM that were made with and without macromolecular crowders. Chapter 5 showed distinctly different β-cell responses, morphologically and genetically, to the crowded and uncrowded matrix. Further investigations into specific differences that exist between the two ECMs such as presence of growth factors embedded in the matrix, surface roughness and chemical composition can all help to elucidate the reasons behind the differential responses from the β-cells. Experimental tools such as Raman spectroscopy (Hanlon et al., 2000; Votteler et al., 2012), fourier transform infrared (FTIR) imaging spectroscopy (Cheheltani et al., 2012; Federman et al., 2002; Lui et al., 1996) and atomic force microscopy (AFM) (Zeiger et al., 2012) can provide information about the composition of the different ECMs at the molecular level. Infrared and AFM images of cells surrounded by their deposited matrix with and without crowders may provide more chemical and structural information. Previous studies that used AFM was able to detect differences in ECM alignment in normal and crowded mesenchymal stem cells (Zeiger et al., 2012). Similar differences may potentially help to explain why isolated islets responded so differently to the normal and crowded endothelial ECM.

Other cells types such as murine islet endothelial cells (closer in type to endothelial cells found in proximity to β-cells *in vivo*) and fibroblasts (negative control to endothelial ECM) may also be crowded to compare ECM morphology and subsequent islet/β-cell responses. Furthermore, alternative macromolecular crowders may be used to tailor the spatial orientation and pattern of the deposited ECM to one

more suited to β-cells. Collagen I and fibronectin matrices produced under Ficoll crowding by fibroblasts were shown to be more reticular, whereas dextran sulfate produced a course granular pattern (Lareu et al., 2007c). Similarly, Ficoll crowded mesenchymal stem cells produced fibronectin and collagen IV fibers that were more aligned than uncrowded cells and in doing so, increased the actin cytoskeleton alignment of the mesenchymal stem cells seeded onto this ECM (Zeiger et al., 2012). It would therefore be interesting to investigate the effect of different endothelial ECM structures on β-cell function.

6.2.3 Incorporation of endothelial ECM into 3D hydrogels

The interactions between islets and ECM have mostly been studied on 2D ECM-coated surfaces. However, there is increasing interest in simulating *in vivo* characteristic of tissues, whereby cell-matrix interactions occur on a 3D level. Studies with collagen-based hydrogels (Nagata et al., 2002) and Matrigel® (Knight et al., 2006a; Oberg-Welsh, 2001; Perfetti et al., 1996) have all shown better islet viability and function than when cultured on 2D culture plates. However, even though hydrogels containing ECM peptides have shown some promise (Lin et al., 2009; Weber et al., 2007), they do not provide the plethora of ECM components that islets require for long-term survival and functionality. Therefore, incorporation of endothelial ECM into hydrogels may be a solution.

A method for harvesting *in vitro* crowded ECM could be developed for the incorporation of the components into 3D synthetic scaffolds such as hydrogels. The endothelial cells could be crowded and cultured on a thermo-responsive polymer, such as poly(N-isopropylacrylamide) (PNIPAAm) (Moran et al., 2007), then

decellularized. The residual ECM may then be lifted off the polymer surface at the correct temperature and freeze-dried for downstream incorporation into hydrogels and encapsulation of islets/β-cells.

6.2.4 Co-culture of β-cells with crowded endothelial cells

Alternatively, endothelial cells and islets can be cultured together in a 2D or encapsulated 3D system. Current focus has been to co-culture the two cell types in order to improve vascularization and protect islets from blood-mediated inflammatory reaction (Johansson et al., 2005; Paget et al., 2011; Pan et al., 2011; Song et al., 2009). However, the ability for endothelial cells to supply islets with ECM components in co-culture has not yet been explored.

In a 2D system, macromolecular crowding of endothelial cells could first enhance ECM deposition. Islets or β-cells can then be added to the culture and tested for functionality and differentiation. In a 3D system, islets/β-cells can be encapsulated with endothelial cells in a degradable hydrogel system and cultured under crowded conditions. Ideally, the hydrogel would degrade at a similar rate to the rate at which the endothelial cells produce and deposit ECM around the islets/β-cells. In this manner, a mixture of islet-promoting ECM components that is not denatured, bioactive and containing vital growth factors could be directly constructed around the islets/β-cells and eventually replace the original hydrogel system.

In addition to *in vitro* studies, *in vivo* studies using animal models are vital for determining whether these methods for helping isolated islets recover from the isolation process have any clinical relevance. The *in vivo* environment is complex and thus the ability for these islets to survive the engraftment procedure will be a

future hurdle that cannot be predicted through *in vitro* testing alone. Rodent models are easier to manipulate and with many models of diabetes in mice being currently available for use, they are optimal for preliminary investigations into initial clinical outcomes.

6.3 Concluding statement

This thesis has provided the groundwork for understanding the constituents of healthy pancreatic islet ECM that may be important for maintaining islet longevity. In addition to this, a method was developed for the easy production of an ECM mixture that does not require lengthy and complex extraction steps and contains all the components identified in a healthy islet ECM. This ECM mixture has shown much promise in supporting and maintaining the function, viability and differentiation of isolated islets and thus also holds potential for the improvement of future islet transplantation efficiencies and outcomes.

Appendix

Appendix A

Comparison of healthy and diabetic human islet gene expression

Microarray data from healthy and Type 2 diabetic human islets is available from the website of the Diabetes Genome Anatomy Project (Gunton et al., 2005; Kahn, 2005). Human pancreatic islets were isolated from 7 healthy donors with normal glucose tolerance, and 5 Type 2 diabetic donors. All donors either suffered a cerebrovascular accident or intracerebral haemorrhage. RNA was isolated (no samples were pooled), cRNA made and hybridized to U133A and U133B Affymetrix arrays. This data was analysed for differences in expression levels of syndecans in healthy and diabetic islets. Figure A.1 shows an individual value plot of the arbitrary fluorescence intensity values that represent gene expression levels from each donor. Student t-tests were performed to determine statistical significance in differences between healthy and diabetic gene expression.

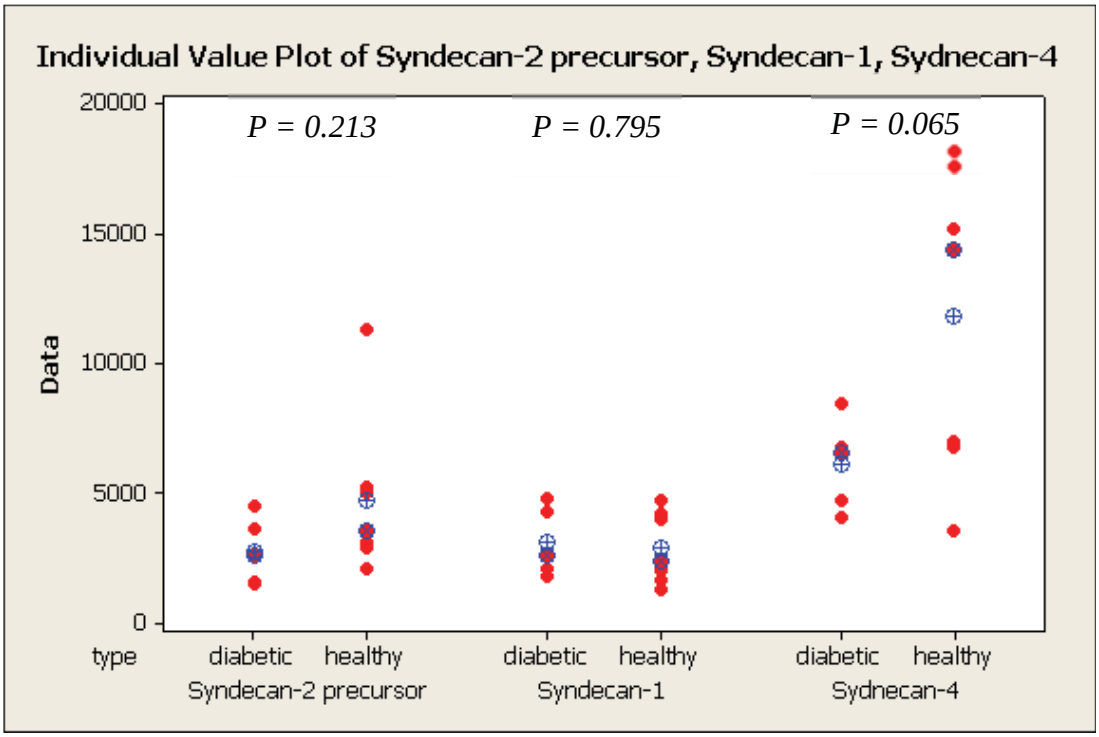

Figure A.1 Individual value plot of Syndecan gene expression levels in Type 2 diabetic and healthy human islets. Data values are arbitrary fluorescence intensity values that reflect the expression level of the gene. ⊗ represents the position of the median and ⊕ represents the position of the mean. Student t-test was performed to obtain the corresponding P-values.

Appendix B

Identification of islet ECM by mass spectrometry

Identification of ECM proteins and/or proteoglycans from isolated islets was attempted by mass spectrometry. Pages 193 to 195 shows an example of the peptide sequences identified by the database search program, Mascot. Direct tryptic digestion of protein extracts as well as semi-purification by SDS-PAGE both resulted in identification of intracellular proteins only. Both ECM proteins and proteoglycans were not identified in the Mascot peptide search.

Mascot Search Results

User : **Orbi-Proc**
Email :
Search title : **Jenny_14_10_11_islet.raw**
MS data file : **G:\Data\Ling\VelosOrbi\17-10-11\Jenny_14_10_11_islet.raw**
Database : **NCBInr 19_8_11 (14987464 sequences; 5132678026 residues)**
Timestamp : **17 Oct 2011 at 01:01:09 GMT**
Protein hits :

gi|25742763 78 kDa glucose-regulated protein precursor [Rattus norvegicus]
gi|1351907 RecName: Full=Serum albumin; AltName: Full=BSA; AltName: Allergen=Bos d 6; Flags: Precursor
gi|6755863 endoplasmin [Mus musculus]
gi|74267962 ALB protein [Bos taurus]
gi|296482166 78 kDa glucose-regulated protein precursor [Bos taurus]
gi|15010550 heat shock protein gp96 precursor [Homo sapiens]
gi|54777 unnamed protein product [Mus musculus]
gi|157679184 HSP70 protein [Poecilia reticulata]
gi|6807647 hypothetical protein [Homo sapiens]
gi|11230802 alpha-actinin-4 [Mus musculus]
gi|60502437 Protein disulfide isomerase associated 6 [Mus musculus]
gi|58037267 protein disulfide-isomerase A6 [Mus musculus]
gi|6756041 14-3-3 protein zeta/delta [Mus musculus]
gi|6754254 heat shock protein HSP 90-alpha [Mus musculus]
gi|27806751 alpha-2-HS-glycoprotein precursor [Bos taurus]
gi|281485070 heat shock protein [Ctenopharyngodon idella]
gi|253706 14-3-3 protein zeta chain [cattle, brain, Peptide, 245 aa]
gi|6756039 14-3-3 protein theta [Mus musculus]
gi|148238273 inter-alpha-trypsin inhibitor heavy chain H2 [Bos taurus]
gi|9507245 14-3-3 protein gamma [Rattus norvegicus]
gi|5803225 14-3-3 protein epsilon [Homo sapiens]
gi|37492 alpha-tubulin [Homo sapiens]
gi|33438248 mKIAA0034 protein [Mus musculus]
gi|6005942 transitional endoplasmic reticulum ATPase [Homo sapiens]
gi|200283 protein disulfide isomerase-related protein [Mus musculus]
gi|3065925 14-3-3 protein beta [Mus musculus]
gi|27806941 alpha-1-antiproteinase precursor [Bos taurus]
gi|10946574 creatine kinase B-type [Mus musculus]
gi|67782283 actin 5 [Aedes aegypti]
gi|1710248 protein disulfide isomerase-related protein 5 [Homo sapiens]
gi|307188541 Heat shock 70 kDa protein cognate 4 [Camponotus floridanus]
gi|221106594 PREDICTED: similar to predicted protein [Hydra magnipapillata]

gi|6680836 calreticulin precursor [Mus musculus]
gi|1374715 ATP synthase beta subunit [Rattus norvegicus]
gi|38348230 ERO1-like protein beta precursor [Mus musculus]
gi|6680932 chromogranin-A precursor [Mus musculus]
gi|6679891 neutral alpha-glucosidase AB [Mus musculus]
gi|3860051 transcytosis associated protein p115 [Mus musculus]
gi|1002369 coatomer protein [Homo sapiens]
gi|49481 beta tubulin [Cricetulus griseus]
gi|683793 calnexin [Mus musculus]
gi|136429 RecName: Full=Trypsin; Flags: Precursor
gi|2724046 beta-actin [Mustela putorius furo]
gi|148362136 TUBB [Salmo salar]
gi|10720174 RecName: Full=Hypoxia up-regulated protein 1; AltName: Full=150 kDa oxygen-regulated protein; Short=ORP-150; Flags: Precursor
gi|71664 calmodulin - salmon
gi|115893 RecName: Full=Carboxypeptidase E; Short=CPE; AltName: Full=Carboxypeptidase H; Short=CPH; AltName: Full=Enkephalin convertase; AltName: Full=Prohormone·
gi|32358 hnRNP U protein [Homo sapiens]
gi|6756037 14-3-3 protein eta [Mus musculus]
gi|135490 RecName: Full=Tubulin beta chain; AltName: Full=Beta-tubulin
gi|2612797 precursor NEFA protein [Mus musculus]
gi|156322163 hypothetical protein NEMVEDRAFT_v1g225293 [Nematostella vectensis]
gi|156371481 predicted protein [Nematostella vectensis]
gi|128842 RecName: Full=Nucleolin; AltName: Full=Protein C23
gi|312732 beta prime cop [Bos taurus]
gi|78369364 vitamin D-binding protein precursor [Bos taurus]
gi|224148687 PREDICTED: similar to ATP synthase subunit beta, mitochondrial, partial [Taeniopygia guttata]
gi|6679465 glucosidase 2 subunit beta precursor [Mus musculus]

gi|50823	unnamed protein product [Mus musculus]
gi|291395669	PREDICTED: histone cluster 1, H2bc-like [Oryctolagus cuniculus]
gi|309215	EndoA' cytokeratin (5' end put.); putative [Mus musculus]
gi|1346784	RecName: Full=Proteasome subunit alpha type-7; AltName: Full=Proteasome subunit RC6-1
gi|16506279	testican-2 precursor [Mus musculus]
gi|78000201	tropomyosin alpha-1 chain isoform h [Rattus norvegicus]
gi|121496	RecName: Full=Glucagon; Contains: RecName: Full=Glicentin; Contains: RecName: Full=Glicentin-related polypeptide; Short=GRPP; Contains: RecName: Full=O›
gi|67043503	heat shock protein 70 [Cyclospora colobi]
gi|9789985	isovaleryl-CoA dehydrogenase, mitochondrial precursor [Mus musculus]
gi|37403	unnamed protein product [Homo sapiens]
gi|473947	KIAA0115 [Homo sapiens]
gi|38566236	UDP-glucose ceramide glucosyltransferase-like 1 [Mus musculus]
gi|50409	unnamed protein product [Mus musculus]
gi|205065	ORF with similarities to Kex2 and furin proteins; putative [Rattus norvegicus]
gi|478813	nonhistone chromosomal protein HMG-1 - human
gi|1588409	dynactin:SUBUNIT=50kD
gi|50349[illegible]	nascent polypeptide associated complex subunit alpha isoform b [Homo sapiens]
gi|2935[illegible]	endo B cytokeratin [Mus musculus]
gi|1398903	Ca2+ dependent activator protein for secretion [Mus musculus]
gi|4885371	histone H1.0 [Homo sapiens]
gi|83764016	prepro complement component C3 [Bos taurus]
gi|110331845	inter-alpha (globulin) inhibitor H3 [Bos taurus]
gi|83745120	60S acidic ribosomal protein P2 [Mus musculus]
gi|19072792	endoplasmic reticulum resident protein 44 precursor [Mus musculus]
gi|4503481	elongation factor 1-gamma [Homo sapiens]
gi|4506661	60S ribosomal protein L7a [Homo sapiens]
gi|1763275	acidic nuclear phosphoprotein pp32 [Mus musculus]
gi|488	kininogen I precursor [Bos taurus]
gi|12841359	unnamed protein product [Mus musculus]
gi|6755204	proteasome subunit beta type-5 [Mus musculus]
gi|8567338	coatomer subunit gamma isoform 1 [Mus musculus]
gi|59857769	inter-alpha (globulin) inhibitor H4 (plasma Kallikrein-sensitive glycoprotein) [Bos taurus]
gi|7110705	prothymosin alpha [Mus musculus]
gi|6677865	secretogranin-2 precursor [Mus musculus]
gi|157954061	alpha-2-macroglobulin [Bos taurus]
gi|122555	RecName: Full=Hemoglobin subunit beta; AltName: Full=Beta-globin; AltName: Full=Hemoglobin beta chain
gi|306875	C protein [Homo sapiens]
gi|1093617	major vault protein
gi|12314088	dJ604K5.1 (15 kDa selenoprotein) [Homo sapiens]
gi|149633330	PREDICTED: similar to tubulin alpha-3 chain - Chinese hamster [Ornithorhynchus anatinus]
gi|296736	macropain subunit iota [Homo sapiens]
gi|292160	heat shock protein 70 [Homo sapiens]
gi|77735479	alpha-fetoprotein precursor [Bos taurus]
gi|116643090	beta-tubulin [Erratomyces patelii]
gi|47225622	unnamed protein product [Tetraodon nigroviridis]
gi|122597	RecName: Full=Hemoglobin subunit beta; AltName: Full=Beta-globin; AltName: Full=Hemoglobin beta chain
gi|5114051	HSPC029 [Homo sapiens]
gi|34228	unnamed protein product [Homo sapiens]
gi|148232266	fibulin-1 [Bos taurus]
gi|27806743	protein AMBP precursor [Bos taurus]
gi|223130	fibrinogen betaB 1-118
gi|26328385	unnamed protein product [Mus musculus]
gi|6755202	proteasome subunit beta type-3 [Mus musculus]
gi|227229	ribosomal protein S4
gi|162719	ATP synthase alpha subunit precursor [Bos taurus]
gi|7657176	protein canopy homolog 2 isoform 1 precursor [Homo sapiens]
gi|26353732	unnamed protein product [Mus musculus]
gi|4506195	proteasome subunit beta type-2 isoform 1 [Homo sapiens]
gi|1907268	proteasome subunit C9-like protein [Sus scrofa]
gi|21913299	ribosomal protein L15 [Gadus morhua]
gi|13959396	RecName: Full=Ras GTPase-activating-like protein IQGAP1
gi|2935466	taipoxin-associated calcium binding protein 49 [Mus musculus]
gi|5902076	serine/arginine-rich splicing factor 1 isoform 1 [Homo sapiens]
gi|148230585	thioredoxin-like 1 [Xenopus laevis]
gi|32532	unnamed protein product [Homo sapiens]
gi|132827	RecName: Full=60S ribosomal protein L26
gi|4507669	translationally-controlled tumor protein [Homo sapiens]
gi|1917813	OCP2 [Homo sapiens]

gi|1617813	UCP2 [Homo sapiens]
gi|6981672	tropomyosin alpha-4 chain [Rattus norvegicus]
gi|52545896	hypothetical protein [Homo sapiens]
gi|4503513	eukaryotic translation initiation factor 3 subunit I [Homo sapiens]
gi|50527	cytochrome c oxidase subunit Va preprotein [Mus musculus]
gi|1498589	20S proteasome alpha subunit PSMA5 [Drosophila melanogaster]
gi|78045497	vitronectin [Bos taurus]
gi|57506	zinc binding protein [Rattus norvegicus]
gi|12843046	unnamed protein product [Mus musculus]
gi|418316	RecName: Full=DNA damage-binding protein 1; AltName: Full=DDB p127 subunit; AltName: Full=DDBa; AltName: Full=Damage-specific DNA-binding protein 1; Alt
gi|220659	unnamed protein product [Rattus norvegicus]
gi|145349855	predicted protein [Ostreococcus lucimarinus CCE9901]
gi|200812	LLRep3 protein [Mus musculus]
gi|12857342	unnamed protein product [Mus musculus]
gi|1372988	cytochrome c oxidase subunit IV [Mus musculus]
gi|34234	laminin-binding protein [Homo sapiens]
gi|397800	cyclophilin C-associated protein [Mus musculus]
gi|5902663	elongation factor 1-beta homolog [Mus musculus]
gi|286248	proteasome subunit R-DELTA [Rattus sp.]
gi|627739	heparin-binding protein 15 - bovine
gi|135806	RecName: Full=Prothrombin; AltName: Full=Coagulation factor II; Contains: RecName: Full=Activation peptide fragment 1; Contains: RecName: Full=Activatio
gi|57708	unnamed protein product [Rattus rattus]
gi|52741	J1 protein [Mus musculus]
gi|4506203	proteasome subunit beta type-7 proprotein [Homo sapiens]
gi|158767	ubiquitin [Drosophila melanogaster]
gi|122272	RecName: Full=Hemoglobin subunit alpha-1; AltName: Full=Alpha-1-globin; AltName: Full=Hemoglobin alpha-1 chain
gi|3264859	translation initiation factor eIF3 p44 subunit [Homo sapiens]
gi|223590	oxidase IV,cytochrome
gi|9955246	Chain A, Crystal Structure Of A Chimera Of Beta-Catenin And Alpha- Catenin
gi|73958475	PREDICTED: similar to major vault protein [Canis familiaris]
gi|36049	unnamed protein product [Homo sapiens]
gi|6753490	COP9 signalosome complex subunit 4 [Mus musculus]
gi|71413905	hypothetical protein [Trypanosoma cruzi strain CL Brener]
gi|4506711	40S ribosomal protein S27 [Homo sapiens]
gi|194760821	GF22263 [Drosophila ananassae]
gi|[illegible]	ES/130 [Homo sapiens]
gi|551547	prosome beta-subunit [Homo sapiens]
gi|30377	cytokeratin 13 [Homo sapiens]
gi|293675	IFN-response element binding factor 2 [Mus musculus]
gi|195977848	positive transcriptional regulator MutR family [Streptococcus equi subsp. zooepidemicus MGCS10565]

	NCBInr	Decoy	False discovery rate
Peptide matches above identity threshold	310	5	1.61 %
Peptide matches above homology or identity threshold	431	19	4.41 %

Mascot Score Histogram

Ions score is -10*Log(P), where P is the probability that the observed match is a random event.
Individual ions scores > 44 indicate identity or extensive homology ($p<0.05$).
Protein scores are derived from ions scores as a non-probabilistic basis for ranking protein hits.

Appendix C

Selection of housekeeping gene for MIN6 and islets

Housekeeping genes TATA-binding protein (TBP) and cyclophilin were the initial candidates for qPCR normalization. However, the expression of these genes was found to fluctuate not only between each condition but also across each trial in the MIN6 cell line (Figure B.1), with both genes often being upregulated in normal (unstressed) MIN6 cells cultured on +MMC ECM.

Similarly, variations in TBP and cyclophilin expression between experimental conditions were observed in isolated murine pancreatic islets (Figure B.2). Interestingly, in contrast to the MIN6 cells, significant downregulation of both housekeeping genes were observed in islets cultured on ECM.

The 18S rRNA was found to be the most stable housekeeping gene in both MIN6 and islets, with very slight variances between each cell support and trial. The 18S rRNA was thus used for subsequent normalization in the comparative analyses of mRNA expression levels in β-cells.

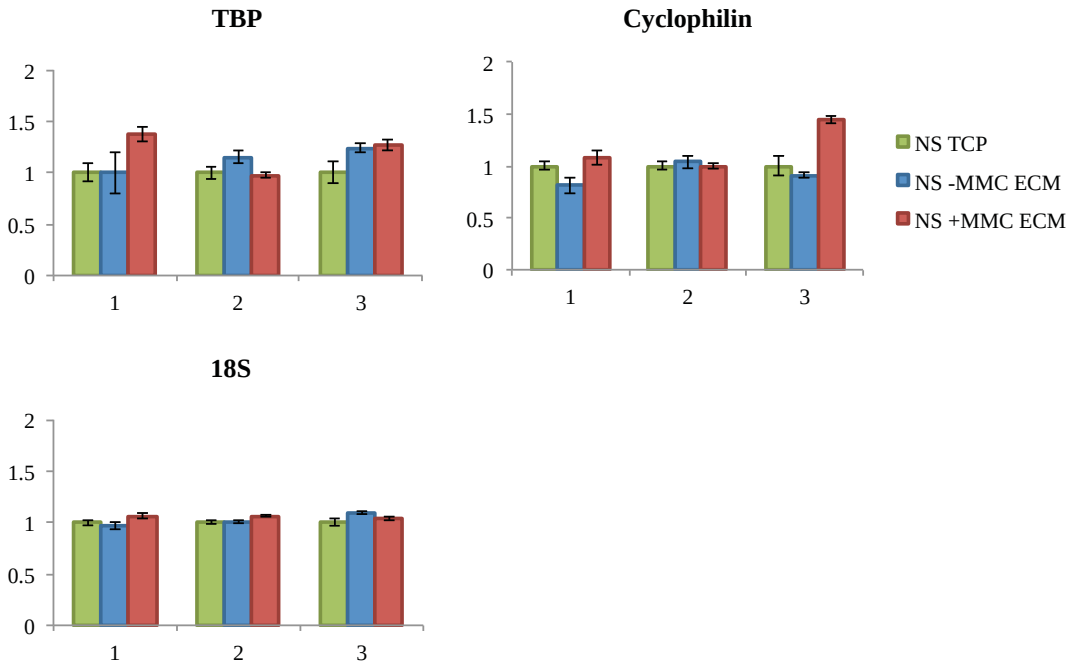

Figure B.1 Comparison of housekeeping gene expression levels in normal MIN6 cells at 2 days of culture on TCP (NS TCP), uncrowded matrix (NS –MMC ECM) and crowded matrix (NS +MMC ECM) in 3 separate experiments.

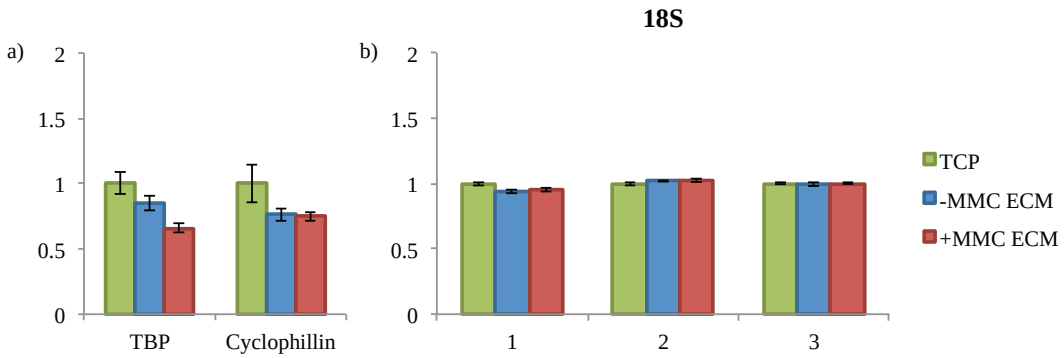

Figure B.2 Comparison of housekeeping gene expression levels in murine pancreatic islets at 7 days of culture on TCP, –MMC ECM and +MMC ECM in (a) 1 experiment for TBP and cyclophilin and (b) 3 separate experiments for 18S.

References

Akerfeldt, M.C., and D.R. Laybutt. 2011. Inhibition of Id1 augments insulin secretion and protects against high-fat diet-induced glucose intolerance. *Diabetes*. 60:2506-2514.

Alberts, B., A. Johnson, J. Lewis, M. Raff, and K.R.P. Walter. 2007. Molecular biology of the cell - fifth edition. Garland Science, Taylor \& Francis Group.

Alexopoulou, A.N., H.A. Multhaupt, and J.R. Couchman. 2007. Syndecans in wound healing, inflammation and vascular biology. *Int J Biochem Cell Biol*. 39:505-528.

Alves, F., W. Vogel, K. Mossie, B. Millauer, H. Höfler, and A. Ullrich. 1995. Distinct structural characteristics of discoidin I subfamily receptor tyrosine kinases and complementary expression in human cancer. *Oncogene*. 10:609--618.

Andres, J.L., L. Rönnstrand, S. Cheifetz, and J. Massagué. 1991. Purification of the transforming growth factor-beta (TGF-beta) binding proteoglycan betaglycan. *J Biol Chem*. 266:23282--23287.

Antonio, J.D.S., M.J. Karnovsky, S. Gay, R.D. Sanderson, and A.D. Lander. 1994. Interactions of syndecan-1 and heparin with human collagens. *Glycobiology*. 4:327--332.

Antonio, J.D.S., J. Slover, J. Lawler, M.J. Karnovsky, and A.D. Lander. 1993. Specificity in the interactions of extracellular matrix proteins with subpopulations of the glycosaminoglycan heparin. *Biochemistry*. 32:4746--4755.

Armanet, M., A. Wojtusciszyn, P. Morel, G. Parnaud, P. Rousselle, C. Sinigaglia, T. Berney, and D. Bosco. 2009. Regulated laminin-332 expression in human islets of Langerhans. *FASEB J*. 23:4046--4055.

Asundi, V.K., and D.J. Carey. 1995. Self-association of N-syndecan (syndecan-3) core protein is mediated by a novel structural motif in the transmembrane domain and ectodomain flanking region. *J Biol Chem*. 270:26404-26410.

Aukland, K., G.C. Kramer, and E.M. Renkin. 1984. Protein concentration of lymph and interstitial fluid in the rat tail. *Am J Physiol*. 247:H74-79.

Aviezer, D., D. Hecht, M. Safran, M. Eisinger, G. David, and A. Yayon. 1994. Perlecan, basal lamina proteoglycan, promotes basic fibroblast growth factor-receptor binding, mitogenesis, and angiogenesis. *Cell*. 79:1005--1013.

Azevedo-Martins, A.K., S. Lortz, S. Lenzen, R. Curi, D.L. Eizirik, and M. Tiedge. 2003. Improvement of the mitochondrial antioxidant defense status prevents cytokine-induced nuclear factor-kappaB activation in insulin-producing cells. *Diabetes*. 52:93-101.

Ballian, N., and F.C. Brunicardi. 2007. Islet vasculature as a regulator of endocrine pancreas function. *World J Surg*. 31:705-714.

Bao, X., E.A. Moseman, H. Saito, B. Petryniak, A. Thiriot, S. Hatakeyama, Y. Ito, H. Kawashima, Y. Yamaguchi, J.B. Lowe, U.H. von Andrian, and M. Fukuda. Endothelial heparan sulfate controls chemokine presentation in recruitment of lymphocytes and dendritic cells to lymph nodes. *Immunity*. 33:817-829.

Bateman, J.F., W.G. Cole, J.J. Pillow, and J.A.M. Ramshaw. 1986. Induction of procollagen processing in fibroblast cultures by neutral polymers. *Journal of Biological Chemistry*. 261:4198-4203.

Bates, D.O., J.R. Levick, and P.S. Mortimer. 1993. Change in macromolecular composition of interstitial fluid from swollen arms after breast cancer treatment, and its implications. *Clin Sci (Lond)*. 85:737-746.

Baudin, B., A. Bruneel, N. Bosselut, and M. Vaubourdolle. 2007. A protocol for isolation and culture of human umbilical vein endothelial cells. *Nature protocols*. 2:481-485.

Beattie, G.M., A.M.P. Montgomery, A.D. Lopez, E. Hao, B. Perez, M.L. Just, J.R.T. Lakey, M.E. Hart, and A. Hayek. 2002. A novel approach to increase human islet cell mass while preserving beta-cell function. *Diabetes*. 51:3435--3439.

Belkin, A.M., and N.R. Smalheiser. 1996. Localization of cranin (dystroglycan) at sites of cell-matrix and cell-cell contact: recruitment to focal adhesions is dependent upon extracellular ligands. *Cell Adhes Commun*. 4:281--296.

Bengtsson, E., M. Mörgelin, T. Sasaki, R. Timpl, D. Heinegård, and A. Aspberg. 2002. The leucine-rich repeat protein PRELP binds perlecan and collagens and may function as a basement membrane anchor. *J Biol Chem*. 277:15061--15068.

Bernfield, M., M. Götte, P.W. Park, O. Reizes, M.L. Fitzgerald, J. Lincecum, and M. Zako. 1999. Functions of cell surface heparan sulfate proteoglycans. *Annu Rev Biochem*. 68:729--777.

Bernfield, M., and R.D. Sanderson. 1990. Syndecan, a developmentally regulated cell surface proteoglycan that binds extracellular matrix and growth factors. *Philos Trans R Soc Lond B Biol Sci*. 327:171--186.

Bezakova, G., and M.A. Ruegg. 2003. New insights into the roles of agrin. *Nat Rev Mol Cell Biol*. 4:295--308.

Biarnes, M., M. Montolio, V. Nacher, M. Raurell, J. Soler, and E. Montanya. 2002. Beta-cell death and mass in syngeneically transplanted islets exposed to short- and long-term hyperglycemia. *Diabetes*. 51:66-72.

Billestrup, N. 2011. ID'ing a novel inhibitor of beta-cell function, Id1. *Diabetes*. 60:2455-2456.

Bix, G., J. Fu, E.M. Gonzalez, L. Macro, A. Barker, S. Campbell, M.M. Zutter, S.A. Santoro, J.K. Kim, M. Höök, C.C. Reed, and R.V. Iozzo. 2004. Endorepellin causes endothelial cell disassembly of actin cytoskeleton and focal adhesions through alpha2beta1 integrin. *J Cell Biol*. 166:97--109.

Bix, G., and R.V. Iozzo. 2008. Novel interactions of perlecan: unraveling perlecan's role in angiogenesis. *Microsc Res Tech*. 71:339--348.

Blasi, F. 1997. uPA, uPAR, PAI-1: key intersection of proteolytic, adhesive and chemotactic highways? *Immunol Today*. 18:415--417.

Blinman, T.A., I. Gukovsky, M. Mouria, V. Zaninovic, E. Livingston, S.J. Pandol, and A.S. Gukovskaya. 2000. Activation of pancreatic acinar cells on isolation from tissue: cytokine upregulation via p38 MAP kinase. *Am J Physiol Cell Physiol*. 279:C1993-2003.

Bode-Lesniewska, B., M.T. Dours-Zimmermann, B.F. Odermatt, J. Briner, P.U. Heitz, and D.R. Zimmermann. 1996. Distribution of the large aggregating proteoglycan versican in adult human tissues. *J Histochem Cytochem*. 44:303--312.

Bonner-Weir, S., M. Taneja, G.C. Weir, K. Tatarkiewicz, K.H. Song, A. Sharma, and J.J. O'Neil. 2000. In vitro cultivation of human islets from expanded ductal tissue. *Proc Natl Acad Sci U S A*. 97:7999--8004.

Bornstein, P., and E.H. Sage. 2002. Matricellular proteins: extracellular modulators of cell function. *Curr Opin Cell Biol*. 14:608--616.

Borun, T.W., M.D. Scharff, and E. Robbins. 1967. Preparation of mammalian polyribosomes with the detergent Nonidet P-40. *Biochim Biophys Acta*. 149:302-304.

Bosco, D., P. Meda, P.A. Halban, and D.G. Rouiller. 2000. Importance of cell-matrix interactions in rat islet beta-cell secretion in vitro: role of alpha6beta1 integrin. *Diabetes*. 49:233-243.

Bottino, R., A.N. Balamurugan, S. Bertera, M. Pietropaolo, M. Trucco, and J.D. Piganelli. 2002. Preservation of human islet cell functional mass by anti-oxidative action of a novel SOD mimic compound. *Diabetes*. 51:2561-2567.

Bowers, S.L.K., I. Banerjee, and T.A. Baudino. 2010. The extracellular matrix: at the center of it all. *J Mol Cell Cardiol*. 48:474--482.

Buchanan, C., I. Stigliano, H.M. Garay-Malpartida, L.R. Gomes, L. Puricelli, M.C. Sogayar, E.B. de Kier Joffé, and M.G. Peters. 2010. Glypican-3 reexpression regulates apoptosis in murine adenocarcinoma mammary cells modulating PI3K/Akt and p38MAPK signaling pathways. *Breast Cancer Res Treat*. 119:559--574.

Buruzula, G.K., H.W.T. Matthew, and J.F.Eliason. 2004. Differentiation of CD34+ cord blood cells in glycosaminoglycan microcapsules. *Proceedings of the IEEE 30th Annual Northeast*:114-115.

Cabric, S., J. Sanchez, U. Johansson, R. Larsson, B. Nilsson, O. Korsgren, and P.U. Magnusson. 2010. Anchoring of vascular endothelial growth factor to surface-immobilized heparin on pancreatic islets: implications for stimulating islet angiogenesis. *Tissue Eng Part A*. 16:961--970.

Caiazzo, R., V. Gmyr, T. Hubert, N. Delalleau, R. Lamberts, E. Moerman, J. Kerr-Conte, and F. Pattou. 2007. Evaluation of alternative sites for islet transplantation in the minipig: interest and limits of the gastric submucosa. *Transplant Proc*. 39:2620-2623.

Carey, D.J. 1997. Syndecans: multifunctional cell-surface co-receptors. *Biochem J*. 327 (Pt 1):1-16.

Carlsson, P.O., F. Palm, and G. Mattsson. 2002. Low revascularization of experimentally transplanted human pancreatic islets. *J Clin Endocrinol Metab*. 87:5418-5423.

Chakravarti, S., M.F. Tam, and A.E. Chung. 1990. The basement membrane glycoprotein entactin promotes cell attachment and binds calcium ions. *J Biol Chem*. 265:10597--10603.

Chan, S.L., and V.C. Yu. 2004. Proteins of the bcl-2 family in apoptosis signalling: from mechanistic insights to therapeutic opportunities. *Clinical and experimental pharmacology & physiology*. 31:119-128.

Chao, C.S., Z.L. Loomis, J.E. Lee, and L. Sussel. 2007. Genetic identification of a novel NeuroD1 function in the early differentiation of islet alpha, PP and epsilon cells. *Dev Biol*. 312:523-532.

Chebotareva, N.A., B.I. Kurganov, and N.B. Livanova. 2004. Biochemical effects of molecular crowding. *Biochemistry. Biokhimiia*. 69:1239-1251.

Cheheltani, R., J.M. Rosano, B. Wang, A.K. Sabri, N. Pleshko, and M.F. Kiani. 2012. Fourier transform infrared spectroscopic imaging of cardiac tissue to detect collagen deposition after myocardial infarction. *Journal of biomedical optics*. 17:056014.

Chen, C., F. Loe, A. Blocki, Y.X. Peng, and M. Raghunath. 2011. Applying macromolecular crowding to enhance extracellular matrix deposition and its remodeling in vitro for tissue engineering and cell-based therapies. *Adv Drug Deliver Rev*. 63:277-290.

Chen, C.Z.C., Y.X. Peng, Z.B. Wang, P.V. Fish, J.L. Kaar, R.R. Koepsel, A.J. Russell, R.R. Lareu, and M. Raghunath. 2009. The Scar-in-a-Jar: studying potential antifibrotic compounds from the epigenetic to extracellular level in a single well. *Brit J Pharmacol*. 158:1196-1209.

Cheng, J.Y., M. Raghunath, J. Whitelock, and L. Poole-Warren. 2011. Matrix components and scaffolds for sustained islet function. *Tissue Eng Part B Rev*. 17:235-247.

Cheng, K., K. Ho, R. Stokes, C. Scott, S.M. Lau, W.J. Hawthorne, P.J. O'Connell, T. Loudovaris, T.W. Kay, R.N. Kulkarni, T. Okada, X.L. Wang, S.H. Yim, Y. Shah, S.T. Grey, A.V. Biankin, J.G. Kench, D.R. Laybutt, F.J. Gonzalez, C.R. Kahn, and J.E. Gunton. 2010. Hypoxia-inducible factor-1alpha regulates beta cell function in mouse and human islets. *J Clin Invest*. 120:2171-2183.

Cheung, A.L. 2007. Isolation and culture of human umbilical vein endothelial cells (HUVEC). *Current protocols in microbiology*. Appendix 4:Appendix 4B.

Chiao, E., P. Fisher, L. Crisponi, M. Deiana, I. Dragatsis, D. Schlessinger, G. Pilia, and A. Efstratiadis. 2002. Overgrowth of a mouse model of the Simpson-Golabi-Behmel syndrome is independent of IGF signaling. *Dev Biol*. 243:185--206.

Chin, G.S., S. Lee, M. Hsu, W. Liu, W.J.H. Kim, H. Levinson, and M.T. Longaker. 2001. Discoidin domain receptors and their ligand, collagen, are temporally regulated in fetal rat fibroblasts in vitro. *Plastic and Reconstructive Surgery*. 107:769-776.

Cho, C.H., J.F. Eliason, and H.W.T. Matthew. 2008. Application of porous glycosaminoglycan-based scaffolds for expansion of human cord blood stem cells in perfusion culture. *J Biomed Mater Res A*. 86:98--107.

Chuang, C.Y., M. Lord, J. Melrose, M.D. Rees, S.M. Knox, C. Freeman, R.V. Iozzo, and J.M. Whitelock. 2010. Heparan sulfate-dependent signaling of fibroblast growth factor 18 by chondrocyte-derived perlecan. *Biochemistry*. 49:5524-5532.

Cirulli, V., G.M. Beattie, G. Klier, M. Ellisman, C. Ricordi, V. Quaranta, F. Frasier, J.K. Ishii, A. Hayek, and D.R. Salomon. 2000. Expression and function of alpha(v)beta(3) and alpha(v)beta(5) integrins in the developing pancreas: roles in the adhesion and migration of putative endocrine progenitor cells. *J Cell Biol*. 150:1445--1460.

Colognato, H., M. MacCarrick, J.J. O'Rear, and P.D. Yurchenco. 1997. The laminin alpha2-chain short arm mediates cell adhesion through both the alpha1beta1 and alpha2beta1 integrins. *J Biol Chem*. 272:29330--29336.

Corless, C.L., A. Mendoza, T. Collins, and J. Lawler. 1992. Colocalization of thrombospondin and syndecan during murine development. *Dev Dyn*. 193:346--358.

Costell, M., R. Carmona, E. Gustafsson, M. González-Iriarte, R. Fässler, and R. Muñoz-Chápuli. 2002. Hyperplastic conotruncal endocardial cushions and transposition of great arteries in perlecan-null mice. *Circ Res*. 91:158--164.

Cowley, M.J., A. Weinberg, N. Zammit, S.N. Walters, W.J. Hawthorne, T. Loudovaris, H. Thomas, T. Kay, J.E. Gunton, S.I. Alexander, W. Kaplan, J. Chapman, P.J. O'Connell, and S.T. Grey. 2012. Human Islets Express a Marked Pro-Inflammatory Molecular Signature Prior to Transplantation. *Cell Transplant*.

Daoud, J., M. Petropavlovskaia, L. Rosenberg, and M. Tabrizian. 2009. The effect of extracellular matrix components on the preservation of human islet function in vitro. *Biomaterials*.

Davalli, A.M., Y. Ogawa, C. Ricordi, D.W. Scharp, S. Bonner-Weir, and G.C. Weir. 1995. A selective decrease in the beta cell mass of human islets transplanted into diabetic nude mice. *Transplantation*. 59:817-820.

Davalli, A.M., L. Scaglia, D.H. Zangen, J. Hollister, S. Bonner-Weir, and G.C. Weir. 1996. Vulnerability of islets in the immediate posttransplantation period. Dynamic changes in structure and function. *Diabetes*. 45:1161-1167.

David, G., X.M. Bai, B. Van der Schueren, J.J. Cassiman, and H. Van den Berghe. 1992. Developmental changes in heparan sulfate expression: in situ detection with mAbs. *J Cell Biol*. 119:961-975.

Davis, G.E., and D.R. Senger. 2005. Endothelial extracellular matrix: biosynthesis, remodeling, and functions during vascular morphogenesis and neovessel stabilization. *Circ Res*. 97:1093-1107.

de Pereda, J.M., G. Wiche, and R.C. Liddington. 1999. Crystal structure of a tandem pair of fibronectin type III domains from the cytoplasmic tail of integrin alpha6beta4. *EMBO J*. 18:4087--4095.

De Vos, A., H. Heimberg, E. Quartier, P. Huypens, L. Bouwens, D. Pipeleers, and F. Schuit. 1995. Human and rat beta cells differ in glucose transporter but not in glucokinase gene expression. *J Clin Invest*. 96:2489-2495.

Dedhar, S., K. Jewell, M. Rojiani, and V. Gray. 1992. The receptor for the basement membrane glycoprotein entactin is the integrin alpha 3/beta 1. *J Biol Chem*. 267:18908--18914.

Deijnen, J.H.V., P.T.V. Suylichem, G.H. Wolters, and R.V. Schilfgaarde. 1994. Distribution of collagens type I, type III and type V in the pancreas of rat, dog, pig and man. *Cell Tissue Res*. 277:115--121.

Deters, N.A., R.A. Stokes, and J.E. Gunton. 2011. Islet transplantation: factors in short-term islet survival. *Archivum immunologiae et therapiae experimentalis*. 59:421-429.

Devendra, D., E. Liu, and G.S. Eisenbarth. 2004. Type 1 diabetes: recent developments. *BMJ*. 328:750-754.

Dhodapkar, M.V., E. Abe, A. Theus, M. Lacy, J.K. Langford, B. Barlogie, and R.D. Sanderson. 1998. Syndecan-1 is a multifunctional regulator of myeloma pathobiology: control of tumor cell survival, growth, and bone cell differentiation. *Blood*. 91:2679-2688.

Drenckhahn, D., and T.D. Pollard. 1986. Elongation of actin filaments is a diffusion-limited reaction at the barbed end and is accelerated by inert macromolecules. *J Biol Chem*. 261:12754-12758.

Dror, V., V. Nguyen, P. Walia, T.B. Kalynyak, J.A. Hill, and J.D. Johnson. 2007. Notch signalling suppresses apoptosis in adult human and mouse pancreatic islet cells. *Diabetologia*. 50:2504-2515.

Drzeniek, Z., G. Stocker, B. Siebertz, U. Just, T. Schroeder, W. Ostertag, and H.D. Haubeck. 1999. Heparan sulfate proteoglycan expression is induced during early erythroid differentiation of multipotent hematopoietic stem cells. *Blood*. 93:2884-2897.

Duvillie, B., M. Heinis, and V. Stetsyuk. 2007. In vivo and in vitro techniques to study pancreas development and islet cell function. *Endocrine development*. 12:46-54.

Echtermeyer, F., P.C. Baciu, S. Saoncella, Y. Ge, and P.F. Goetinck. 1999. Syndecan-4 core protein is sufficient for the assembly of focal adhesions and actin stress fibers. *J Cell Sci*. 112:3433-3441.

Eickelberg, O., M. Centrella, M. Reiss, M. Kashgarian, and R.G. Wells. 2002. Betaglycan inhibits TGF-beta signaling by preventing type I-type II receptor complex formation. Glycosaminoglycan modifications alter betaglycan function. *J Biol Chem*. 277:823--829.

Ellis, R.J. 2001. Macromolecular crowding: an important but neglected aspect of the intracellular environment. *Current opinion in structural biology*. 11:114-119.

Ettner, N., W. Göhring, T. Sasaki, K. Mann, and R. Timpl. 1998. The N-terminal globular domain of the laminin alpha1 chain binds to alpha1beta1 and alpha2beta1 integrins and to the heparan sulfate-containing domains of perlecan. *FEBS Lett*. 430:217--221.

Evans, J.L., I.D. Goldfine, B.A. Maddux, and G.M. Grodsky. 2003. Are oxidative stress-activated signaling pathways mediators of insulin resistance and beta-cell dysfunction? *Diabetes*. 52:1-8.

Federman, S., L.M. Miller, and I. Sagi. 2002. Following matrix metalloproteinases activity near the cell boundary by infrared micro-spectroscopy. *Matrix Biol*. 21:567-577.

Felding-Habermann, B., and D.A. Cheresh. 1993. Vitronectin and its receptors. *Curr Opin Cell Biol*. 5:864--868.

Ferdous, Z., and K.J. Grande-Allen. 2007. Utility and control of proteoglycans in tissue engineering. *Tissue Eng*. 13:1893--1904.

Filmus, J. 2001. Glypicans in growth control and cancer. *Glycobiology*. 11:19R--23R.

Foghandersen, N., B.M. Altura, B.T. Altura, and O. Siggaardandersen. 1995. Composition of Interstitial Fluid. *Clin Chem*. 41:1522-1525.

Folkow, B., M. Gurevich, M. Hallback, Y. Lundgren, and L. Weiss. 1971. The hemodynamic consequences of regional hypotension in spontaneously hypertensive and normotensive rats. *Acta physiologica Scandinavica*. 82:9A-10A.

Fransson, L.-A., M. Belting, F. Cheng, M. Jönsson, K. Mani, and S. Sandgren. 2004. Novel aspects of glypican glycobiology. *Cell Mol Life Sci*. 61:1016--1024.

Friedlander, M., P.C. Brooks, R.W. Shaffer, C.M. Kincaid, J.A. Varner, and D.A. Cheresh. 1995. Definition of two angiogenic pathways by distinct alpha v integrins. *Science*. 270:1500--1502.

Frisch, S.M., and R.A. Screaton. 2001. Anoikis mechanisms. *Current Opinion in Cell Biology*. 13:555-562.

Gao, R., J. Ustinov, M.-A. Pulkkinen, K. Lundin, O. Korsgren, and T. Otonkoski. 2003. Characterization of endocrine progenitor cells and critical factors for their differentiation in human adult pancreatic cell culture. *Diabetes*. 52:2007--2015.

Gauthier, B.R., T. Brun, E.J. Sarret, H. Ishihara, O. Schaad, P. Descombes, and C.B. Wollheim. 2004. Oligonucleotide microarray analysis reveals PDX1 as an essential regulator of mitochondrial metabolism in rat islets. *J Biol Chem*. 279:31121-31130.

Gershengorn, M.C., A.A. Hardikar, C. Wei, E. Geras-Raaka, B. Marcus-Samuels, and B.M. Raaka. 2004. Epithelial-to-mesenchymal transition generates proliferative human islet precursor cells. *Science*. 306:2261-2264.

Geutskens, S.B., F. Homo-Delarche, J.-M. Pleau, S. Durant, H.A. Drexhage, and W. Savino. 2004. Extracellular matrix distribution and islet morphology in the early postnatal pancreas: anomalies in the non-obese diabetic mouse. *Cell Tissue Res*. 318:579--589.

Giuliani, M., W. Moritz, E. Bodmer, D. Dindo, P. Kugelmeier, R. Lehmann, M. Gassmann, P. Groscurth, and M. Weber. 2005. Central necrosis in isolated hypoxic human pancreatic islets: evidence for postisolation ischemia. *Cell Transplant*. 14:67-76.

Gonzalez, A.D., M. Kaya, W. Shi, H. Song, J.R. Testa, L.Z. Penn, and J. Filmus. 1998. OCI-5/GPC3, a glypican encoded by a gene that is mutated in the Simpson-Golabi-Behmel overgrowth syndrome, induces apoptosis in a cell line-specific manner. *J Cell Biol*. 141:1407--1414.

González-Iriarte, M., R. Carmona, J.M. Pérez-Pomares, D. Macías, M. Costell, and R. Muñoz-Chápuli. 2003. Development of the coronary arteries in a murine model of transposition of great arteries. *J Mol Cell Cardiol*. 35:795--802.

Gotte, M. 2003. Syndecans in inflammation. *Faseb Journal*. 17:575-591.

Green, R.A., N.H. Lovell, and L.A. Poole-Warren. 2010a. Impact of co-incorporating laminin peptide dopants and neurotrophic growth factors on conducting polymer properties. *Acta Biomater*. 6:63--71.

Green, R.A., P.J. Martens, R. Norden, and L.A. Poole-Warren. 2010b. Stem Cell Engineering. G. Artmann, J. Hescheler, and S. Minger, editors. Springer.

Grewal, I.S., K.D. Grewal, F.S. Wong, H. Wang, D.E. Picarella, C.A. Janeway, and R.A. Flavell. 2002. Expression of transgene encoded TGF-beta in islets prevents autoimmune diabetes in NOD mice by a local mechanism. *J Autoimmun*. 19:9--22.

Grey, S.T., C. Longo, T. Shukri, V.I. Patel, E. Csizmadia, S. Daniel, M.B. Arvelo, V. Tchipashvili, and C. Ferran. 2003. Genetic engineering of a suboptimal islet graft with A20 preserves beta cell mass and function. *J Immunol*. 170:6250-6256.

Griffith, L.G., and M.A. Swartz. 2006. Capturing complex 3D tissue physiology in vitro. *Nat Rev Mol Cell Biol*. 7:211--224.

Gu, W.L., S.L. Fu, Y.X. Wang, Y. Li, H.Z. Lu, X.M. Xu, and P.H. Lu. 2009. Chondroitin sulfate proteoglycans regulate the growth, differentiation and migration of multipotent neural precursor cells through the integrin signaling pathway. *Bmc Neuroscience*. 10:-.

Guillam, M.T., E. Hummler, E. Schaerer, J.I. Yeh, M.J. Birnbaum, F. Beermann, A. Schmidt, N. Deriaz, and B. Thorens. 1997. Early diabetes and abnormal postnatal pancreatic islet development in mice lacking Glut-2. *Nat Genet*. 17:327-330.

Gunton, J.E., R.N. Kulkarni, S. Yim, T. Okada, W.J. Hawthorne, Y.H. Tseng, R.S. Roberson, C. Ricordi, P.J. O'Connell, F.J. Gonzalez, and C.R. Kahn. 2005. Loss of ARNT/HIF1beta mediates altered gene expression and pancreatic-islet dysfunction in human type 2 diabetes. *Cell*. 122:337-349.

Hall, H., D. Bozic, K. Michel, and J.A. Hubbell. 2003. N-terminal alpha-dystroglycan binds to different extracellular matrix molecules expressed in regenerating peripheral nerves in a protein-mediated manner and promotes neurite extension of PC12 cells. *Mol Cell Neurosci*. 24:1062--1073.

Hamamoto, K., S. Yamada, A. Hara, T. Kodera, M. Seno, and I. Kojima. 2011. Extracellular matrix modulates insulin production during differentiation of AR42J cells: functional role of Pax6 transcription factor. *J Cell Biochem*. 112:318-329.

Hammar, E., G. Parnaud, D. Bosco, N. Perriraz, K. Maedler, M. Donath, D.G. Rouiller, and P.A. Halban. 2004. Extracellular matrix protects pancreatic beta-cells against apoptosis: role of short- and long-term signaling pathways. *Diabetes*. 53:2034-2041.

Hamon, M., E. Mbemba, N. Charnaux, H. Slimani, S. Brule, L. Saffar, R. Vassy, C. Prost, N. Lievre, A. Starzec, and L. Gattegno. 2004. A syndecan-4/CXCR4 complex expressed on human primary lymphocytes and macrophages and HeLa cell line binds the CXC chemokine stromal cell-derived factor-1 (SDF-1). *Glycobiology*. 14:311-323.

Hanley, S.C., A. Pilotte, B. Massie, and L. Rosenberg. 2008. Cellular origins of adult human islet in vitro dedifferentiation. *Lab Invest*. 88:761-772.

Hanlon, E.B., R. Manoharan, T.W. Koo, K.E. Shafer, J.T. Motz, M. Fitzmaurice, J.R. Kramer, I. Itzkan, R.R. Dasari, and M.S. Feld. 2000. Prospects for in vivo Raman spectroscopy. *Physics in medicine and biology*. 45:R1-59.

Hardikar, A.A., B. Marcus-Samuels, E. Geras-Raaka, B.M. Raaka, and M.C. Gershengorn. 2003. Human pancreatic precursor cells secrete FGF2 to stimulate clustering into hormone-expressing islet-like cell aggregates. *Proceedings of the National Academy of Sciences of the United States of America*. 100:7117-7122.

Harve, K.S., R. Lareu, R. Rajagopalan, and M. Raghunath. 2010. Understanding how the crowded interior of cells stabilizes DNA/DNA and DNA/RNA hybrids-in silico predictions and in vitro evidence. *Nucleic Acids Res*. 38:172-181.

Hayek, A., A.D. Lopez, and G.M. Beattie. 1989. Enhancement of pancreatic islet cell monolayer growth by endothelial cell matrix and insulin. *In Vitro Cell Dev Biol*. 25:146--150.

Henderson, J.R., and M.C. Moss. 1985. A morphometric study of the endocrine and exocrine capillaries of the pancreas. *Q J Exp Physiol*. 70:347-356.

Heremans, A., B.D. Cock, J.J. Cassiman, H.V. den Berghe, and G. David. 1990. The core protein of the matrix-associated heparan sulfate proteoglycan binds to fibronectin. *J Biol Chem*. 265:8716--8724.

Heyninck, K., and R. Beyaert. 2005. A20 inhibits NF-kappaB activation by dual ubiquitin-editing functions. *Trends in biochemical sciences*. 30:1-4.

Hinek, A. 1996. Biological roles of the non-integrin elastin/laminin receptor. *Biol Chem*. 377:471--480.

Ho, E., and T.M. Bray. 1999. Antioxidants, NFkappaB activation, and diabetogenesis. *Proc Soc Exp Biol Med*. 222:205-213.

Høgåsen, K., T.E. Mollnes, and M. Harboe. 1992. Heparin-binding properties of vitronectin are linked to complex formation as illustrated by in vitro polymerization and binding to the terminal complement complex. *J Biol Chem*. 267:23076--23082.

Hojima, Y., B. Behta, A.M. Romanic, and D.J. Prockop. 1994. Cleavage of type I procollagen by C- and N-proteinases is more rapid if the substrate is aggregated with dextran sulfate or polyethylene glycol. *Analytical biochemistry*. 223:173-180.

Hoogewerf, A.J., G.S. Kuschert, A.E. Proudfoot, F. Borlat, I. Clark-Lewis, C.A. Power, and T.N. Wells. 1997. Glycosaminoglycans mediate cell surface oligomerization of chemokines. *Biochemistry*. 36:13570--13578.

Horowitz, A., E. Tkachenko, and M. Simons. 2002. Fibroblast growth factor-specific modulation of cellular response by syndecan-4. *J Cell Biol*. 157:715-725.

Horton, M.A. 1999. Arg-gly-Asp (RGD) peptides and peptidomimetics as therapeutics: relevance for renal diseases. *Exp Nephrol*. 7:178--184.

Hughes, C.S., L.M. Postovit, and G.A. Lajoie. 2010. Matrigel: a complex protein mixture required for optimal growth of cell culture. *Proteomics*. 10:1886--1890.

Hughes, S.D., C. Quaade, J.H. Johnson, S. Ferber, and C.B. Newgard. 1993. Transfection of AtT-20ins cells with GLUT-2 but not GLUT-1 confers glucose-stimulated insulin secretion. Relationship to glucose metabolism. *J Biol Chem*. 268:15205-15212.

Hughes, S.J., A. Clark, P. McShane, H.H. Contractor, D.W.R. Gray, and P.R.V. Johnson. 2006. Characterisation of collagen VI within the islet-exocrine interface of the human pancreas: implications for clinical islet isolation? *Transplantation*. 81:423--426.

Hulinsky, I., S. Cooney, J. Harrington, and M. Silink. 1995a. In vitro growth of neonatal rat islet cells is stimulated by adhesion to matrix. *Horm Metab Res*. 27:209--215.

Hulinsky, I., J. Harrington, S. Cooney, and M. Silink. 1995b. Insulin secretion and DNA synthesis of cultured islets of Langerhans are influenced by the matrix. *Pancreas*. 11:309--314.

Iozzo, R.V. 1984. Proteoglycans and neoplastic--mesenchymal cell interactions. *Hum Pathol*. 15:2--10.

Iozzo, R.V. 2000. Proteoglycans. CRC Press.

Iozzo, R.V. 2001. Heparan sulfate proteoglycans: intricate molecules with intriguing functions. *J Clin Invest*. 108:165-167.

Irving-Rodgers, H.F., A.F. Ziolkowski, C.R. Parish, Y. Sado, Y. Ninomiya, C.J. Simeonovic, and R.J. Rodgers. 2008. Molecular composition of the peri-islet basement membrane in NOD mice: a barrier against destructive insulitis. *Diabetologia*. 51:1680--1688.

Islam, S. 2010. The Islets of Langerhans. Springer.

Jackers, P., F. Minoletti, D. Belotti, N. Clausse, G. Sozzi, M.E. Sobel, and V. Castronovo. 1996. Isolation from a multigene family of the active human gene of the metastasis-associated multifunctional protein 37LRP/p40 at chromosome 3p21.3. *Oncogene*. 13:495--503.

Jang, E., H. Albadawi, M.T. Watkins, E.R. Edelman, and A.B. Baker. 2012. Syndecan-4 proteoliposomes enhance fibroblast growth factor-2 (FGF-2)-induced proliferation, migration, and neovascularization of ischemic muscle. *Proc Natl Acad Sci U S A*. 109:1679-1684.

Jarvis, T.C., D.M. Ring, S.S. Daube, and P.H. von Hippel. 1990. "Macromolecular crowding": thermodynamic consequences for protein-protein interactions within the T4 DNA replication complex. *J Biol Chem*. 265:15160-15167.

Javazon, E.H., D.C. Colter, E.J. Schwarz, and D.J. Prockop. 2001. Rat marrow stromal cells are more sensitive to plating density and expand more rapidly from single-cell-derived colonies than human marrow stromal cells. *Stem Cells*. 19:219--225.

Jiang, F.X., E. Georges-Labouesse, and L.C. Harrison. 2001. Regulation of laminin 1-induced pancreatic beta-cell differentiation by alpha6 integrin and alpha-dystroglycan. *Mol Med*. 7:107--114.

Jiang, F.X., G. Naselli, and L.C. Harrison. 2002. Distinct Distribution of Laminin and Its Integrin Receptors in the Pancreas. *J Histochem Cytochem*. 50:1625-1632.

Jikko, A., S.E. Harris, D. Chen, D.L. Mendrick, and C.H. Damsky. 1999. Collagen integrin receptors regulate early osteoblast differentiation induced by BMP-2. *Journal of Bone and Mineral Research*. 14:1075-1083.

Johansson, A., J. Lau, M. Sandberg, L. Borg, P. Magnusson, and P.-O. Carlsson. 2009. Endothelial cell signalling supports pancreatic beta cell function in the rat. *Diabetologia*.

Johansson, S., G. Svineng, K. Wennerberg, A. Armulik, and L. Lohikangas. 1997. Fibronectin-integrin interactions. *Front Biosci*. 2:d126--d146.

Johansson, U., G. Elgue, B. Nilsson, and O. Korsgren. 2005. Composite islet-endothelial cell grafts: a novel approach to counteract innate immunity in islet transplantation. *American journal of transplantation : official journal of the American Society of Transplantation and the American Society of Transplant Surgeons*. 5:2632-2639.

Juárez, P., M.M. Vilchis-Landeros, J. Ponce-Coria, V. Mendoza, R. Hernández-Pando, N.A. Bobadilla, and F. López-Casillas. 2007. Soluble betaglycan reduces renal damage progression in db/db mice. *Am J Physiol Renal Physiol*. 292:F321--F329.

Kahn, C.R. 2005. Human pancreatic islets from normal and Type 2 diabetic subjects.

Kaido, T., B. Perez, M. Yebra, J. Hill, V. Cirulli, A. Hayek, and A.M. Montgomery. 2004a. Alphav-integrin utilization in human beta-cell adhesion, spreading, and motility. *J Biol Chem*. 279:17731--17737.

Kaido, T., M. Yebra, V. Cirulli, and A.M. Montgomery. 2004b. Regulation of human beta-cell adhesion, motility, and insulin secretion by collagen IV and its receptor alpha1beta1. *J Biol Chem*. 279:53762--53769.

Kaido, T., M. Yebra, V. Cirulli, C. Rhodes, G. Diaferia, and A.M. Montgomery. 2006. Impact of defined matrix interactions on insulin production by cultured human beta-cells. Effects on insulin content, secretion and gene transcription. *Diabetes*. 55:2723-2729.

Kaiser, N., A.P. Corcos, A. Tur-Sinai, Y. Ariav, and E. Cerasi. 1988. Monolayer culture of adult rat pancreatic islets on extracellular matrix: long term maintenance of differentiated B-cell function. *Endocrinology*. 123:834--840.

Kajikawa, M., S. Fujimoto, Y. Tsuura, E. Mukai, T. Takeda, Y. Hamamoto, M. Takehiro, J. Fujita, Y. Yamada, and Y. Seino. 2002. Ouabain suppresses glucose-induced mitochondrial ATP production and insulin release by generating reactive oxygen species in pancreatic islets. *Diabetes*. 51:2522-2529.

Kantengwa, S., D. Baetens, K. Sadoul, C.A. Buck, P.A. Halban, and D.G. Rouiller. 1997. Identification and characterization of alpha 3 beta 1 integrin on primary and transformed rat islet cells. *Exp Cell Res*. 237:394--402.

Kato, M., H. Wang, V. Kainulainen, M.L. Fitzgerald, S. Ledbetter, D.M. Ornitz, and M. Bernfield. 1998. Physiological degradation converts the soluble syndecan-1 ectodomain from an inhibitor to a potent activator of FGF-2. *Nat Med*. 4:691--697.

Kidszun, A., D. Schneider, D. Erb, G. Hertl, V. Schmidt, M. Eckhard, K.T. Preissner, G. Breier, R.G. Bretzel, and T. Linn. 2006. Isolated pancreatic

islets in three-dimensional matrices are responsive to stimulators and inhibitors of angiogenesis. *Cell Transplant*. 15:489--497.

Kikkawa, Y., and J.H. Miner. 2005. Review: Lutheran/B-CAM: a laminin receptor on red blood cells and in various tissues. *Connect Tissue Res*. 46:193--199.

Kikkawa, Y., C.L. Moulson, I. Virtanen, and J.H. Miner. 2002. Identification of the binding site for the Lutheran blood group glycoprotein on laminin alpha 5 through expression of chimeric laminin chains in vivo. *J Biol Chem*. 277:44864--44869.

Kim, J.S., and A. Yethiraj. 2009. Effect of macromolecular crowding on reaction rates: a computational and theoretical study. *Biophysical journal*. 96:1333-1340.

Kim, S., S.W. Kim, and Y.H. Bae. 2005. Synthesis, bioactivity and specificity of glucagon-like peptide-1 (7-37)/polymer conjugate to isolated rat islets. *Biomaterials*. 26:3597--3606.

Kleeff, J., T. Ishiwata, A. Kumbasar, H. Friess, M.W. Büchler, A.D. Lander, and M. Korc. 1998. The cell-surface heparan sulfate proteoglycan glypican-1 regulates growth factor action in pancreatic carcinoma cells and is overexpressed in human pancreatic cancer. *J Clin Invest*. 102:1662--1673.

Knight, K.R., Y. Uda, M.W. Findlay, D.L. Brown, K.J. Cronin, E. Jamieson, T. Tai, E. Keramidaris, A.J. Penington, J. Rophael, L.C. Harrison, and W.A. Morrison. 2006a. Vascularized tissue-engineered chambers promote survival and function of transplanted islets and improve glycemic control. *FASEB J*. 20:565-567.

Knight, K.R., Y. Uda, M.W. Findlay, D.L. Brown, K.J. Cronin, E. Jamieson, T. Tai, E. Keramidaris, A.J. Penington, J. Rophael, L.C. Harrison, and W.A. Morrison. 2006b. Vascularized tissue-engineered chambers promote survival and function of transplanted islets and improve glycemic control. *FASEB J*. 20:565--567.

Knox, S., A.J. Fosang, K. Last, J. Melrose, and J. Whitelock. 2005. Perlecan from human epithelial cells is a hybrid heparan/chondroitin/keratan sulfate proteoglycan. *FEBS Letters*. 579:5019-5023.

Knox, S., C. Merry, S. Stringer, J. Melrose, and J. Whitelock. 2002. Not all perlecans are created equal: interactions with fibroblast growth factor (FGF) 2 and FGF receptors. *J Biol Chem*. 277:14657--14665.

Kojima, T., C.W. Leone, G.A. Marchildon, J.A. Marcum, and R.D. Rosenberg. 1992. Isolation and characterization of heparan sulfate proteoglycans produced by cloned rat microvascular endothelial cells. *J Biol Chem*. 267:4859-4869.

Kröger, S., and J.E. Schröder. 2002. Agrin in the developing CNS: new roles for a synapse organizer. *News Physiol Sci*. 17:207--212.

Kühn, K., and J. Eble. 1994. The structural bases of integrin-ligand interactions. *Trends Cell Biol*. 4:256--261.

Kulkarni, R.N., J.N. Winnay, M. Daniels, J.C. Bruning, S.N. Flier, D. Hanahan, and C.R. Kahn. 1999. Altered function of insulin receptor substrate-1-deficient mouse islets and cultured beta-cell lines. *J Clin Invest*. 104:R69-75.

Kumar, C. 2006. Tissue, cell and organ engineering. Wiley-VCH.

Kure, S., and O. Yoshie. 1986. A syngeneic monoclonal antibody to murine Meth-A sarcoma (HepSS-1) recognizes heparan sulfate glycosaminoglycan (HS-GAG): cell density and transformation dependent alteration in cell surface HS-GAG defined by HepSS-1. *J Immunol*. 137:3900-3908.

Kuroda, M., T. Oka, Y. Oka, T. Yamochi, K. Ohtsubo, S. Mori, T. Watanabe, R. Machinami, and S. Ohnishi. 1995. Colocalization of Vascular Endothelial Growth-Factor (Vascular-Permeability Factor) and Insulin in Pancreatic-Islet Cells. *Journal of Clinical Endocrinology & Metabolism*. 80:3196-3200.

Lammert, E., G.Q. Gu, M. McLaughlin, D. Brown, R. Brekken, L.C. Murtaugh, H.P. Gerber, N. Ferrara, and D.A. Melton. 2003. Role of VEGF-A in vascularization of pancreatic islets. *Current Biology*. 13:1070-1074.

Lareu, R.R., I. Arsianti, H.K. Subramhanya, P. Yanxian, and M. Raghunath. 2007a. In vitro enhancement of collagen matrix formation and crosslinking for applications in tissue engineering: a preliminary study. *Tissue Eng*. 13:385-391.

Lareu, R.R., K.S. Harve, and M. Raghunath. 2007b. Emulating a crowded intracellular environment in vitro dramatically improves RT-PCR performance. *Biochem Biophys Res Commun*. 363:171-177.

Lareu, R.R., K.H. Subrainhanya, Y.X. Peng, P. Benny, C. Chen, Z.B. Wang, R. Rajagopalan, and M. Raghunath. 2007c. Collagen matrix deposition is dramatically enhanced in vitro when crowded with charged macromolecules: The biological relevance of the excluded volume effect. *FEBS Letters*. 581:2709-2714.

Larrain, J., G. Cizmeci-Smith, V. Troncoso, R.C. Stahl, D.J. Carey, and E. Brandan. 1997. Syndecan-1 expression is down-regulated during myoblast terminal differentiation. Modulation by growth factors and retinoic acid. *J Biol Chem*. 272:18418-18424.

Laschke, M.W., M. Rücker, G. Jensen, C. Carvalho, R. Mülhaupt, N.-C. Gellrich, and M.D. Menger. 2008. Incorporation of growth factor containing Matrigel promotes vascularization of porous PLGA scaffolds. *J Biomed Mater Res A*. 85:397--407.

Lechner, A., A.L. Nolan, R.A. Blacken, and J.F. Habener. 2005. Redifferentiation of insulin-secreting cells after in vitro expansion of adult human pancreatic islet tissue. *Biochem Biophys Res Commun*. 327:581--588.

Lee, B.-W., J.-H. Jee, J.-S. Heo, S.-H. Choi, K.-T. Jang, J.-H. Noh, I.-K. Jeong, S.-H. Oh, Y.-R. Ahn, H.-Y. Chae, Y.-K. Min, J.-H. Chung, M.-K. Lee, M.-S. Lee, and K.-W. Kim. 2005. The favorable outcome of human islet transplantation in Korea: experiences of 10 autologous transplantations. *Transplantation*. 79:1568--1574.

Lee, D., E.S. Oh, A. Woods, J.R. Couchman, and W. Lee. 1998. Solution structure of a syndecan-4 cytoplasmic domain and its interaction with phosphatidylinositol 4,5-bisphosphate. *J Biol Chem*. 273:13022--13029.

Leibowitz, G., G. Uckaya, A.I. Oprescu, E. Cerasi, D.J. Gross, and N. Kaiser. 2002. Glucose-regulated proinsulin gene expression is required for adequate insulin production during chronic glucose exposure. *Endocrinology*. 143:3214-3220.

Lelièvre, S., V.M. Weaver, and M.J. Bissell. 1996. Extracellular matrix signaling from the cellular membrane skeleton to the nuclear skeleton: a model of gene regulation. *Recent Prog Horm Res*. 51:417--432.

Lewis, K.A., P.C. Gray, A.L. Blount, L.A. MacConell, E. Wiater, L.M. Bilezikjian, and W. Vale. 2000. Betaglycan binds inhibin and can mediate functional antagonism of activin signalling. *Nature*. 404:411-414.

Li, N., T. Brun, M. Cnop, D.A. Cunha, D.L. Eizirik, and P. Maechler. 2009. Transient oxidative stress damages mitochondrial machinery inducing persistent beta-cell dysfunction. *J Biol Chem*. 284:23602-23612.

Lin, C.-C., and K.S. Anseth. 2009. Glucagon-like peptide-1 functionalized PEG hydrogels promote survival and function of encapsulated pancreatic beta-cells. *Biomacromolecules*. 10:2460--2467.

Lin, C.C., A.T. Metters, and K.S. Anseth. 2009. Functional PEG-peptide hydrogels to modulate local inflammation induced by the pro-inflammatory cytokine TNFalpha. *Biomaterials*. 30:4907-4914.

Lin, X. 2004. Functions of heparan sulfate proteoglycans in cell signaling during development. *Development*. 131:6009--6021.

Linetsky, E., R. Bottino, R. Lehmann, R. Alejandro, L. Inverardi, and C. Ricordi. 1997. Improved human islet isolation using a new enzyme blend, liberase. *Diabetes*. 46:1120-1123.

Linn, T., K. Schneider, H.P. Hammes, K.T. Preissner, H. Brandhorst, E. Morgenstern, F. Kiefer, and R.G. Bretzel. 2003. Angiogenic capacity of endothelial cells in islets of Langerhans. *FASEB J*. 17:881--883.

López-Casillas, F., S. Cheifetz, J. Doody, J.L. Andres, W.S. Lane, and J. Massagué. 1991. Structure and expression of the membrane proteoglycan betaglycan, a component of the TGF-beta receptor system. *Cell*. 67:785--795.

Lucas-clerc, C., C. Massart, J.P. Campion, B. Launois, and M. Nicol. 1993. Long-Term Culture of Human Pancreatic-Islets in an Extracellular-Matrix - Morphological and Metabolic Effects. *Molecular and Cellular Endocrinology*. 94:9-20.

Lui, K., M. Jackson, M.G. Sowa, H. Ju, I.M. Dixon, and H.H. Mantsch. 1996. Modification of the extracellular matrix following myocardial infarction monitored by FTIR spectroscopy. *Biochim Biophys Acta*. 1315:73-77.

Luo, Y., and M.S. Shoichet. 2004. A photolabile hydrogel for guided three-dimensional cell growth and migration. *Nat Mater*. 3:249--253.

Madden, T.L., and J. Herzfeld. 1993. Crowding-induced organization of cytoskeletal elements: I. Spontaneous demixing of cytosolic proteins and model filaments to form filament bundles. *Biophysical journal*. 65:1147-1154.

Madihally, S.V., A.W. Flake, and H.W. Matthew. 1999. Maintenance of CD34 expression during proliferation of CD34+ cord blood cells on glycosaminoglycan surfaces. *Stem Cells*. 17:295--305.

Maechler, P., L. Jornot, and C.B. Wollheim. 1999. Hydrogen peroxide alters mitochondrial activation and insulin secretion in pancreatic beta cells. *J Biol Chem*. 274:27905-27913.

Magnuson, V.L., M. Young, D.G. Schattenberg, M.A. Mancini, D.L. Chen, B. Steffensen, and R.J. Klebe. 1991. The alternative splicing of fibronectin pre-mRNA is altered during aging and in response to growth factors. *J Biol Chem*. 266:14654--14662.

Malaisse, W.J. 1997. Physiology, pathology and pharmacology of insulin secretion: recent acquisitions. *Diabetes & metabolism*. 23 Suppl 3:6-15.

Mann, K., R. Deutzmann, and R. Timpl. 1988. Characterization of proteolytic fragments of the laminin-nidogen complex and their activity in ligand-binding assays. *Eur J Biochem*. 178:71--80.

Marano, R.P.C., and S. Vilaró. 1994. The role of fibronectin, laminin, vitronectin and their receptors on cellular adhesion in proliferative vitreoretinopathy. *Invest Ophthalmol Vis Sci*. 35:2791--2803.

Martin, M.J., A. Muotri, F. Gage, and A. Varki. 2005. Human embryonic stem cells express an immunogenic nonhuman sialic acid. *Nature Medicine*. 11:228-232.

Mauri, P., A. Scarpa, A.C. Nascimbeni, L. Benazzi, E. Parmagnani, A. Mafficini, M.D. Peruta, C. Bassi, K. Miyazaki, and C. Sorio. 2005. Identification of proteins released by pancreatic cancer cells by multidimensional protein

identification technology: a strategy for identification of novel cancer markers. *FASEB J*. 19:1125--1127.

Mayer, U., K. Mann, L.I. Fessler, J.H. Fessler, and R. Timpl. 1997. Drosophila laminin binds to mammalian nidogen and to heparan sulfate proteoglycan. *Eur J Biochem*. 245:745--750.

McCall-Culbreath, K.D., and M.M. Zutter. 2008. Collagen receptor integrins: rising to the challenge. *Curr Drug Targets*. 9:139--149.

McCarthy, K.J., and J.R. Couchman. 1990. Basement membrane chondroitin sulfate proteoglycans: localization in adult rat tissues. *J Histochem Cytochem*. 38:1479--1486.

Mecham, R.P., and J.E. Heuser. 1991. The elastic fiber. *In* Cell biology of extracellular matrix. E.D. Hay, editor. Plenum Press, New York. 97.

Meglasson, M.D., and F.M. Matschinsky. 1986. Pancreatic islet glucose metabolism and regulation of insulin secretion. *Diabetes/metabolism reviews*. 2:163-214.

Mercurio, A.M. 1995. Laminin receptors: achieving specificity through cooperation. *Trends Cell Biol*. 5:419--423.

Meyer, T., C. Bühler, S. Czub, U. Beutner, C. Otto, A. Thiede, and K. Ulrichs. 1998a. Selection of donor pigs for pancreatic islet transplantation may depend on the expression level of connective tissue proteins in the islet capsule. *Transplant Proc*. 30:2471--2473.

Meyer, T., I. Chodnewska, S. Czub, W. Hamelmann, U. Beutner, C. Otto, A. Thiede, and K. Ulrichs. 1998b. Extracellular matrix proteins in the porcine pancreas: a structural analysis for directed pancreatic islet isolation. *Transplant Proc*. 30:354.

Miller, S.J., A.M. Hoggat, and W.P. Faulk. 1998. Heparin regulates ICAM-1 expression in human endothelial cells: an example of non-cytokine-mediated endothelial activation. *Thromb Haemost*. 80:481--487.

Miner, J.H., and P.D. Yurchenco. 2004. Laminin functions in tissue morphogenesis. *Annu Rev Cell Dev Biol*. 20:255--284.

Minton, A.P. 1997. Influence of excluded volume upon macromolecular structure and associations in 'crowded' media. *Curr Opin Biotechnol*. 8:65-69.

Miralles, F., P. Czernichow, K. Ozaki, N. Itoh, and R. Scharfmann. 1999. Signaling through fibroblast growth factor receptor 2b plays a key role in the development of the exocrine pancreas. *Proc Natl Acad Sci U S A*. 96:6267--6272.

Miyazaki, J., K. Araki, E. Yamato, H. Ikegami, T. Asano, Y. Shibasaki, Y. Oka, and K. Yamamura. 1990. Establishment of a pancreatic beta cell line that retains glucose-inducible insulin secretion: special reference to expression of glucose transporter isoforms. *Endocrinology*. 127:126-132.

Mizushima, H., H. Takamura, Y. Miyagi, Y. Kikkawa, N. Yamanaka, H. Yasumitsu, K. Misugi, and K. Miyazaki. 1997. Identification of integrin-dependent and -independent cell adhesion domains in COOH-terminal globular region of laminin-5 alpha 3 chain. *Cell Growth Differ*. 8:979--987.

Modrowski, D., A. Orosco, J. Thevenard, O. Fromigue, and P.J. Marie. 2005. Syndecan-2 overexpression induces osteosarcoma cell apoptosis: Implication of syndecan-2 cytoplasmic domain and JNK signaling. *Bone*. 37:180-189.

Mongiat, M., J. Fu, R. Oldershaw, R. Greenhalgh, A.M. Gown, and R.V. Iozzo. 2003. Perlecan protein core interacts with extracellular matrix protein 1 (ECM1), a glycoprotein involved in bone formation and angiogenesis. *J Biol Chem*. 278:17491--17499.

Mongiat, M., J. Otto, R. Oldershaw, F. Ferrer, J.D. Sato, and R.V. Iozzo. 2001. Fibroblast growth factor-binding protein is a novel partner for perlecan protein core. *J Biol Chem*. 276:10263--10271.

Mongiat, M., K. Taylor, J. Otto, S. Aho, J. Uitto, J.M. Whitelock, and R.V. Iozzo. 2000. The protein core of the proteoglycan perlecan binds specifically to fibroblast growth factor-7. *J Biol Chem*. 275:7095--7100.

Montesano, R., P. Mouron, M. Amherdt, and L. Orci. 1983. Collagen matrix promotes reorganization of pancreatic endocrine cell monolayers into islet-like organoids. *J Cell Biol*. 97:935--939.

Moran, M.T., W.M. Carroll, A. Gorelov, and Y. Rochev. 2007. Intact endothelial cell sheet harvesting from thermoresponsive surfaces coated with cell adhesion promoters. *Journal of the Royal Society, Interface / the Royal Society*. 4:1151-1157.

Murakami, M., A. Horowitz, S. Tang, J.A. Ware, and M. Simons. 2002. Protein kinase C (PKC) delta regulates PKCalpha activity in a Syndecan-4-dependent manner. *J Biol Chem*. 277:20367-20371.

Murugesan, S., J. Xie, and R.J. Linhardt. 2008. Immobilization of heparin: approaches and applications. *Curr Top Med Chem*. 8:80--100.

Mythreye, K., and G.C. Blobe. 2009. The type III TGFbeta receptor regulates directional migration: new tricks for an old dog. *Cell Cycle*. 8:3069--3070.

Nagata, N., Y. Gu, H. Hori, A.N. Balamurugan, M. Touma, Y. Kawakami, W. Wang, T.T. Baba, A. Satake, M. Nozawa, Y. Tabata, and K. Inoue. 2001. Evaluation of insulin secretion of isolated rat islets cultured in extracellular matrix. *Cell Transplant*. 10:447--451.

Nagata, N.A., K. Inoue, and Y. Tabata. 2002. Co-culture of extracellular matrix suppresses the cell death of rat pancreatic islets. *J Biomater Sci Polym Ed*. 13:579-590.

Narang, A.S., and R.I. Mahato. 2006. Biological and biomaterial approaches for improved islet transplantation. *Pharmacological reviews*. 58:194-243.

Naso, M.F., D.R. Zimmermann, and R.V. Iozzo. 1994. Characterization of the complete genomic structure of the human versican gene and functional analysis of its promoter. *J Biol Chem*. 269:32999--33008.

Nathan, D.M., J.B. Buse, M.B. Davidson, E. Ferrannini, R.R. Holman, R. Sherwin, and B. Zinman. 2009. Medical management of hyperglycaemia in type 2 diabetes mellitus: a consensus algorithm for the initiation and adjustment of therapy: a consensus statement from the American Diabetes Association and the European Association for the Study of Diabetes. *Diabetologia*. 52:17-30.

Negi, S., A. Jetha, R. Aikin, C. Hasilo, R. Sladek, and S. Paraskevas. 2012. Analysis of beta-cell gene expression reveals inflammatory signaling and evidence of dedifferentiation following human islet isolation and culture. *PloS one*. 7:e30415.

Nikolova, G., N. Jabs, I. Konstantinova, A. Domogatskaya, K. Tryggvason, L. Sorokin, R. FaÂ¨ssler, G. Gu, H.-P. Gerber, N. Ferrara, D.A. Melton, and E. Lammert. 2006. The vascular basement membrane: a niche for insulin gene expression and beta-cell proliferation. *Dev Cell*. 10:397--405.

Nilasaroya, A., L.A. Poole-Warren, J.M. Whitelock, and P.J. Martens. 2008. Structural and functional characterisation of poly(vinyl alcohol) and heparin hydrogels. *Biomaterials*. 29:4658--4664.

Noguchi, H., M. Ueda, S. Matsumoto, N. Kobayashi, and S. Hayashi. 2007. BETA2/NeuroD protein transduction requires cell surface heparan sulfate proteoglycans. *Hum Gene Ther*. 18:10--17.

Nolan, A.L. 2009. In vitro culture of isolated islets of Langerhans: analysis of function. *Methods Mol Biol*. 560:65--71.

Nomizu, M., Y. Kuratomi, S.Y. Song, M.L. Ponce, M.P. Hoffman, S.K. Powell, K. Miyoshi, A. Otaka, H.K. Kleinman, and Y. Yamada. 1997. Identification of cell binding sequences in mouse laminin gamma1 chain by systematic peptide screening. *J Biol Chem*. 272:32198--32205.

Oberg-Welsh, C. 2001. Long-term culture in matrigel enhances the insulin secretion of fetal porcine islet-like cell clusters in vitro. *Pancreas*. 22:157--163.

Ogawa, T., Y. Tsubota, J. Hashimoto, Y. Kariya, and K. Miyazaki. 2007. The short arm of laminin gamma2 chain of laminin-5 (laminin-332) binds syndecan-1

and regulates cellular adhesion and migration by suppressing phosphorylation of integrin beta4 chain. *Mol Biol Cell*. 18:1621--1633.

Ogneva, V., and Y. Martinova. 2002. The effect of in vitro fibroblast growth factors on cell proliferation in pancreas from normal and streptozotocin-treated rats. *Diabetes Res Clin Pract*. 57:11-16.

Oh, E.S., A. Woods, and J.R. Couchman. 1997. Multimerization of the cytoplasmic domain of syndecan-4 is required for its ability to activate protein kinase C. *J Biol Chem*. 272:11805-11811.

Olofsson, A.M., M. Vestberg, H. Herwald, J. Rygaard, G. David, K.E. Arfors, V. Linde, H. Flodgaard, J. Dedio, W. Müller-Esterl, and E. Lundgren-Akerlund. 1999. Heparin-binding protein targeted to mitochondrial compartments protects endothelial cells from apoptosis. *J Clin Invest*. 104:885--894.

Otonkoski, T., M. Banerjee, O. Korsgren, L.-E. Thornell, and I. Virtanen. 2008. Unique basement membrane structure of human pancreatic islets: implications for beta-cell growth and differentiation. *Diabetes Obes Metab*. 10 Suppl 4:119--127.

Otonkoski, T., G.M. Beattie, J.S. Rubin, A.D. Lopez, A. Baird, and A. Hayek. 1994. Hepatocyte growth factor/scatter factor has insulinotropic activity in human fetal pancreatic cells. *Diabetes*. 43:947-953.

Paget, M.B., H.E. Murray, C.J. Bailey, P.R. Flatt, and R. Downing. 2011. Rotational co-culture of clonal beta-cells with endothelial cells: effect of PPAR-gamma agonism in vitro on insulin and VEGF secretion. *Diabetes Obes Metab*. 13:662-668.

Pan, X., W. Xue, Y. Li, X. Feng, X. Tian, and C. Ding. 2011. Islet graft survival and function: concomitant culture and transplantation with vascular endothelial cells in diabetic rats. *Transplantation*. 92:1208-1214.

Pan, Y., A. Woodbury, J.D. Esko, K. Grobe, and X. Zhang. 2006. Heparan sulfate biosynthetic gene Ndst1 is required for FGF signaling in early lens development. *Development*. 133:4933-4944.

Paraskevas, S., D. Maysinger, R. Wang, T.P. Duguid, and L. Rosenberg. 2000. Cell loss in isolated human islets occurs by apoptosis. *Pancreas*. 20:270-276.

Parish, C.R. 2006. The role of heparan sulphate in inflammation. *Nat Rev Immunol*. 6:633--643.

Parish, C.R., C. Freeman, and M.D. Hulett. 2001. Heparanase: a key enzyme involved in cell invasion. *Biochim Biophys Acta*. 1471:M99--108.

Parnaud, G., E. Hammar, D.G. Rouiller, M. Armanet, P.A. Halban, and D. Bosco. 2006. Blockade of beta1 integrin-laminin-5 interaction affects spreading and insulin secretion of rat beta-cells attached on extracellular matrix. *Diabetes*. 55:1413--1420.

Perfetti, R., T.E. Henderson, Y. Wang, C. Montrose-Rafizadeh, and J.M. Egan. 1996. Insulin release and insulin mRNA levels in rat islets of Langerhans cultured on extracellular matrix. *Pancreas*. 13:47--54.

Phillips, R., J. Kondev, and J. Theriot. 2008. What and Where: Construction Plans for Cells and Organisms. *In* Physical Biology of the Cell. Taylor & Francis Group.

Pierschbacher, M.D., and E. Rouslahti. 1984. Cell attachment activity of fibronectin can be duplicated by small synthetic fragments of the molecule. *Nature*. 309:30--33.

Pileggi, A., R.D. Molano, T. Berney, P. Cattan, C. Vizzardelli, R. Oliver, C. Fraker, C. Ricordi, R.L. Pastori, F.H. Bach, and L. Inverardi. 2001. Heme oxygenase-1 induction in islet cells results in protection from apoptosis and improved in vivo function after transplantation. *Diabetes*. 50:1983-1991.

Pillarisetti, S. 2000. Lipoprotein modulation of subendothelial heparan sulfate proteoglycans (perlecan) and atherogenicity. *Trends Cardiovasc Med*. 10:60--65.

Pinkse, G.G.M., W.P. Bouwman, R. Jiawan-Lalai, O.T. Terpstra, J.A. Bruijn, and E. de Heer. 2006. Integrin signaling via RGD peptides and anti-beta1 antibodies confers resistance to apoptosis in islets of Langerhans. *Diabetes*. 55:312--317.

Pontoglio, M., S. Sreenan, M. Roe, W. Pugh, D. Ostrega, A. Doyen, A.J. Pick, A. Baldwin, G. Velho, P. Froguel, M. Levisetti, S. Bonner-Weir, G.I. Bell, M. Yaniv, and K.S. Polonsky. 1998. Defective insulin secretion in hepatocyte nuclear factor 1alpha-deficient mice. *J Clin Invest*. 101:2215-2222.

Pozzi, M., K.K. Wary, F.G. Giancotti, and H.A. Gardner. 1998. Integrin alpha 1 beta 1 mediates a unique collagen-dependent proliferation pathway in vivo. *Journal of Cell Biology*. 142:587-594.

Pye, D.A., R.R. Vives, P. Hyde, and J.T. Gallagher. 2000. Regulation of FGF-1 mitogenic activity by heparan sulfate oligosaccharides is dependent on specific structural features: differential requirements for the modulation of FGF-1 and FGF-2. *Glycobiology*. 10:1183-1192.

Ricordi, C., and T.B. Strom. 2004. Clinical islet transplantation: advances and immunological challenges. *Nat Rev Immunol*. 4:259-268.

Ris, F., E. Hammar, D. Bosco, C. Pilloud, K. Maedler, M.Y. Donath, J. Oberholzer, E. Zeender, P. Morel, D. Rouiller, and P.A. Halban. 2002. Impact of integrin-matrix matching and inhibition of apoptosis on the survival of purified human beta-cells in vitro. *Diabetologia*. 45:841--850.

Robertson, R.P. 2004a. Chronic oxidative stress as a central mechanism for glucose toxicity in pancreatic islet beta cells in diabetes. *J Biol Chem*. 279:42351-42354.

Robertson, R.P. 2004b. Islet transplantation as a treatment for diabetes - a work in progress. *N Engl J Med*. 350:694-705.

Robertson, R.P., J. Harmon, P.O. Tran, and V. Poitout. 2004. Beta-cell glucose toxicity, lipotoxicity, and chronic oxidative stress in type 2 diabetes. *Diabetes*. 53 Suppl 1:S119-124.

Ross, R.H., and W. Pawlina. 2006. Histology: A Text and Atlas: With Correlated Cell and Molecular Biology. Lippincott Williams & Wilkins.

Ross, R.S., and T.K. Borg. 2001. Integrins and the myocardium. *Circulation Research*. 88:1112-1119.

Rozario, T., and D.W. DeSimone. 2010. The extracellular matrix in development and morphogenesis: a dynamic view. *Dev Biol*. 341:126--140.

Russ, H.A., P. Ravassard, J. Kerr-Conte, F. Pattou, and S. Efrat. 2009. Epithelial-mesenchymal transition in cells expanded in vitro from lineage-traced adult human pancreatic beta cells. *PloS one*. 4:e6417.

Ryan, E.A., J.R. Lakey, R.V. Rajotte, G.S. Korbutt, T. Kin, S. Imes, A. Rabinovitch, J.F. Elliott, D. Bigam, N.M. Kneteman, G.L. Warnock, I. Larsen, and A.M. Shapiro. 2001. Clinical outcomes and insulin secretion after islet transplantation with the Edmonton protocol. *Diabetes*. 50:710--719.

Ryan, E.A., B.W. Paty, P.A. Senior, D. Bigam, E. Alfadhli, N.M. Kneteman, J.R. Lakey, and A.M. Shapiro. 2005. Five-year follow-up after clinical islet transplantation. *Diabetes*. 54:2060-2069.

Sakiyama-Elbert, S.E., and J.A. Hubbell. 2000. Controlled release of nerve growth factor from a heparin-containing fibrin-based cell ingrowth matrix. *J Control Release*. 69:149--158.

Sakko, A.J., C. Ricciardelli, K. Mayne, S. Suwiwat, R.G. LeBaron, V.R. Marshall, W.D. Tilley, and D.J. Horsfall. 2003. Modulation of prostate cancer cell attachment to matrix by versican. *Cancer Res*. 63:4786--4791.

Salek-Ardakani, S., J.R. Arrand, D. Shaw, and M. Mackett. 2000. Heparin and heparan sulfate bind interleukin-10 and modulate its activity. *Blood*. 96:1879--1888.

Salmivirta, M., F. Safaiyan, K. Prydz, M.S. Andresen, M. Aryan, and S.O. Kolset. 1998. Differentiation-associated modulation of heparan sulfate structure and function in CaCo-2 colon carcinoma cells. *Glycobiology*. 8:1029-1036.

Salvay, D.M., C.B. Rives, X. Zhang, F. Chen, D.B. Kaufman, W.L. Lowe, and L.D. Shea. 2008. Extracellular matrix protein-coated scaffolds promote the

reversal of diabetes after extrahepatic islet transplantation. *Transplantation*. 85:1456--1464.

Sanvito, F., P.L. Herrera, J. Huarte, A. Nichols, R. Montesano, L. Orci, and J.D. Vassalli. 1994. TGF-beta 1 influences the relative development of the exocrine and endocrine pancreas in vitro. *Development*. 120:3451--3462.

Schofield, K.P., J.T. Gallagher, and G. David. 1999. Expression of proteoglycan core proteins in human bone marrow stroma. *Biochem J*. 343 Pt 3:663-668.

Schuppin, G.T., S. Bonner-Weir, E. Montana, N. Kaiser, and G.C. Weir. 1993. Replication of adult pancreatic-beta cells cultured on bovine corneal endothelial cell extracellular matrix. *In vitro cellular & developmental biology. Animal*. 29A:339-344.

Shapiro, A.M., J.R. Lakey, E.A. Ryan, G.S. Korbutt, E. Toth, G.L. Warnock, N.M. Kneteman, and R.V. Rajotte. 2000. Islet transplantation in seven patients with type 1 diabetes mellitus using a glucocorticoid-free immunosuppressive regimen. *N Engl J Med*. 343:230-238.

Shapiro, A.M., C. Ricordi, and B. Hering. 2003. Edmonton's islet success has indeed been replicated elsewhere. *Lancet*. 362:1242.

Shin, H., S. Jo, and A.G. Mikos. 2003. Biomimetic materials for tissue engineering. *Biomaterials*. 24:4353--4364.

Sigrist, S., A. Mechine-Neuville, K. Mandes, V. Calenda, S. Braun, G. Legeay, J.P. Bellocq, M. Pinget, and L. Kessler. 2003. Influence of VEGF on the viability of encapsulated pancreatic rat islets after transplantation in diabetic mice. *Cell Transplant*. 12:627--635.

Simoneau, S., S. Haïk, C. Leucht, D. Dormont, J.-P. Deslys, S. Weiss, and C. Lasmézas. 2003. Different isoforms of the non-integrin laminin receptor are present in mouse brain and bind PrP. *Biol Chem*. 384:243--246.

Simons, M., and A. Horowitz. 2001. Syndecan-4-mediated signalling. *Cell Signal*. 13:855-862.

Skandalis, S.S., D. Kletsas, D. Kyriakopoulou, M. Stavropoulos, and D.A. Theocharis. 2006. The greatly increased amounts of accumulated versican and decorin with specific post-translational modifications may be closely associated with the malignant phenotype of pancreatic cancer. *Biochim Biophys Acta*. 1760:1217--1225.

Smith, J.W., and D.A. Cheresh. 1990. Integrin (alpha v beta 3)-ligand interaction. Identification of a heterodimeric RGD binding site on the vitronectin receptor. *J Biol Chem*. 265:2168--2172.

Song, H.J., W.J. Xue, Y. Li, X.H. Tian, Y. Song, X.M. Ding, X.S. Feng, P.X. Tian, and Z.L. Li. 2009. Improved islet survival and funtion with rat endothelial cells in vitro co-culture. *Transplant Proc*. 41:4302-4306.

Steffens, G.C.M., C. Yao, P. Prével, M. Markowicz, P. Schenck, E.M. Noah, and N. Pallua. 2004. Modulation of angiogenic potential of collagen matrices by covalent incorporation of heparin and loading with vascular endothelial growth factor. *Tissue Eng*. 10:1502--1509.

Stendahl, J.C., D.B. Kaufman, and S.I. Stupp. 2009. Extracellular matrix in pancreatic islets: relevance to scaffold design and transplantation. *Cell Transplant*. 18:1--12.

Stendahl, J.C., L.-J. Wang, L.W. Chow, D.B. Kaufman, and S.I. Stupp. 2008. Growth factor delivery from self-assembling nanofibers to facilitate islet transplantation. *Transplantation*. 86:478--481.

Stokes, R.A., K. Cheng, N. Deters, S.M. Lau, W.J. Hawthorne, P.J. O'Connell, J. Stolp, S. Grey, T. Loudovaris, T.W. Kay, H.E. Thomas, F.J. Gonzalez, and J.E. Gunton. 2012. Hypoxia-inducible factor 1alpha (HIF-1alpha) potentiates beta-cell survival after islet transplantation of human and mouse islets. *Cell Transplant*.

Strigini, M. 2005. Mechanisms of morphogen movement. *J Neurobiol*. 64:324--333.

Su, G., S.A. Blaine, D. Qiao, and A. Friedl. 2007. Shedding of syndecan-1 by stromal fibroblasts stimulates human breast cancer cell proliferation via FGF2 activation. *J Biol Chem*. 282:14906-14915.

Sutherland, D.E., R.W. Gruessner, and A.C. Gruessner. 2001. Pancreas transplantation for treatment of diabetes mellitus. *World J Surg*. 25:487-496.

Swarm, R.L. 1963. Transplantion of murine chondrosarcoma in mice of idfferent inbred strains. *J Natl Cancer Inst*. 31:953--975.

Szot, G.L., P. Koudria, and J.A. Bluestone. 2007. Murine pancreatic islet isolation. *Journal of visualized experiments : JoVE*:255.

Takahashi, I., N. Noguchi, K. Nata, S. Yamada, T. Kaneiwa, S. Mizumoto, T. Ikeda, K. Sugihara, M. Asano, T. Yoshikawa, A. Yamauchi, N.J. Shervani, A. Uruno, I. Kato, M. Unno, K. Sugahara, S. Takasawa, H. Okamoto, and A. Sugawara. 2009. Important role of heparan sulfate in postnatal islet growth and insulin secretion. *Biochem Biophys Res Commun*. 383:113--118.

Taylor, S.J., J.W. McDonald, and S.E. Sakiyama-Elbert. 2004. Controlled release of neurotrophin-3 from fibrin gels for spinal cord injury. *J Control Release*. 98:281--294.

Thivolet, C.H., P. Chatelain, H. Nicoloso, A. Durand, and J. Bertrand. 1985. Morphological and functional effects of extracellular matrix on pancreatic islet cell cultures. *Exp Cell Res*. 159:313--322.

Thomas, F.T., J.L. Contreras, G. Bilbao, C. Ricordi, D. Curiel, and J.M. Thomas. 1999. Anoikis, extracellular matrix, and apoptosis factors in isolated cell transplantation. *Surgery*. 126:299-304.

Tkachenko, E., E. Lutgens, R.V. Stan, and M. Simons. 2004. Fibroblast growth factor 2 endocytosis in endothelial cells proceed via syndecan-4-dependent activation of Rac1 and a Cdc42-dependent macropinocytic pathway. *J Cell Sci*. 117:3189-3199.

Tumova, S., A. Woods, and J.R. Couchman. 2000. Heparan sulfate chains from glypican and syndecans bind the Hep II domain of fibronectin similarly despite minor structural differences. *J Biol Chem*. 275:9410--9417.

Tunggal, P., N. Smyth, M. Paulsson, and M.C. Ott. 2000. Laminins: structure and genetic regulation. *Microsc Res Tech*. 51:214--227.

Turnbull, J.E., D.G. Fernig, Y. Ke, M.C. Wilkinson, and J.T. Gallagher. 1992. Identification of the basic fibroblast growth factor binding sequence in fibroblast heparan sulfate. *J Biol Chem*. 267:10337-10341.

Ueda, M., S. Matsumoto, S. Hayashi, N. Kobayashi, and H. Noguchi. 2008. Cell surface heparan sulfate proteoglycans mediate the internalization of PDX-1 protein. *Cell Transplant*. 17:91--97.

Utani, A., M. Nomizu, H. Matsuura, K. Kato, T. Kobayashi, U. Takeda, S. Aota, P.K. Nielsen, and H. Shinkai. 2001. A unique sequence of the laminin alpha 3 G domain binds to heparin and promotes cell adhesion through syndecan-2 and -4. *J Biol Chem*. 276:28779-28788.

Uygun, B.E., S.E. Stojsih, and H.W.T. Matthew. 2009. Effects of immobilized glycosaminoglycans on the proliferation and differentiation of mesenchymal stem cells. *Tissue Eng Part A*. 15:3499--3512.

Vainionpää, N., Y. Kikkawa, K. Lounatmaa, J.H. Miner, P. Rousselle, and I. Virtanen. 2006. Laminin-10 and Lutheran blood group glycoproteins in adhesion of human endothelial cells. *Am J Physiol Cell Physiol*. 290:C764--C775.

van Deijnen, J.H., C.E. Hulstaert, G.H. Wolters, and R. van Schilfgaarde. 1992a. Significance of the peri-insular extracellular matrix for islet isolation from the pancreas of rat, dog, pig, and man. *Cell Tissue Res*. 267:139--146.

van Deijnen, J.H., C.E. Hulstaert, G.H. Wolters, and R. van Schilfgaarde. 1992b. Significance of the peri-insular extracellular matrix for islet isolation from the pancreas of rat, dog, pig, and man. *Cell Tissue Res*. 267:139-146.

van den Born, J., K. Salmivirta, T. Henttinen, N. Ostman, T. Ishimaru, S. Miyaura, K. Yoshida, and M. Salmivirta. 2005. Novel heparan sulfate structures revealed by monoclonal antibodies. *J Biol Chem*. 280:20516-20523.

Velasco-Loyden, G., J. Arribas, and F. López-Casillas. 2004. The shedding of betaglycan is regulated by pervanadate and mediated by membrane type matrix metalloprotease-1. *J Biol Chem*. 279:7721--7733.

Velten, F., C. Laue, and J. Schrezenmeir. 1999. The effect of alginate and hyaluronate on the viability and function of immunoisolated neonatal rat islets. *Biomaterials*. 20:2161--2167.

Venkatasubbarao, K., M.M. Ahmed, M. Mohiuddin, C. Swiderski, E. Lee, W.R. Gower, K.F. Salhab, P. McGrath, W. Strodel, and J.W. Freeman. 2000. Differential expression of transforming growth factor beta receptors in human pancreatic adenocarcinoma. *Anticancer Res*. 20:43--51.

Villar, M.J., J.R. Hassell, and E. Brandan. 1999. Interaction of skeletal muscle cells with collagen type IV is mediated by perlecan associated with the cell surface. *J Cell Biochem*. 75:665--674.

Virtanen, I., M. Banerjee, J. Palgi, O. Korsgren, A. Lukinius, L.-E. Thornell, Y. Kikkawa, K. Sekiguchi, M. Hukkanen, Y.T. Konttinen, and T. Otonkoski. 2008. Blood vessels of human islets of Langerhans are surrounded by a double basement membrane. *Diabetologia*. 51:1181--1191.

Vischer, P., K. Feitsma, P. Schön, and W. Völker. 1997. Perlecan is responsible for thrombospondin 1 binding on the cell surface of cultured porcine endothelial cells. *Eur J Cell Biol*. 73:332--343.

Votteler, M., D.A. Carvajal Berrio, M. Pudlas, H. Walles, and K. Schenke-Layland. 2012. Non-contact, Label-free Monitoring of Cells and Extracellular Matrix using Raman Spectroscopy. *Journal of visualized experiments : JoVE*.

Vukicevic, S., H.K. Kleinman, F.P. Luyten, A.B. Roberts, N.S. Roche, and A.H. Reddi. 1992. Identification of multiple active growth factors in basement membrane Matrigel suggests caution in interpretation of cellular activity related to extracellular matrix components. *Exp Cell Res*. 202:1--8.

Vuoriluoto, K., J. Jokinen, K. Kallio, M. Salmivirta, J. Heino, and J. Ivaska. 2008. Syndecan-1 supports integrin alpha 2 beta 1-mediated adhesion to collagen. *Experimental Cell Research*. 314:3369-3381.

Waanders, L.F., K. Chwalek, M. Monetti, C. Kumar, E. Lammert, and M. Mann. 2009. Quantitative proteomic analysis of single pancreatic islets. *Proc Natl Acad Sci U S A*. 106:18902-18907.

Wadsworth, G.R., and C.J. Oliveiro. 1953. Plasma protein concentration of normal adults living in Singapore. *British medical journal*. 2:1138-1139.

Wang, F.H., Y.C. Yip, M. Zhang, H.T. Vong, K.I. Chan, K.C. Wai, and J.M. Wen. 2010. Diagnostic utility of glypican-3 for hepatocellular carcinoma on liver needle biopsy. *J Clin Pathol*. 63:599--603.

Wang, J., T. Yoshida, F. Nakaki, H. Hiai, T. Okazaki, and T. Honjo. 2005a. Establishment of NOD-Pdcd1-/- mice as an efficient animal model of type I diabetes. *Proc Natl Acad Sci U S A*. 102:11823--11828.

Wang, R., J. Li, K. Lyte, N.K. Yashpal, F. Fellows, and C.G. Goodyer. 2005b. Role for beta1 integrin and its associated alpha3, alpha5, and alpha6 subunits in development of the human fetal pancreas. *Diabetes*. 54:2080--2089.

Wang, R.N., S. Paraskevas, and L. Rosenberg. 1999. Characterization of integrin expression in islets isolated from hamster, canine, porcine, and human pancreas. *J Histochem Cytochem*. 47:499--506.

Wang, R.N., and L. Rosenberg. 1999. Maintenance of beta-cell function and survival following islet isolation requires re-establishment of the islet-matrix relationship. *J Endocrinol*. 163:181--190.

Watkins, D., Cooperst.Sj, P.K. Dixit, and A. Lazarow. 1968. Insulin Secretion from Toadfish Islet Tissue Stimulated by Pyridine Nucleotides. *Science*. 162:283-284.

Weber, L.M., and K.S. Anseth. 2008. Hydrogel encapsulation environments functionalized with extracellular matrix interactions increase islet insulin secretion. *Matrix Biol*. 27:667--673.

Weber, L.M., K.N. Hayda, and K.S. Anseth. 2008. Cell-matrix interactions improve beta-cell survival and insulin secretion in three-dimensional culture. *Tissue Eng Part A*. 14:1959--1968.

Weber, L.M., K.N. Hayda, K. Haskins, and K.S. Anseth. 2007. The effects of cell-matrix interactions on encapsulated beta-cell function within hydrogels functionalized with matrix-derived adhesive peptides. *Biomaterials*. 28:3004--3011.

Weinberg, N., L. Ouziel-Yahalom, S. Knoller, S. Efrat, and Y. Dor. 2007. Lineage tracing evidence for in vitro dedifferentiation but rare proliferation of mouse pancreatic beta-cells. *Diabetes*. 56:1299-1304.

Whipple, C.A., A.D. Lander, and M. Korc. 2008. Discovery of a novel molecule that regulates tumor growth and metastasis. *ScientificWorldJournal*. 8:1250--1253.

Whitelock, J.M., L.D. Graham, J. Melrose, A.D. Murdoch, R.V. Iozzo, and P.A. Underwood. 1999. Human perlecan immunopurified from different endothelial cell sources has different adhesive properties for vascular cells. *Matrix Biol*. 18:163--178.

Whitelock, J.M., A.D. Murdoch, R.V. Iozzo, and P.A. Underwood. 1996. The degradation of human endothelial cell-derived perlecan and release of bound

basic fibroblast growth factor by stromelysin, collagenase, plasmin, and heparanases. *J Biol Chem*. 271:10079--10086.

WHO. 2011. Diabetes. Vol. 2012, World Health Organization.

Wolters, G.H., G.H. Vos-Scheperkeuter, J.H. van Deijnen, and R. van Schilfgaarde. 1992. An analysis of the role of collagenase and protease in the enzymatic dissociation of the rat pancreas for islet isolation. *Diabetologia*. 35:735-742.

Woods, A., M. Hook, L. Kjellen, C.G. Smith, and D.A. Rees. 1984. Relationship of heparan sulfate proteoglycans to the cytoskeleton and extracellular matrix of cultured fibroblasts. *J Cell Biol*. 99:1743-1753.

Woods, A., R.L. Longley, S. Tumova, and J.R. Couchman. 2000a. Syndecan-4 binding to the high affinity heparin-binding domain of fibronectin drives focal adhesion formation in fibroblasts. *Arch Biochem Biophys*. 374:66--72.

Woods, A., R.L. Longley, S. Tumova, and J.R. Couchman. 2000b. Syndecan-4 binding to the high affinity heparin-binding domain of fibronectin drives focal adhesion formation in fibroblasts. *Arch Biochem Biophys*. 374:66-72.

Wrenshall, L.E., R.B. Stevens, F.B. Cerra, and J.L. Platt. 1999. Modulation of macrophage and B cell function by glycosaminoglycans. *J Leukoc Biol*. 66:391--400.

Wu, Y., L. Chen, P.-S. Zheng, and B.B. Yang. 2002. beta 1-Integrin-mediated glioma cell adhesion and free radical-induced apoptosis are regulated by binding to a C-terminal domain of PG-M/versican. *J Biol Chem*. 277:12294--12301.

Wu, Y., J. Wu, D.Y. Lee, A. Yee, L. Cao, Y. Zhang, C. Kiani, and B.B. Yang. 2005a. Versican protects cells from oxidative stress-induced apoptosis. *Matrix Biol*. 24:3--13.

Wu, Y.J., D.P.L. Pierre, J. Wu, A.J. Yee, and B.B. Yang. 2005b. The interaction of versican with its binding partners. *Cell Res*. 15:483--494.

Xian, X., S. Gopal, and J.R. Couchman. 2010. Syndecans as receptors and organizers of the extracellular matrix. *Cell Tissue Res*. 339:31-46.

Xu, X., V.L. Browning, and J.S. Odorico. 2011. Activin, BMP and FGF pathways cooperate to promote endoderm and pancreatic lineage cell differentiation from human embryonic stem cells. *Mechanisms of development*. 128:412-427.

Yamaoka, T., C. Idehara, M. Yano, T. Matsushita, T. Yamada, S. Li, M. Moritani, J. Hata, H. Sugino, S. Noji, and M. Itakura. 1998. Hypoplasia of pancreatic islets in transgenic mice expressing activin receptor mutants. *Journal of Clinical Investigation*. 102:294-301.

Yi, X.Y., E.A. Wayner, Y. Kim, and A.J. Fish. 1998. Adhesion of cultured human kidney mesangial cells to native entactin: role of integrin receptors. *Cell Adhes Commun*. 5:237--248.

Yuan, D.-H., H.-H. Xie, Y. Wang, C.-Y. Meng, L.-P. Yang, Y.-C. Feng, J.-G. Song, X. Zou, K.-C. Wu, and J. Liu. 2008. Expression and significance of glypican-3 in colorectal cancer. *Zhonghua Yi Xue Za Zhi*. 88:1540--1542.

Yung, S., A. Woods, T.M. Chan, M. Davies, J.D. Williams, and J.R. Couchman. 2001. Syndecan-4 up-regulation in proliferative renal disease is related to microfilament organization. *FASEB J*. 15:1631-1633.

Zanone, M.M., E. Favaro, and G. Camussi. 2008. From endothelial to beta cells: insights into pancreatic islet microendothelium. *Curr Diabetes Rev*. 4:1-9.

Zeiger, A.S., F.C. Loe, R. Li, M. Raghunath, and K.J. Van Vliet. 2012. Macromolecular crowding directs extracellular matrix organization and mesenchymal stem cell behavior. *PloS one*. 7:e37904.

Zertal-Zidani, S., A. Bounacer, and R. Scharfmann. 2007. Regulation of pancreatic endocrine cell differentiation by sulphated proteoglycans. *Diabetologia*. 50:585--595.

Zhang, C., T. Moriguchi, M. Kajihara, R. Esaki, A. Harada, H. Shimohata, H. Oishi, M. Hamada, N. Morito, K. Hasegawa, T. Kudo, J.D. Engel, M. Yamamoto, and S. Takahashi. 2005. MafA is a key regulator of glucose-stimulated insulin secretion. *Mol Cell Biol*. 25:4969-4976.

Zhou, Y.P., J.C. Pena, M.W. Roe, A. Mittal, M. Levisetti, A.C. Baldwin, W. Pugh, D. Ostrega, N. Ahmed, V.P. Bindokas, L.H. Philipson, D. Hanahan, C.B. Thompson, and K.S. Polonsky. 2000. Overexpression of Bcl-x(L) in beta-cells prevents cell death but impairs mitochondrial signal for insulin secretion. *American journal of physiology. Endocrinology and metabolism*. 278:E340-351.

Ziolkowski, A.F., S.K. Popp, C. Freeman, C.R. Parish, and C.J. Simeonovic. 2012. Heparan sulfate and heparanase play key roles in mouse beta cell survival and autoimmune diabetes. *J Clin Invest*. 122:132-141.